

**8-PSK SIGNALING OVER NON-LINEAR
SATELLITE CHANNELS**

**Ruben Caballero, B. ENG.
Dr. Sheila Horan**

NMSU-ECE-96-010 May 1996

8-PSK SIGNALING
OVER NON-LINEAR
SATELLITE CHANNELS
BY
RUBÉN CABALLERO, B.ENG.

A Thesis submitted to the Graduate School
in partial fulfillment of the requirements
for the Degree
Master of Science in Electrical Engineering

New Mexico State University

Las Cruces, New Mexico

May 1996

ACKNOWLEDGMENTS

Throughout my young career as an engineer, I always had a particular feeling, that was well expressed, by the French philosopher and mathematician Descartes in the 17th century:

*“... à la vue d’ingénieuse découvertes, je me demandais si je ne pourrais pas
inventer par moi-même sans m’appuyer sur la lecture d’un auteur ...”*

My two years of graduate study and this thesis allowed me to answer to this affirmation.

First, I would like to thank Dr. Sheila Horan, my thesis advisor, for her help, direction and advice toward the completion of my research. To Dr. Stephen Horan and Dr. William Ryan, I also wish to give my thanks for sharing with me their engineering expertise and advice. I also would like to thank Dr. James P. Reilly who served on my thesis committee and the students in the Center for Space Telemetry and Telecommunications Systems in the Klipsch School of Electrical and Computer Engineering Department for their dedication towards Telemetry and Space-Communications.

I am also deeply grateful to the Canadian Air Force and the Canadian Government for their support in the completion of my Master’s degree. I also thank NASA for their support under Grant # NAG 5-1491 and for giving me the chance to work on this project.

Finalmente, no existen suficientes palabras para describir el cariño y amor que le tengo a mi familia, Los Caballero, sin quienes nunca habría llegado hasta donde hoy estoy. Muchísimas gracias a mi padre, Luis, mi madre, Luz, y a mi dos hermanitas, María-Paz y Joanna Manuela.

ABSTRACT

**8-PSK SIGNALING
OVER NON-LINEAR
SATELLITE CHANNELS**

BY

RUBÉN CABALLERO, B.ENG.

Master of Science in Electrical Engineering

New Mexico State University

Las Cruces, New Mexico, 1996

Dr. Sheila B. Horan, Chair

Space agencies are under pressure to utilize better bandwidth-efficient communication methods due to the actual allocated frequency bands becoming more congested. Also budget reductions is another problem that the space agencies must deal with. This budget constraint results in simpler spacecraft carrying less communication capabilities and also the reduction in staff to capture data in the earth stations. It is then imperative that the most bandwidth efficient communication methods be utilized. This thesis presents a study of 8-ary Phase Shift Keying (8PSK) modulation with respect to bandwidth, power efficiency, spurious emissions and interference susceptibility over a non-linear satellite channel.

An end-to-end system performance, including the InterSymbol Interference (ISI) and the Symbol Error Rate (SER) as a function of E_b/N_0 on 8PSK modulation was conducted on Signal Processing Worksystem (SPW) software installed on a SUN Sparc Station 10 and a Hewlett Packard (HP) Model 715/100 Unix Station. The simulations were based on the Non-Return-to-Zero (NRZ) data format. The end-to-end system evaluation was performed using ideal and non-ideal data with ideal system components and three baseband filter types: 5th Order Butterworth, 3rd Order Bessel and Square Root Raised Cosine (SRRC), $\alpha = 0.25, 0.5$ and 1 , to observe the effect of pulse shaping on bandwidth and SER.

The simulations show that in-band spurious emissions are greater in number and more evident for the Bessel Filter than the Butterworth Filter with a Bandwidth (3dB)-Time product equal to 1 ($BT=1$). With respect to the sideband attenuation, it was found that the values of attenuation for the 3rd Order Bessel filter are comparable to the 5th Order Butterworth filter. For SRRC filters with $\alpha = 0.25$ and $\alpha = 0.5$, the bandwidth is narrower than the Butterworth and Bessel Filters, but the attenuation is less at high frequencies. Nonetheless, the absence of spurious emissions is a net advantage. For SRRC $\alpha = 1$, the bandwidth is wider than the two previous SRRC filters and the absence of in-band spurious emissions was again noticed. Less sideband attenuation was recorded for this roll-off factor compared with $\alpha = 0.25$ and $\alpha = 0.5$. For SER, it was found that the Butterworth and Bessel Filters just barely meet the threshold of ISI loss < 0.4 dB at $SER = 10^{-3}$. Also the SRRC filters do not meet this specification. From these results, it can be stipulated that the 5th Order Butterworth filter has a small advantage compared to the other filters. Overall, it was shown by using baseband filtering that the bandwidth utilization can be improved by a factor of 12 to 24 with $BT=1$ and 8PSK which can significantly increase the spectrum utilization. Also a study on the tradeoffs between non-constant envelope and bandwidth in a non-linear system, Solid State Power Amplifier (SSPA), is discussed.

TABLE OF CONTENTS

LIST OF TABLES	ix
LIST OF FIGURES	x
LIST OF ABBREVIATIONS	xiii
Chapter	
1. INTRODUCTION AND BACKGROUND	1
2. THEORY	8
2.1 Eight (8) Level Phase Shift Keying (8PSK).....	8
2.2 NRZ-L Ideal and Non-Ideal Data	11
2.3 Intersymbol Interference (ISI)	13
2.4 Spectrum Shaping and Filters	14
2.4.1 Butterworth Filters	14
2.4.2 Bessel Filters	15
2.4.3 Raised Cosine Filters	16
2.5 Solid State Power Amplifier (SSPA)	20
2.6 Additive White Gaussian Noise (AWGN)	21
2.7 Matched Filter for White Noise	23
3. 8PSK SIMULATIONS.....	25
3.1 Simulation Procedures.....	25
3.2 Power Containment and Spurious Emissions Simulations.....	28
3.3 End-to-End System Performance: Symbol Error Rate (SER)	64
3.4 Non-Constant Envelope 8PSK Simulations.....	73
4. CONCLUSIONS AND RECOMMENDATIONS.....	98
REFERENCES	101

APPENDIX A. SPW Detail Diagrams for PSD and SER Simulations	103
A.1 PSD Detailed Diagram.....	103
A.2 SEP. Detailed Diagram.....	108
APPENDIX B. SSPA, ESA 10 Watts.....	111
APPENDIX C. Non-Constant Envelope Simulation Block Diagram.....	118
APPENDIX D. Program Listing: “SPWSOBRE.M”.....	122
APPENDIX E. Scatter Plots: 5th Order Butterworth Filter.....	126
E.1 Scatter Plots.....	126
E.2 Program Listing: BUTTPLOT.M.....	145
APPENDIX F. Scatter Plots: 3rd Order Bessel Filter.....	151
F.1 Scatter Plots.....	151
F.2 Program Listing: BESSPLOT.M.....	170
APPENDIX G. Scatter Plots: SRRC Filter.....	176
G.1 Scatter Plots.....	176
G.2 Program Listing: SRRCPLOT.M.....	196

LIST OF TABLES

Table 1.1 - Summary of PCM/PM/NRZ Modulation Simulation.....	5
Table 2.1 - Values of C_i for the BPSK, QPSK, 8PSK Simulation Model.....	11
Table 3.1 - Power Spectrum Simulations.....	29
Table 3.2 - Comparison of Theoretical and Simulated Amplitudes for 8PSK using SPW with Ideal Data	30
Table 3.3 - Spectrum Levels Relative to First Data Sideband (SSPA at Saturation Level and Ideal Data).....	50
Table 3.4 - Spectrum Levels Relative to First Data Sideband (SSPA at Saturation Level and Non-Ideal Data).....	50
Table 3.5 - SER for 8PSK Simulations.....	66
Table 3.6 - Baseband Filters ISI Loss Measurements at 10^{-3} SER.....	68
Table 3.7 - Optimum Baseband Filter.....	69
Table 3.8 - Utilization Ratio Improvement for Various Spectrum Shaping.....	71
Table 3.9 - Rotation of 8PSK Symbols due to PM Conversion on SSPA.....	86
Table 3.10 - Mean and Variance of SSPA Output (Saturation Level) with 5th Order Butterworth (BT=1).....	91
Table 3.11 - Non-Constant Envelope Simulations: Filters and BW Used.....	92

LIST OF FIGURES

Figure 2.1 - 8 PSK Digital Transmission System.....	8
Figure 2.2 - 8PSK Signal Constellation.....	9
Figure 2.3 - Block Diagram for the BPSK, QPSK and 8PSK Modulator on SPW.....	10
Figure 2.4 - NRZ-L Digital Data Format.....	11
Figure 2.5 - Intersymbol Interference (ISI).....	13
Figure 2.6 - Amplitude Response of Various Orders of Butterworth Filters.....	15
Figure 2.7 - Amplitude Response of Various Orders of Bessel Filters.....	16
Figure 2.8 - Frequency Response: Raised Cosine Characteristics with Different α	17
Figure 2.9 - Time Response of Raised Cosine Filters for Different α	18
Figure 2.10 - SSPA, ESA 10 Watts, Output Characteristics Curve.....	20
Figure 2.11 - Block Diagram for the AWGN.....	22
Figure 2.12 - Matched Filter Diagram.....	23
Figure 3.1 - Simulation Block Diagram.....	25
Figure 3.2 - Power Spectra of Unfiltered 8PSK Baseband Ideal Data using SSPA at Saturation Level	31
Figure 3.3 - Power Spectra of Unfiltered 8PSK Baseband Non-Ideal Data using SSPA at Saturation Level	34
Figure 3.4 - Power Spectra of Filtered 8PSK Baseband Ideal Data using 5th Order Butterworth Filter (BT=1) & SSPA at Saturation Level	36
Figure 3.5 - Power Spectra of Filtered 8PSK Baseband Non-Ideal Data using 5th Order Butterworth Filter (BT=1) & SSPA at Saturation Level	37
Figure 3.6 - Power Spectra of Filtered 8PSK Baseband Ideal Data using 3rd Order Bessel Filter (BT=1) & SSPA at Saturation Level	39
Figure 3.7 - Power Spectra of Filtered 8PSK Baseband Non-Ideal Data using 3rd Order Bessel Filter (BT=1) & SSPA at Saturation Level	40
Figure 3.8 - Power Spectra of Filtered 8PSK Baseband Ideal Data using SRRC ($\alpha = 0.25$) Filter & SSPA at Saturation Level	43
Figure 3.9 - Power Spectra of Filtered 8PSK Baseband Non-Ideal Data using SRRC ($\alpha = 0.25$) Filter & SSPA at Saturation Level	44

Figure 3.10 - Power Spectra of Filtered 8PSK Baseband Ideal Data using SRRC ($\alpha = 0.5$) Filter & SSPA at Saturation Level	46
Figure 3.11 - Power Spectra of Filtered 8PSK Baseband Non-Ideal Data using SRRC ($\alpha = 0.5$) Filter & SSPA at Saturation Level	47
Figure 3.12 - Power Spectra of Filtered 8PSK Baseband Ideal Data using SRRC ($\alpha = 1$) Filter & SSPA at Saturation Level	48
Figure 3.13 - Power Spectra of Filtered 8PSK Baseband Non-Ideal Data using SRRC ($\alpha = 1$) Filter & SSPA at Saturation Level	49
Figure 3.14 - Power Spectra of Unfiltered 8PSK Baseband Ideal Data using SSPA at 10dB backoff	52
Figure 3.15 - Power Spectra of Unfiltered 8PSK Baseband Non-Ideal Data using SSPA at 10dB backoff	53
Figure 3.16 - Power Spectra of Filtered 8PSK Baseband Ideal Data using 5th Order Butterworth Filter (BT=1) & SSPA at 10dB backoff	54
Figure 3.17 - Power Spectra of Filtered 8PSK Baseband Non-Ideal Data using 5th Order Butterworth Filter (BT=1) & SSPA at 10dB backoff	55
Figure 3.18 - Power Spectra of Filtered 8PSK Baseband Ideal Data using 3rd Order Bessel Filter (BT=1) & SSPA at 10dB backoff	56
Figure 3.19 - Power Spectra of Filtered 8PSK Baseband Non-Ideal using 3rd Order Bessel Filter (BT=1) & SSPA at 10dB backoff	57
Figure 3.20 - Power Spectra of Filtered 8PSK Baseband Ideal Data using SRRC Filter ($\alpha = 0.25$) & SSPA at 10dB backoff.....	58
Figure 3.21 - Power Spectra of Filtered 8PSK Baseband Non-Ideal Data using SRRC ($\alpha = 0.25$) Filter & SSPA at 10dB backoff	59
Figure 3.22 - Power Spectra of Filtered 8PSK Baseband Ideal Data using SRRC ($\alpha = 0.5$) Filter & SSPA Filter at 10dB backoff	60
Figure 3.23 - Power Spectra of Filtered 8PSK Baseband Non-Ideal Data: using SRRC ($\alpha = 0.5$) Filter & SSPA at 10dB backoff	61
Figure 3.24 - Power Spectra of Filtered 8PSK Baseband Ideal Data using SRRC ($\alpha = 1$) Filter & SSPA at 10dB backoff	62
Figure 3.25 - Power Spectra of Filtered 8PSK Baseband Non-Ideal Data using SRRC ($\alpha = 1$) Filter & SSPA at 10dB backoff	63
Figure 3.26 - SER for 8PSK curves: Ideal and Non-Ideal Data with BT = ∞	65

Figure 3.27 - SER for 8PSK: 5th Order Butterworth BT = 1, 2 and 3 (SSPA at Saturation & Ideal Data).....	67
Figure 3.28 - SER for 8PSK: 3rd Order Bessel BT = 1, 2 and 3 (SSPA at Saturation & Ideal Data).....	67
Figure 3.29 - SER for 8PSK: SRRC $\alpha = 1$ (no SSPA), $\alpha = 0.25, 0.5$, and 1 (SSPA at Saturation & Ideal Data).....	68
Figure 3.30 - 8PSK Modulator Output: Real & Imaginary Part	75
Figure 3.31 - 8PSK Modulator Output: Magnitude & Phase	76
Figure 3.32 - 5th Order Butterworth Filter (BT = 1) Output: Real & Imaginary Part	77
Figure 3.33 - 5th Order Butterworth Filter (BT = 1) Output: Magnitude & Phase	78
Figure 3.34 - Output of SSPA (Input = Output of 5th Order Butterworth Filter (BT = 1)) Real & Imaginary Part	79
Figure 3.35 - Output of SSPA (Input = Output of 5th Order Butterworth Filter (BT = 1)) Magnitude & Phase	80
Figure 3.36 - Output of SSPA (Input = Output of 8PSK Modulator (Constant Envelope)) Real & Imaginary Part	81
Figure 3.37 - Output of SSPA (Input = Output of 8PSK Modulator (Constant Envelope)) Magnitude & Phase	82
Figure 3.38 - Non-Constant Envelope Simulations Block Diagram	84
Figure 3.39 - SSPA, ESA 10 Watts, Zoomed Magnitude Characteristic Curve	84
Figure 3.40 - SSPA, ESA 10 Watts, Phase (degrees) Characteristic Curve	85
Figure 3.41 - Scatter Plot: 8PSK Modulator, 5th Order Butterworth Filter (BT = 1), and SSPA (Saturation Level) Output.....	87
Figure 3.42 - Mean and Variance in Decision Region.....	91
Figure 3.43 - 5th Order Butterworth Filter: Average Symbol Variance vs. BT.....	93
Figure 3.44 - Zoom of Average Symbol Variance vs. BT for 5th Order Butterworth Filter.....	94
Figure 3.45 - 3rd Order Bessel Filter: Average Symbol Variance vs. BT.....	95
Figure 3.46 - Zoom of Average Symbol Variance vs. BT for 3rd Order Bessel Filter.....	95
Figure 3.47 - SRRC Filter: Average Symbol Variance vs. Rolloff Factor (α).....	96

LIST OF ABBREVIATIONS

α or r	Rolloff Factor for SRRC filters
ρ	Band Utilization Ratio
AM	Amplitude Modulation
AWGN	Additive White Gaussian Noise
ASCII	American Information Code for Information Interchange
dB	Decibels
BER	Bit Error Rate
Bi- ϕ	Bi-Phase (Manchester)
BPSK	Binary Phase Shift Keying
BW	Bandwidth
BT	Bandwidth-Time (symbol) product
CCSDS	Consultative Committee for Space Data Systems
DC	Direct Current
E_s/N_0	Energy (symbol) to Noise ratio
ESA	European Space Agency
f_s	Sampling Frequency
FFT	Fast Fourier Transform
FSK	Frequency Shift Keying
FSE	Fractionally-Spaced Equalizer
FTP	File Transfer Protocol
GMSK	Gaussian Minimum Shift Keying
Hz	Hertz
HP	Hewlett Packard

IF	Intermediate Frequency
IIR	Infinite Impulse Response (filter)
ISI	InterSymbol Interference
JPL	Jet Propulsion Laboratory
LSB	Least Significant Bit
MSB	Most Significant Bit
MSK	Minimum Shift Keying
NASA	National Aeronautics and Space Administration
NMSU	New Mexico State University
NRZ-L	Non-Return-to-Zero Logic
OQPSK	Offset Quaternary Phase Shift Keying
PA	Power Amplifier
PC	Personal Computer
PCM	Pulse Coded Modulation
PM	Phase Modulation
PSD	Power Spectral Density
PSK	Phase Shift Keying
QPSK	Quaternary Phase Shift Keying
R_B	Bit Rate
R_S	Symbol or Baud Rate
RC	Raised Cosine
RF	Radio Frequency
sec	Seconds
SER	Symbol Error Rate
SFCG	Space Frequency Coordination Group

SNR	Signal-to-Noise Ratio
SPC	Serial-to-Parallel Converter
SPW	Signal Processing Worksystem
SSPA	Solid State Power Amplifier
SRRC	Square Root Raised Cosine
T_B	Bit Period
TWT	Traveling Wave Tube
V	Volts

Chapter 1

INTRODUCTION AND BACKGROUND

This thesis gives the results of a study on 8 Level Phase Shift Keying (8PSK) modulation with respect to bandwidth, power efficiency, spurious emissions, interference susceptibility and the non-constant envelope effect through a non-linear channel. This work was conducted at New Mexico State University (NMSU) in the Center for Space Telemetry and Telecommunications Systems in the Klipsch School of Electrical and Computer Engineering Department and is supported by a grant from the National Aeronautics and Space Administration (NASA) # NAG 5-1491.

The first chapter of this report gives a brief summary of the work completed by the Jet Propulsion Laboratory (JPL) on various modulation schemes and previous studies performed on non-constant envelope signals. In Chapter 2, some theoretical concepts will be explained which are directly related to the simulations that were performed for the 8PSK modulation. Finally in Chapter 3, results on the simulations for 8PSK will be given. The simulations were performed on a Signal Processing Worksystem (SPW) [†] (software installed on a SUN SPARC 10 Unix Station and Hewlett Packard Model 715/100 Unix Station) where the power containment, spurious emissions, symbol error rates and non-constant envelope effect on the bandwidth are measured for different types of spectrum shaping filters. Conclusions and suggestions for further work are given at the end of this report in Chapter 4.

[†] SPW is a registered trademark of COMDISCO systems, a Business Unit of Cadence Design Systems, Inc. 919 East Hillsdale Blvd., Foster City, CA 94404.

During its 12th annual meeting (November 1992 in Australia), the Space Frequency Coordination Group (SFCG-12) requested the Consultative Committee for Space Data Systems (CCSDS) Radio Frequency (RF) and Modulation Subpanel to study and compare various modulation schemes with respect to:

- (a) - bandwidth needed;
- (b) - power efficiency;
- (c) - spurious emissions; and
- (d) - interference susceptibility.

This study has to be conducted due to the fact that frequency bands are becoming more and more congested and space agencies are under constant pressure to reduce costs. To date, four position papers have been presented (References [1], [2], [3], and [4]). These reports divided the study into three logical phases:

Phase I (a) - Bandwidth (BW) utilization of various modulation schemes, explores traditional modulation schemes that were used in the past and compares them with newer ones that could improve the communication channel efficiencies. From this first paper, the following was concluded. The traditional modulation methods utilize subcarriers which have some advantages and disadvantages. The subcarrier greatly facilitates the separation of data types and also separates the data transmitted from the RF carrier. On the other hand, subcarriers significantly increased the spacecraft complexity. It also produces additional losses in the modulator and demodulator and occupies a large bandwidth. The new modulation techniques (and data formatting) such as PCM/PM/Bi- ϕ (Pulse Coded Modulated/ Phase Modulation: data are Bi-Phase (Manchester) modulated directly on a residual RF carrier), PCM/PM/NRZ (NRZ data are phase modulated directly on a residual RF carrier), BPSK/Bi- ϕ (data is Bi-Phase (Manchester) modulated on an RF carrier fully suppressing it) and BPSK/NRZ (Binary Phase Shift Keying/NRZ data is phase modulated directly on an RF carrier fully suppressing it) were examined.

It was noted, as expected, that these new types of modulation significantly reduce the amount of BW. Therefore use of subcarriers should be limited. A new definition of required bandwidth was proposed (required BW is equal to 95% of the corresponding ideally modulated square pulse shaping signal) due to the ambiguities of the present definitions. For more information refer to [1].

Phase I (b) - A comparison of Quaternary Phase Shift Keying (QPSK), Offset Quaternary Phase Shift Keying (OQPSK), BPSK, and Gaussian Minimum Shift Keying (GMSK) [2] is a complimentary paper for Phase I (a) which studies modulations that seem more promising for this study (BPSK was used as reference). First, it was concluded that by doing some spectral shaping on the data, a reduction of the bandwidth can be achieved. The unfiltered data spectrum can be as much as 5 to 10 times the width of the filtered data spectrum. Also the signal degradation due to power losses, pulse distortions and ISI is between 0.2 and 0.4 dB (for QPSK, OQPSK, BPSK, and GMSK) if a matched receiver is used. With respect to the pulse shaping filtering, it was mentioned that such filtering at the Intermediate Frequency (IF) level would require hardware that would be considered acceptable for RF filtering. With respect to the modulation schemes it was noticed that GMSK is a bit better than QPSK and filtered BPSK in non-linear channels unless filtering is applied after the power amplifier (PA). In the case of pulse shaping filtering, the GMSK and filtered OQPSK offered practically identical performance.

Phase II - Spectrum Shaping [3] is analyzed and simulated. The benefits accruing from the spectrum shaping of the transmitted signal are presented. This paper shows that several types of filters and location for these filters can be used. Also it was shown that spectrum shaping, with an efficient type of modulation, can increase the utilization ratio. This would allow more signals to be placed into a given frequency band. The paper also gives the frequency spectra simulations performed on PCM/PM/NRZ data on the SPW (COMDISCO) simulation software. Non-ideal and ideal data were used with 4 different types of spectrum shaping filters (Butterworth 5th Order, Bessel 3rd Order, Raised Cosine ($\alpha = 0.25, 0.5$ and 1 with NRZ-L data and sampled data), SRRC ($\alpha = 1$ with NRZ-L

data and sampled data)). All these simulations were performed using a non-ideal system and at passband. Power Spectral plots (Power Containment versus R_B) were generated for these different types of filters at the output of the baseband filter, SSPA and 2nd Harmonic filter (refer to [3] for more information) and were compared with the case where no baseband filtering is performed. It was shown that this baseband filtering in fact improves the frequency band Utilization Ratio. Studies were also performed to determine the filter amplitude response and ISI of these filters. The Raised Cosine filter was found to be amplitude unstable at high data transition rates therefore it was not included in Phase III.

As mentioned in the paper of Phase II, Phase III should apply the techniques (Power Containment Plots, Utilization Ratio...) described in Phase II to each of the modulation schemes identified in Phase I, i.e.,

- (a) - PCM/PM/NRZ (NRZ Data Modulated directly on RF Carrier);
- (b) - PCM/PM/Bi- ϕ (Split-Phase Data Modulated directly on RF carrier) ;
- (c) - BPSK/NRZ (NRZ Data modulated on suppressed carrier);
- (d) - BPSK/ Bi- ϕ (Split-Phase Data Modulated on suppressed RF Carrier);
- (e) - QPSK (NRZ Data Quadri-Phase Modulated RF Carrier);
- (f) - OQPSK (NRZ Data Offset QPSK Modulated on RF Carrier);
- (g) - 8PSK (NRZ Data 8-Phase Shift Keyed Modulated on RF Carrier);
- (h) - MSK (NRZ Data Minimum Shift Keyed on RF Carrier); and
- (I) - GMSK (NRZ Data Gaussian Minimum Shift Keyed on RF Carrier).

End-to-end system performance, including the ISI and the SER as function of E_b/N_0 should be determined. Therefore at the end of Phase III, the modulation techniques providing the most efficient frequency spectrum utilization should become clear.

Phase III (a) - End-to-End System Performance for PCM/PM/NRZ. Reference [4] contains the simulations performed on SPW software. The simulations were based on the PCM/PM/NRZ modulation format. The end-to-end performance was performed using non-ideal data, non-ideal system components and three baseband filter types

- (a) - Butterworth 5th Order;
- (b) - Bessel 3rd Order; and
- (c) - SRRC ($\alpha = 1$).

Again note that the Raised Cosine filters were not included in Phase III since they were discovered to be amplitude unstable at high data transition rates. The idea is to have a design utilizing the narrowest possible transmitted RF Spectrum and yet be consistent with reasonable system losses, (i.e. maximize bandwidth efficiency with acceptable ISI loss). The optimum filter is found by selecting the filter that provides the lowest Bandwidth-Time product (BT) where T is the duration of one symbol (for PCM/PM/NRZ the duration of one bit is equal to the duration of one symbol or $1/R_B$ where R_B is the bit rate) . From these simulations the following conclusions were derived for PCM/PM/NRZ modulation. The simulations show that a practical system can be built with filtering ISI losses below 0.4 dB and the total end-to-end performance system losses below 0.75 dB at $SER = 10^{-3}$. Also excellent utilization ratios are achieved based on -50 dB sideband attenuation. The following table summarizes the results for the different types of baseband spectrum filters used:

Table 1.1 - Summary of PCM/PM/NRZ Modulation Simulation

PARAMETER	BUTTERWORTH	BESSEL	SRRC
BT or α	2	2	1
ISI LOSS (dB)	0.28	0.37	0.19
TOTAL SYSTEM LOSS (dB)	0.64	0.73	0.55
UTILIZATION RATIO, ρ	8.5	7.4	8.1

As shown in this table, significant bandwidth savings (Utilization Ratio) is possible by selecting the proper baseband filter. Different modulation types will also affect the bandwidth savings. Therefore, future work will involve the same measurements as described above for the different types of modulation. It will then be possible to identify the most efficient modulation type(s) based upon the application, the system performance and the preferred frequency band. In this case, this report contains the simulations performed on an 8PSK signal being filtered (spectrum shaping) by the three filters mentioned earlier.

To complete this work, the relationship between the non-constant envelope introduced by pulse shaping the 8PSK signal and the bandwidth of the filter was to be investigated. Therefore the following question had to be answered:

*How much variation is introduced by the non-constant envelope
as the bandwidth of the filter is made smaller?*

A literature search was conducted to see if any kind of investigation had been performed with respect to an 8PSK non-constant envelope signal going through a non-linear channel (amplifier). The analysis of the non-linear distortion caused by the amplifier, more specifically for a non-constant envelope, is very complicated. Although many analyses have been published in the literature, none has been entirely applicable here. The research conducted in [5] shows how a bandlimited spectrum filter and the shape of the frequency pulse affect the error probability of a frequency shift keying (FSK) signal with differential phase detection. The investigation was conducted using a Butterworth filter (order = 4 and 3 for the transmitter and receiver respectively) and the frequency shaping pulse is raised cosine or rectangular. This investigation was then performed for a FSK signal as opposed to a PSK signal. In [6], an experiment more related to the one described in this thesis was performed. This paper investigates the effect of filtering PSK, FSK and MSK signals in a theoretical way. A Butterworth Filter (4th Order) is used and the ISI and BER are measured.

However, this paper does not consider an amplifier in their study. In [7], the performance of a satellite channel using a software package (developed at Telecom Research Laboratories) was measured.

The results of this experiment (using the software) were then validated by experiments on a hardware simulator. It was shown that both results from the software and actual measurements are very similar (minor differences due to the ideal demodulator used in the software package). Even though the satellite channel in this paper uses spectrum shaping filters and non-linearities (TWT Amplifier), there was no experiment conducted to measure the effect of non-constant envelope through this non-linear system.

Although other similar studies were performed on pulse shaping, non-constant envelope and non-linear channels, none of them involved the measurement of the effect of a non-constant envelope signal (8PSK for this case) through a non-linear channel (SSPA). The following thesis gives the results on simulations performed on an 8PSK bandlimited signal (bandlimited with the three filters enumerated earlier) going through a non-linear amplifier. The effect of the non-constant envelope through this channel will be demonstrated.

Chapter 2

THEORY

This section will briefly describe some of the concepts that were used for the simulations performed on the SPW simulation software (from COMDISCO) that is installed on a SUN Sparc Station 10 and HP Model 715/100 Unix Station in the Center for Space Telemetry and Telecommunications Systems in the Klipsch School of Electrical and Computer Engineering Department at NMSU.

2.1 Eight (8) Level Phase Shift Keying (8PSK)

8 level PSK is a multi-phase signaling technique meaning that 8 modulation phases (with constant amplitude) are produced at the transmitter output. Figure 2.1 shows how an 8-phase signal can be generated from a serial binary input stream using a 3 bit Serial-to-Parallel Converter (SPC). In this case, since the data rate is R_B bits/sec, then the Symbol Rate (baud), R_S , of the multi-phase signal will be

$$R_S = R_B/\lambda \text{ where } \lambda = \log_2 8 = 3 \text{ thus } R_S = R_B/3 \text{ (symbols/sec).}$$

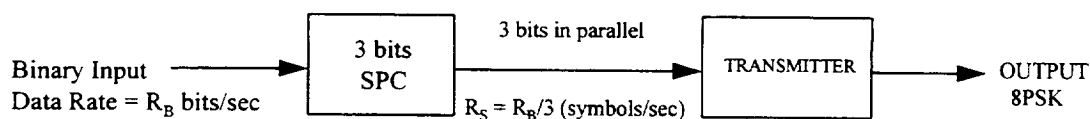


Figure 2.1 - 8PSK Digital Transmission System

A plot of the complex envelope of the 8PSK signal, $g(t) = A_c e^{j\theta(t)}$, is shown in Figure 2.2. This figure is usually referred as the 8PSK constellation.

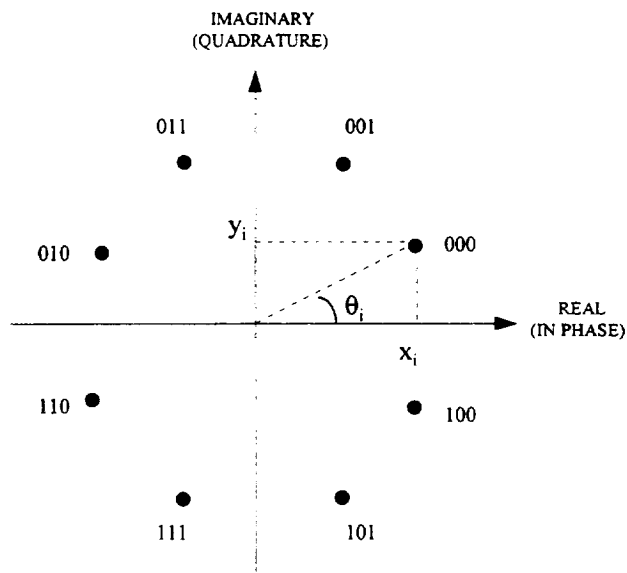


Figure 2.2 - 8PSK Signal Constellation

As shown in Figure 2.2, each point on the constellation corresponds to one of the 8 multi-phase values (or symbols) which corresponds to one of the phases that θ is allowed to have. In the above figure each point corresponds to a symbol where the PSK phases are

$$\theta_1 = 22.5^\circ \text{ for symbol } 000 \text{ (decision region: } 0^\circ \text{ to } 45^\circ)$$

$$\theta_2 = 67.5^\circ \text{ for symbol } 001 \text{ (decision region: } 45^\circ \text{ to } 90^\circ)$$

$$\theta_3 = 112.5^\circ \text{ for symbol } 011 \text{ (decision region: } 90^\circ \text{ to } 135^\circ)$$

$$\theta_4 = 157.5^\circ \text{ for symbol } 010 \text{ (decision region: } 135^\circ \text{ to } 180^\circ)$$

$$\theta_5 = 202.5^\circ \text{ for symbol } 110 \text{ (decision region: } 180^\circ \text{ to } 225^\circ)$$

$$\theta_6 = 247.5^\circ \text{ for symbol } 111 \text{ (decision region: } 225^\circ \text{ to } 270^\circ)$$

$$\theta_7 = 292.5^\circ \text{ for symbol } 101 \text{ (decision region: } 270^\circ \text{ to } 315^\circ)$$

$$\theta_8 = 337.5^\circ \text{ for symbol } 100 \text{ (decision region: } 315^\circ \text{ to } 360^\circ)$$

Another way of expressing 8PSK is by using two orthogonal carriers modulated by x and y components of the complex envelope (no phase modulator is used in this case) thus

$$g(t) = A_c e^{j\theta(t)} = x(t) + jy(t)$$

where $x_i = A_c \cos \theta_i$ and $y_i = A_c \sin \theta_i$, where $i = 1$ to 8 for 8PSK as shown in Figure 2.2.

For the bandpass physical signal, the waveform can then be represented by

$$v(t) = \text{Re}\{g(t)e^{j\omega_c t}\} \text{ where } \omega_c = 2\pi f_c, f_c \text{ is the carrier frequency in hertz (Hz).}$$

For the simulations performed on SPW, the 8PSK modulator in the library was slightly modified to be able to implement the non-ideal data. By changing some of the constants, this 8PSK modulator can become a BPSK or QPSK modulator. The complex envelope form of 8-PSK was used to develop this baseband modulator. Figure 2.3 shows the block diagram used in SPW. The “Control Block” in the figure connects one of its two inputs (x1 or x2) to the output depending on the state of the logical “control” input. When the control input is 0, x1 is used; when the control input is 1, x2 is used.

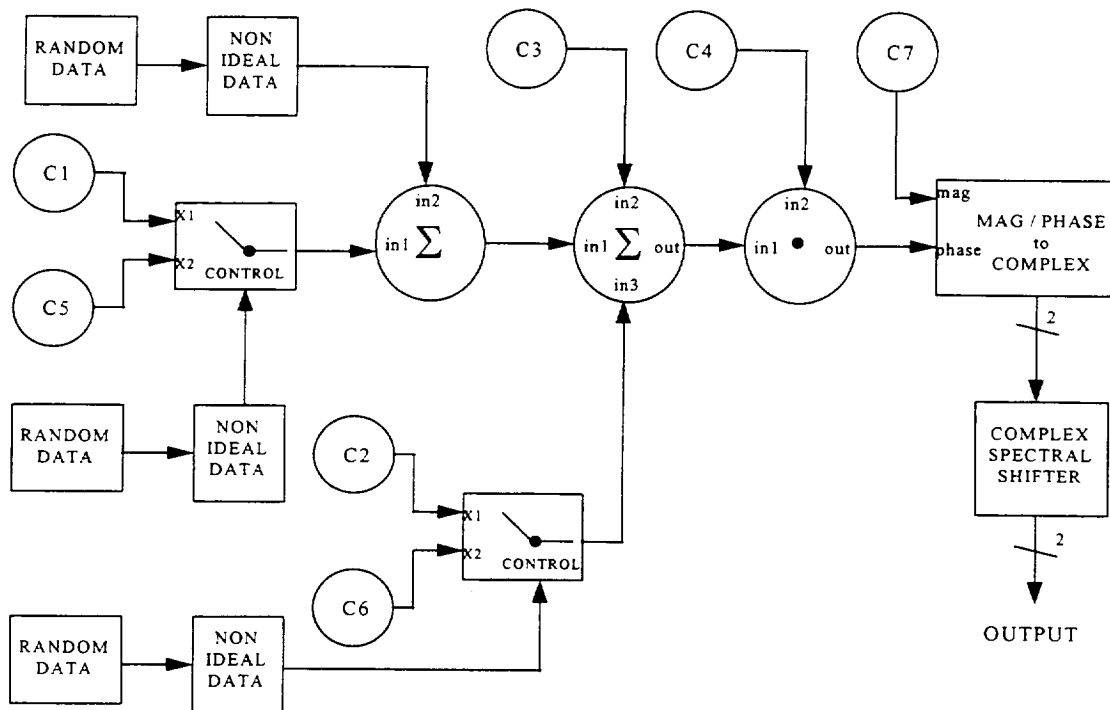


Figure 2.3 - Block Diagram for the BPSK, QPSK and 8PSK Modulator on SPW

The values of C_i are given in Table 2.1 and vary depending on the desired modulator (BPSK, QPSK or 8-PSK)

Table 2.1 - Values of C_i for the BPSK, QPSK, 8PSK Simulation Model

MODULATION TYPE	VALUES OF CONSTANT " C_i "						
	C1	C2	C3	C4	C5	C6	C7
BPSK	0.0	0.0	0.0	$2\pi/2$	0.0	0.0	$\sqrt{2}$
QPSK	2.0	0.0	0.5	$2\pi/4$	0.0	0.0	$\sqrt{2}$
8PSK	2.0	4.0	0.5	$2\pi/8$	0.0	0.0	$\sqrt{2}$

2.2 NRZ-L Ideal And Non-Ideal Data

The binary input or data format that is used throughout these simulations is referred as NRZ-L which stands for Non-Return-to-Zero Logic level. NRZ-L has the logic 0 or 1 represented by the appropriate voltage level for the duration of the bit period. The following convention will be used: a logic 0 will be represented by a $-A$ Volt (V) signal level and a logic 1 will be represented by a logic $+A$ V signal level (which is the convention used in these simulations). Figure 2.4 shows this digital data format.

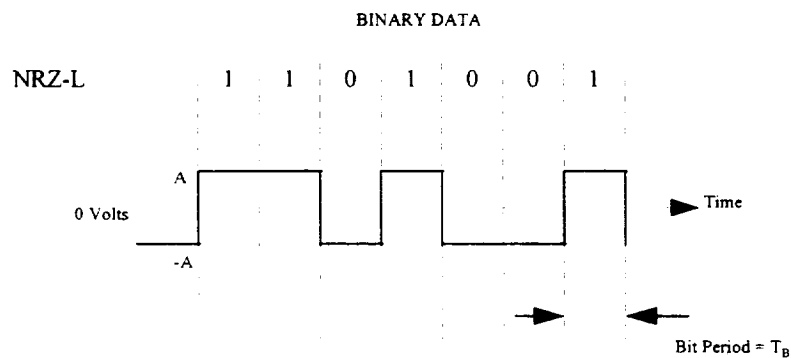


Figure 2.4 - NRZ-L Digital Data Format

All the simulations were done using ideal and non-ideal data. Ideal data are defined as having a perfect symmetry, i.e., the duration of a digit one (1) is equal to the time duration of a digit zero (0) and it also has a perfect data balance, i.e., the probability of getting a zero is equal to the probability of getting a 1 ($\Pr(0) = \Pr(1) = 0.5$ or 50%). For non-ideal data these two conditions, data symmetry and data balance, are not respected. The CCSDS limits are $\pm 2\%$ for data asymmetry and a data imbalance of 0.45 (probability of getting a 1 vs probability of a 0) as mentioned in [3]. The data asymmetry can be increased by the stray capacitance in spacecraft wiring and data imbalance can be produced by long runs of 1s and 0s in the random data. If non-ideal data are present (i.e., the mean value or expected value, m_a , of the signal is not equal to 0), the Power Spectrum Density (PSD) of the digital signal will then consist not only of a continuous spectrum that depends on the pulse-shape spectrum of the signal data (rectangular pulse for NRZ-L), but will also contain spectral lines (delta functions) spaced at approximately the harmonics of the symbol rate, R_s . The PSD equation of a baseband digital signal for the case of uncorrelated data, derived in [8] shows these results:

$$PSD_x(f) = \sigma_a^2 \cdot R_s \cdot |F(f)|^2 + (m_a \cdot R_s)^2 \cdot \sum_{n=-\infty}^{\infty} |F(nR_s)|^2 \delta(f - nR_s)$$

Continuous spectrum

Discrete Spectrum

where m_a is the mean of the data

σ_a^2 is the variance of the data

$R_s = 1/T_s =$ Baud or Symbol Rate

$F(f)$ is the pulse shape spectrum (sinc^2 shape for NRZ-L data).

2.3 Intersymbol Interference (ISI)

ISI can be introduced into a system by improperly filtering pulses as they pass through a communication system. As it is known in communications, the absolute BW of flat-top multilevel pulses is infinity, therefore since the channel is always bandlimited, the pulse waveforms passing through it will be dispersed or spread. This spreading will exceed the time duration of the pulse or symbol and will overlap with the next symbol. This interference is called ISI which will cause system degradation or higher error rates. Figure 2.5 shows two examples of ISI.

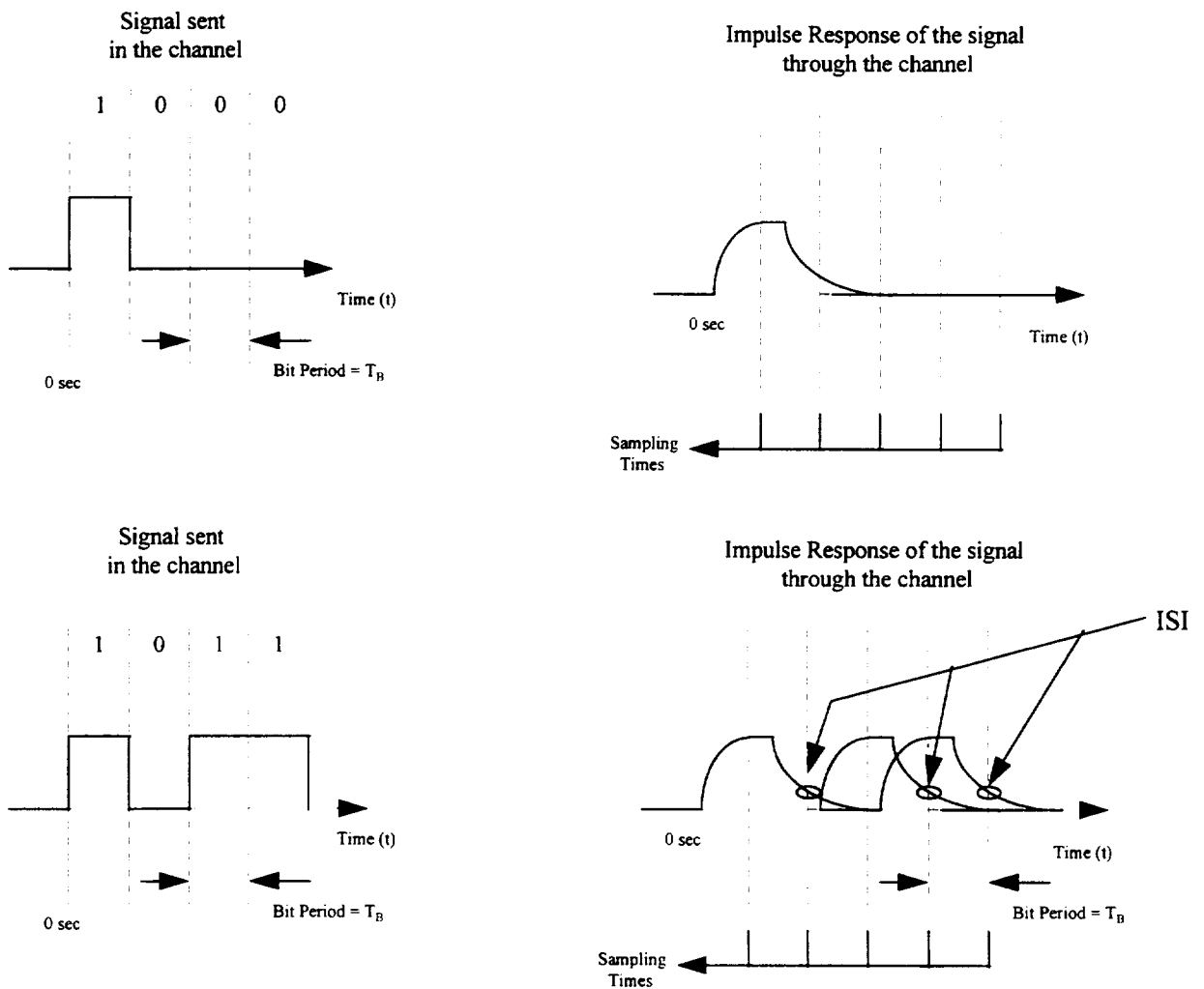


Figure 2.5 - Intersymbol Interference (ISI)

In 1928, Nyquist discovered three different methods to eliminate ISI by having rounded tops pulses instead of flat tops [8]. The BW can then be restricted without introducing ISI. One of these methods includes the utilization of Raised Cosine - Rolloff Filtering that will be described below.

2.4 Spectrum Shaping And Filters

Spectrum Shaping is a technique that allows the signal energy to be concentrated near the carrier and therefore reduce the power contained in the sidelobes (baseband and RF). This is done by filtering the signal. Such a technique can also yield a significant savings in the required BW. Nonetheless, this type of filtering causes loss of energy (if filtering is done at the RF level) and ISI or pulse distortion (if the BW limitation is too restrictive since the pulses are not rectangular any more). These losses can be reduced if the receiver compensates for the distortions (i.e., if a matched filter is used). Thus baseband filtering is effective in limiting spectrum width.

The filters that were used for the simulations are Butterworth, Bessel and Raised Cosine. They will be described in the following paragraphs.

2.4.1 Butterworth Filters

The Butterworth family of filters is known to have a “maximally” flat response in the passband region [9]. In other words the amplitude response in the passband region comes very close to a perfectly flat response (at a given order). This is why Butterworth Filters are commonly used. Figure 2.6 shows the amplitude response for different orders of Butterworth filters. Note again how flat the amplitude is in the passband region. All orders of this filter pass through the 3 dB cut-off point. Also as the order of the filter increases, the sharpness of the slope after the 3dB cutoff point also increases.

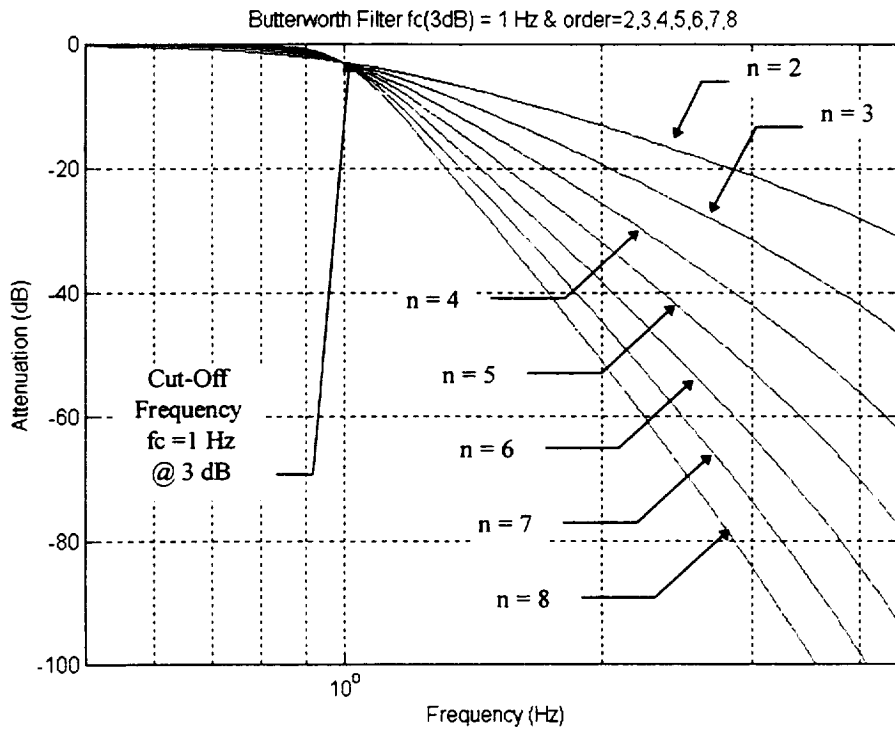


Figure 2.6 - Amplitude Response of Various Orders of Butterworth Filters

2.4.2 Bessel Filters

The main characteristic of the Bessel family of filters is that they have an approximately linear phase in the passband region. This linear phase will have a tendency to prevent dispersion of the signal and therefore can be good for digital pulses. Figure 2.7 shows the amplitude response of various orders of Bessel Filters. Note that the amplitude is not as flat in the passband region as for the Butterworth filter. Also the transition from the passband to the stopband region is not as rapid as for the Butterworth Filters for the various orders of filters.

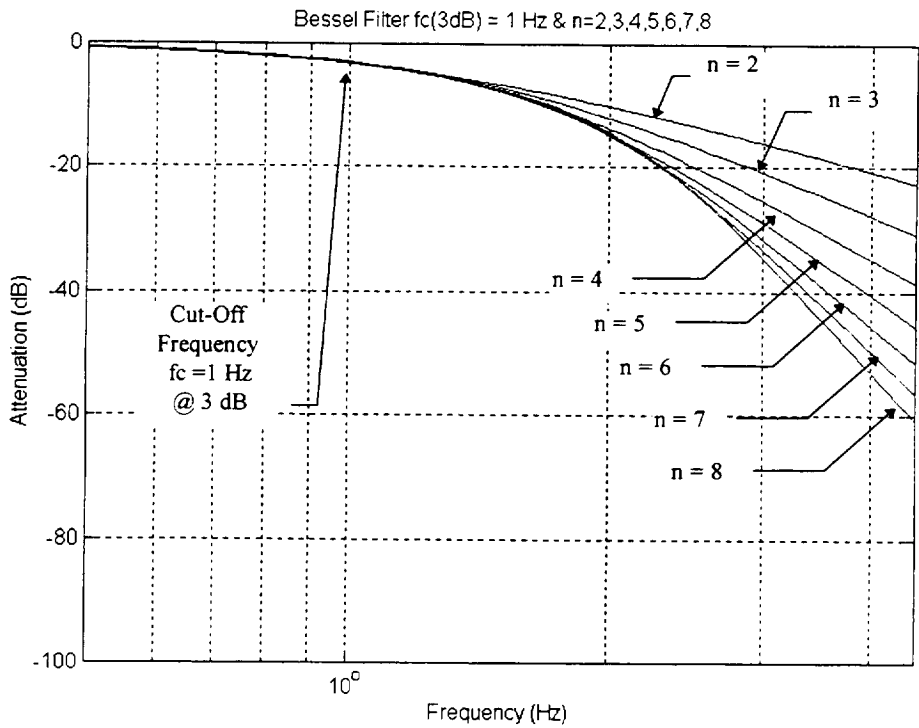


Figure 2.7 - Amplitude Response of Various Orders of Bessel Filters

For the simulations performed in this paper, a 5th Order Butterworth Filter and a 3rd Order Bessel Filter were selected. These orders of filters are the same as those selected for comparison during Phase III of this study.

2.4.3 Raised Cosine Filters

As mentioned earlier, if the Raised Cosine filters are used the ISI will be eliminated in a linear channel. The idea behind the Raised Cosine Filter is that the time signal goes through zero at adjacent sampling points therefore eliminating the interference of other symbols. Also it has the important property of having an envelope that decays fast enough so that clock phase jitter at the sampling times do not introduce to much ISI.

The transfer function of the Raised Cosine Filter is

$$X(f) = \begin{cases} T, & 0 \leq |f| < \frac{(1-\alpha)}{2T} \\ \frac{T}{2} \left(1 - \sin \left[\frac{(2\pi|f|T - \pi)}{2\alpha} \right] \right), & \frac{(1-\alpha)}{2T} \leq |f| \leq \frac{(1+\alpha)}{2T} \\ 0, & |f| > \frac{(1+\alpha)}{2T} \end{cases}$$

where the zeros will occur at $t=nT$ (T is the sampling interval) and α is the rolloff factor or the excess bandwidth over the Nyquist Band Filter which can be varied from 0 to 1. The rolloff factor, α , determines the bandwidth of a Raised Cosine Filter. For $\alpha = 0$, the filter's transfer function approximates that of a "Brick Wall" filter with bandwidth $1/(2T)$ while an $\alpha=1$ yields a sinusoidal transfer function having a total width of $1/T$. Figure 2.8 shows the frequency response of the Raised Cosine Function with different rolloff factors ($\alpha = 0, 0.25, 0.5$ and 1) and $T=1$ seconds.

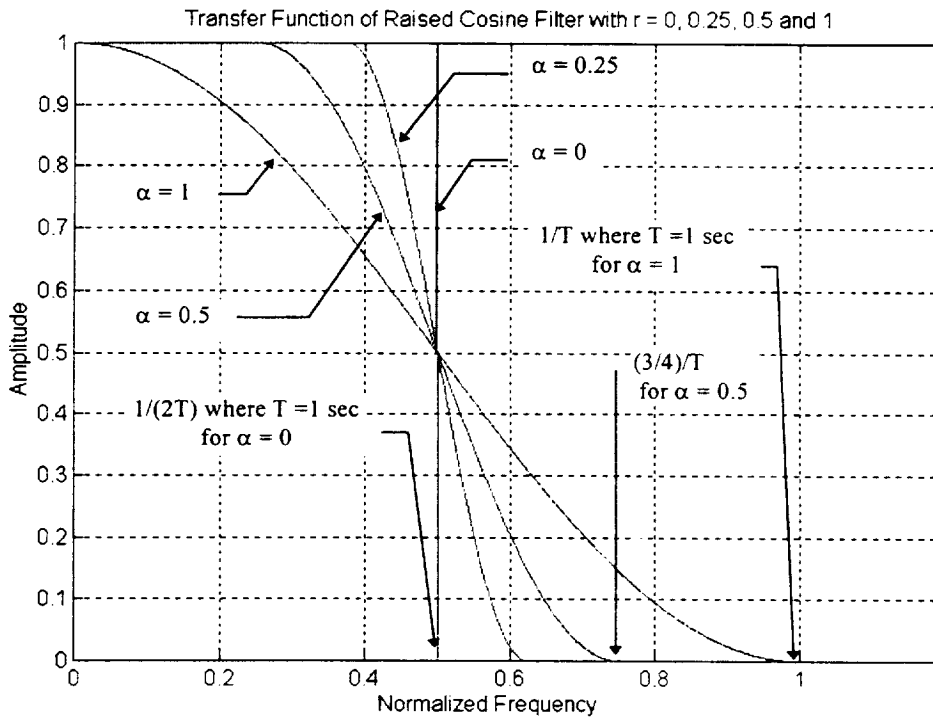


Figure 2.8 - Frequency Response: Raised Cosine Characteristics with Different α

Figure 2.9 gives the time domain response for different rolloff factors.

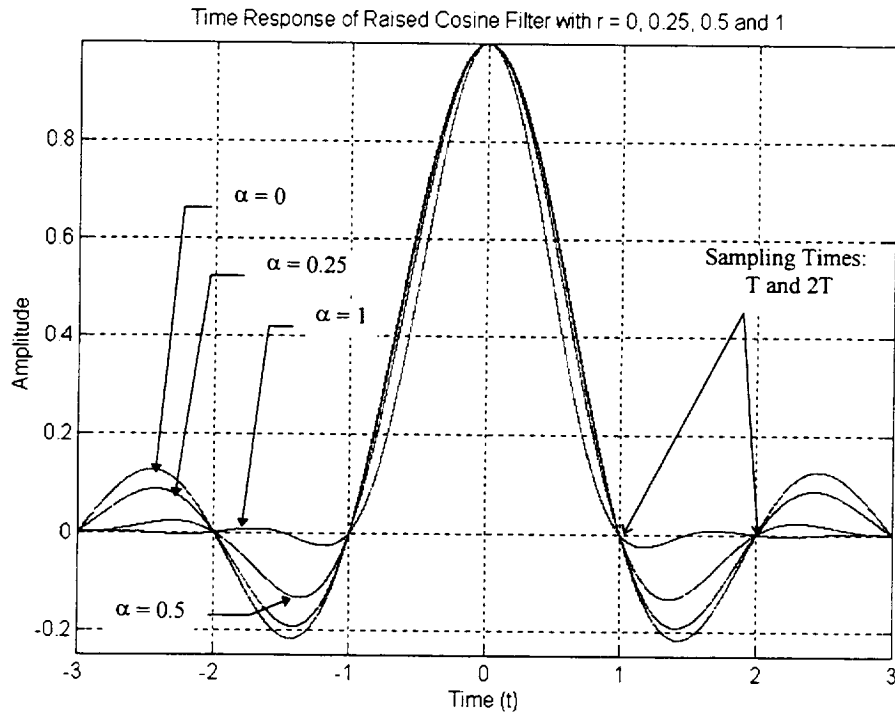


Figure 2.9 - Time Response of Raised Cosine Filters for Different α

From Figure 2.9, it can be seen that if the symbols are sampled at the nulls of the sinc function then the symbol interference from the previous and next symbols will not exist. This is why the Raised Cosine filters are used since it is a class of filter that satisfies Nyquist's first criterion (see [8]). To produce a zero ISI channel the impulse response shown above has to be created. This can be done by utilizing a Square Root Raised Cosine filter in both the transmitter and the receiver. The overall filtering characteristics of the channel will be a Nyquist Channel or a Raised Cosine Filter:

$$X(f) = T(f) \cdot H(f) \cdot R(f) = \begin{cases} \frac{1}{T}, & 0 \leq |f| \leq T \\ 0, & \text{elsewhere} \end{cases}$$

where $T(f)$ is the frequency response of the transmitter;
 $H(f)$ is the frequency response of the channel;
 $R(f)$ is the frequency response of the receiver; and
 $X(f)$ is the overall frequency response of the system.

If the channel has a large bandwidth compared to the transmitter and receiver frequency response then

$$X(f) = T(f) \cdot R(f) = RC(f)$$

where $RC(f)$ is the frequency response of the Raised Cosine Filter. Thus

$$T(f) = R(f) = \sqrt{RC(f)} = SRRC(f)$$

where $SRRC(f)$ is a Square Root Raised Cosine Filter for both the transmitter and the receiver which maximizes the data transmission efficiency (both the transmitter and receiver are matched). Therefore, the channel will be a Nyquist Channel (or Raised Cosine Function) with zero ISI for optimum data detection. This does not apply for a non-linear channel as will be shown when a non-linear device such as a Solid State Power Amplifier (SSPA) is present in the channel.

As stated in [3]: "Raised Cosine Filters were selected for evaluation because the linearity of their phase-frequency relationship should help to eliminate the ringing found in the Butterworth filters at the cut-off frequency. Their comparatively narrow bandwidth, combined with a smooth response, should provide a signal which concentrates most of the data sideband energy near the main lobe significantly attenuating the sidebands. Such filters are commonly employed to pack a multiplicity of signals in a confined frequency band."

2.5 Solid State Power Amplifier (SSPA)

Amplifiers are classified into two main categories: linear and non-linear circuits. Devices such as Traveling-Wave Tubes (TWT) and Solid State Power Amplifier's (SSPA) can be linear amplifiers when operated well below the saturation level. If this drive level is increased, the efficiency, i.e., RF output/Direct Current (DC) input is improved, but the amplifier then becomes a non-linear device. Therefore constant envelope signals such as PSK are preferred so that the distortion due to the non-linear amplifier will be minimized. In this case, the power amplifier will be used in its non-linear region to maximize the signal power. Figure 2.10 shows the SSPA, European Space Agency (ESA) 10 Watts, Magnitude Characteristics Curve.

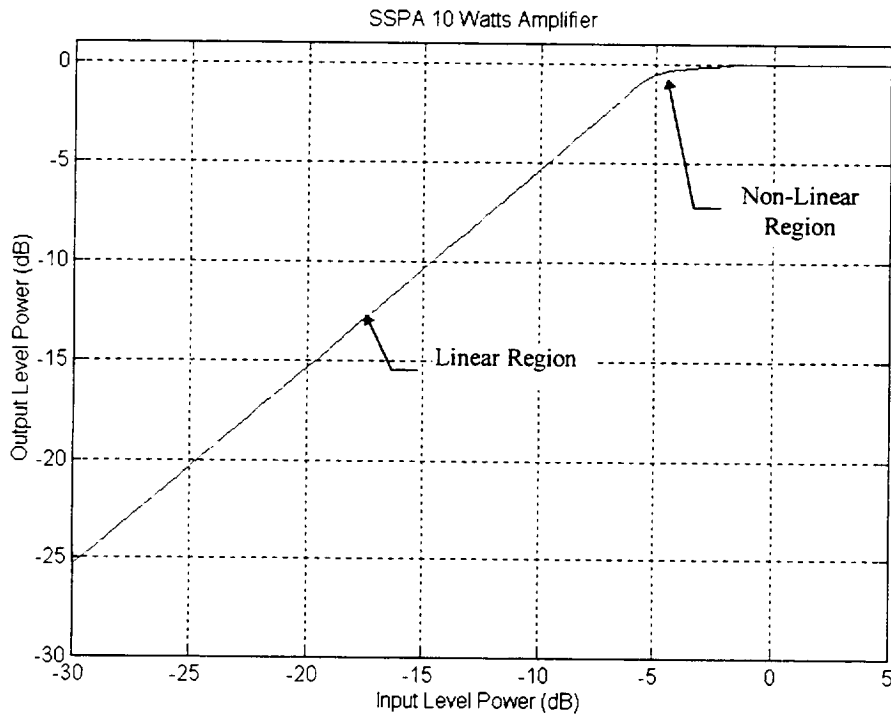


Figure 2.10 - SSPA, ESA 10 Watts, Magnitude Characteristic Curve

The non-linearities that occur in the nonlinear region of this amplifier will cause non-linear distortion and Amplitude Modulation-to-Phase Modulation (AM-to-PM) and AM-to-AM conversion effects (linear channels are channels without AM-AM and AM-PM conversions). As mentioned in [8], the analysis of these non-linearities are very complicated.

In this study the non-linear channel will be considered (the power amplifier will be operated in its saturation region). Even if SRRC filters are used for the transmitter and receiver, ISI-free sample points no longer exist because of the distortion introduced by the system. This will be shown and discussed in Chapter 3 - 8PSK Simulations. Thus, the objective of this study is not only to find a bandwidth efficient communications system which can increase frequency band-utilization, but also, to identify an implementation that can be realized.

NMSU used the SSPA model for their simulation which is based upon specifications provided by the European Space Agency (ESA) for their 10 Watts, solid state, S-band power amplifier. This power amplifier was selected since all the simulations performed in Phases II and III (refer to [3], [4]) were done using this amplifier.

2.6 Additive White Gaussian Noise (AWGN)

In the channel being simulated, white gaussian noise was added to the signal. In AWGN, the term additive means that the noise is added to the signal. Also by Gaussian it is meant that the random process representing the noise, $n(t)$, is Gaussian and has a Power Spectral Density (PSD) of

$$PSD_n(f) = \begin{cases} N_0/2, & |f| \leq B \\ 0, & otherwise \end{cases}$$

where B is a positive constant which represents the BW and the noise is bandlimited as long as B is finite. If $B \rightarrow \infty$, the noise is completely white, i.e., all the frequencies are present.

Gaussian processes give a good approximation of naturally occurring behaviors. Addition of the noise, $n(t)$, will give $r(t) = s(t) + n(t)$ where

- $n(t)$ is the AWGN with variance $= \sigma_n^2 = N_0/2$ and mean $= m_n = 0$;
- $s(t)$ is the signal; and
- $r(t)$ is the resulting signal with the noise added.

This resulting signal (random process) will have a Gaussian distribution with mean $= s(t_0)$ where t_0 is the sampling time and a variance $\sigma_n^2 = N_0/2$. Figure 2.11, shows a block diagram of how the noise was added to the initial signal on SPW. Figure A.4 in Appendix A contains a more detailed diagram of the circuit used in SPW. As shown in Figure 2.11, the variance (and therefore the standard deviation) is calculated by using the average complex power of the signal and E_s/N_0 (dB) which was entered by the user. The output of this block gives the input signal added with a Gaussian Noise.

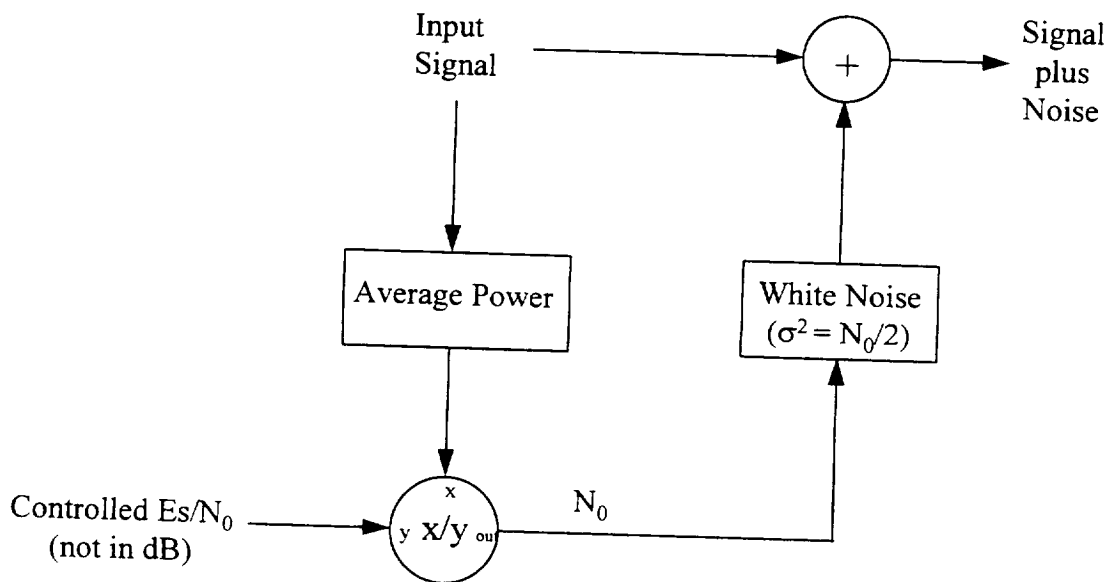


Figure 2.11 - Block Diagram for the AWGN

In our simulations, a variation of the integrate-and-dump filter was used. This was possible since the digital signaling format has a rectangular bit shape. For the integrate-and-dump filter, the digital input signal plus the noise is integrated over one symbol period T and the output of the integrator is dumped at the end of the symbol period which is the value that is required. Therefore for proper operation of this optimum filter, an external clocking signal called bit sync is required.

Chapter 3

8PSK SIMULATIONS

3.1 Simulation Procedures

To simulate the non linear satellite link, a Signal Processing Worksystem (SPW) which is a COMDISCO simulation software was utilized on a SUN Sparc Station 10 and HP Model 715/100 Unix Station. The following diagram shows the different blocks that were simulated on the workstation.

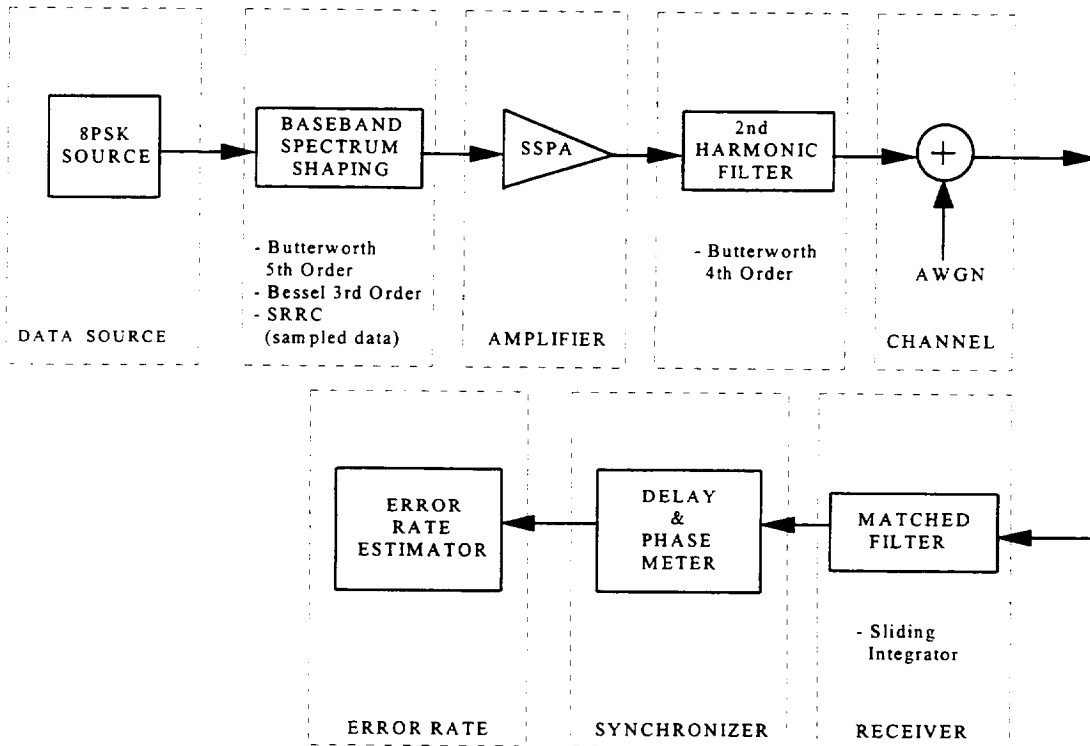


Figure 3.1 - Simulation Block Diagram

First a Data Source or Modulator was used to produce the 8PSK signal. The data source also contained a block that could produce data asymmetry on the data. All simulations were produced at baseband using the complex envelope signal representation. The results do not vary if the simulations are done in baseband or passband. The advantage of going to baseband is the computer execution time, i.e., it takes longer to simulate at passband since the sampling frequency must be at least twice the Nyquist rate. The next block after the modulator is the baseband spectrum shaping filter. The three types of filters that were used for these simulations were 5th Order Butterworth, 3rd Order Bessel, and finally Square Root Raised Cosine (SRRC) with Sampled Data and Roll-Off factors of 0.25, 0.5 and 1.

The next blocks include the SSPA, a bandlimiting filter and the noise (channel). Simulations were performed using the SSPA at the saturation level to maximize the power. Simulations at saturation were then followed by simulations with the SSPA backed off by -10 dB. This amplifier was followed by a 2nd Harmonic filter (4th Order Butterworth with a bandwidth of $\pm 20R_s$) which reduces the interference between different channels. This bandlimiting filter is followed by the variable AWGN (variable to be able to control the E_s/N_0 values).

These blocks were followed by the Receiver, Symbol Synchronizer and finally the Error Estimator. A matched filter (sliding integrator) was used as the receiver for the Butterworth and Bessel Filters. The matched filter was matched to the NRZ-L baseband data. For the SRRC, the receiver was also a SRRC to minimize the ISI. The SRRC will minimize the ISI and the matched filter is an optimum filter which optimizes the Signal-to-Noise ratio (SNR). The synchronizer that was used consisted in a Delay and Phase Meter that would correlate, as best as it could, the initial data with the data that went through the channel.

After these two signals went through the phase and delay meter, the initial data were delayed to be synchronized with the distorted data (the delay between the initial and distorted data were caused by the filters). After the data were synchronized (the best correlation was found), an Error Rate Estimator was used to measure the differences in symbols and calculate the Symbol Error Rate (SER).

When the Power Containments were needed a Spectrum Analyzer from SPW was placed after the 2nd Harmonic Filter.

The following variables and systems were implemented in SPW for the simulations:

(a) - SPW Simulation Variables:

- i - Bit rate = 1 bps ($R_s = \text{symbol rate} = (1/3) \text{ symbols/s}$ for 8PSK)
- ii - Sample Rate = $f_s = 16 \text{ samples/sec}$
- iii - Data: NRZ-L
- iv - Carrier Frequency = 0Hz (Baseband Simulations)

(b) - Transmitting System:

i - Data Generator: Ideal and Non-Ideal Data:

- data asymmetry = 2%
- data imbalance = 0.45

ii - Baseband filters (do not include resistive and reactive losses):

- Butterworth 5th Order (BT = 1,2,3);
- Bessel 3rd Order (BT=1,2,3)
- SRRC ($\alpha = 0.25, 0.5$ and 1) with 256 taps

Note - BT represents the product of the bandwidth (3 dB single-sided) with the symbol time; thus if BT = 1 it means that

$$B = (1/3) \text{ since } T = (1/R_s) = (1/(1/3)) = 3.$$

- Also 256 taps were chosen because we will have:

$(256 \text{ taps}/16 \text{ samples/sec})/2 = 8$ symbols interfering with the one being sampled. It was noted that using more taps on the Infinite Impulse Response (IIR) filter did not affect the output.

iii - Power Amplifier based on:

- European Space Agency (ESA) 10-Watt

Solid State Power Amplifier (SSPA);

- 4th Order Butterworth (cutoff at $\pm 20 R_s$) - 2nd Harmonic Filter

- protects user's of other bands.

(c) - Receiving System:

i - Matched Filter: Sliding Integrator

ii - Delay and Phase Meter (synchronization); and

iii - Error Rate Estimator.

The following simulations were performed with the system described above

(a) - Power Containment and Spurious Emissions;

(b) - End-to-End System Performance : Symbol Error Rate (SER); and

(c) - Non-Constant Envelope Simulations (a variation of the circuit shown in Figure 3.1 was utilized).

3.2 Power Containment and Spurious Emissions Simulations

Table 3.1, summarizes the simulations performed for 8PSK (the numbers in parenthesis, (1) etc. indicate individual runs that were performed):

Table 3.1 - Power Spectrum Simulations

SIMULATION NUMBER	MODULATION TYPE	FILTER LOCATION	FILTER TYPE	FILTER CHAR.	DATA CHAR.	SPECTRUM PLOTS	PLOTS LOCATION
1	8PSK	none	none	none	ideal NRZ-L	(1) - $\pm 5 R_B$ (2) - $\pm 50R_B$ (3) - $\pm 150 R_B$	(1) - Modulator Output (2) - Output of the SSPA (3) - 2 nd Harmonic Filter Output
2	8PSK	none	none	none	non-ideal NRZ-L	(1) - $\pm 5 R_B$ (2) - $\pm 50R_B$ (3) - $\pm 150 R_B$	(1) - Modulator Output (2) - Output of the SSPA (3) - 2 nd Harmonic Filter Output
3	8PSK	baseband	Butterworth	5th Order (BT=1)	ideal NRZ-L	(1) - $\pm 5 R_B$ (2) - $\pm 50R_B$	(1) - Spectrum Filter Output (2) - Output of the SSPA (3) - 2 nd Harmonic Filter Output
4	8PSK	baseband	Butterworth	5th Order (BT=1)	non-ideal NRZ-L	(1) - $\pm 5 R_B$ (2) - $\pm 50R_B$	(1) - Spectrum Filter Output (2) - Output of the SSPA (3) - 2 nd Harmonic Filter Output
5	8PSK	baseband	Bessel	3rd Order (BT=1)	ideal NRZ-L	(1) - $\pm 5 R_B$ (2) - $\pm 50R_B$	(1) - Spectrum Filter Output (2) - Output of the SSPA (3) - 2 nd Harmonic Filter Output
6	8PSK	baseband	Bessel	3rd Order (BT=1)	non-ideal NRZ-L	(1) - $\pm 5 R_B$ (2) - $\pm 50R_B$	(1) - Spectrum Filter Output (2) - Output of the SSPA (3) - 2 nd Harmonic Filter Output
7	8PSK	baseband	SRRC	$\alpha = 0.25$	ideal NRZ-L	(1) - $\pm 5 R_B$ (2) - $\pm 8 R_B$	(1) - Spectrum Filter Output (2) - Output of the SSPA (3) - 2 nd Harmonic Filter Output
8	8PSK	baseband	SRRC	$\alpha = 0.25$	non-ideal NRZ-L	(1) - $\pm 5 R_B$ (2) - $\pm 8R_B$	(1) - Spectrum Filter Output (2) - Output of the SSPA (3) - 2 nd Harmonic Filter Output
9	8PSK	baseband	SRRC	$\alpha = 0.5$	ideal NRZ-L	(1) - $\pm 5 R_B$ (2) - $\pm 8 R_B$	(1) - Spectrum Filter Output (2) - Output of the SSPA (3) - 2 nd Harmonic Filter Output
10	8PSK	baseband	SRRC	$\alpha = 0.5$	non-ideal NRZ-L	(1) - $\pm 5 R_B$ (2) - $\pm 8 R_B$	(1) - Spectrum Filter Output (2) - Output of the SSPA (3) - 2 nd Harmonic Filter Output
11	8PSK	baseband	SRRC	$\alpha = 1.0$	ideal NRZ-L	(1) - $\pm 5 R_B$ (2) - $\pm 8 R_B$	(1) - Spectrum Filter Output (2) - Output of the SSPA (3) - 2 nd Harmonic Filter Output
12	8PSK	baseband	SRRC	$\alpha = 1.0$	non-ideal NRZ-L	(1) - $\pm 5 R_B$ (2) - $\pm 8 R_B$	(1) - Spectrum Filter Output (2) - Output of the SSPA (3) - 2 nd Harmonic Filter Output

SIMULATION (1) - UNFILTERED BASEBAND IDEAL DATA

Figure 3.2a shows the power spectrum of the NRZ-L Ideal data using 8PSK. The abscissa is the frequency with respect to the bit rate R_B thus the first lobe for 8PSK ends at $\pm R_B/3$ ($R_B/3$ represents the baud rate or symbol rate R_S) which was to be expected. The following table shows the comparison of the theoretical and simulated amplitudes for 8PSK using SPW with Ideal data. The values in the simulated amplitude column were taken from Figure 3.2a by moving the cursor on the peak of each lobe at the frequencies indicated; the accuracy of the readings of the simulated amplitude was approximated to be around ± 1.5 dB. It is to be noted that the results of the simulations are very close to theory. The following formula was used to calculate the theoretical power spectrum [8]:

$$PSD(f) = \left(\frac{\sin(\pi f \lambda T_b)}{\pi f \lambda T_b} \right)^2$$

where $M=2^\lambda$ is the number of points in the signal constellation (in this case $\lambda= 3$ for 8PSK) and the bit rate is $R_B = 1/T_B$ (1 bit/sec in this case).

Table 3.2 - Comparison of Theoretical and Simulated Amplitudes for 8PSK using SPW (Ideal Data)

OFFSET FROM CENTER FREQUENCY ($\pm R_B$)	THEORETICAL AMPLITUDE (dB)	SIMULATED AMPLITUDE (dB)
0	0	0
0.5	-13.46	-13.5
0.8333	-17.90	-18.8
1.16667	-20.82	-21.3
1.5	-23.01	-23.9
1.8333	-24.75	-25.6
2.1667	-26.20	-27.1
2.5	-27.44	-28.3
2.8333	-28.53	-29.2
3.1667	-29.50	-30.9
3.5	-30.37	-31.0
3.8333	-31.16	-31.9
4.1667	-31.88	-32.5
4.5	-32.55	-33.2
4.8333	-33.17	-33.7
5.1667	-33.75	-34.5

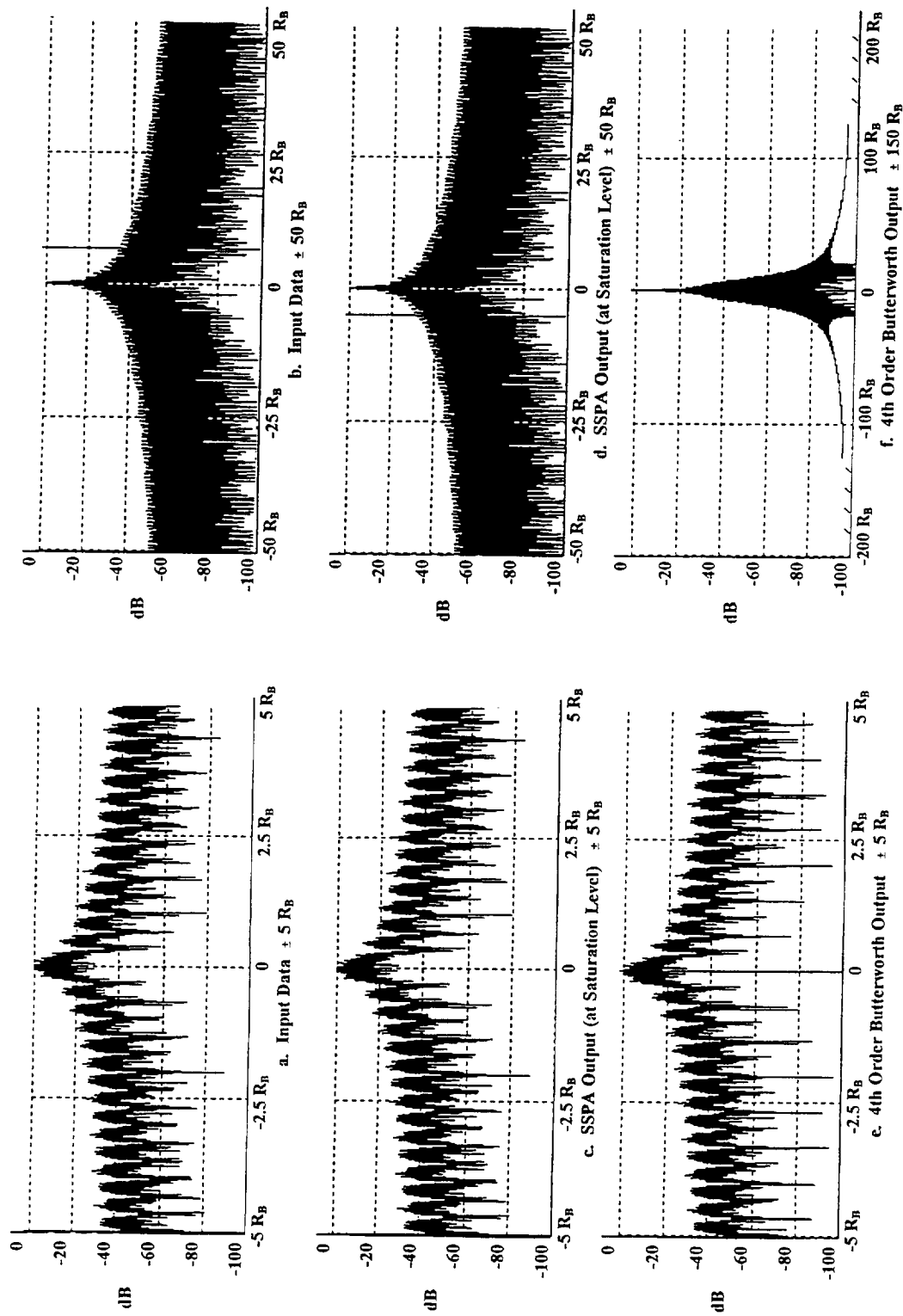


Figure 3.2 - Power Spectra of Unfiltered 8PSK Baseband Ideal Data using SSPA at Saturation Level

These data and Figure 3.2a will be used as reference for the next figures. To produce Figure 3.2a, a sampling frequency, f_s , of 250 samples/sec was chosen. The sampling frequency was chosen much higher than the Nyquist rate (2 times the highest frequency) to be able to have a spectrum going from $-125R_B$ to $+125R_B$. Also 300 000 samples (to have 1200 symbols, i.e., 1 symbol/sec*300 000 samples/ 250 samples/sec) were taken therefore an FFT of $N=262144$ (power of 2) was utilized. Hence the frequency resolution, f_1 , [10] of the plots is given by:

$$\text{frequency resolution} = f_1 = \frac{f_s}{N} = \frac{250}{262144} = 9.537 \times 10^{-4} \text{ Hz}$$

Figure 3.2b shows the same results as Figure 3.2a but the frequency abscissa was set to $\pm 50 R_B$. Figure 3.2c shows the output spectrum of the SSPA with ideal data. The SSPA was used at its saturation level (0 dB). Simulations were later done with the SSPA set to 10 dB away from saturation (10 dB Backoff). The output of the SSPA is identical to its input due to the constant envelope of the input signal. Figure 3.2d is the same as Figure 3.2c but at $\pm 50 R_B$ instead of at $\pm 5 R_B$. Finally Figure 3.2e shows the output of the 4th Order Butterworth ($\pm 20 R_B$) 2nd Harmonic filter which has no effect in the region of $\pm 5 R_B$. This filter is used to reduce unwanted emissions on other bands. Figure 3.2f is the same as Figure 3.2e but $\pm 150 R_B$ was used in the abscissa to see the effect on the other bands.

SIMULATION (2) - UNFILTERED BASEBAND NON-IDEAL DATA

For this simulation, the data symmetry was set to 2% and the probability of zero = 0.45. Figure 3.3a shows the unfiltered baseband data (Non-Ideal Data) at the output of the 8PSK modulator. The presence of spurs at approximately $f = n \cdot R_s$ (where $n=0,1,2..$) are due to the probability of zero which is not equiprobable, i.e., equal to 0.5, and to the data asymmetry. The spurs are more evident in Figure 3.3b.

Figure 3.3c and 3.3d show the output of the SSPA (at saturation level) and as mentioned earlier there is no effect or difference with the input data since it is a constant envelope signal (no spectrum shaping filter present) going through the amplifier. Figure 3.3e and 3.3f show the output of the 4th Order Butterworth filter at $\pm 5R_B$ and $\pm 150R_B$.

Simulations (1) and (2) will be used as references for the spectrum shaping filter simulations.

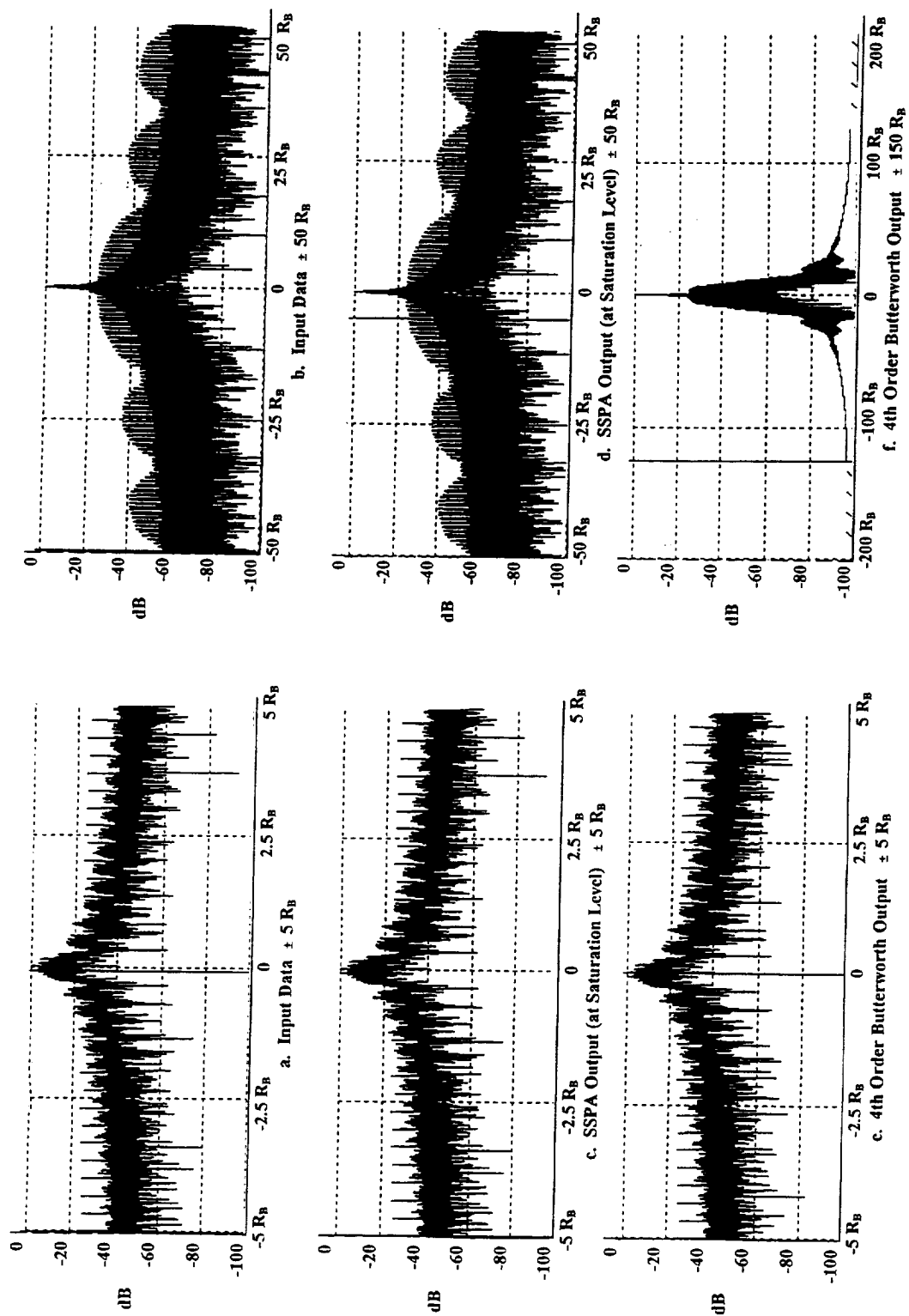


Figure 3.3 - Power Spectra of Unfiltered 8PSK Baseband Non-Ideal Data using SSPA at Saturation Level

SIMULATION (3) AND (4) - 5TH ORDER BUTTERWORTH FILTERED BASEBAND DATA
(IDEAL AND NON-IDEAL DATA)

For this simulation, the sampling frequency (f_s) was set to 250 samples/sec, the symbol rate (R_s) = (1/3) symbols/sec, the number of samples set to 300 000 and the number of FFT points (N) = 524 288. The BT product was set to 1 thus the bandwidth $B = R_s$ and $T = 1/R_s$ which is the symbol interval. For the non-ideal data, the data asymmetry was again set to 2% and the probability of zero was set to 0.45.

Figure 3.4a and 3.5a show the result of the baseband data going through the 5th Order Butterworth Filter for ideal and non-ideal data, respectively. Note that at approximately $\pm 2R_s$ the filter attenuates the data sidebands by approximately 40 dB. Figures 3.4c and 3.5c show the output of the SSPA for the ideal and non-ideal data. Note that due to the non-constant envelope of the data (since some spectrum shaping was performed), the output of the SSPA is quite different from Figure 3.2c and 3.3c. In fact, it seems like the SSPA is trying to recreate the sidelobes that were attenuated by the filter. Also, the spurious emissions encountered in Figure 3.3d for the non-ideal case are not present or are fairly attenuated. In [3] for PCM/PM/NRZ it was reported that the Butterworth Baseband Filter introduced large in-band spurious emissions which does not seem to appear here. Comparing Figures 3.4d and 3.5d seems to demonstrate that there is no difference at the output of the SSPA for ideal and non-ideal data using the Butterworth Filter, compared to the plots with no filter and non-ideal data in Figures 3.2d and 3.3d where the spurs are obvious. Figures 3.4e/3.4f and 3.5e/3.5f show the output of the 4th order Butterworth with ideal and non-ideal data.

If the amount of attenuation from baseband filtering is examined by comparing with Figures 3.2c/3.2d and 3.3c/3.3d with 3.4c/3.4d and 3.5c/3.5d (Butterworth Filter), it can be seen that at approximately $\pm 0.5R_B$, the Butterworth filter attenuates the sidebands by approximately 23 dB. At approximately $\pm 2.5 R_B$, the attenuation is around 50dB below the peak of the main lobe, placing the absolute level of the sidebands under 50 dB after this point.

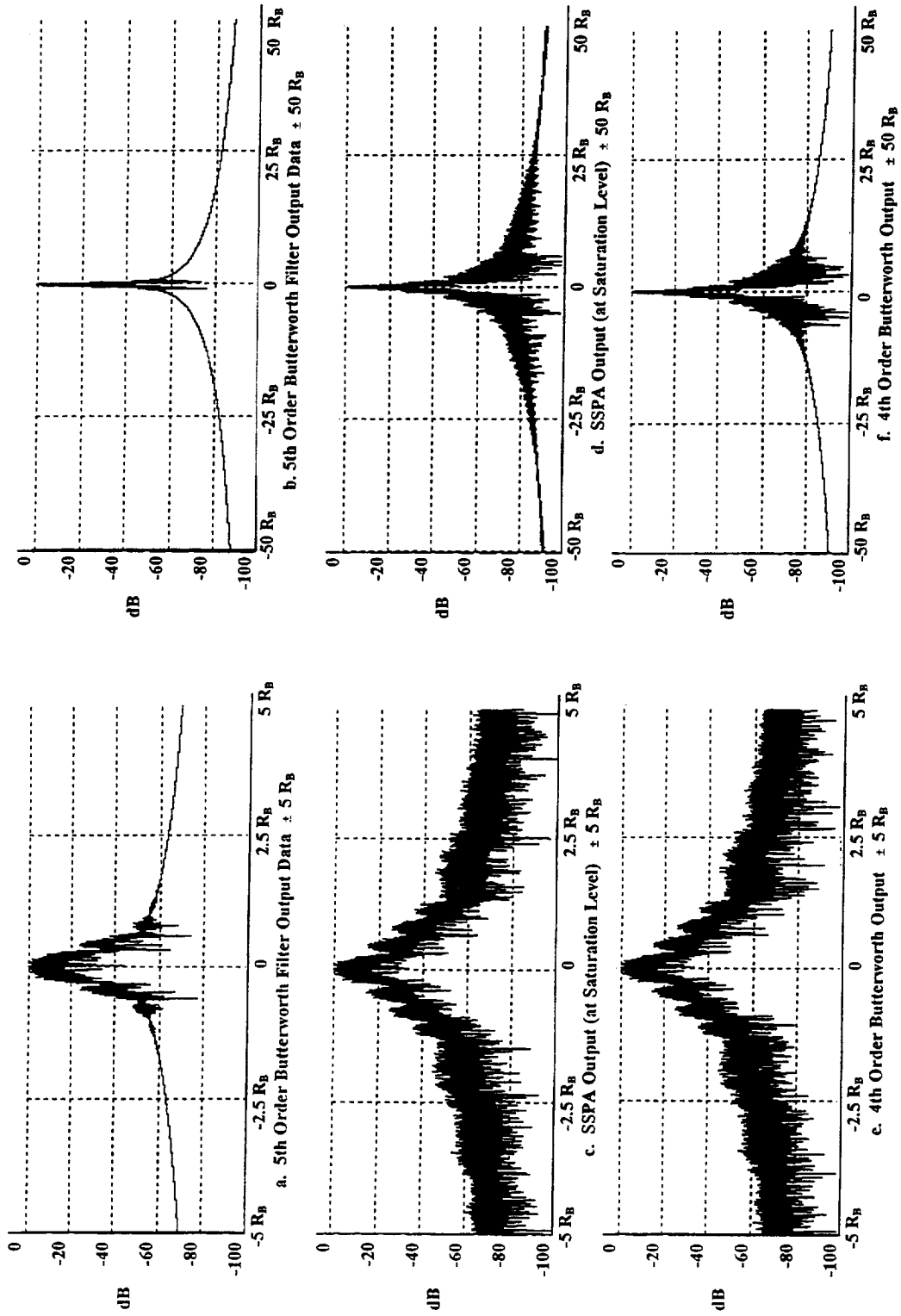


Figure 3.4 - Power Spectra of Filtered 8PSK Baseband Ideal Data using 5th Order Butterworth Filter ($BT=1$) & SSPA at Saturation Level

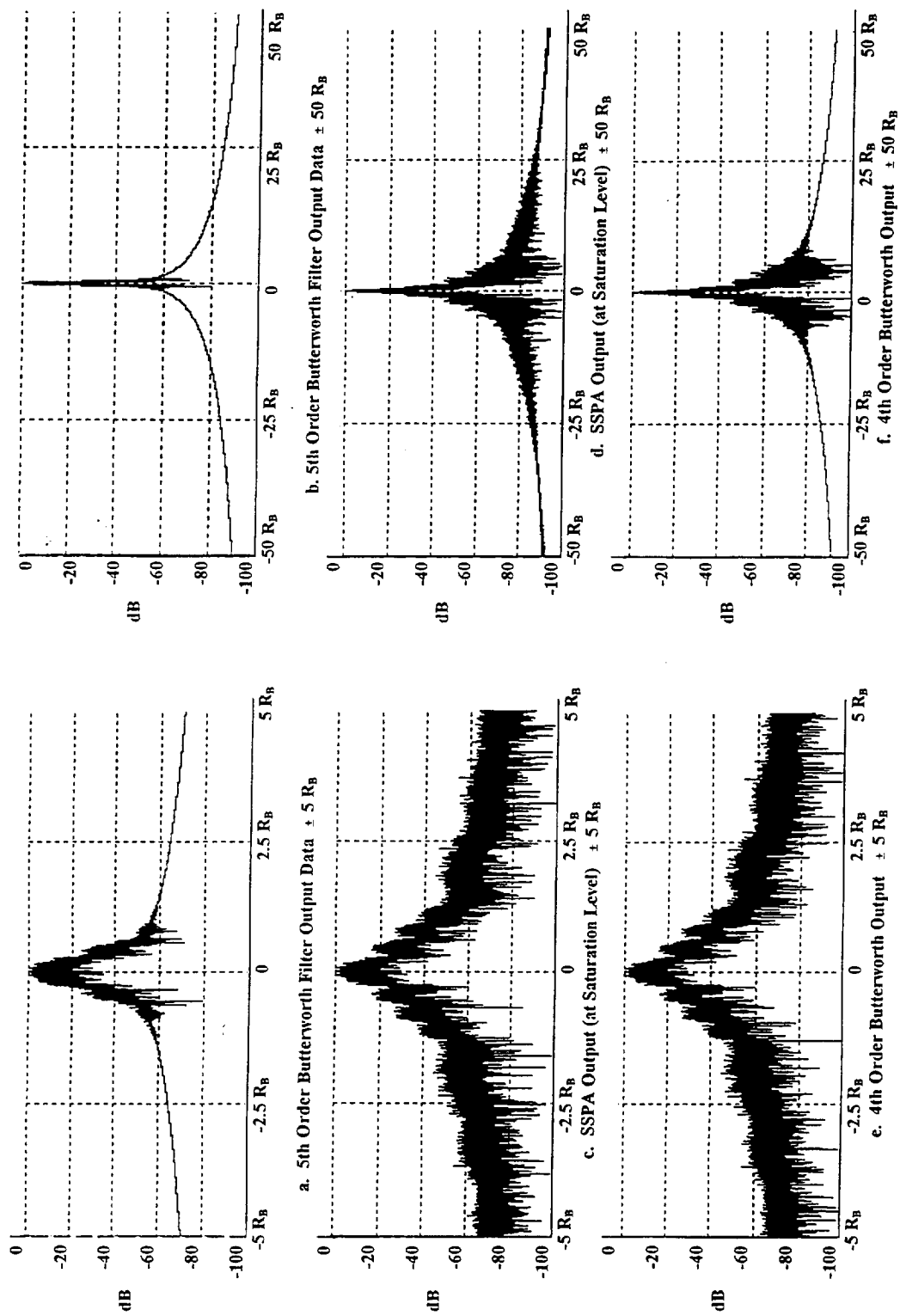


Figure 3.5 - Power Spectra of Filtered 8PSK Baseband Non-Ideal Data using 5th Order Butterworth Filter ($BT=1$) & SSPA at Saturation Level

Tables 3.3 and 3.4, at the end of this Chapter, summarize the attenuation spectrum levels relative to the first data sideband for Ideal and Non-Ideal data. This information about sideband attenuation will be important when discussing the utilization ratio (ρ) and band utilization in a latter section.

SIMULATION (5) AND (6) - 3rd ORDER BESSEL FILTERED BASEBAND DATA

(IDEAL AND NON-IDEAL DATA)

Again these two simulations used the same parameters as those discussed for the 5th Order Butterworth filter. In the case of the Bessel filter the effect of in-band spurious emissions are more present and more evident than for the Butterworth filter as shown in Figure 3.7a compared to Figure 3.6a. The output of the SSPA (Figures 3.6c/3.6d and 3.7c/3.7d for ideal and non-ideal data respectively) show some small spurs emissions caused by the non-ideal data.

With respect to the sideband attenuation, the values of attenuation for the Bessel (3rd Order) are comparable to the 5th Order Butterworth filter (see Tables 3.3 and 3.4).

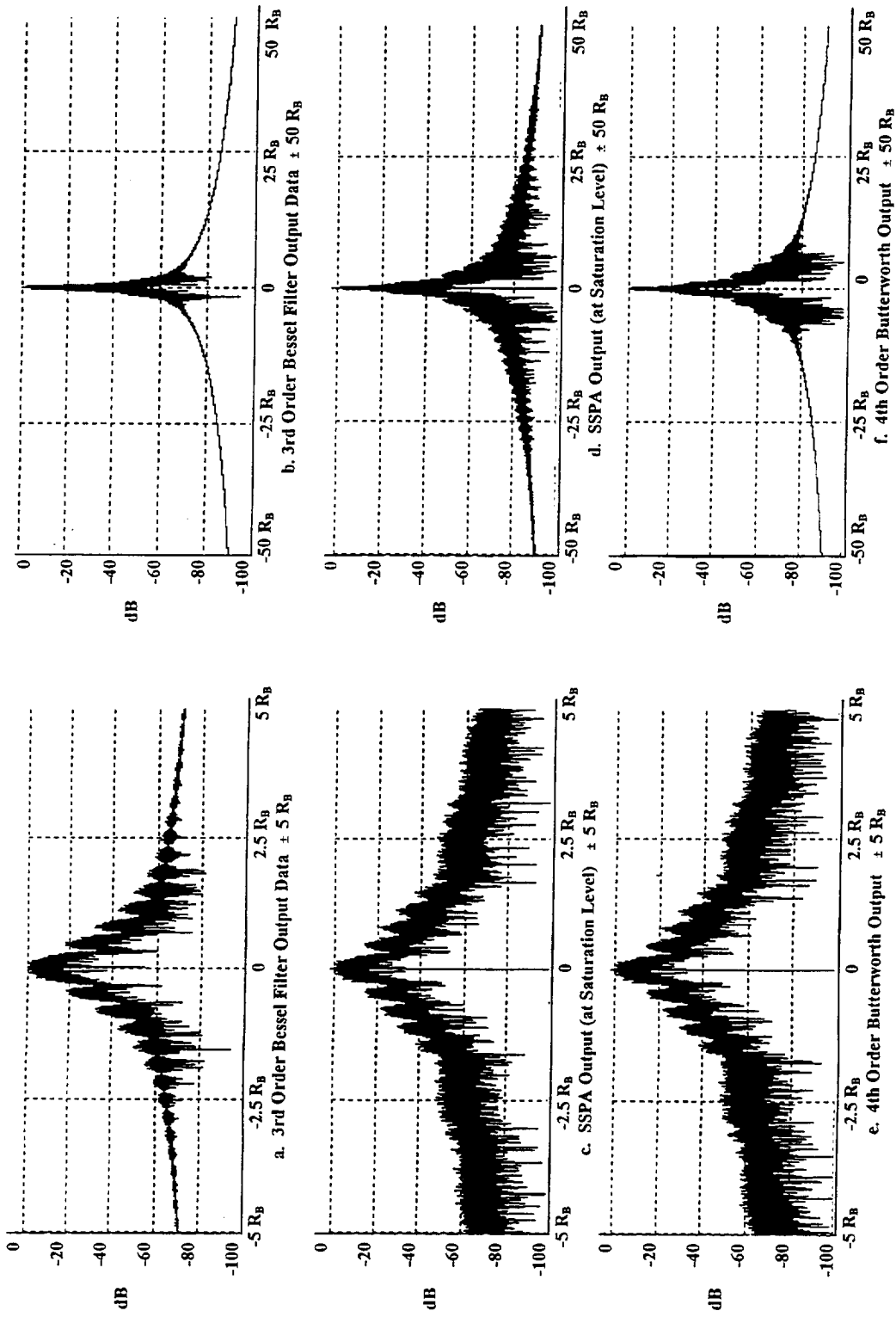


Figure 3.6 - Power Spectra of Filtered 8PSK Baseband Ideal Data using 3rd Order Bessel Filter ($BT=1$) & SSPA at Saturation Level

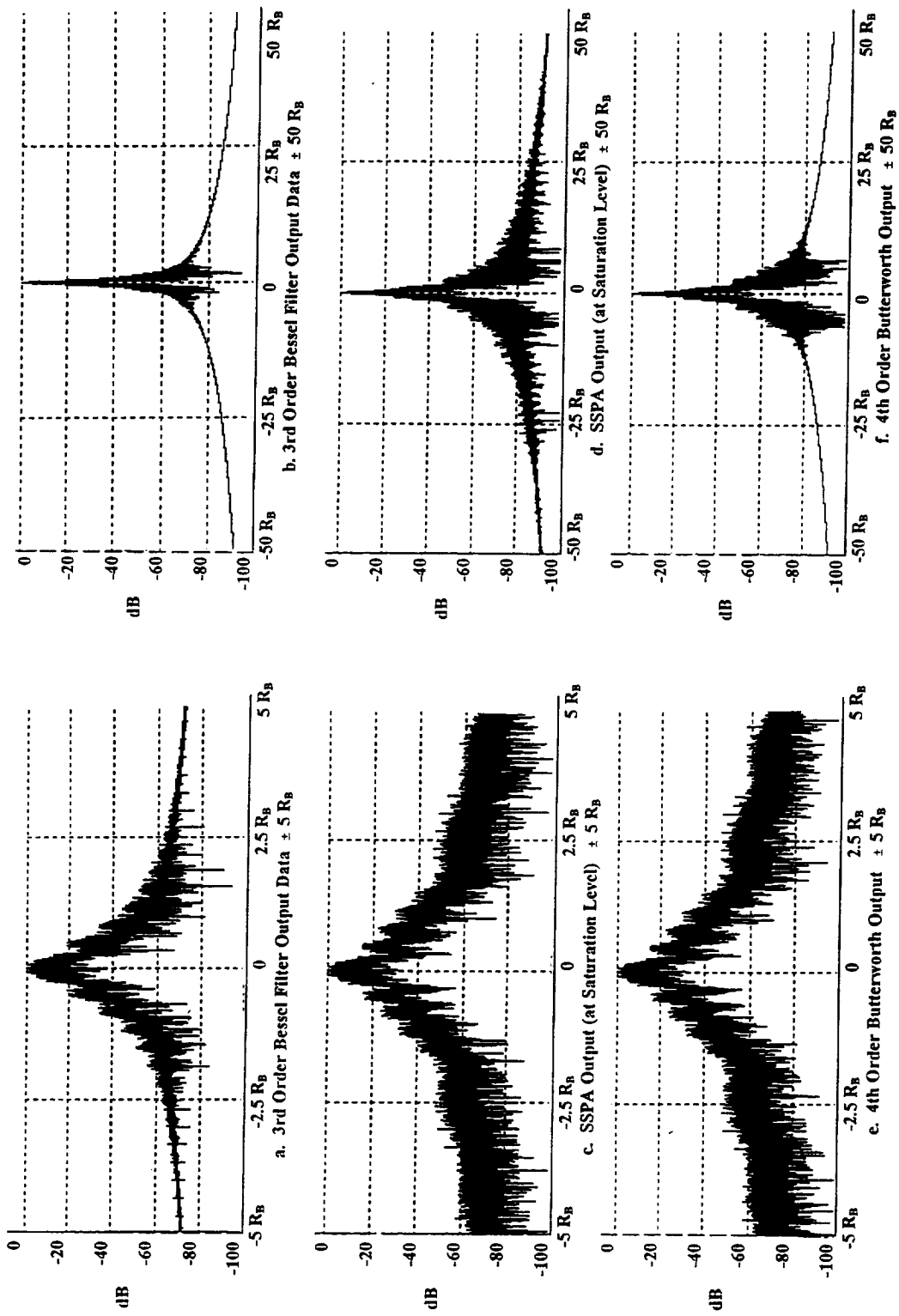


Figure 3.7 - Power Spectra of Filtered 8PSK Baseband Non-Ideal Data using 3rd Order Bessel Filter (BT=1) & SSPA at Saturation Level

SIMULATION (7) TO (12) - SRRC FILTER WITH IDEAL AND NON-IDEAL DATA

The SRRC block in SPW was used as the transmitter and receiver to simulate the SRRC filter as a spectrum filter. To simulate a SRRC transmitter filter non-sampled data were used by cascading the SRRC with a 1/sinc filter (function already implemented in SPW). For the receiving SRRC no 1/sinc filter was cascaded. Three different rolloff factors were used during the simulation to see the difference in bandwidth. The rolloff factors that were used were $\alpha = 0.25, 0.5$ and 1 . In the SRRC filter block, the tap length or FIR length was set to 256 which takes into account 8 intersymbol interferences from neighboring pulses since the sampling frequency, f_s , was set to 16 samples/sec:

$$\frac{256 \text{ taps}}{2 \cdot (f_s)} = 8 \text{ samples interfering before and after.}$$

It is to be noted that the sampling frequency was changed or lowered from 250 samples/sec to 16 samples/sec. Nothing is gained by oversampling (only higher frequencies are seen in the graphs). By having a high f_s , simulations take more time to terminate.

Therefore, the following parameters were used for the simulations performed with the SRRC filters:

- f_s = sampling frequency = 16 samples/sec (gives the same results as using 250 samples/sec and it is faster)
- R_s = symbol rate = (1/3) symbols/sec;
- FFT Points = 16384;
- # samples = 20K; and
- Tap length (FIR length) = 256.

Also for data asymmetry a 2% value was used with a probability of zero equal to 0.45.

Thus in this section, spectra for SRRC with a 1/sinc filter in cascade at the transmitter are shown. The SRRC filters have advantages and disadvantages with respect to Butterworth and Bessel filters which can only be demonstrated by comparing the several types. Thus, to make the comparison, power spectra using several different SRRC filters must be examined.

Square Root Raised Cosine Filter ($\alpha = 0.25$).

Comparing Figures 3.8a and 3.9a of a SRRC filter with a roll-off factor of $\alpha = 0.25$ with Figures 3.4a and 3.5a for Butterworth and Figures 3.6a and 3.7a for Bessel Filters, it is immediately noted that the SRRC filters offers a significant advantage over both of the Butterworth and Bessel filters (BT=1 for both these filters). The spectrum is narrower, better defined and cleaner than the spectra for other filter types. On the other hand, the attenuation is less than that for the Butterworth or Bessel filters at high R_B ($\approx \pm 20 R_B$) as indicated in Tables 3.3 and 3.4. In-band spurious emissions are absent, even for non-ideal data. This is the narrowest bandwidth SRRC filter that is considered in this study.

Outputs from the power amplifier (see Figures 3.8b/3.8c and 3.9b/3.9c for ideal and non-ideal data respectively) shows that the nonlinearity (and non constant-envelope signal going in) in the SSPA causes an increase in amplitude in the 1 to 4 R_B region. Finally Figures 3.8d/3.8e and 3.9d/3.9e shows the output of the 4th Order Butterworth Filter. Note how the attenuation remains fairly constant around $-7R_B$ with a value of approximately -68 dB.

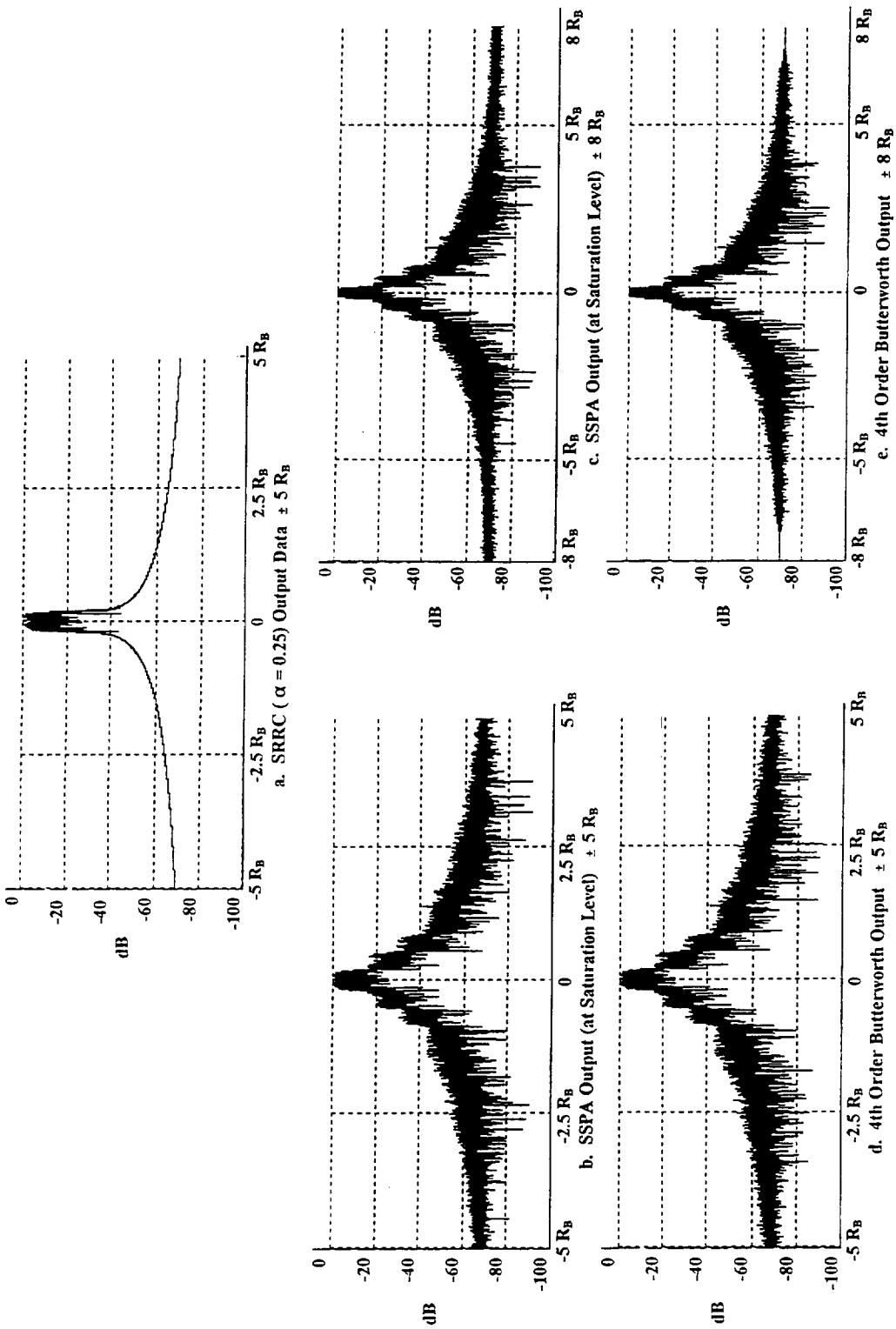


Figure 3.8 - Power Spectra of Filtered 8PSK Baseband Ideal Data using SRRC ($\alpha = 0.25$) Filter & SSPA at Saturation Level

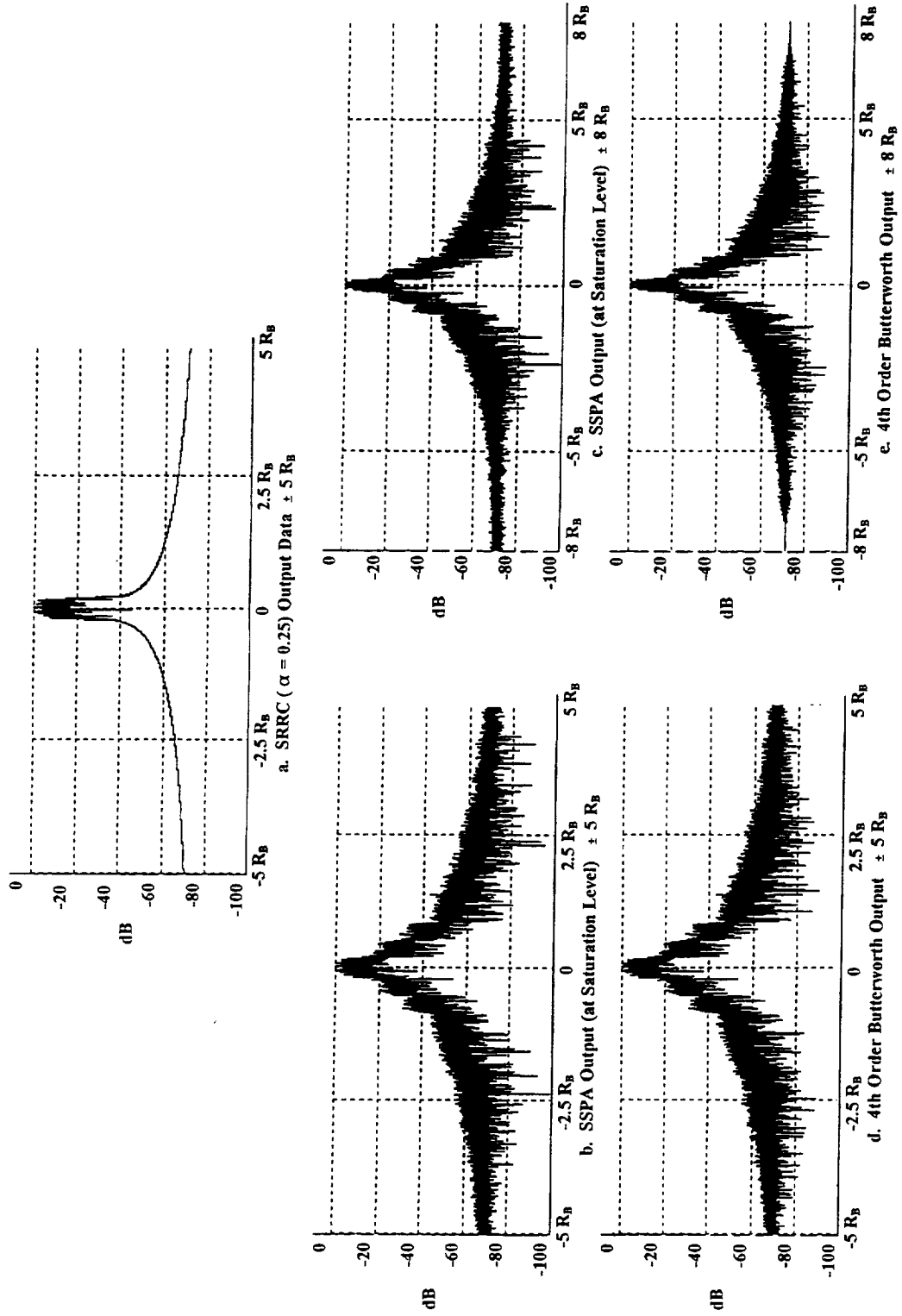


Figure 3.9 - Power Spectra of Filtered 8PSK Baseband Non-Ideal Data using SRRC ($\alpha = 0.25$) Filter & SSPA at Saturation Level

Square Root Raised Cosine Filter ($\alpha = 0.5$)

Similar power spectrum plots are found for the case of $\alpha = 0.5$ (Figures 3.10a and 3.11a) compared to Figures 3.8a and 3.9a. The bandwidth is slightly wider for this case ($\alpha = 0.5$). Nonetheless as with SRRC ($\alpha = 0.25$), the transmitted power spectrum (Figures 3.10e or 3.11e for ideal and non-ideal data respectively) is smooth and the absence of in-band spurious emissions is obvious, even for non-ideal data. But again, the attenuation produced by the Butterworth or Bessel Filter is much superior at higher frequencies than the SRRC (refer to Tables 3.3 and 3.4). Therefore since there appears to be no significant difference in the spectra between the SRRC with $\alpha = 0.25$ and $\alpha = 0.5$, the selection must depend upon other factors such as ISI, implementation complexity, etc.

Square Root Raised Cosine Filter ($\alpha = 1$)

A SRRC filter with an $\alpha = 1$ has a larger bandwidth than filters with smaller values of α , therefore the baseband data spectrum using ideal and non-ideal data (Figures 3.12a and 3.13a) are wider (than for $\alpha = 0.25$ and $\alpha = 0.5$). Also, it is to be noted in Figures 3.12b/3.12c and 3.13b/3.13c, the higher order sidebands (2nd, 3rd, .. lobes) are more visible in contrast to the other SRRC filters.

Nonetheless, again at the power amplifier's output (Figures 3.12b/3.12c or 3.13b/3.13c for ideal and non-ideal data respectively), the spectrum is characterized by a smooth roll-off with no-in band spurious emissions evident. Due to this filter's wider bandwidth, the attenuation is slightly less than that for filters with smaller values of α especially with the non-ideal data (refer to Tables 3.3 and 3.4).

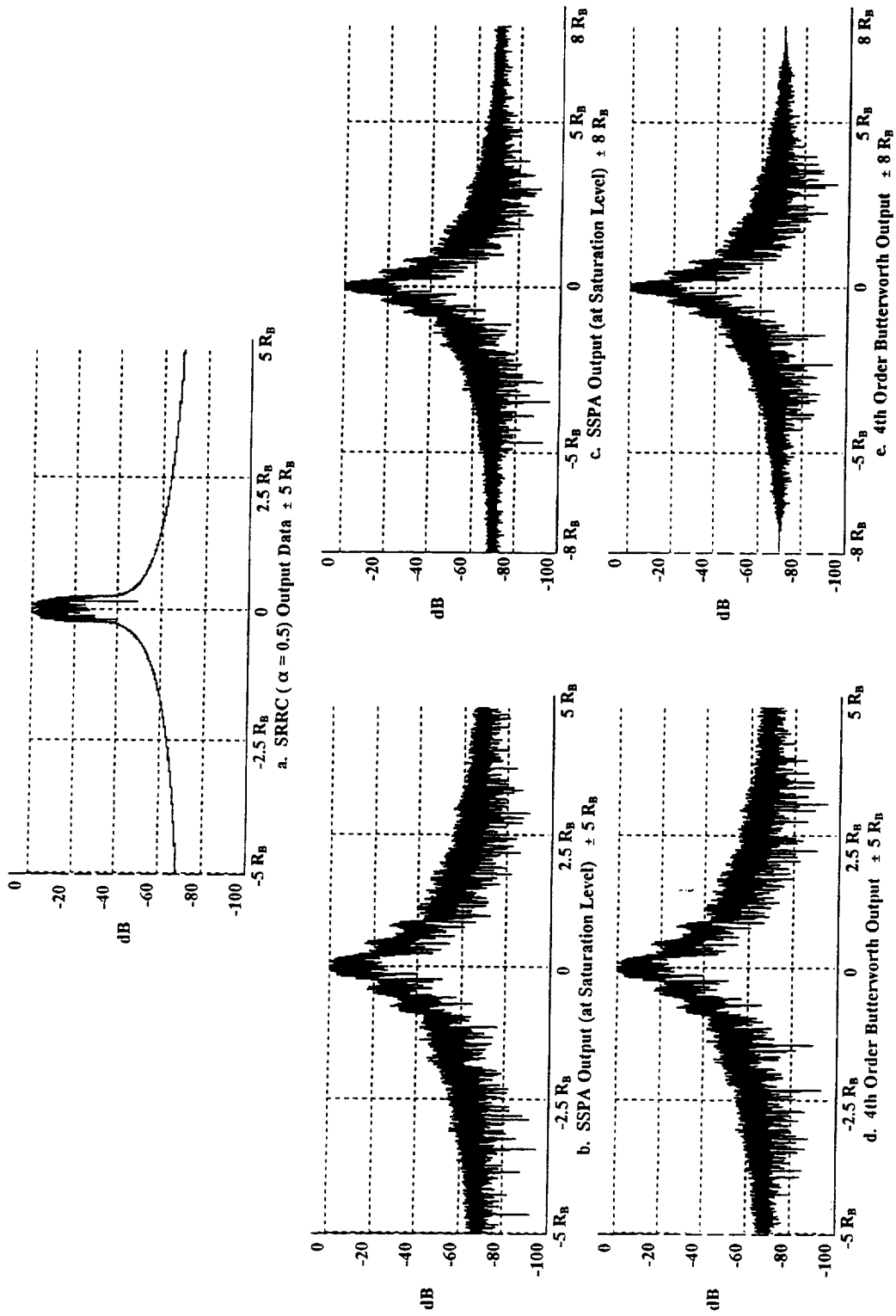


Figure 3.10 - Power Spectra of Filtered 8PSK Baseband Ideal Data using SRRC ($\alpha = 0.5$) Filter & SSQA at Saturation Level

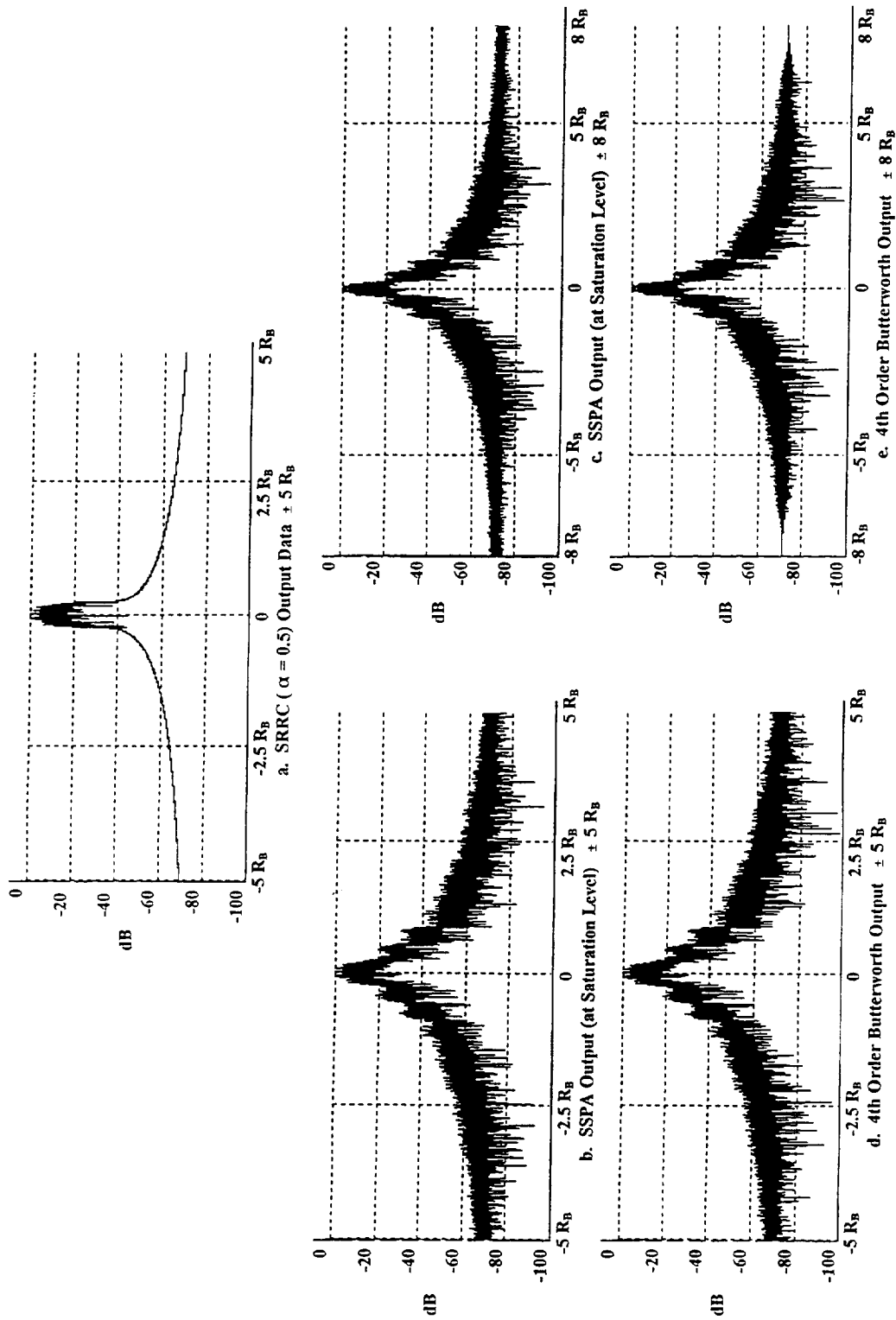


Figure 3.11 - Power Spectra of Filtered 8PSK Baseband Non-Ideal Data using SRRC ($\alpha = 0.5$) Filter & SSPA at Saturation Level

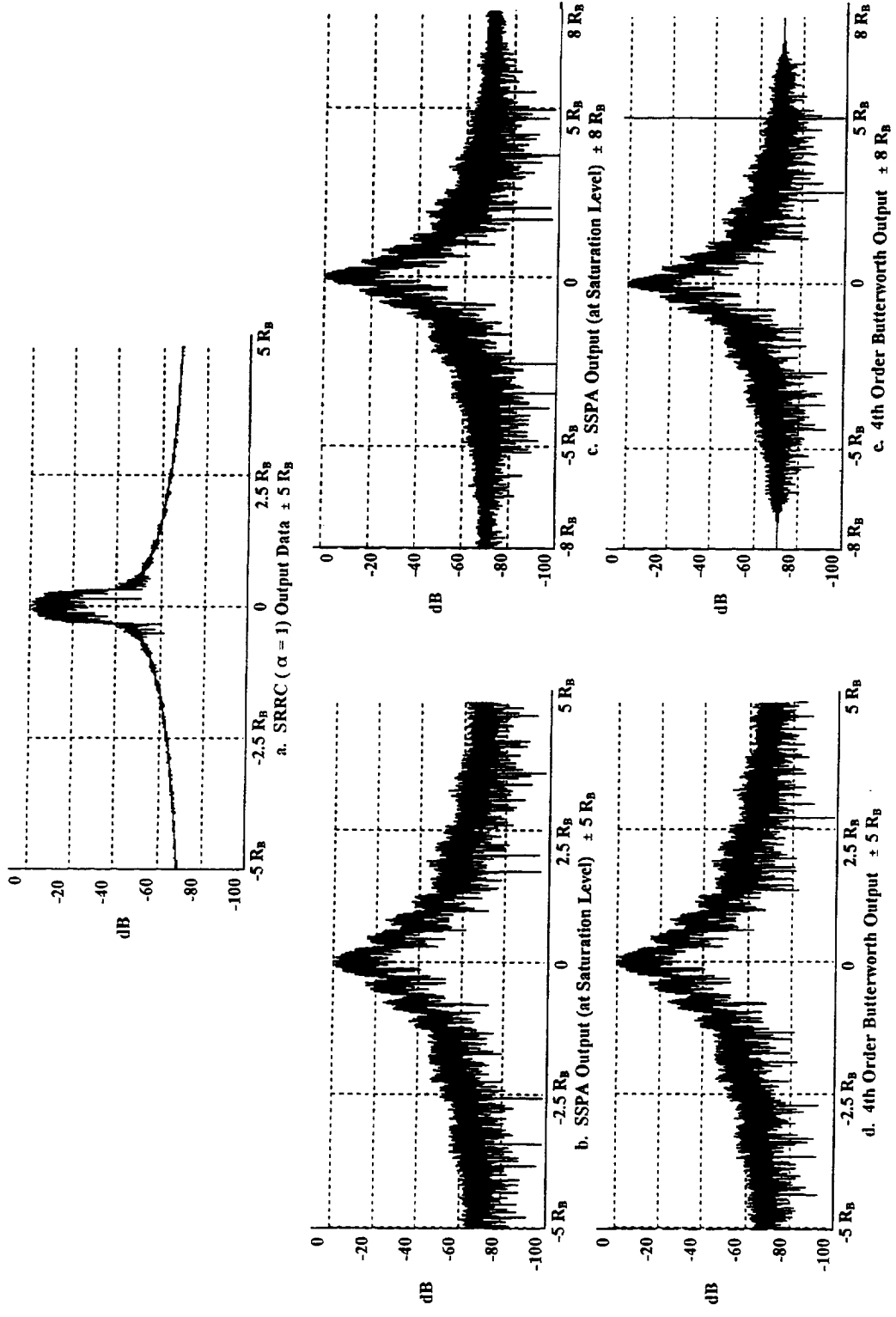


Figure 3.12 - Power Spectra of Filtered 8PSK Baseband Ideal Data using SRRC ($\alpha = 1$) Filter & SSPA at Saturation Level

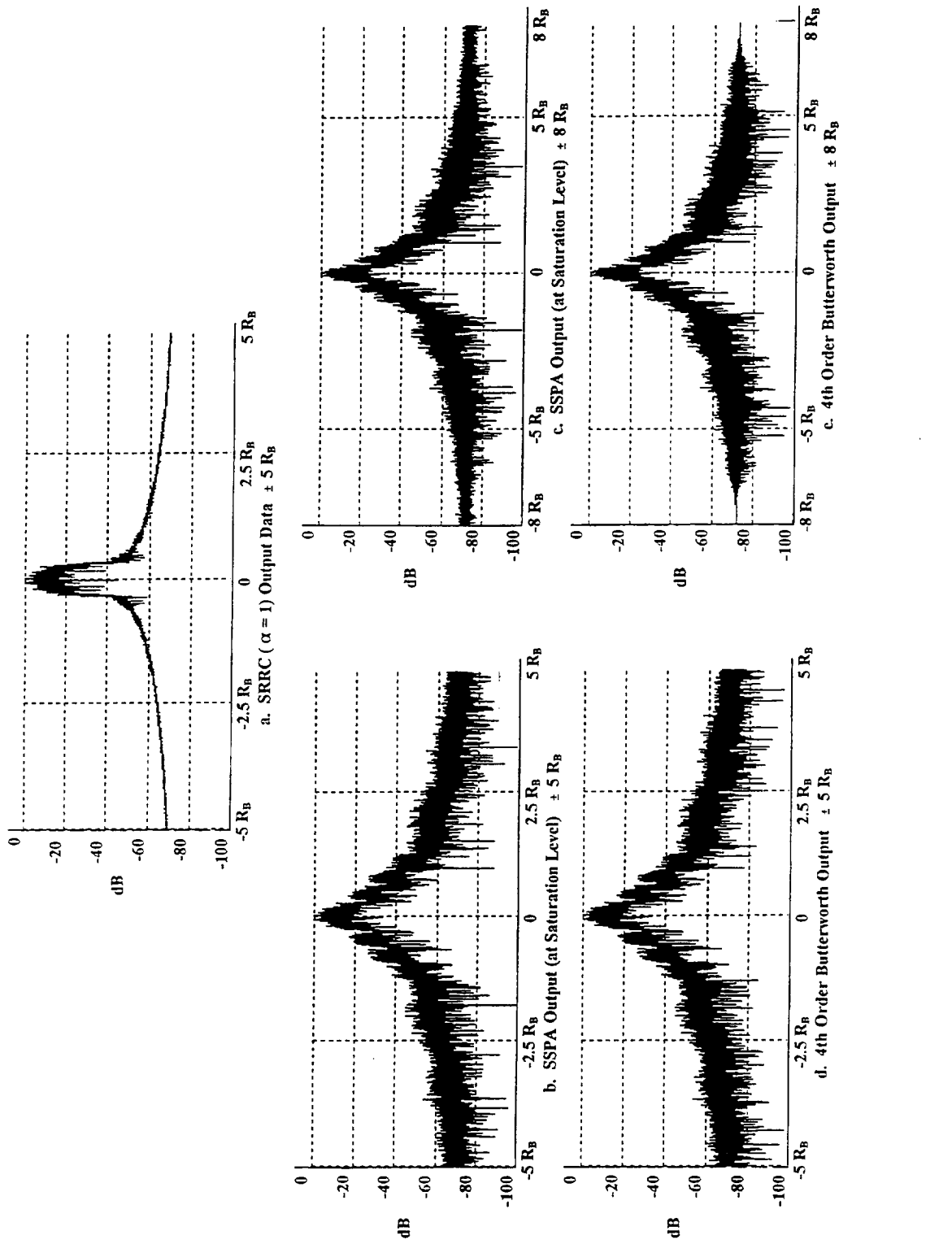


Figure 3.13 - Power Spectra of Filtered 8PSK Baseband Non-Ideal Data using SRRC ($\alpha = 1$) Filter & SSQA at Saturation Level

Summary of Baseband Filter Simulations:

Table 3.3 - Spectrum Levels Relative to First Data Sideband
(SSPA at Saturation Level and Ideal Data)

FILTER TYPE	$\pm 0 R_B$ dB	$\pm 5 R_B$ dB	$\pm 10 R_B$ dB	$\pm 20 R_B$ dB
None, Unfiltered Data (Reference)	0	-40	-44	-44
Butterworth, 5th Order (BT=1)	0	-63	-72	-81
Bessel, 3rd Order (BT=1)	0	-65	-72	-80
Square Root Raised Cosine ($\alpha = 0.25$), Sampled Data	0	-65	-67	-71
Square Root Raised Cosine ($\alpha = 0.5$), Sampled Data	0	-64	-67	-70
Square Root Raised Cosine ($\alpha = 1$), Sampled Data	0	-63	-66	-70

Table 3.4 - Spectrum Levels Relative to First Data Sideband
(SSPA at Saturation Level and Non-Ideal Data)

FILTER TYPE	$\pm 0 R_B$ dB	$\pm 5 R_B$ dB	$\pm 10 R_B$ dB	$\pm 20 R_B$ dB
None, Unfiltered Data (Reference)	0	-39	-42	-43
Butterworth, 5th Order (BT=1)	0	-63	-73	-82
Bessel, 3rd Order (BT=1)	0	-66	-74	-83
Square Root Raised Cosine ($\alpha = 0.25$), Sampled Data	0	-67	-68	-72
Square Root Raised Cosine ($\alpha = 0.5$), Sampled Data	0	-66	-68	-71
Square Root Raised Cosine ($\alpha = 1$), Sampled Data	0	-63	-67	-70

POWER SPECTRA FOR NON-FILTERED AND FILTERED 8 PSK
WITH SSPA BACKED OFF FROM SATURATION

All of the previous simulations were repeated for the SSPA backed off from saturation by 10 dB, so that it is operating in the linear region. Results of these simulations are given in Figures 3.14 to 3.25. Since the system is operating in the linear region, the power spectra plots remain the same through the SSPA, and the 2nd Harmonic Butterworth filter.

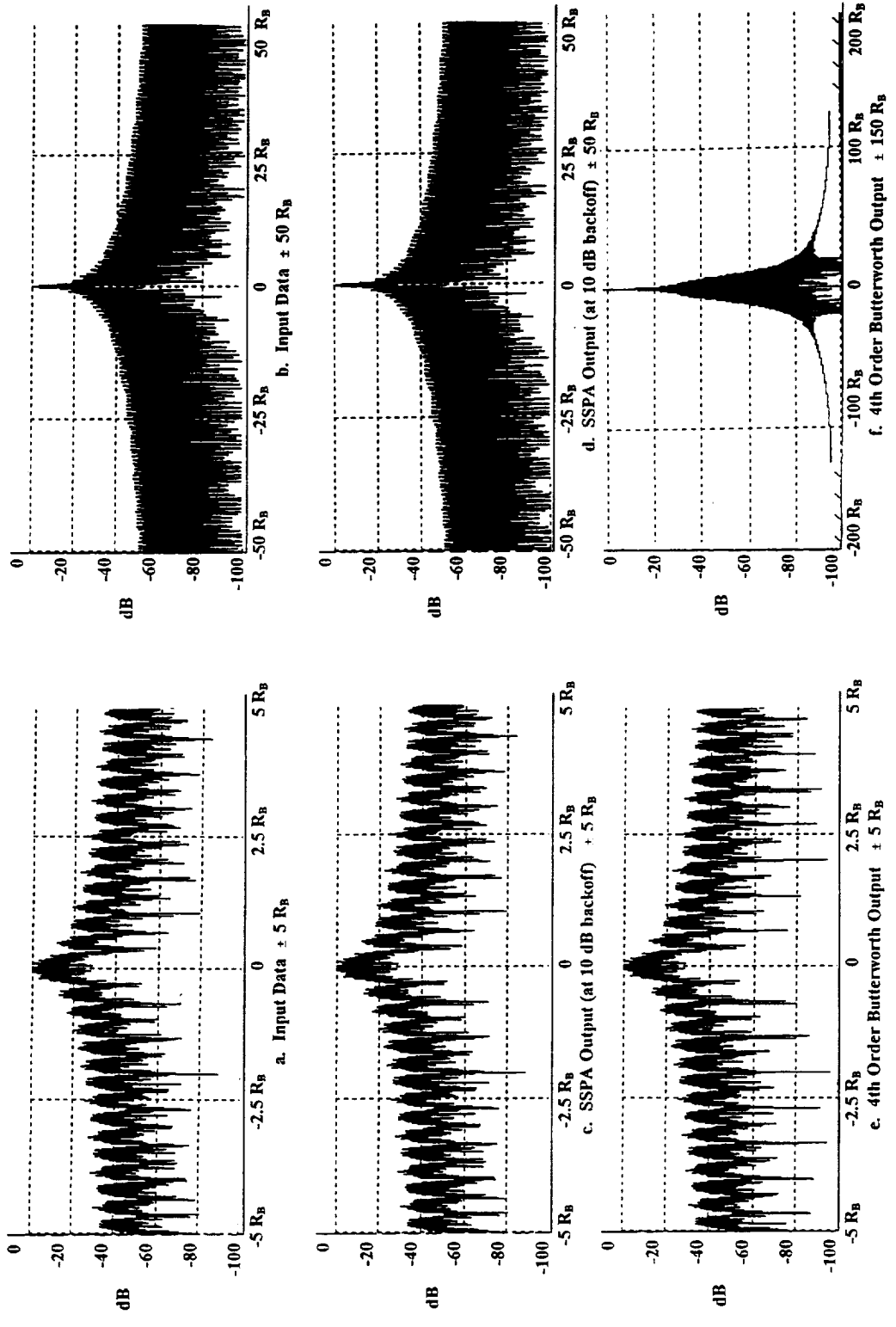


Figure 3.14 - Power Spectra of Unfiltered 8PSK Baseband Ideal Data using SSPA at 10 dB backoff

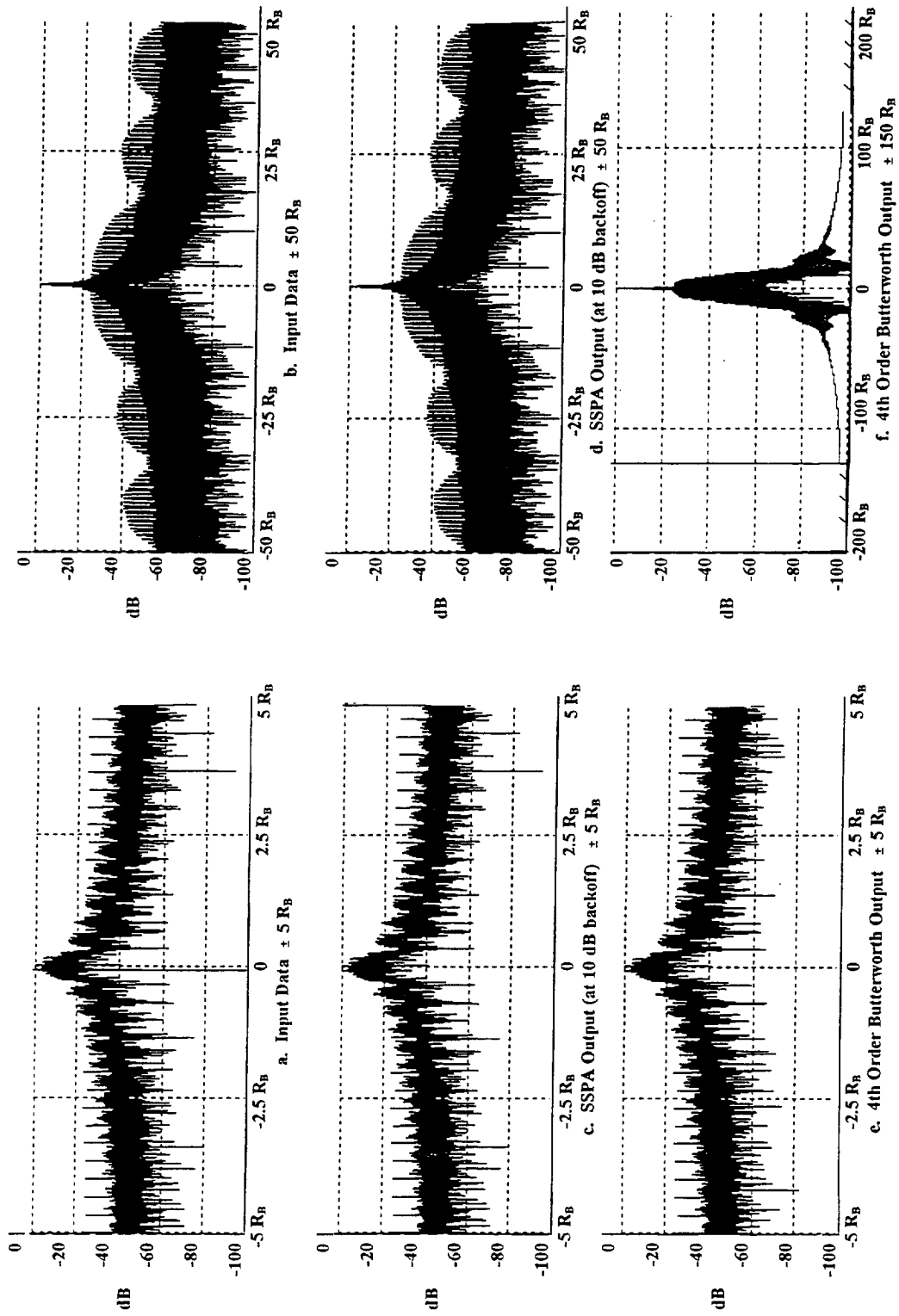


Figure 3.15 - Power Spectra of Unfiltered 8PSK Baseband Non-Ideal Data using SSPA at 10 dB backoff

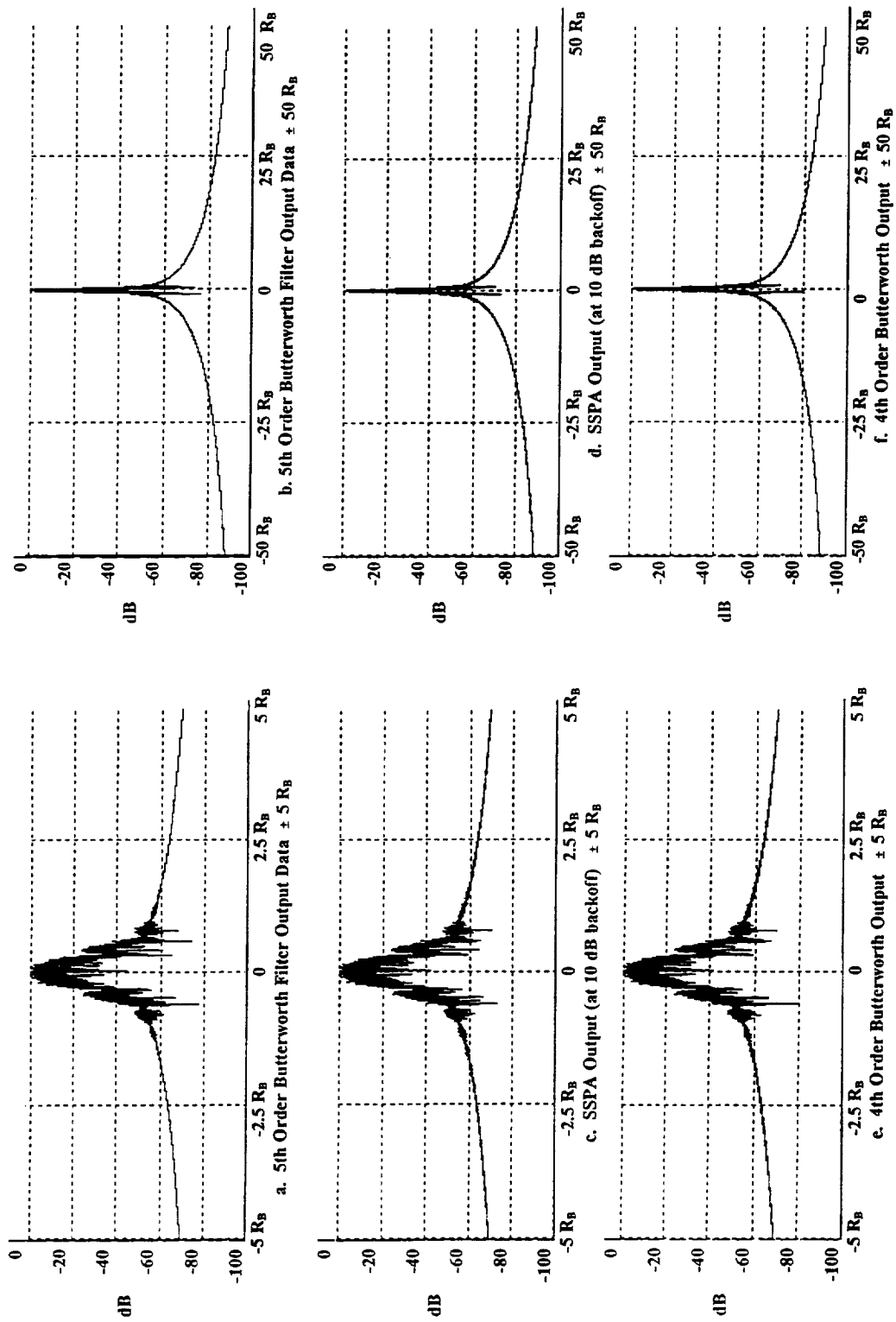


Figure 3.16 - Power Spectra of Filtered 8PSK Baseband Ideal Data using 5th Order Butterworth Filter ($BT=1$) & SSPA at 10 dB backoff

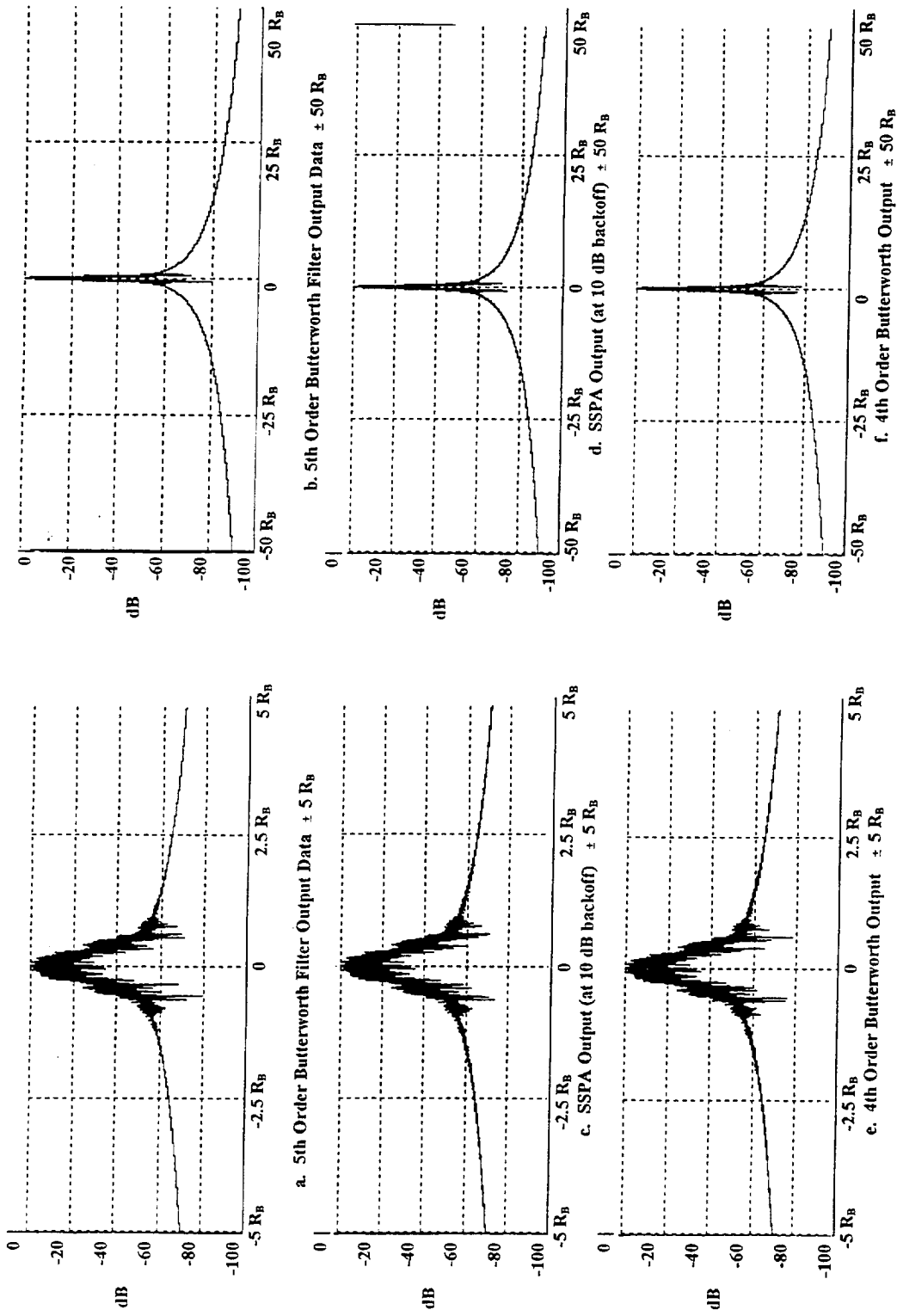


Figure 3.17 - Power Spectra of Filtered 8PSK Baseband Non-Ideal Data using 5th Order Butterworth Filter (BT=1) & SSPA at 10 dB Backoff

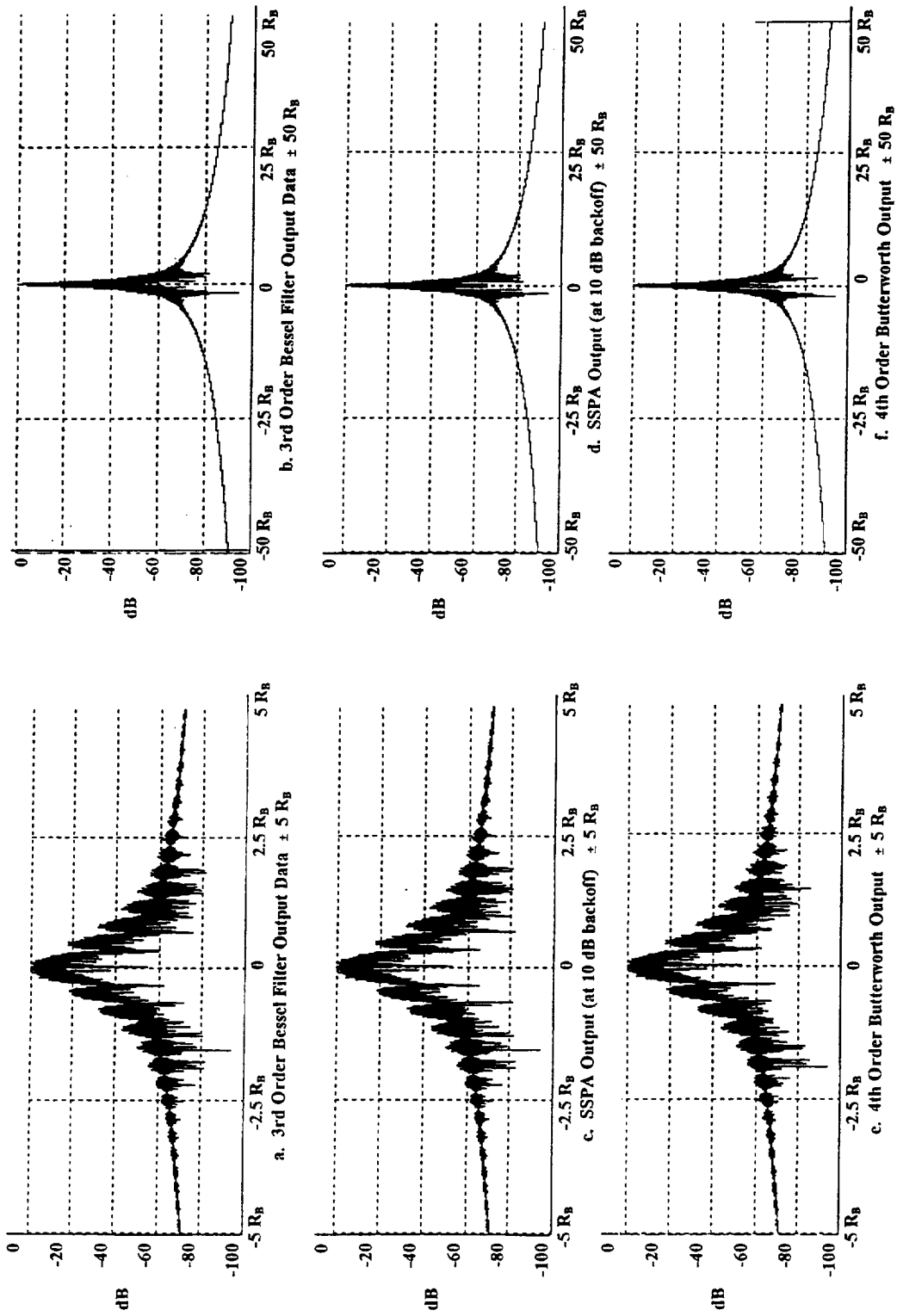


Figure 3.18 - Power Spectra of Filtered 8PSK Baseband Ideal Data using 3rd Order Bessel Filter ($BT=1$) & SSPA at 10 dB backoff

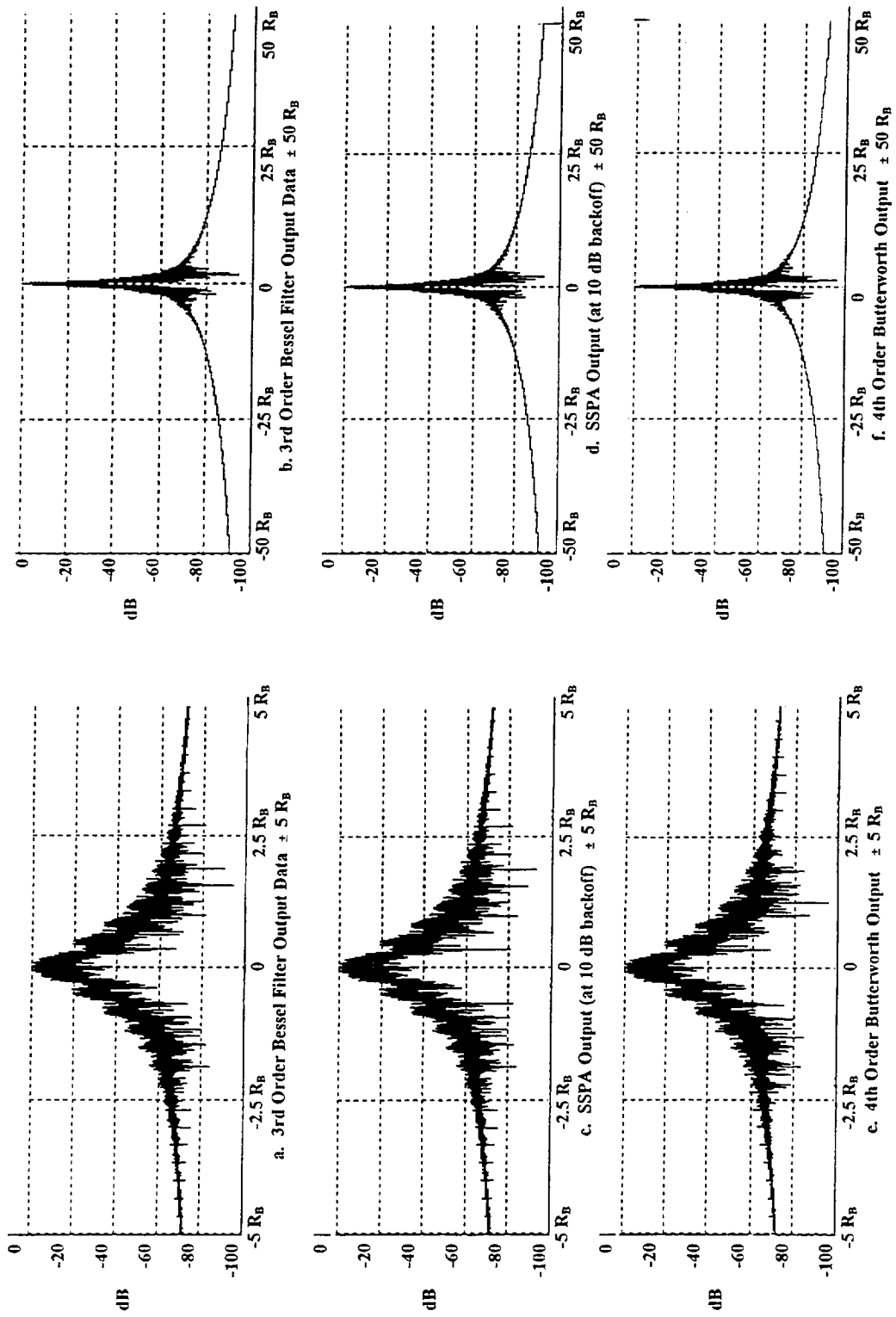


Figure 3.19 - Power Spectra of Filtered 8PSK Baseband Non-Ideal Data using 3rd Order Bessel Filter ($BT=1$) & SSPA at 10 dB backoff

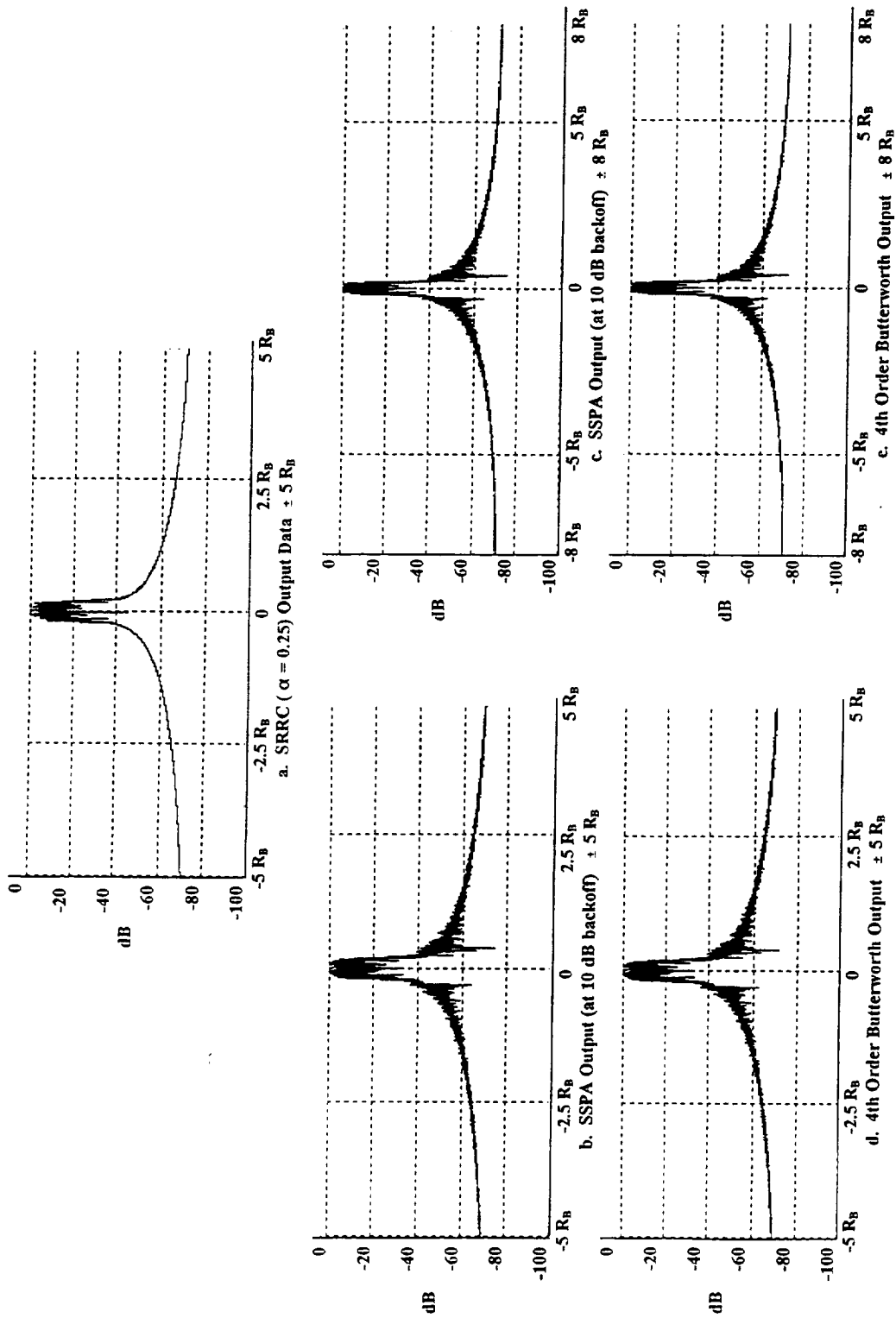


Figure 3.20 - Power Spectra of Filtered 8PSK Baseband Ideal Data using SRRC ($\alpha = 0.25$) Filter & SSQA at 10 dB backoff

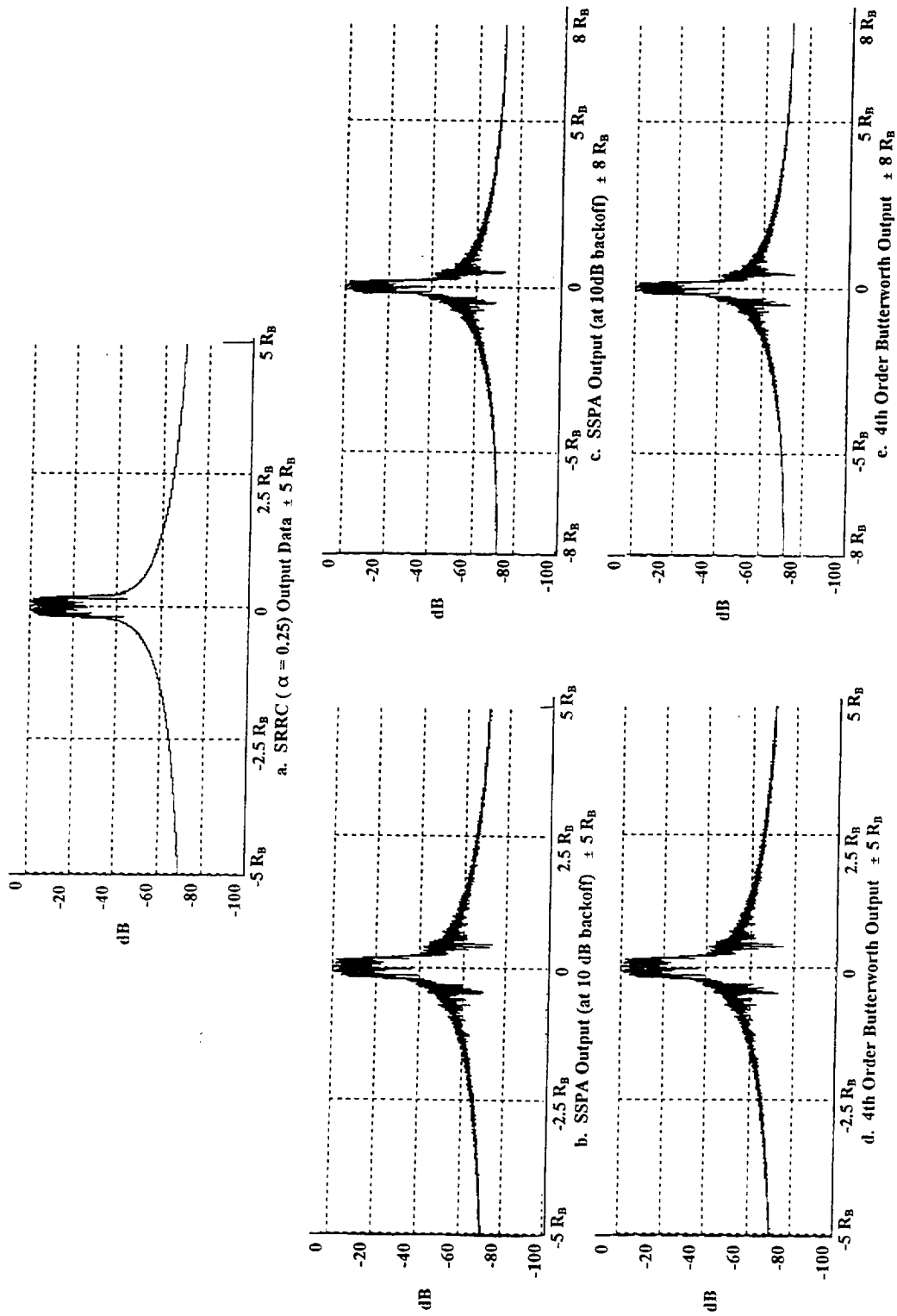


Figure 3.21 - Power Spectra of Filtered 8PSK Baseband Non-Ideal Data using SRRC ($\alpha = 0.25$) Filter & SSPA at 10 dB backoff

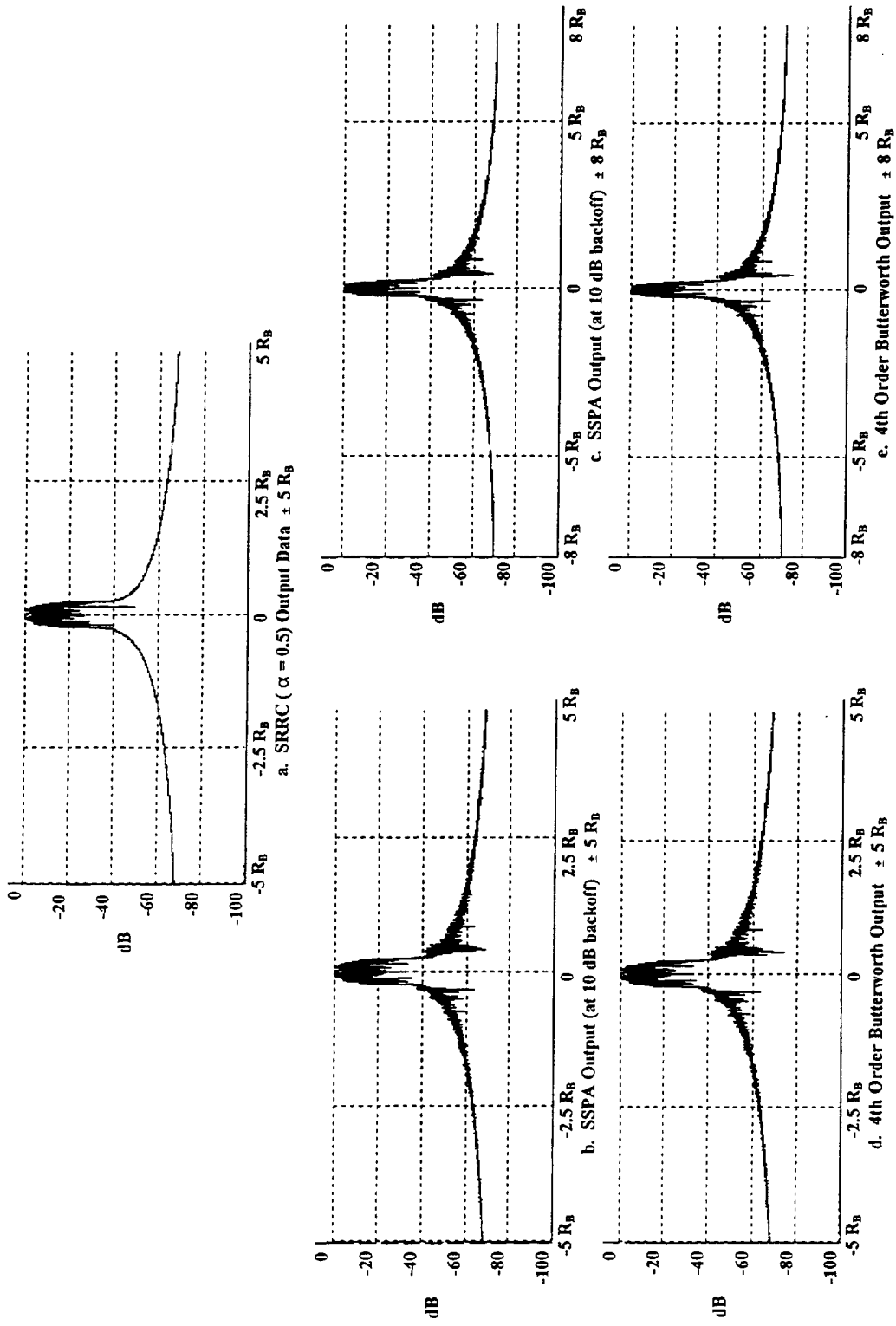


Figure 3.22 - Power Spectra of Filtered 8PSK Baseband Ideal Data using SRRC ($\alpha = 0.5$) Filter at 10 dB backoff

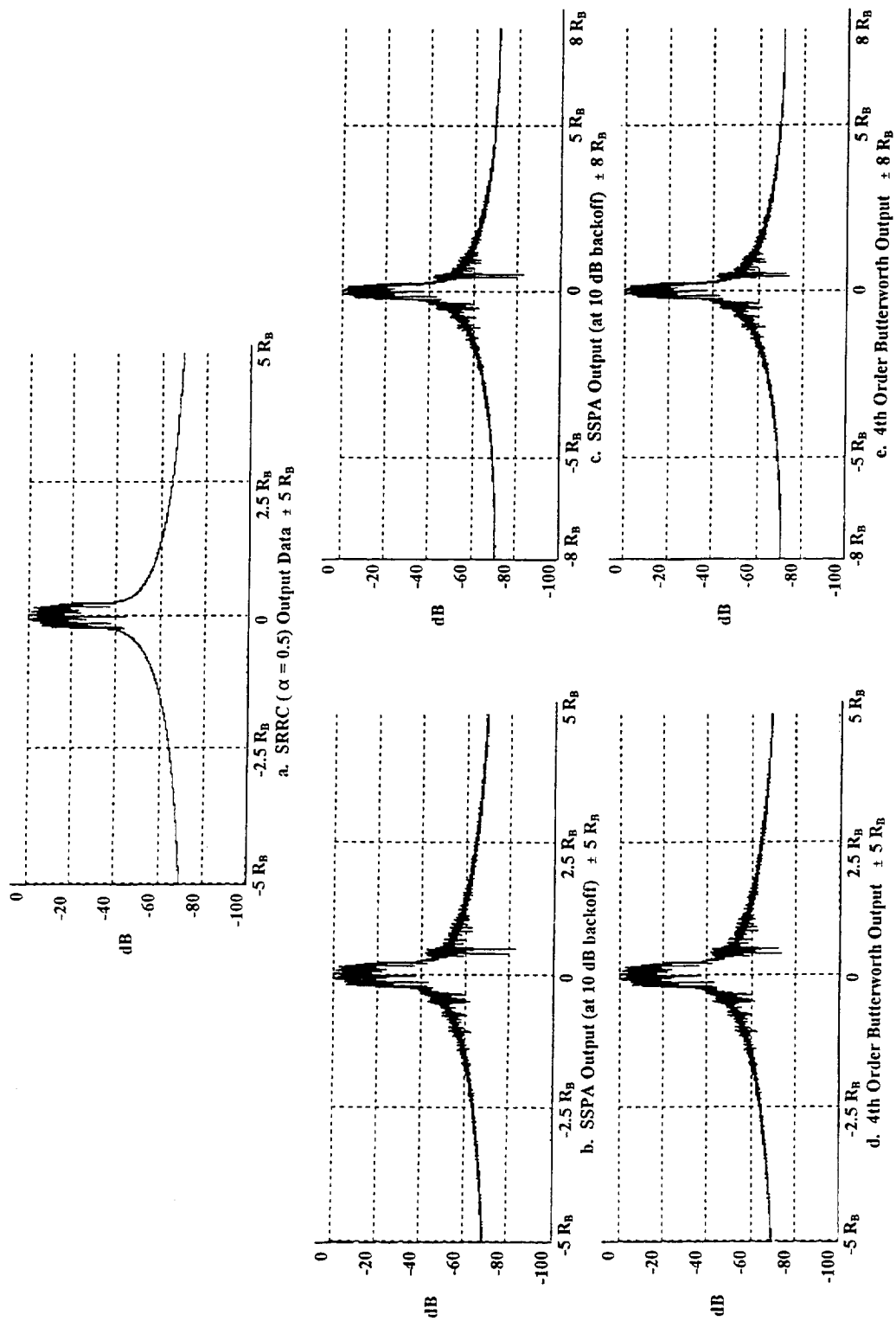


Figure 3.23 - Power Spectra of Filtered 8PSK Baseband Non-Ideal Data using SRRC ($\alpha=0.5$) Filter & SSPA at 10 dB backoff

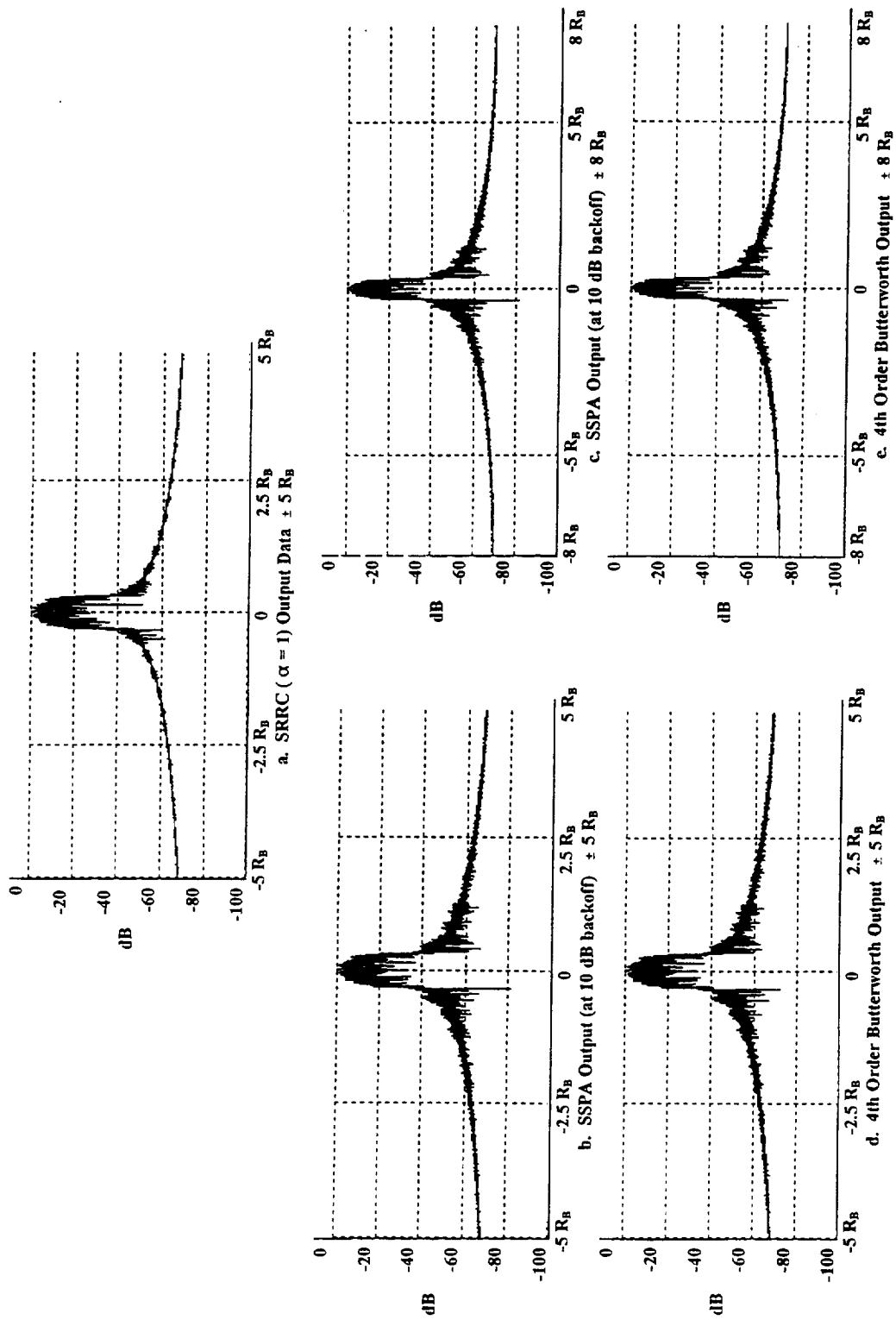


Figure 3.24 - Power Spectra of Filtered 8PSK Baseband Ideal Data using SRRC ($\alpha = 1$) Filter & SSPA at 10dB backoff

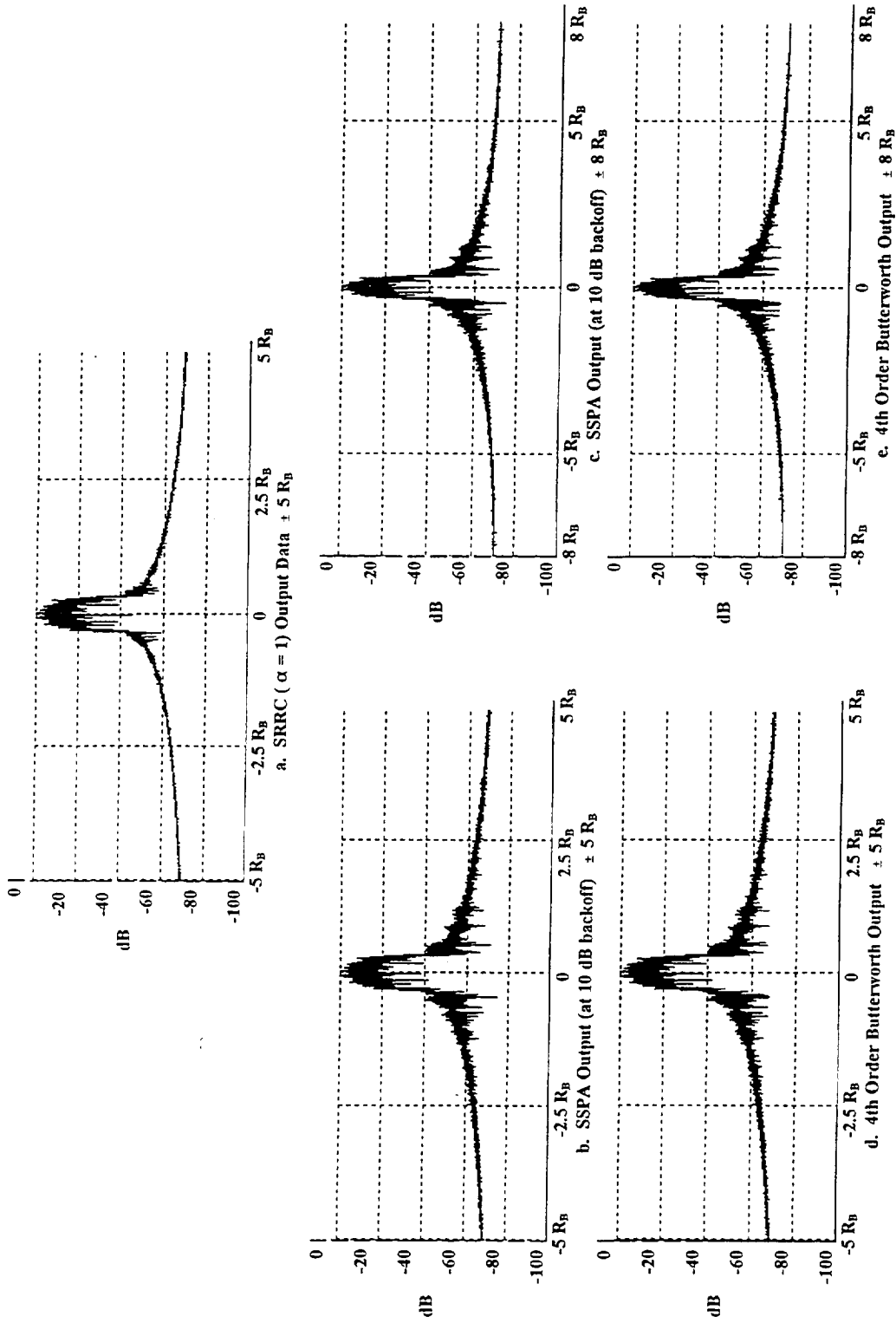


Figure 3.25 - Power Spectra of Filtered 8PSK Baseband Non-Ideal Data using SRRC ($\alpha=1$) Filter & SSPA at 10 dB backoff

3.3 End-to-End System Performance: Symbol Error Rate (SER).

To measure the end-to-end system performance, the symbol error rate was measured for different values of average symbol energy to noise ratios (E_s/N_0). Such a measurement was performed using SPW and the system described previously. The three types of baseband filters described earlier were used. To choose the best filter from such a study one selects the filter that has a BT product such that the filter ISI loss is < 0.4 dB [4]. To obtain a measure of the filter ISI loss, a reference needs to be established. An ideal linear system is used where ideal data and hardware are utilized to provide a reference for comparisons with the system being studied (a plot of Probability of error versus E_s/N_0 is derived and called Theoretical plot in this case for 8PSK). The proper reference system to measure filter loss would be a system where measurements are made by using non-ideal components and data.

From the experience of the NMSU Center for Space Telemetry and Telecommunications Systems, the effect of non-ideal data and system are negligible overall and usually the error produced by such non-idealities are approximately 0.5-1.0 dB. To see how small this effect is, a simulation was performed using no baseband filter ($BT = \infty$), the non-linear SSPA and non-ideal data. The SER curve is plotted as a function of the SNR. This plot was then compared with the ideal and theoretical curves described above and shown in Figure 3.26. The theoretical curve was plotted using the Symbol Error Performance expression derived from [8], i.e., for equally likely coherent M-ary PSK signaling:

$$P_E(M) \cong 2Q\left(\sqrt{\frac{2E_s}{N_0}} \sin\left(\frac{\pi}{M}\right)\right)$$

where $P_E(M)$ is the probability of symbol error, $E_s = E_b (\log_2 M)$ is the energy per symbol, and $M=2^\lambda$ is the size of the symbol set i.e $\lambda=3$ then $M=8$ since 8PSK signaling is used.

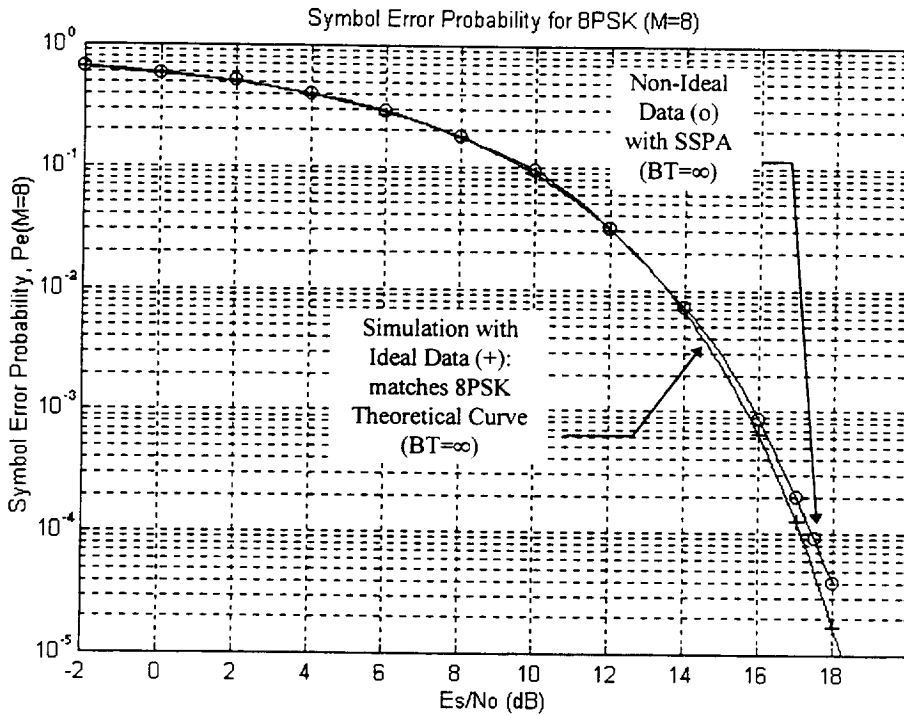


Figure 3.26 - SER for 8PSK curves: Ideal and Non-Ideal data with $BT = \infty$

From Figure 3.26 it can be seen that the difference between the theoretical curve and the non-ideal one is very small. Around $SER=10^{-3}$, the SNR difference between the two curves is approximately 0.2 dB (15.873 dB - 15.68 dB). Note that the last portion of the curve was extrapolated. For this reason the simulations for the SER curves were performed using ideal-data (which overlaps with the theoretical curve) keeping in mind that there will be a small SNR deviation due to the non-idealities of the system. In the CCSDS reports ([3], [4]), simulations were made using non-ideal data and non-ideal system components.

These non-idealities reflect those found in specific equipment and may vary from system-to-system. Perhaps measurements of the non-idealities could be made at a later time and then incorporated into the overall results of the project. The system performance was then done with ideal data (SSPA at saturation level) for the Butterworth and Bessel filter set to $BT=1,2$ and 3 and also the SRRC filters set to $\alpha = 0.25, 0.5$ and 1 (worse case for SRRC filter).

The symbol error rate was then plotted as a function of the average symbol SNR. Table 3.5, summarizes the simulations performed for the 8PSK SER using the system mentioned above:

Table 3.5 - SER for 8PSK Simulations

SIMULATION NUMBER	MODULATION TYPE	FILTER LOCATION	FILTER TYPE	FILTER CHAR.	DATA CHAR.
1	8PSK	none	none	none	Ideal NRZ-L
2	8PSK	Baseband	Butterworth (BT=1)	5th Order	Ideal NRZ-L
3	8PSK	Baseband	Butterworth (BT=2)	5th Order	Ideal NRZ-L
4	8PSK	Baseband	Butterworth (BT=3)	5th Order	Ideal NRZ-L
5	8PSK	Baseband	Bessel (BT=1)	3rd Order	Ideal NRZ-L
6	8PSK	Baseband	Bessel (BT=2)	3rd Order	Ideal NRZ-L
7	8PSK	Baseband	Bessel (BT=3)	3rd Order	Ideal NRZ-L
8	8PSK	Baseband	SRRC	$\alpha = 0.25$	Ideal NRZ-L
9	8PSK	Baseband	SRRC	$\alpha = 0.5$	Ideal NRZ-L
10	8PSK	Baseband	SRRC	$\alpha = 1.0$	Ideal NRZ-L

Figures 3.27, 3.28 and 3.29, respectively, show the SER for 8PSK: 5th Order Butterworth BT=1, 2 and 3 (SSPA at Saturation & Ideal-Data), SER for 8PSK: 3rd Order Bessel BT=1, 2 and 3 (SSPA at Saturation & Ideal-Data) and SER for 8PSK: SRRC $\alpha=1$ (no SSPA), $\alpha=0.25$, 0.5 and 1 (SSPA at Saturation & Ideal-Data).

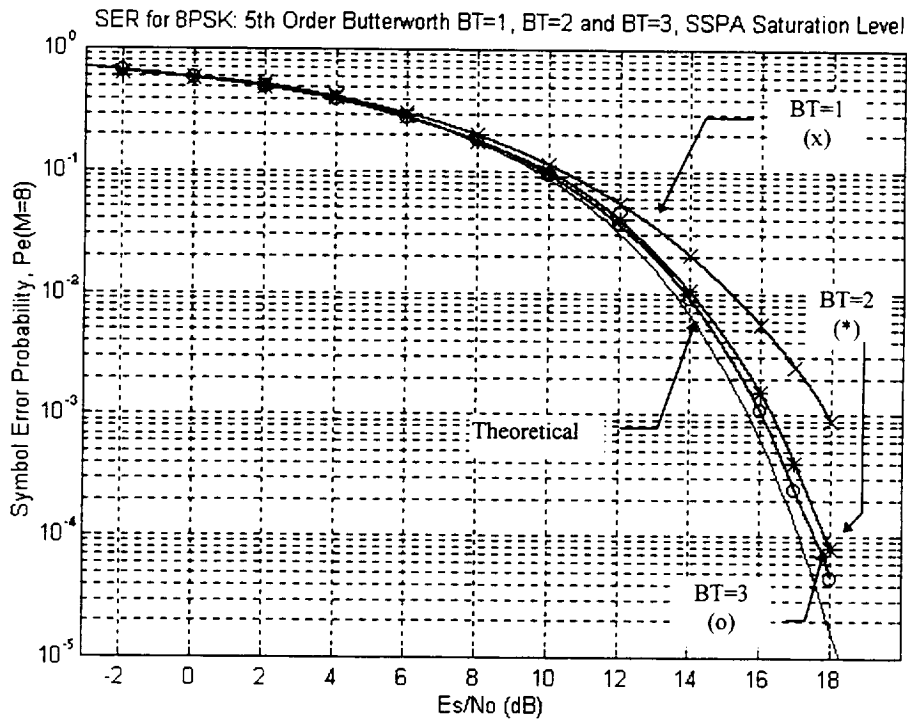


Figure 3.27 - SER for 8PSK:5th Order Butterworth BT=1,2 and 3 (SSPA at Saturation & Ideal Data)

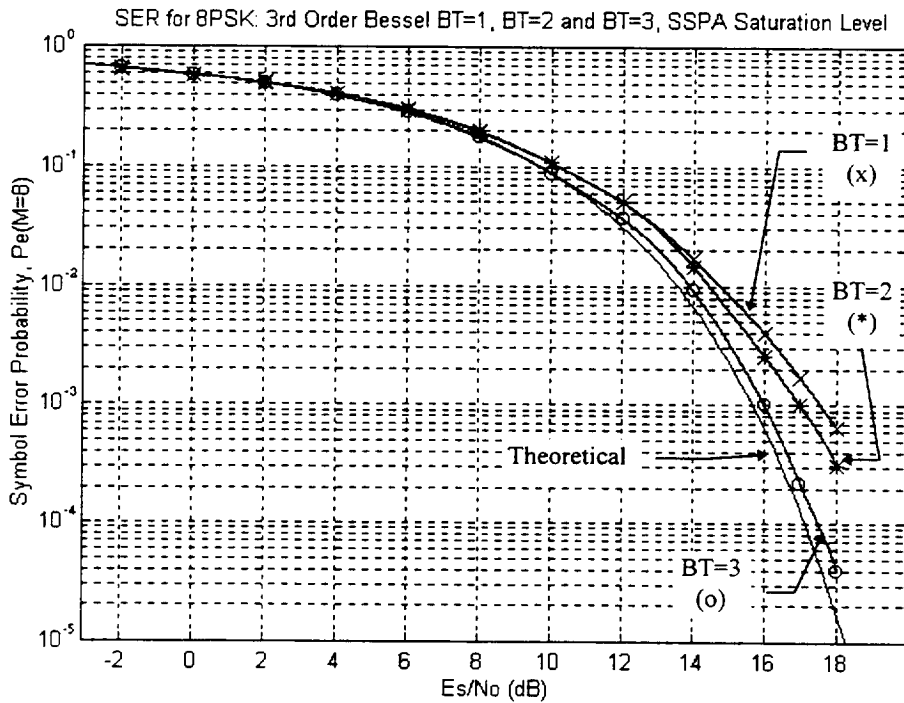


Figure 3.28 - SER for 8PSK: 3rd Order Bessel BT=1, 2 and 3 (SSPA at Saturation & Ideal Data)

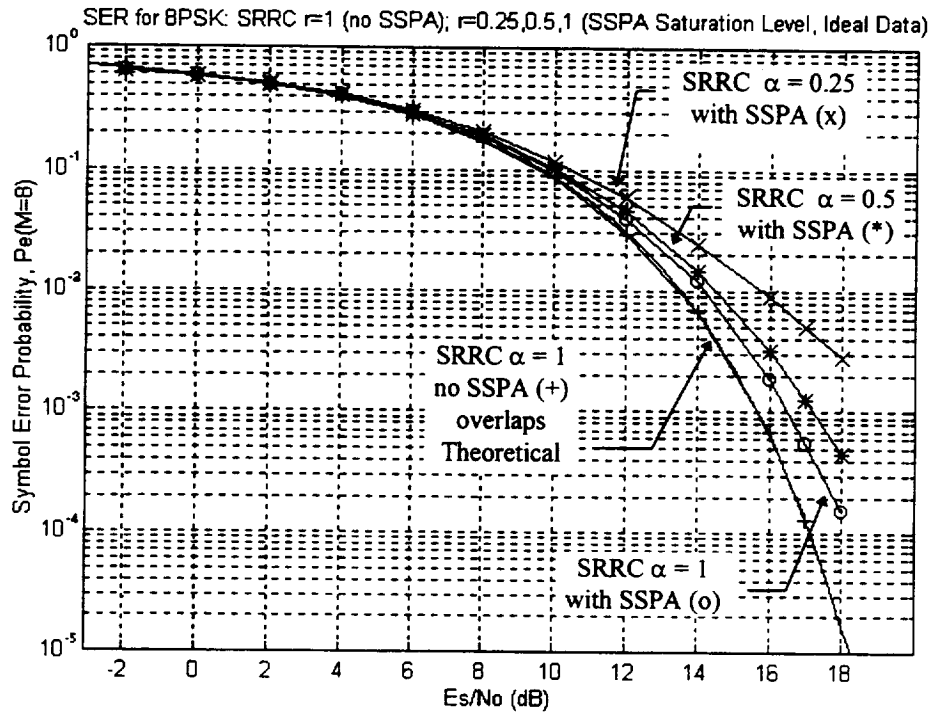


Figure 3.29 - SER for 8PSK: SRRC $\alpha = 1$ (no SSPA), $\alpha = 0.25, 0.5$ and 1 (SSPA at Saturation & Ideal Data)

From these simulations it is then possible to determine the ISI loss due to the system. This is found by taking the difference between the E_s/N_0 values measured with and without the filter. As indicated in [4], the losses are measured over values of $10^{-3} \leq \text{SER} \leq 10^{-2}$ which is the normal operating region for CCSDS encoded data. Losses are then tabulated for $BT = 1, 2, 3$ (see Table 3.6). Also as indicated in that same report the optimal filter is found by selecting the lowest BT providing acceptable ISI loss (in this case a threshold of ISI loss < 0.4 dB). The following table gives the results of the baseband filter ISI losses at 10^{-3} SER using the Figures above:

Table 3.6 - Baseband Filters ISI Loss Measurements at 10^{-3} SER

FILTER TYPE	LOSS (BT=1) (dB)	LOSS (BT=2) (dB)	LOSS (BT=3) (dB)
Butterworth 5th Order	17.86-15.68 = 2.18	16.294-15.68= 0.614	16.048-15.68 = 0.368
Bessel 3rd Order	17.515 - 15.68 = 1.835	16.9734 - 15.68 = 1.2934	16.088 - 15.68 = 0.408
SRRC ($\alpha=1.0$)	16.498 - 15.68 = 0.818	-----	-----

Note that only the loss of the SRRC with $\alpha=1.0$ is shown in the table since the other SRRC filters have higher values of losses (as shown in Figure 3.29) and their bandwidths are much smaller than $BT=1$ therefore they can not be compared with the Butterworth or Bessel filters.

Again as stipulated in [4], the optimum filter is the one that has the smallest BT value providing losses < 0.4 dB. Therefore with the results shown in the previous table, the following can be stipulated as to which filter is the optimum:

Table 3.7 - Optimum Baseband Filter

FILTER TYPES	OPTIMUM BT VALUE
Butterworth (5th Order)	BT = 3
Bessel (3rd Order)	BT = 3
SRRC ($\alpha=1.0$)	none

It must be emphasized that these simulations were performed with ideal data therefore since these values of BT barely meet the $ISI < 0.4$ requirement, with a non-ideal system this threshold would not be met (add approximately 0.5 to 1.0 dB to the values measured). Thus a simulation with a higher order of BT should be performed (example $BT = 4$) which would certainly meet the above requirement since the bandwidth would be increased.

In Phase II [3], a Band Utilization Ratio (ρ) was defined. The interpretation of this ratio can be explained as follows. First with the investigation on the baseband filters performed with the 8PSK modulation, it was noticed that such filters significantly narrow the RF spectrum bandwidth.

As shown in Tables 3.3 and 3.4, reductions of approximately 24 to 28 dB and 26 to 31 dB were achieved at $\pm 5R_B$ and $\pm 10 R_B$ respectively. As stated in [3] "these reductions were obtained with ideal data (non-ideal data gave similar results) and with no effort devoted to filter optimization. With some effort, greater attenuations may be obtainable."

From this, two questions were raised in Phase II about the significant change in the RF spectrum:

- (1) - *Can the number of spacecraft using a specific frequency band be increased if baseband filtering is used ?; and*
- (2) - *If the number of spacecraft using a specific frequency band can be increased, how many more can be accommodated than would be the case if no filtering is used?*

To answer to these questions, a frequency band Utilization Ratio (ρ) can be defined as :

$$\rho = \frac{\text{Number of Spacecraft with Filtering Accommodated in Frequency Band}}{\text{Number of Spacecraft without Filtering Accommodated in Frequency Band}}$$

An important assumption in deriving this ratio was made: the “spectra from spacecraft in adjacent channels will be permitted to overlap one another provided that, at the frequency where the overlap occurs, the signals are at least 50 dB below that of the main telemetry lobe (1st data sideband).” [3].

Using SPW, measurements were made using unfiltered and non-ideal data (the 2nd harmonic filter was removed) to determine the frequency at which the data spectrum was 50 dB below the main lobe. The Power Spectrum plots shown earlier were used to determine this 50 dB level. For example, for ideal data without a spectrum shaping filter the -50dB point is situated at approximately $35 R_B$ (refer to Figure 3.2d) and using the Butterworth Filter (BT=1) with Ideal Data, the -50 dB point is approximately at $2.5 R_B$ (refer to Figure 3.4c), then the Utilization ratio, ρ , is equal to

$$\rho = \frac{35R_B}{2.5R_B} = 14.$$

Note that the way the ratio is calculated in this example is different from the formula given previously but the result is the same. The number of spacecraft with filtering accommodated in the frequency band will be larger than if it was not filtered.

The following table shows the results of Utilization ratio, ρ , for the other filters. The same calculation as performed above were done to complete this table.

Table 3.8 - Utilization Ratio Improvement for Various Spectrum Shaping

FILTER TYPE	Ideal Data -50 dB pt.	Ideal Data Util. Ratio (ρ)	Non-Ideal Data -50 dB pt.	Non-Ideal Data Util. Ratio (ρ)
None, Unfiltered Data (Reference)	$35 R_B$	1	$40 R_B$	1
Butterworth, 5th Order (BT=1)	$2.5 R_B$	14	$2.3 R_B$	17.39
Bessel, 3rd Order (BT=1)	$2.95 R_B$	11.86	$2.5 R_B$	16
Square Root Raised Cosine ($\alpha = 0.25$) Sampled Data	$1.7 R_B$	20.59	$1.7 R_B$	23.5
Square Root Raised Cosine ($\alpha = 0.5$) Sampled Data	$1.8 R_B$	19.4	$1.7 R_B$	23.5
Square Root Raised Cosine ($\alpha = 1$) Sampled Data	$2.5 R_B$	14	$2.2 R_B$	18.18

From this last table it is obvious that baseband filtering offers a significant improvement in the number of spacecraft operating in a frequency band. This improvement is also superior for the case of non-ideal data. In fact by baseband filtering, the bandwidth utilization can increase by a factor of 12 to 24.

As mentioned in [3] : “While these ratios may represent upper bounds, it is clear that a significant increase in spectrum utilization is potentially possible using baseband filtering, even if the ratios are only 3 or 4 to 1. Judging by the auctions now underway in several countries, such additional frequency spectrum will be worth a small fortune and should easily justify expenditures necessary to develop any new filters and/or earth station equipment.”

Finally to complement this section on SER, it can be mentioned that different techniques can be used to mitigate the effects due to the nonlinear bandlimited signal distortion present in these high data rate satellites and therefore improve the End-to-End System Performance (SER). [11] presents a development of the low-pass Volterra discrete-time model for a nonlinear communication channel. More specifically, the dissertation in [11] is a study of adaptive Volterra equalizers on a downlink-limited nonlinear bandlimited satellite channel. It is found that a receiver consisting of a fractionally-spaced equalizer (FSE) followed by a Volterra equalizer (FSE-Volterra) gives improvement beyond that gained by the Volterra equalizer. “ Significant probability of error performance improvement is found for multilevel modulation schemes. Also, it is found that probability of error improvement is more significant for modulation schemes, constant amplitude and multilevel, which require higher signal to noise ratios (i.e., higher modulation orders) for reliable operation”. Furthermore, as discussed in [12], in systems that have a strict power limitation and high data rate demands (example: small satellite transmitting through NASA’s TDRSS network), the dominant noise is present in the uplink rather than the downlink channel. Therefore [12] shows that by modifying the standard receiver for several digital modulation formats and through proper specification of receiver decision regions, pulse shape and receiver filters, significant gains in performance can be produced. On the other hand with respect to the bandwidth utilization, [13] introduces a way to develop technology and equipment that would allow users to maximize their data throughput in an RF spectrum. All these experiments were conducted in the Center for Space Telemetry and Telecommunications Systems at New Mexico State University.

3.4 Non-Constant Envelope 8PSK Simulations

As discussed in the filter section, a finite-duration signal must have infinite bandwidth. Therefore when the signal is filtered (to minimize the bandwidth) and the cutoff frequency of the filter is set smaller and smaller, it was found with simulations that the ISI increases and the eye diagram eventually closes at a point where it exceeds the channel noise. Also, the signal envelope is not constant anymore as it will be shown in Figure 3.33.

The two plots of Figure 3.30 (Figure 3.30a and 3.30b) show the real and imaginary parts respectively of the output of the 8PSK modulator. From Figure 3.31a, it is clear that the envelope of the signal is constant (flat line with an amplitude of $\sqrt{2}$). Figure 3.32 shows, the effect of filtering the signal using a Butterworth Filter 5th Order, $BT=1$. Note how the signal envelope acquires variations in Figure 3.33a and how the transitions during each bit are smooth (1 bit corresponds to 16 samples since $f_s = 16$ samples/bit).

Finally if the output signal from the spectrum filter (for example in this case, the 5th Order Butterworth Filter), goes through a non-linear device (a SSPA or TWT for example) , the signal will be modified in such a way that the performance of the receiver filter will be affected due to the AM-AM and AM-PM conversion produced by the amplifier (this was discussed in the SSPA section). The SSPA is a linear amplifier when operated at the appropriate drive level. If the drive level is increased, the efficiency (RF output/dc input) is improved, but the amplifier becomes nonlinear. In this case constant envelope signals, such as PSK or PM, need to be used so that the intermodulation distortion will not cause a problem. This is the mode of operation that is used on the SSPA. Also as mentioned in [8], many analysis techniques on non-linear distortion have been published in the literature but none of them has been really satisfactory. Figures 3.34 and 3.35 show the output of the SSPA after the output of 5th Order Butterworth ($BT=1$) was used as input.

Thus when PSK (non-filtered and constant envelope) goes through a high powered amplifier (in the non-linear or linear region), the same waveform at the input will be reproduced at the output due to the constant envelope of the data. This can be seen in Figures 3.36 and 3.37, where no spectrum shaping filter was used thus the signal going through the SSPA has a constant envelope.

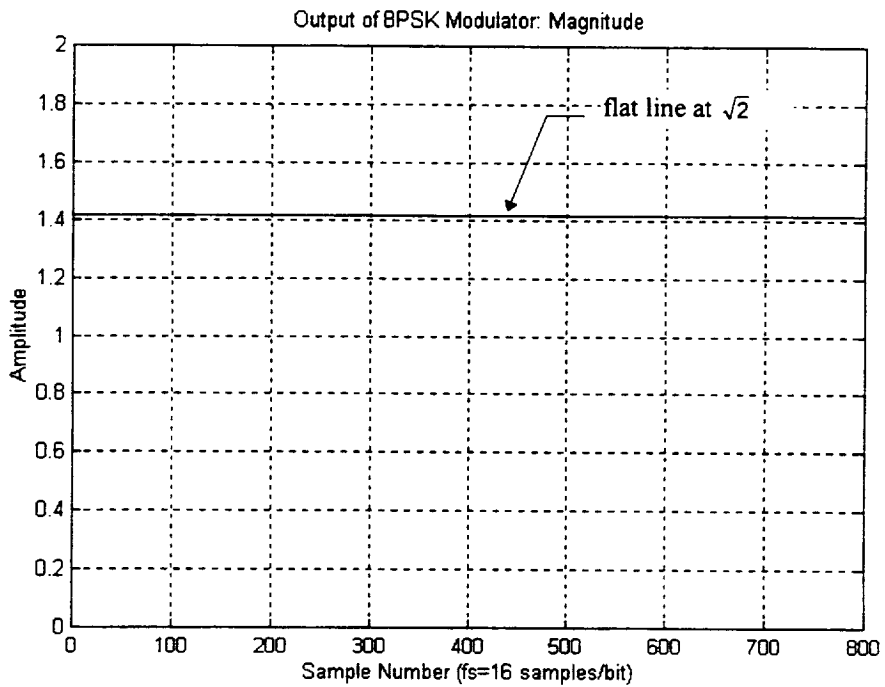


Figure 3.31a - Output of 8PSK Modulator: Magnitude

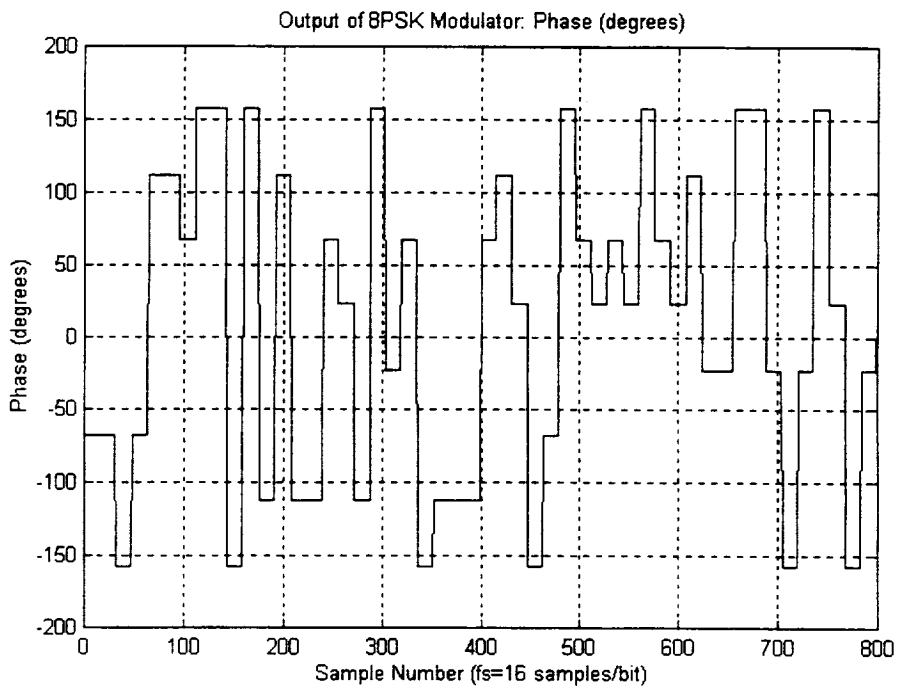


Figure 3.31b - Output of 8PSK Modulator: Phase (degrees)

Figure 3.31 - 8PSK Modulator Output: Magnitude & Phase

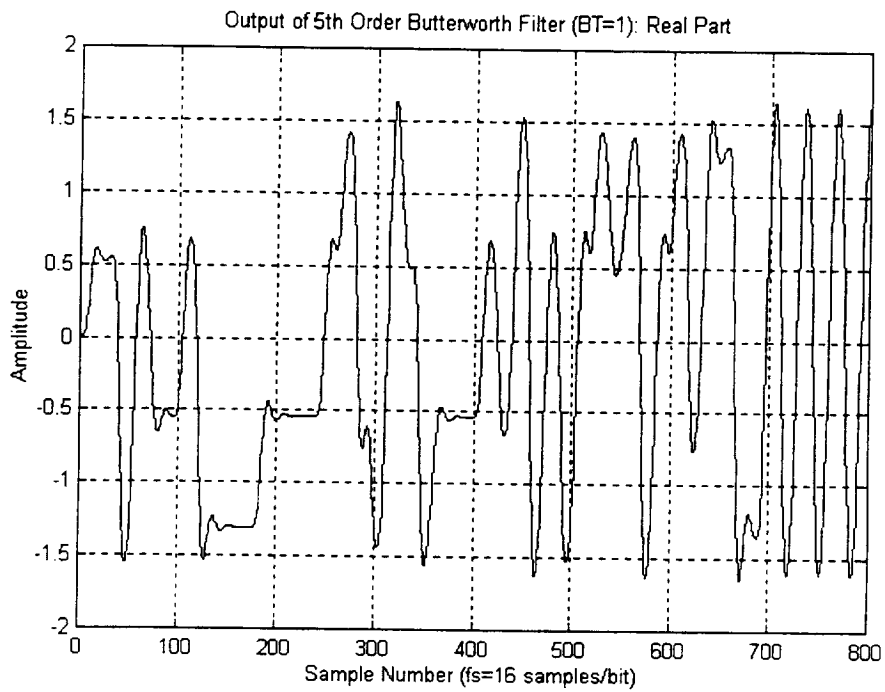


Figure 3.32a - Output of 5th Order Butterworth Filter (BT=1): Real Part

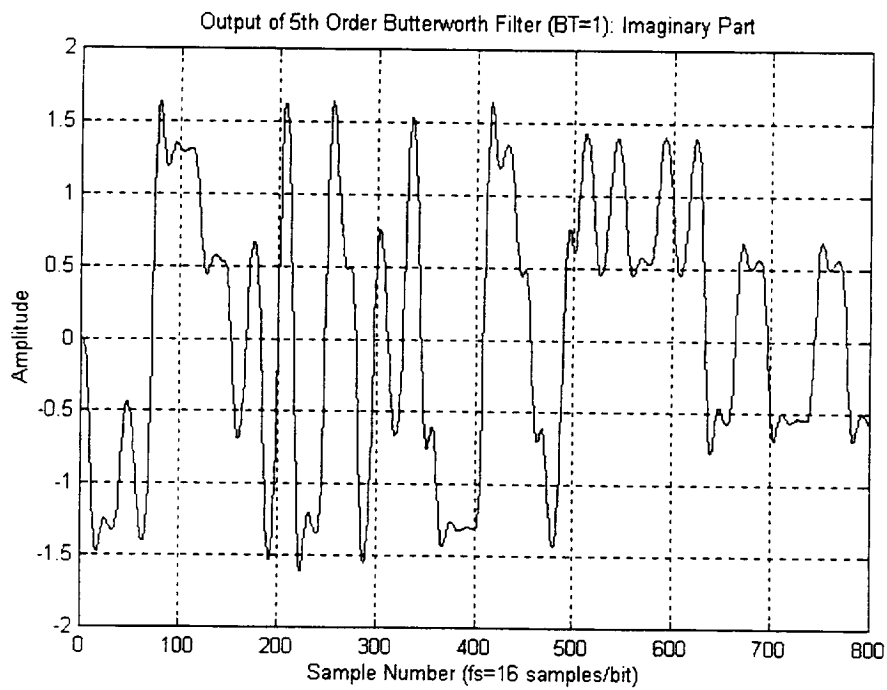


Figure 3.32b - Output of 5th Order Butterworth Filter (BT=1): Imaginary Part

Figure 3.32 - 5th Order Butterworth Filter (BT=1) Output: Real & Imaginary Part

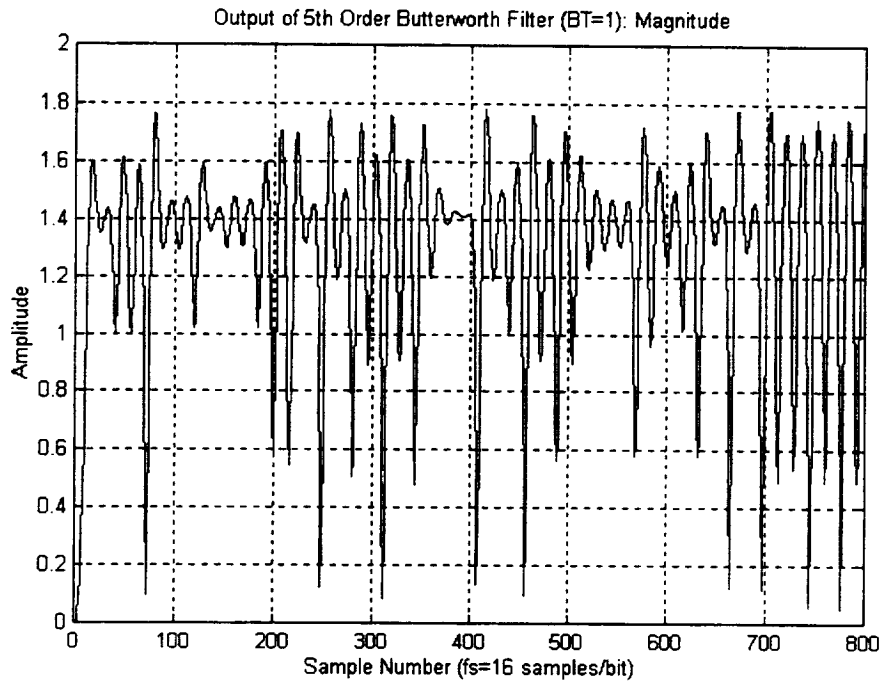


Figure 3.33a - Output of 5th Order Butterworth Filter (BT=1): Magnitude

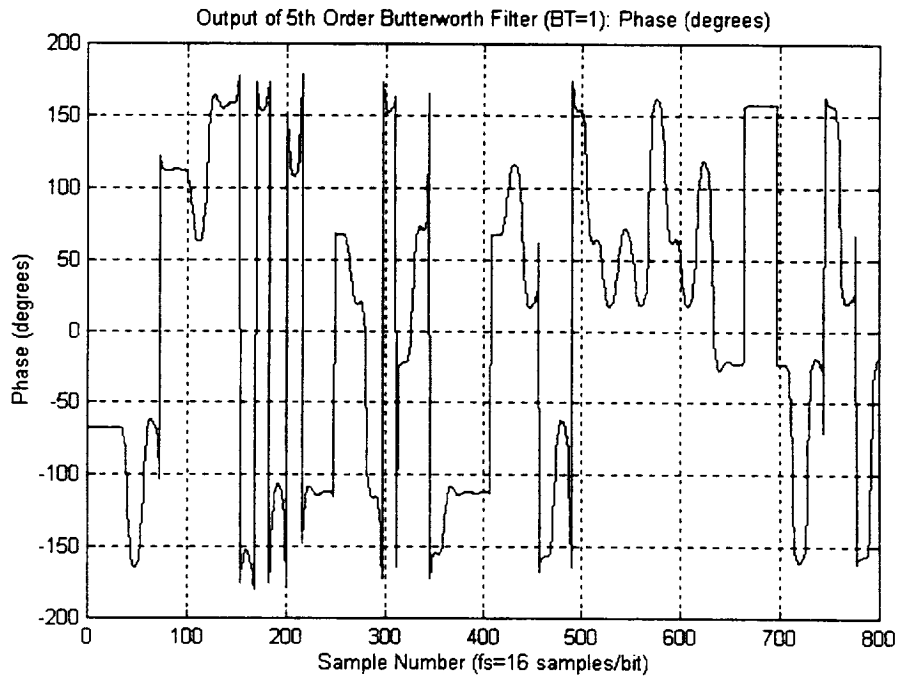


Figure 3.33b - Output of 5th Order Butterworth Filter (BT=1): Phase (degrees)

Figure 3.33 - 5th Order Butterworth Filter (BT=1) Output: Magnitude & Phase

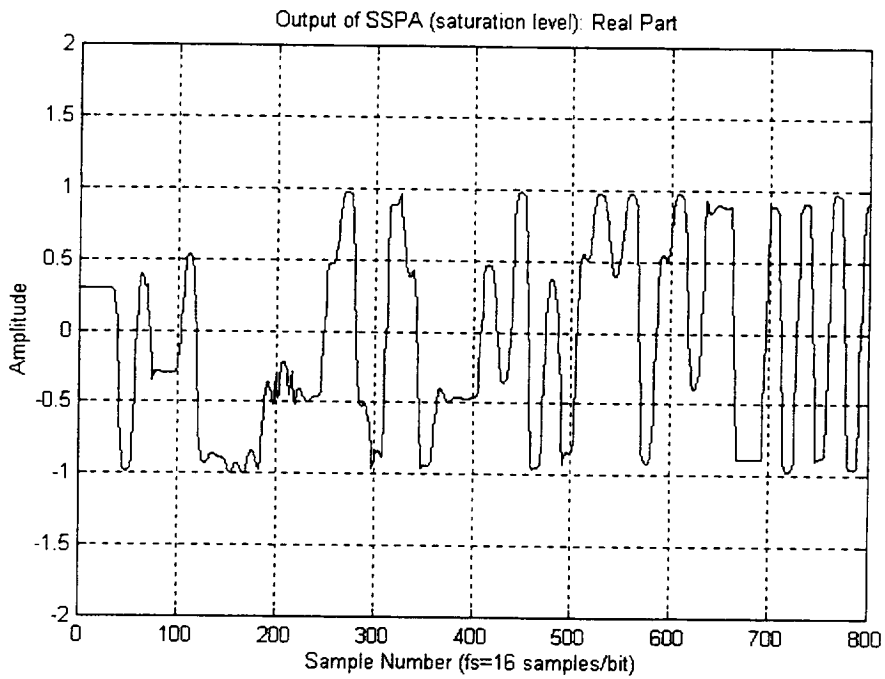


Figure 3.34a - Output of SSPA (Saturation Level): Real Part

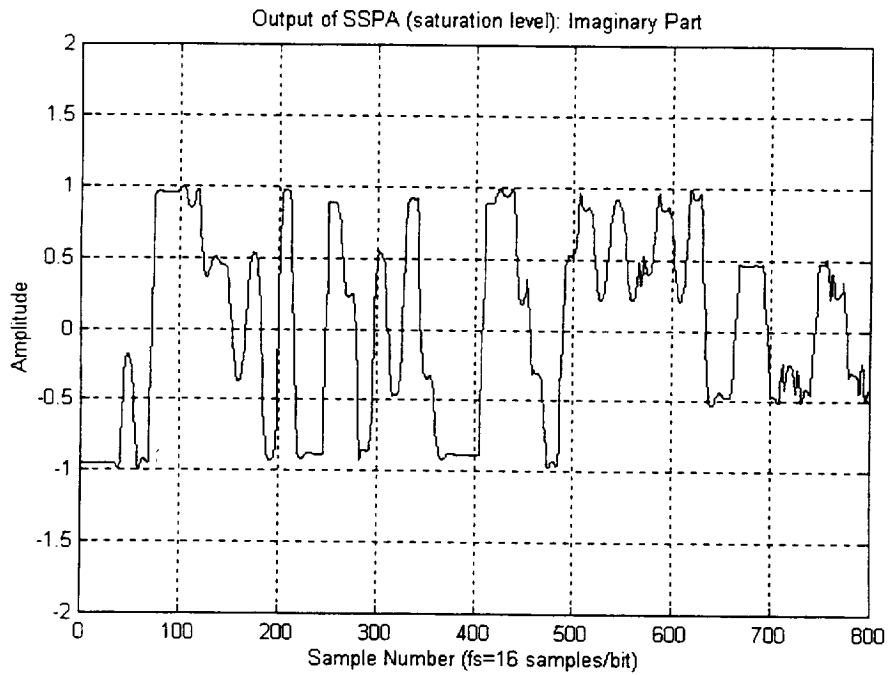


Figure 3.34b - Output of SSPA (Saturation Level): Imaginary Part

Figure 3.34 - Output of SSPA (Input = Output of 5th Order Butterworth Filter (BT=1)): Real & Imaginary Part

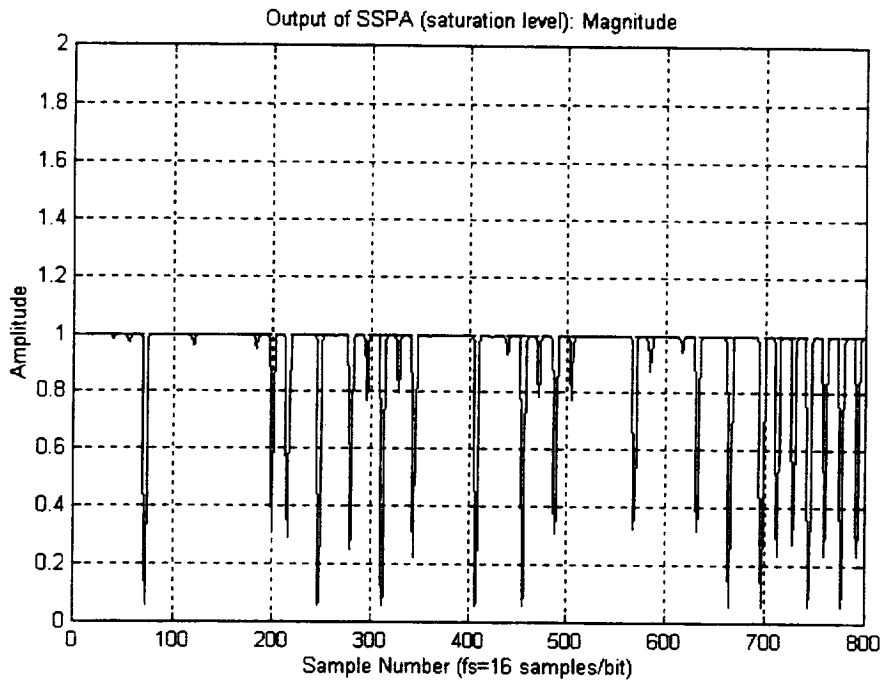


Figure 3.35a - Output of SSPA (Saturation Level): Magnitude

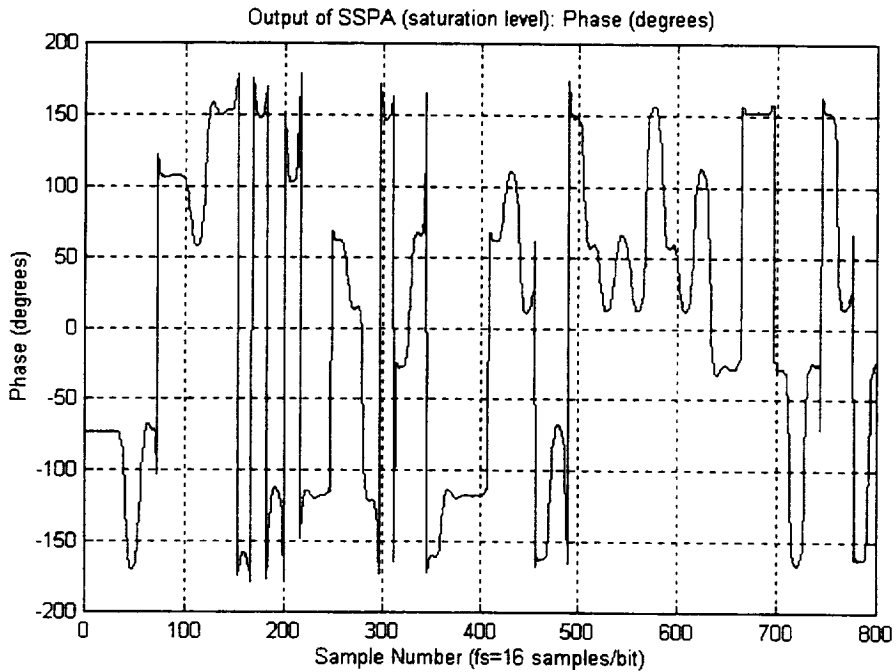


Figure 3.35a - Output of SSPA (Saturation Level): Phase (degrees)

Figure 3.35 - Output of SSPA (Input = Output of 5th Order Butterworth Filter (BT=1)): Magnitude & Phase

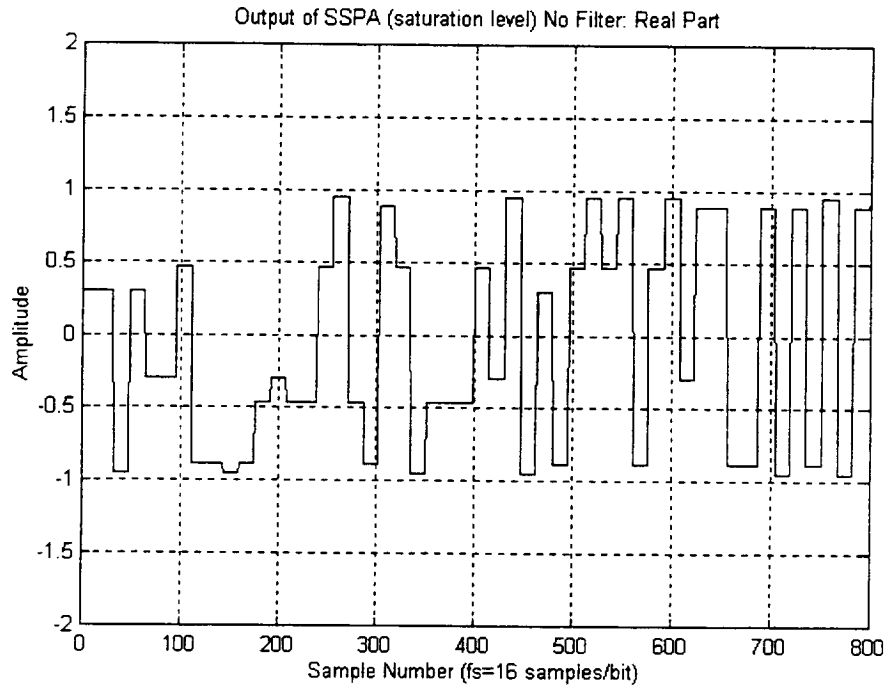


Figure 3.36a - Output of SSPA (Saturation Level) No Filter: Real Part

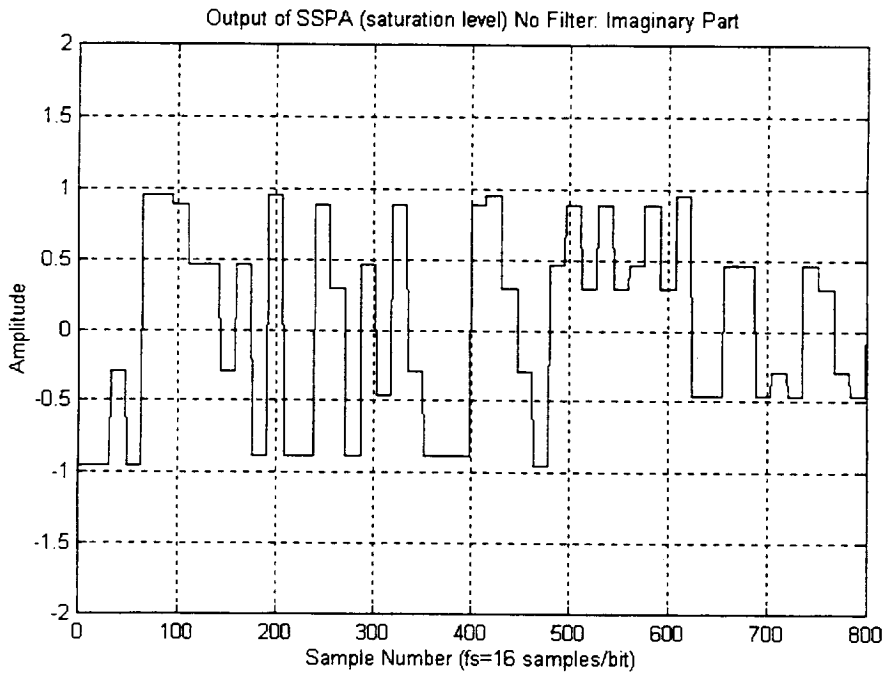


Figure 3.36b - Output of SSPA (Saturation Level) No Filter: Imaginary Part

Figure 3.36 - Output of SSPA (Input = Output of 8PSK Modulator (Constant Envelope)): Real & Imaginary Part

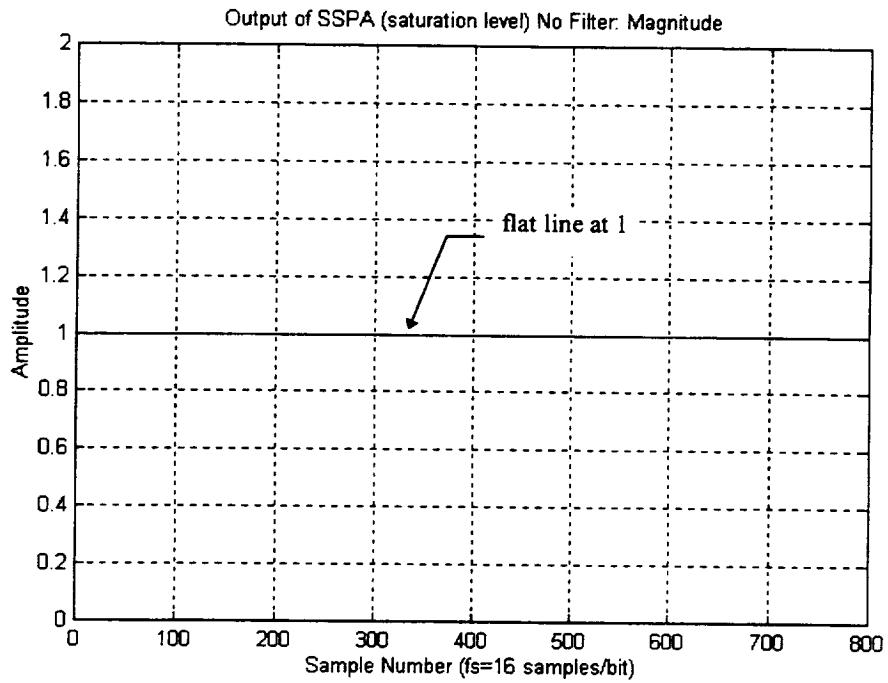


Figure 3.37a - Output of SSPA (Saturation Level) No Filter: Magnitude

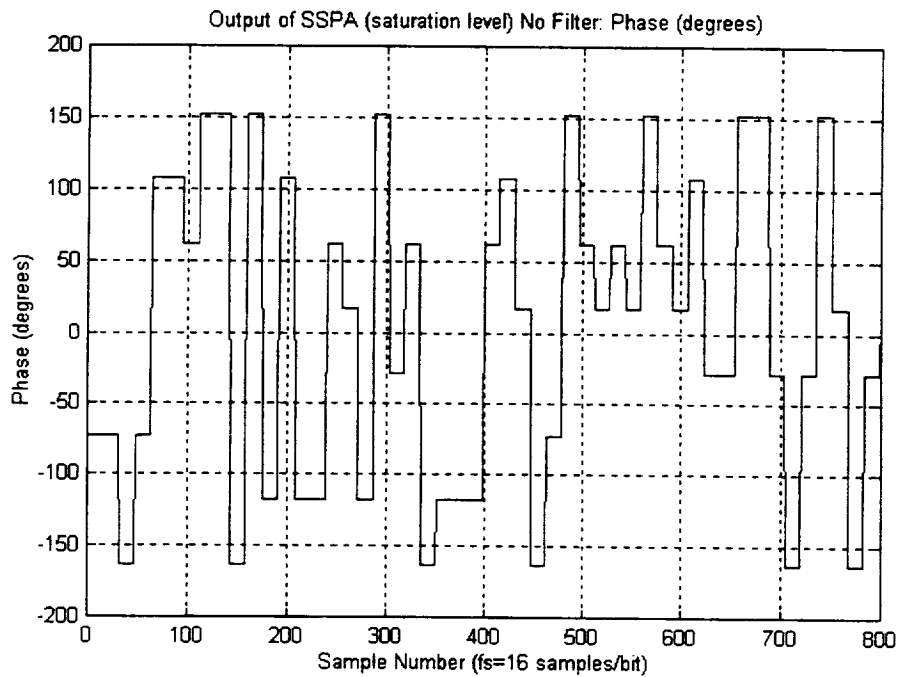


Figure 3.37b - Output of SSPA (Saturation Level) No Filter: Phase (degrees)

Figure 3.37 - Output of SSPA (Input = Output of 8PSK Modulator (Constant Envelope)):

Magnitude & Phase

When amplitude modulation is introduced in the input data (which can be introduced into the PSK signal by pulse shaping - filtering), then the output from the SSPA(at saturation level) will be different from the input, i.e., if ones tries to amplify an AM signal with this type of SSPA (in the non-linear zone) or other nonlinear amplifiers, the AM on the output will be distorted. However, RF signals with a constant envelope, such as FM signals, may be amplified without distortion since a nonlinear amplifier preserves the zero-crossings of the input signal. Therefore pulse shaping gives a smaller bandwidth but a non-constant envelope which reduces the performance of the communication system. On the other hand, no pulse shaping gives a larger BW but the signal has a constant envelope which is a plus on the performance of the receiver filter. It would then be interesting to investigate the trade-off between constant envelope and BW.

A proposed question was:

*How much variation in the constant envelope occurs
as the bandwidth is made smaller due to pulse shaping?*

To answer to this question, it is necessary to measure the bandwidth and envelope variation for different types of pulse shaping. It would then be possible to see what type of relationship these two parameters have. To analyze the effect of non-constant envelope going through the SSPA, different simulations where conducted on SPW with the 3 types of filters used for the power spectrum plots and SER curves performed, in the first and second parts of this report:

- (1) - 5th Order Butterworth Filter;
- (2) - 3rd Order Bessel Filter; and
- (3) - SRRC Filters.

Figure 3.38 shows a block diagram of the circuit used to perform the simulations (Appendix C contains more detailed diagrams and explanations).

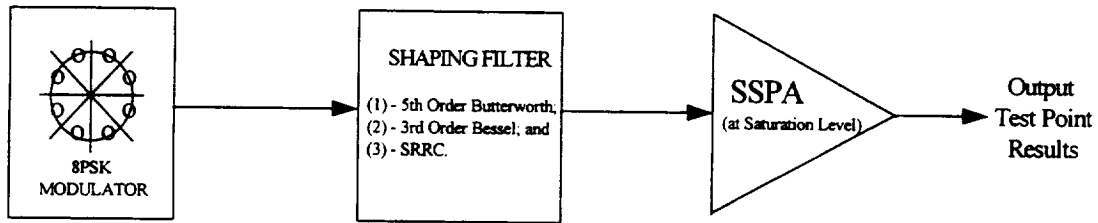


Figure 3.38 - Non-Constant Envelope Simulations Block Diagram

Note that all simulations were performed at baseband and the SSPA was used at saturation level.

Figure 2.10 showed the magnitude characteristic curve of the ESA 10 Watts SSPA that was used in these simulations. Figure 3.39 shows the same curve as Figure 2.10 but zoomed in the non-linear and saturation level regions (between -6 to 1 dB for the Input Level Power).

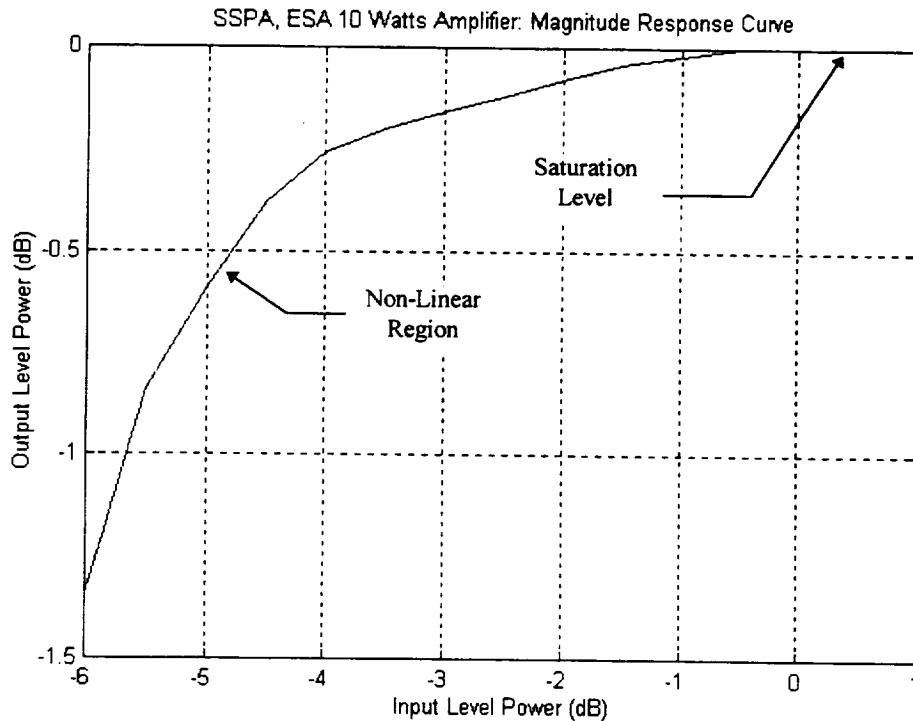


Figure 3.39 - SSPA, ESA 10 Watts, Zoomed Magnitude Characteristic Curve

Note that that the saturation level region and non-linear region are very close, i.e., approximately -2 dB which corresponds to a voltage of $0.794 (10^{-2dB/20})$. A voltage of 1 is at 0dB input level Power. Therefore all simulations were performed using a reference of 0 dB or 1 volt.

In Figure 3.40, the Phase Response of the SSPA that was used is shown.

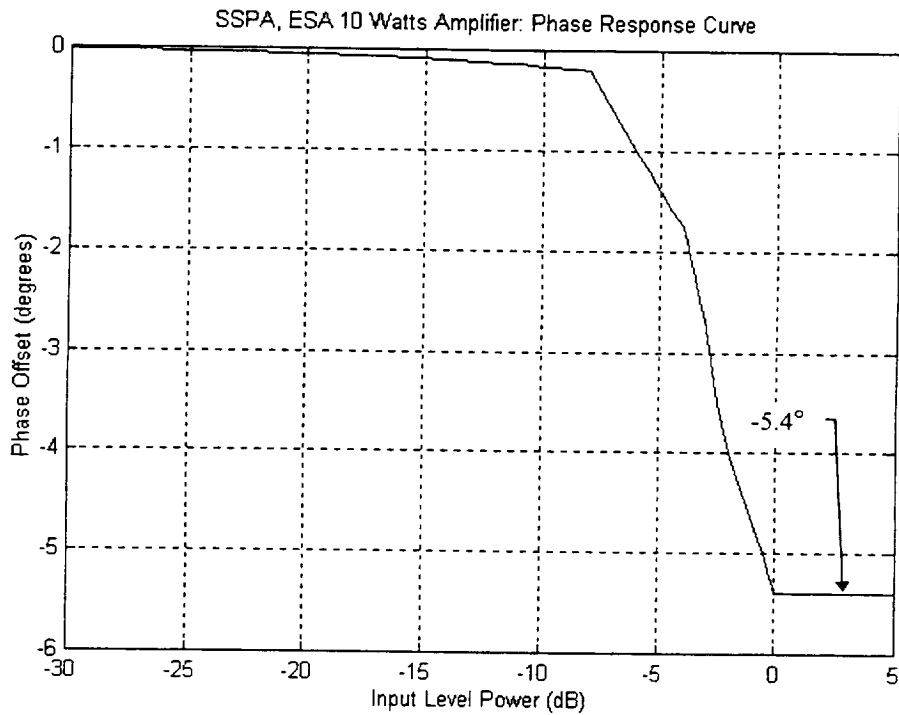


Figure 3.40 - SSPA, ESA 10 Watts, Phase (degrees) Characteristics Curve

Appendix B contains the table of the values of this amplifier and the block diagram used to simulate or interpolate the values from the table. From the phase response curve (Figure 3.40), it is to be noted that a phase rotation of approximately -5.4° occurs at 0 dB of input level. This will cause a rotation of the 8PSK symbols as shown in Table 3.9.

Table 3.9 - Rotation of 8PSK Symbols due to PM Conversion on SSPA

PM CONVERSION AT SATURATION LEVEL (≈ 0 dB Input Level)								
SYMBOLS	1	2	3	4	5	6	7	8
Initial Position ($^{\circ}$)	22.5 $^{\circ}$	67.5 $^{\circ}$	112.5 $^{\circ}$	157.7 $^{\circ}$	202.5 $^{\circ}$	247.5 $^{\circ}$	292.5 $^{\circ}$	337.5 $^{\circ}$
PM Rotation ($^{\circ}$)	-5.4 $^{\circ}$	-5.4 $^{\circ}$	-5.4 $^{\circ}$	-5.4 $^{\circ}$	-5.4 $^{\circ}$	-5.4 $^{\circ}$	-5.4 $^{\circ}$	-5.4 $^{\circ}$
Final Position ($^{\circ}$) = Initial Position - PM Rotation	17.1 $^{\circ}$	62.1 $^{\circ}$	107.1 $^{\circ}$	152.3 $^{\circ}$	197.1 $^{\circ}$ or -162.9 $^{\circ}$	242.1 $^{\circ}$ or -117.9 $^{\circ}$	287.1 $^{\circ}$ or -72.9 $^{\circ}$	332.1 $^{\circ}$ or -27.9 $^{\circ}$

From Table 3.9, a rotation of -5.4° will be introduced to any signal with 0 dB gain (on a 1 volt reference). Thus if a non-constant envelope signal goes through this SSPA, a maximum rotation of -5.4° will be induced but also smaller values of rotation will be introduced ($< |-5.4^{\circ}|$) depending on the input level of the non-constant envelope signal. For example, Figure 3.41 shows the scatter plot of Figures 3.30, 3.32, 3.34, i.e., the 8PSK Modulator, 5th Order Butterworth Filter (BT=1) and SSPA (Saturation Level) Outputs. A scatter plot, also known as the signal “constellation” or “I-Q plot”, shows the location in the complex plane of the in-phase and quadrature-phase components of a complex signal at discrete time samples.

Scatter Plot: 8PSK Modulator, 5th Order Butterworth Filter (BT=1) and SSPA Output (saturation level)

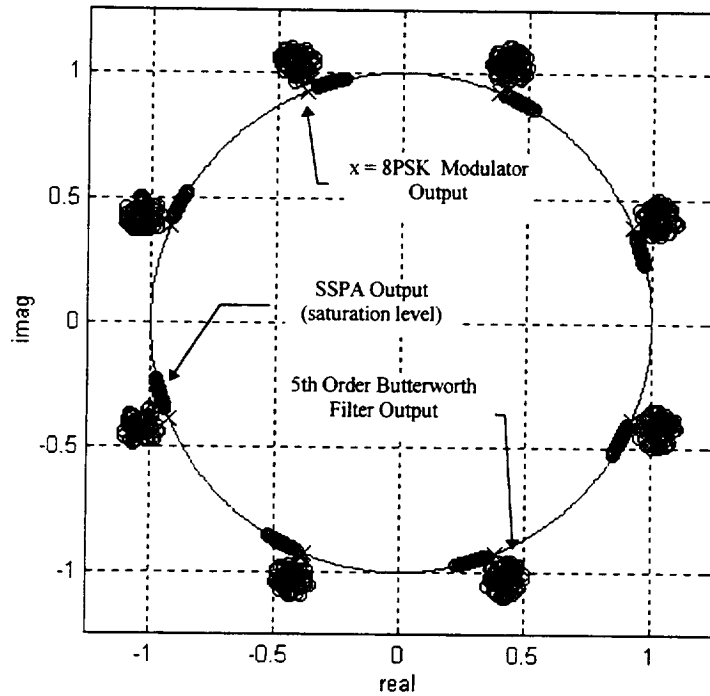


Figure 3.41 - Scatter Plot: 8PSK Modulator, 5th Order Butterworth Filter (BT=1) and SSPA (Saturation Level) Outputs

Note that in this last figure the symbol “x” represents the symbols output from the 8PSK Modulator. The position of these symbols is exactly at $[(\pi/8)*i + (\pi/4)]$ and have an amplitude of 1 (everything was normalized to 1 volt or 0dB). The second set of points (cluster of points outside the unit circle) represents the output of the 5th Order Butterworth Filter with BT=1. Note how the symbols are not shown as a single element anymore; this is due to the non-constant envelope introduced by filtering the input signal (output of the 8PSK Modulator). This cluster will be larger or smaller depending on if the signal has a more constant envelope or non-constant envelope, respectively. The signal was not rotated or phase shifted going through the filter therefore the mean of the cluster is approximately $[(\pi/8)*i + (\pi/4)]$. Finally the last set of points (points aligned on the unit circle) represents the output of the SSPA.

Note that this time the symbols have been rotated ($\approx -5.4^\circ$) due to the AM/PM conversion introduced by the SSPA. Also the symbols are aligned on the unit circle since the SSPA is operating at saturation level (0 dB or 1 volt).

To be able to create this scatter plot from Figures 3.30, 3.32 and 3.34, the following procedure was followed. First a simulation on SPW was performed using the block diagram shown in Figure 3.34 (a more detailed diagram is shown and explained in Appendix C). Then when the simulation was completed, the American Information Code for Information Interchange (ASCII) file containing the complex values of the output of the SSPA for example (signal shown in Figure 3.30) was transferred (File Transfer Protocol (FTP)) to a Personal Computer (PC 486 66 MHz) where the signal was sampled to its optimum value to produce the SSPA Output scatter plot shown in Figure 3.41. For example, for the signal in Figure 3.30, a signal delay equal to 20 samples had to be used to get the optimum scatter plot. This delay of 20 samples was calculated as follows:

First the pulse shaping filter (5th Order Butterworth Filter (BT=1)) and SSPA introduced a delay of 12 samples (includes the delay due to the transition) and since the sampling of the received bit has to occur in the middle of the bit ($f_s/2$ where f_s = sampling frequency = #samples/bit), then

$$T_{\text{sampling time}} = (\text{Delay of 5th Order Butterworth filter (BT=1) and SSPA}) + (f_s/2)$$

where for the 5th Order Butterworth Filter (BT=1), the sampling frequency = $f_s = 16$ samples/bit (for more information on the choice of the value of f_s , refer to Appendix C).

Thus

$$T_{\text{sampling time}} = 12 \text{ samples} + (16 \text{ samples/bit} / 2) = 12 + 8$$

$T_{\text{sampling time}} = 20 \text{ samples}$

All this was processed in a MATLAB^{††} file called SPWSOBRE.M (see Appendix D). This procedure reads the ASCII file transferred from SPW and samples it as discussed above to produce a scatter plot. Afterwards, the mean and variance of each symbol is calculated.

The mean for each symbol, in one of the eight decision regions (described below) is calculated as follows:

$$\theta_{mean(i)} = \text{mean}[\theta(i)] \quad \text{for } i = 0 \text{ to } 7 \text{ inclusively}$$

where

• $\theta(i)$ are all the angles of the symbol contained in one of the eight decision regions

delimited by:

$$\text{region 0: } 0 \leq \theta \leq \pi/4 \quad \text{or} \quad 0 \leq \theta \leq 45^\circ;$$

$$\text{region 1: } \pi/4 < \theta \leq \pi/2 \quad \text{or} \quad 45^\circ < \theta \leq 90^\circ;$$

$$\text{region 2: } \pi/2 < \theta \leq 6\pi/8 \quad \text{or} \quad 90^\circ < \theta \leq 135^\circ;$$

$$\text{region 3: } 6\pi/8 < \theta \leq \pi \quad \text{or} \quad 135^\circ < \theta \leq 180^\circ;$$

$$\text{region 4: } -\pi < \theta \leq -6\pi/8 \quad \text{or} \quad -180^\circ < \theta \leq -135^\circ;$$

$$\text{region 5: } -6\pi/8 < \theta \leq -\pi/2 \quad \text{or} \quad -135^\circ < \theta \leq -90^\circ;$$

$$\text{region 6: } -\pi/2 < \theta \leq -\pi/4 \quad \text{or} \quad -90^\circ < \theta \leq -45^\circ; \text{ and}$$

$$\text{region 7: } -\pi/4 < \theta \leq 0 \quad \text{or} \quad -45^\circ < \theta < 0^\circ;$$

^{††} MATLAB is a registered trademark of The MatWorks Inc., Cochituate Place, 24 Prime Park Way, Natick, Mass. 01760.

• $\text{mean}[x]$ is a function in Matlab that calculates the mean of the vector x . In this case x is a vector containing the angles of the symbols in one of the 8 decision regions. The mean in Matlab is calculated in the following manner:

$$\text{mean}[\theta(i)] = \frac{1}{N} \left[\sum_{x=1}^N \theta_x(i) \right]$$

where i = decision region ($0 \leq i \leq 7$);

x = element in the vector $\theta(i)$; and

N = number of points in the decision region or vector $\theta(i)$.

Also the variance of the symbol vectors are calculated to see the distribution of the symbols around the mean in the decision region. In SPWSOBRE.M the following line calculates the variance:

$$\theta_{\text{variance}(i)} = [\text{std}[\theta(i)]]^2$$

where std = standard deviation which is a function defined in Matlab as being the sample standard deviation normalized by the square root of $(N-1)$, where N is the sequence or vector length. Thus in other words, the variance is calculated as

$$\theta_{\text{variance}(i)} = \frac{1}{(N-1)} \cdot \sum_{x=1}^N (\theta_x(i) - \theta_{\text{mean}(i)})^2$$

where

i = 0 to 7 (decision regions); and

N = number of points in the decision region.

Figure 3.42 graphically shows the mean and variance in a decision region:

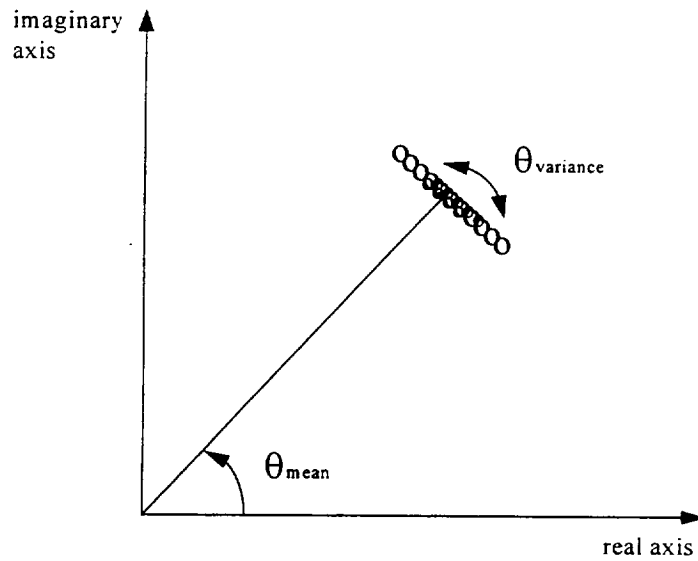


Figure 3.42 - Mean and Variance in Decision Region

Thus, for the 5th Order Butterworth filter with BT=1, the scatter plot due to the SSPA shown in Figure 3.41 has the following values of mean and variance (calculated as shown above) for the 8 symbols:

Table 3.10 - Mean and Variance of SSPA Output (Saturation Level) with 5th Order Butterworth (BT=1)

SYMBOLS	1	2	3	4	5	6	7	8
θ_{mean} (°)	17.020°	62.250°	106.80°	152.58°	-162.98° or 197.02°	-117.86° or 242.14°	-72.650° or 287.35°	-27.753° or 332.247°
$\theta_{variance}$ ($\times 10^{-2}$)°	7.1477	6.3547	5.2001	6.6354	5.4146	5.4370	6.6427	7.4719

If the 2nd row of Table 3.10 is compared with the last row of Table 3.9, it is noted that the results are very similar. The same simulations as described above were conducted for different Bandwidth-Time (BT) products for the 5th Order Butterworth Filter and the 3rd Order Bessel Filter.

Also, the SRRC filter was simulated for roll-off factors varying from 0.1 to 1 ($\alpha = 0.0$ could not be simulated due to software capabilities; the roll-off factor α has to be > 0.0 in SPW). Table 3.11 summarizes the different bandwidth and spectrum filters that were used to see the effect of non-constant envelope through an SSPA.

Table 3.11 - Non-Constant Envelope Simulations: Filters and BW used

SPECTRUM FILTER	BANDWIDTH
5 th Order Butterworth	BT = 1, 1.05, 1.1, 1.2, 1.4, 1.6, 1.8, 2, 2.2, 2.4, 2.6, 2.8, 3, 3.2, 3.4, 3.6, 3.8, 4
3rd Order Bessel	BT = 1, 1.05, 1.1, 1.2, 1.4, 1.6, 1.8, 2, 2.2, 2.4, 2.6, 2.8, 3, 3.2, 3.4, 3.6, 3.8, 4
SRRC	$\alpha = 0.1, 0.15, 0.2, 0.25, 0.3, 0.35, 0.4, 0.45, 0.5, 0.55, 0.6, 0.65, 0.7, 0.75, 0.8, 0.85, 0.9, 0.95, 1.00$

The following figures, i.e., Figure 3.43 - 5th Order Butterworth Filter: Average Symbol Variance vs BT, Figure 3.45 - 3rd Order Bessel Filter: Average Symbol Variance vs BT and Figure 3.47 - SRRC Filter: Average Symbol Variance vs Roll-off factor (α), show the average symbol variance plotted against the bandwidth. The Average Symbol Variance was calculated as follows:

$$\frac{\sum_{i=1}^8 \theta \text{ variance}(i)}{8}$$

which can be explained as being the average of the sum of the variances in the decision regions.

These figures show the effect of varying the non-constant envelope of a signal (by using different BT or α) through an SSPA. The Average Symbol Variance is used as a parameter indicating the spreading of the symbol with respect to the mean for each of the 8 decision regions. For the 5th Order Butterworth Filter in Figure 3.43, it is noted that the variance substantially decreases from BT=1 to BT=1.1. This can be explained by the fact that for BT=1, the filter is narrower and contains only the main lobe of the power spectral density (refer to section 3.2).

Thus the signal in the time domain will be more distorted (non-constant envelope) than when a larger order of BT (or bandwidth) is utilized (the envelope becomes more constant).

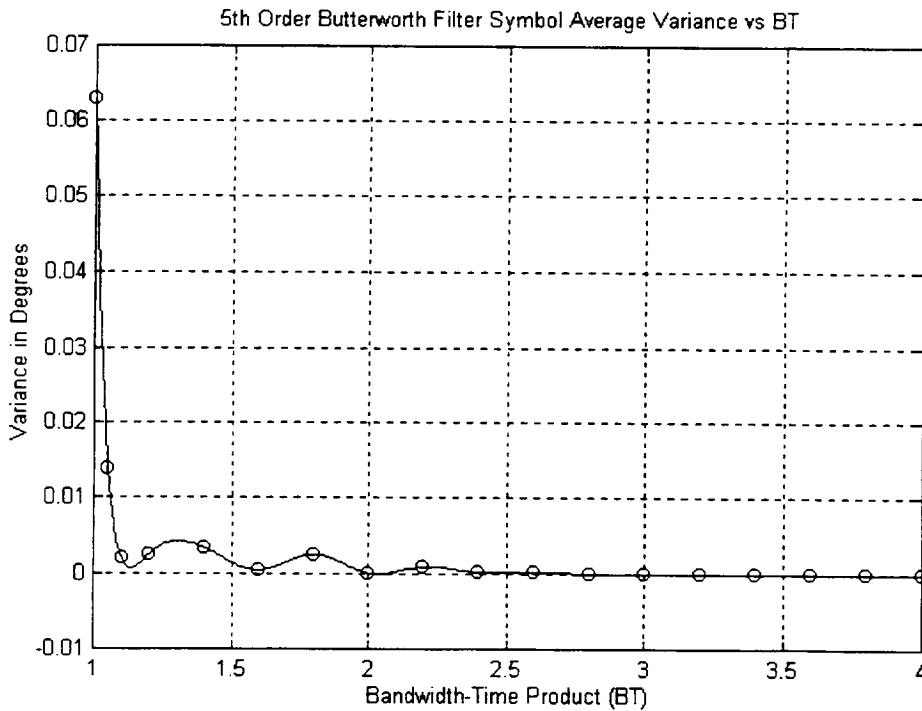


Figure 3.43 - 5th Order Butterworth Filter: Average Symbol Variance vs BT

It is interesting to note how the variance ripples down as the BT is increased. Eventually as BT is very large (at the limit $BT = \infty$), the variance should be equal to 0 since almost all of the PSD (or energy) of the signal is captured.

Figure 3.44 shows a zoomed version, between $BT=1.2$ and 3.2 , of Figure 3.43. Note the symmetry of the ripples as they go to 0. The simulations points “o” were linked together using an interpolation function called “spline” in Matlab.

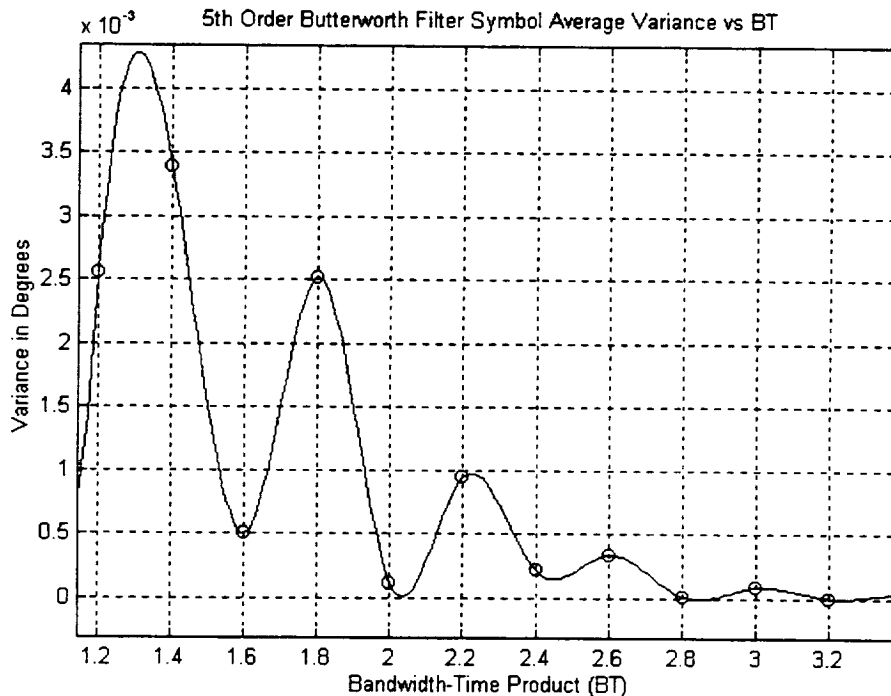


Figure 3.44 - Zoom of Average Symbol Variance vs BT for 5th Order Butterworth Filter

Appendix E contains the scatter plots of the points for Figures 3.43 and 3.44; note that one point in Figure 3.43 corresponds to the average variance of the symbols in one scatter plot. Also a listing of the program (BUTTPLOT.M) written in Matlab, that was used to create the plot, is included.

Figure 3.45, shows the results of variance vs BT for the 3rd Order Bessel Filter. Again as in the Butterworth case presented earlier, the average variance gradually decreases in a sinusoidal form. The damping is more pronounced for the 3rd Order Bessel than the 5th Order Butterworth since the Bessel's variance starts to become a flat line around $BT=1.8$ but for the Butterworth Filter case the steady line becomes present around $BT=3$. Also note that the average variance is appreciably less in magnitude for the Bessel filter (order of magnitude $\approx 10^{-4}$) than the Butterworth filter (order of magnitude $\approx 10^{-2}$). Figure 3.46 shows a zoomed version (between $BT = 1.4$ and 3.7) of Figure 3.45.

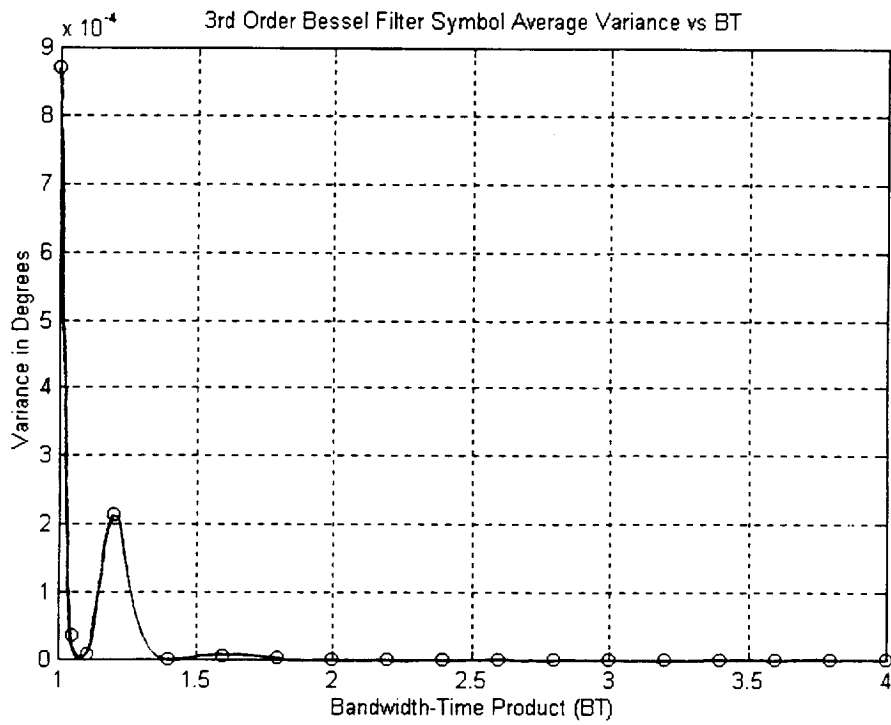


Figure 3.45 - 3rd Order Bessel Filter: Average Symbol Variance vs BT

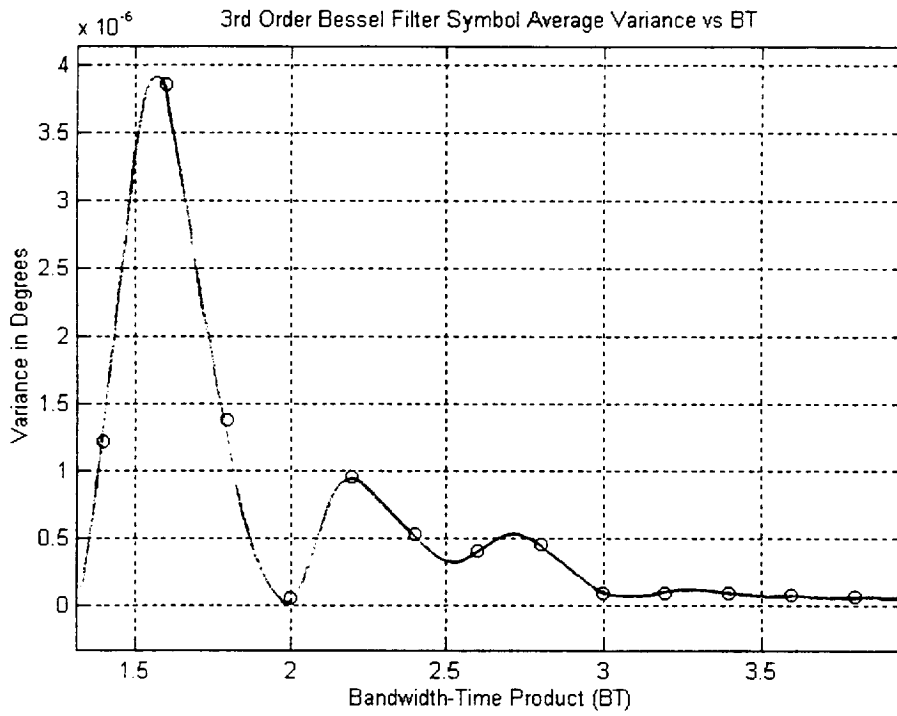


Figure 3.46 - Zoom of Average Symbol Variance vs BT for 3rd Order Bessel Filter

Appendix F contains the scatter plots of the points for Figure 3.45 and 3.46; again, note that one point in Figure 3.45 or 3.46 corresponds to the average variance of the symbols in one scatter plot. Also a listing of the program (BESSPLOT.M) written in Matlab, that was used to create the plot, is included. If the scatter plots in Appendix E and F are compared, it is noted that in fact the average variance is significantly less for the 3rd Order Bessel filter than the 5th Order Butterworth Filter.

Finally Figure 3.47 shows the average variance versus the roll-of factor for the SRRC filter.

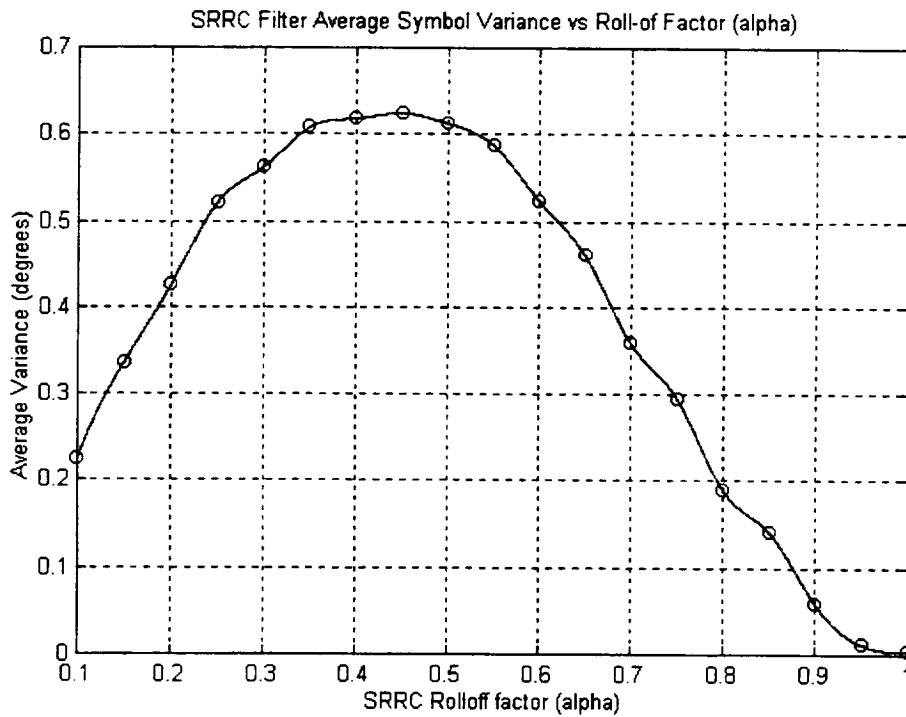


Figure 3.47 - SRRC: Average Symbol Variance vs Roll-off factor (α)

In this case note that the aspect of the plot is really different from the two previous filters. In fact, for the SRRC, the plot appears to have the aspect of a second order parabola with a maximum at approximately $\alpha=0.45$. Note that simulations could not be performed for $0 \leq \alpha < 0.1$ due to SPW software limitations. Nonetheless, it can be seen that the curve gradually decreases to 0 as α reaches 0. This can be explained by the fact that for $\alpha=0$, the frequency response of a SRRC is a pure square wave (or “brick wall”). Thus in the time domain, it would then correspond to a pure sinc ($\sin(x)/x$)

function which would have the zero crossings at the sampling frequency therefore eliminating any ISI. For the case where α reaches 1, the average variance also decreases toward 0 (but it does not reach it). This can be explained since the SRRC filter has a bigger BW for higher α therefore allowing more of the power spectrum to be included in the transmission; this is the same result as increasing the BT for the Butterworth or Bessel Filter. Finally note how the magnitude of the average variance is larger for the SRRC filter than the Butterworth and Bessel.

Appendix G contains the scatter plots of the points for Figure 3.47. Also a listing of the program (SRRCPLOT.M) written in Matlab, that was used to create the plot, is included. If the scatter plots in Appendix E, F and G are compared, it is noted that in fact the average variance is significantly bigger for the SRRC filter than the 3rd Order Bessel filter or the 5th Order Butterworth Filter.

Chapter 4

CONCLUSIONS AND RECOMMENDATIONS

From the simulations on 8PSK Baseband Filtering performed in the Center for Space Telemetry and Telecommunications Systems at NMSU, the following conclusions can be made on the PSD, SER and Non-Constant Envelope:

With respect to PSD and SER for the 8PSK signal which is an extension of the work performed during Phase I, II and III (refer to [1], [2], [3] and [4]) of this study :

- In-band spurious emissions are more present and more evident for the Bessel Filter than the Butterworth Filter (BT=1). With respect to the sideband attenuation, it was found that the values of attenuation for the 3rd Order Bessel are comparable to the 5th Order Butterworth (refer to Tables 3.3 and 3.4 in the report).
- For SRRC filters with $\alpha = 0.25$ and $\alpha = 0.5$, the bandwidth is narrower than the Butterworth and Bessel Filters but the attenuation is less at high frequencies. Nonetheless, the absence of spurious emissions is a net advantage. For SRRC $\alpha = 1$, the bandwidth is wider than the two previous SRRC filters and the absence of in-band spurious emissions was again noticed. Less sideband attenuation was recorded for this roll-off factor compared with $\alpha = 0.25$ and $\alpha = 0.5$.
- For SER, it was found that the Butterworth and Bessel Filters just barely meet the threshold of ISI loss < 0.4 dB at $SER = 10^{-3}$. Also the SRRC filters do not meet this specification. Since this threshold is barely met by the first two filters and this simulation was performed with only ideal data and system it seems reasonable that a simulation with $BT = 4$ should be performed which would certainly meet the threshold.

From these results, it can be stipulated that the 5th Order Butterworth has a small advantage compared to the other filters. Also more simulations should be performed on the power spectrum content depending on the value of BT that meets the threshold mentioned above. Therefore, for example for $BT = 4$, the power spectrum plots should be produced to be able to calculate the new Band Utilization ratio, ρ .

Overall, it was shown by using baseband filtering the bandwidth utilization can be improved by a factor of approximately 12 to 24 with $BT=1$ and 8PSK (see Table 3.8 in this report) which can significantly increase the spectrum utilization. In Phase II (refer to [3]), it was demonstrated that for BPSK, this bandwidth utilization can be potentially increased from 6 to 10 times with $BT=1$. Thus with respect to bandwidth, 8PSK gives better results (using the same bit rate).

To increase our knowledge with respect to a non-linear satellite channel, specific measurements were performed on the Non-Constant Envelope of the signals going through the non-linear SSPA. These simulations have not been previously reported.

- The tradeoffs between constant envelope and bandwidth were observed with simulations for the 5th Order Butterworth Filter, 3rd Order Bessel Filter and SRRC Filter. The more shaped the pulse (to decrease the bandwidth), the more non-constant the envelope of the signal becomes therefore increasing errors due to non-linearities in the system.

⇒ It was found that the amplitude of the Average Symbol Variance of the signal using the 3rd Order Bessel is much less than for the 5th Order Butterworth Filter. Also the amplitude for the 3rd Order Bessel Filter damps toward zero around $BT=1.8$ where for the 5th Order Butterworth Filter this damping will occur around $BT=3$. These curves have the aspect of a sinusoidal function decreasing exponentially toward zero; and

⇒ The Average Symbol Variance vs α for the SRRC was found to be quite different than the two previous spectrum shaping filters. This plot looks more like a second order parabola with a maximum at approximately $\alpha = 0.45$. Also the amplitude is significantly larger than the two previous filters.

Suggestions for further study

- A non-ideal system can be used for future simulations for SER . This non-ideal system should be predetermined with respect to what kind of components have to be used and the amount of error they introduce.
- Increase the BT to 4 and perform more simulations for PSD and SER.
- For the non-constant envelope simulations more simulations should be performed using different orders of filters for Butterworth and Bessel:

⇒ From these simulations it might be possible to find a general expression on how the variance of the symbols is altered by changing BT. This expression should have the following form: $a \cdot \exp(-x) \cdot \sin(x)$ for the Butterworth and Bessel Filters; and

⇒ It would then be possible to predict, with a general equation, when the BT has no real effect on the shaping of a pulse.

REFERENCES

- [1] Warren L. Martin and Tien M. Nguyen, "CCSDC - SFCG Efficient Modulation Methods Study, A Comparison of Modulation Schemes, Phase 1: Bandwidth Utilization (Response to SFCG Action Item 12/32)," SFCG-13, Ottawa Canada, 13-21 October 1993, report dated 24 September 1993.
- [2] Dr. Manfred Otter, "CCSDC - SFCG Efficient Modulation Methods Study, A Comparison of Modulation schemes, Phase 1b: A Comparison of QPSK, OQPSK, BPSK, and GMSK Modulation Systems (Response to SFCG Action Item 12/32)," European Space Agency/ESOC, Member CCSDS Subpanel 1E, (RF and Modulation), June 1994.
- [3] Warren L. Martin and Tien M. Nguyen, "CCSDC - SFCG Efficient Modulation Methods Study, A Comparison of Modulation Schemes, Phase 2: Spectrum Shaping (Response to SFCG Action Item 12/32)," SFCG Meeting, Rothenberg, Germany 14-23 September 1994, report dated August 1994.
- [4] Warren L. Martin, Tien M. Nguyen, Aseel Anabtawi, Sami M. Hinedi, Loc V. Lam and Mazen M. Shihabi, "CCSDC - SFCG Efficient Modulation Methods Study Phase 3: End-to-End System Performance," Jet Propulsion Laboratory, May 1995.
- [5] Israel Korn, "The Effect of Pulse Shaping and Transmitter Filter on the Performance of FSK-DPD and CPM-DPD in Satellite Mobile Channel," IEEE Journal on Selected Areas in Communications, Vol.13, NO. 2, February 1995.
- [6] G. Benelli, V. Capellini, E. Del Re and R. Fantacci, "Evaluation of Constant-Envelope Signals Degradation due to Band-Limited Filtering," IEEE International Conference on Communications '86, Toronto (Ontario) Canada, 1986.
- [7] G. Bharatula, J. Sekfy and J. Millot, "Simulation Studies for Digital Satellite Communications," 20th International Electronics Convention & Exhibition, Melbourne, Australia, October 1985.

- [8] Leon W. Couch II, "Digital and Analog Communication Systems," Macmillan Publishing Company, 1993 , Fourth Edition.

- [9] Stephen Horan, "Introduction to PCM Telemetry Systems," CRC Press Inc. 1993.

- [10] Lonnie C. Ludeman, "Fundamentals of Digital Signal Processing," John Wiley & Sons, 1986.

- [11] Alberto Gutierrez, Jr., "Equalization and Detection for Digital Communication over Non-Linear Bandlimited Satellite Communication Channels," PhD Dissertation by, New Mexico State University, December 1995.

- [12] Theodore John Wolcott, "Uplink-Noise Limited Satellite Communication Systems," Ph.D. Dissertation, New Mexico State University, December 1995.

- [13] Michael Ross, William Osborne and Gregory Jean-Baptiste, " Bandwidth Utilization LDRD, Report for Phase I, Simulation of 32 QAM TCM in SPW," Center for Telemetry Research, Klipsch School of Electrical Engineering, New Mexico State University.

- [14] "SPW - The DSP Framework Communications Library Reference", by Comdisco Systems, Product Number: SPW8015, March 1994.

- [15] "Signal Processing WorkSystem DSP Library Reference", by Alta Group of Cadence Design Systems, Inc. Product Number: SPW8015, March 1995.

APPENDIX A
SPW DETAIL DIAGRAMS
FOR
PSD AND SER SIMULATIONS

This appendix contains the detailed diagrams of the overall system used for the PSD and the SER simulations. Explanations on how these simulations were performed will be given.

A.1 PSD Detailed Diagram

Figure A.1 shows a detailed block diagram of the system used to simulate the PSD with different spectrum shaping filters. First, a MPSK Source block is used and since the simulations were performed for 8PSK the corresponding parameters were given (see right top corner of Figure A.1) to have an 8 level output. The output of this block is saved in a library “rubensigs/modout” for later use. For a more detailed aspect of this block refer to Figure 2.3 in the report. The output of this modulator is then introduced in the “Baseband Spectrum Shaping Filter” (for this case the Butterworth Filter is shown). Figure A.2 shows the contents of this Butterworth Filter Block. When performing simulations the filter order was set to 5 for the Butterworth filter, the attenuation at the passband edge was set to 3dB. These two parameters were kept the same for all the simulations. The sampling frequency was set to 250 samples/bit to be able to have as much spectrum as possible giving a range from $-125 R_B$ to $125 R_B$.

PARAMETERS

sampling rate (Hz) or fs: 250.0
 symbol rate (Hz) or Rsym: (...)
 N (# samples/symbol = fs/Rsym) : (...)
 zeta (data .assymetry: N*0.02) : 0.0
 Carrier Frequency f_c (Hz): 0.0
 Probability of zero: 0.5
 SSPA Backoff (dB): 0.0

MPSK MODULATOR PARAMETERS

MPSK (BPSK = 2, QPSK = 4, 8PSK=8) = 8.0
 C1 (BPSK = 0.0, QPSK = 2.0, 8PSK=2.0) = 2.0
 C2 (BPSK = 0.0, QPSK = 0.0, 8PSK=4.0) = 4.0
 C3 (BPSK = 0.0, QPSK = 0.5, 8PSK=0.5) = 0.5

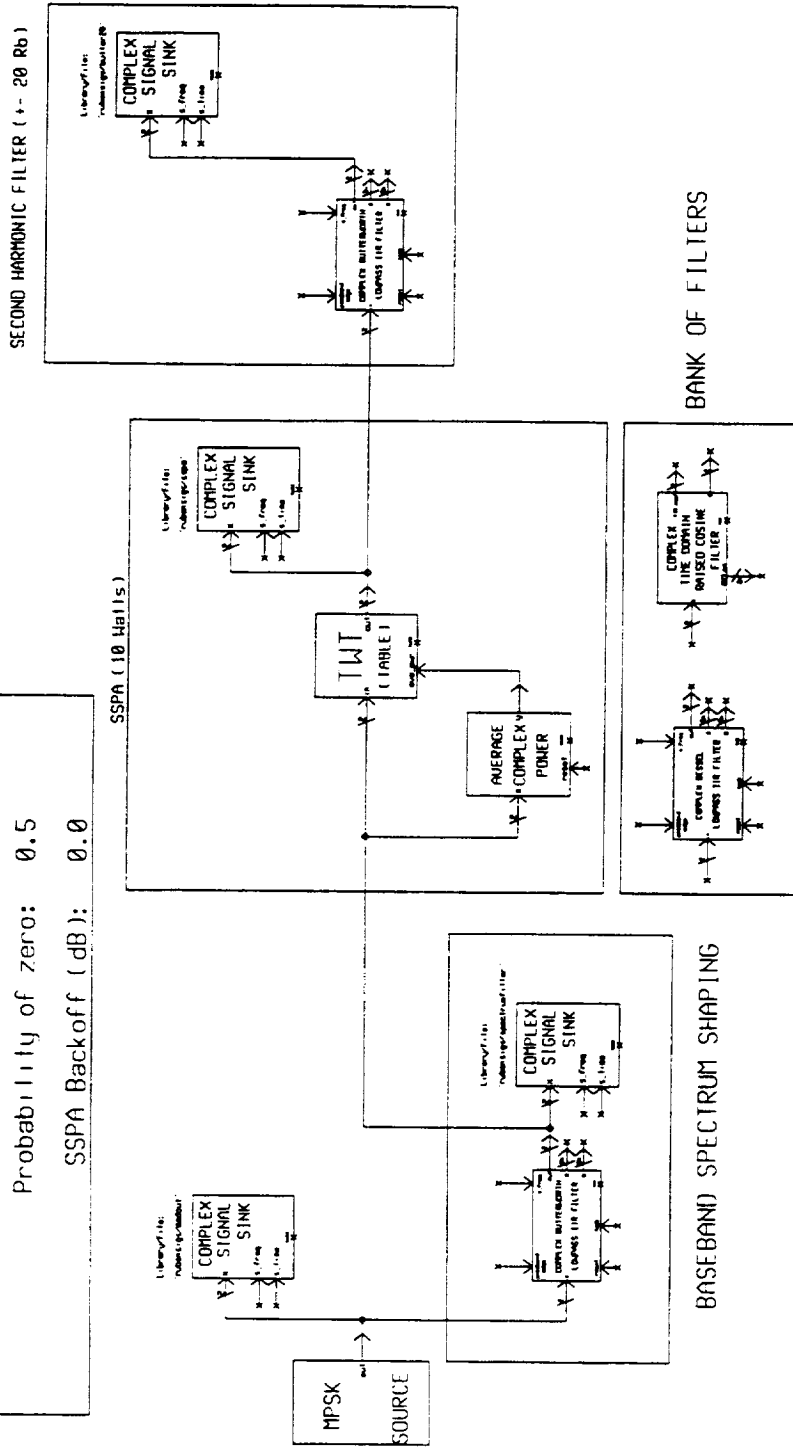


Figure A.1 - PSD Detailed Diagram

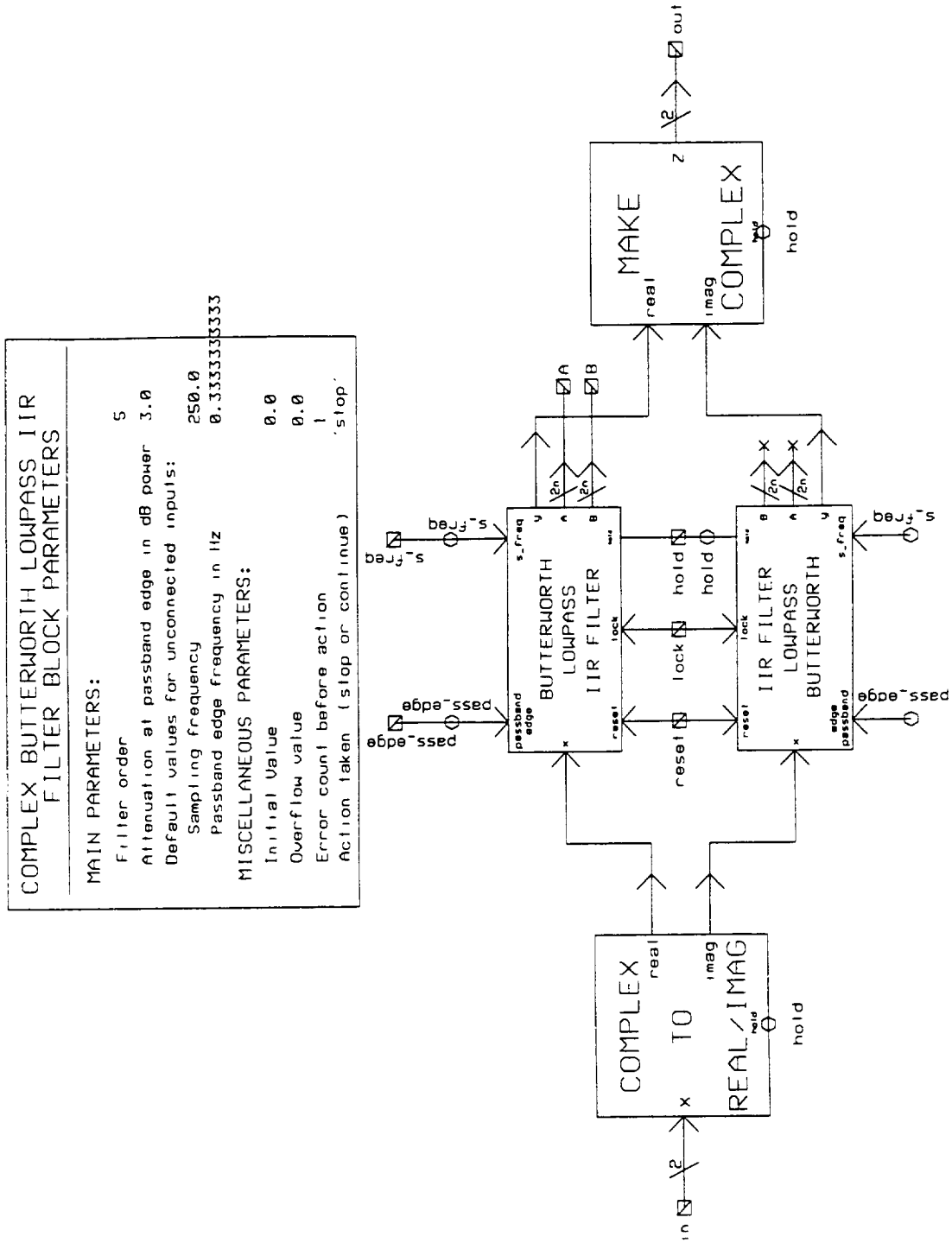


Figure A.2 - Butterworth Filter Block Diagram

For the “Passband Edge Frequency “ parameter, B, the value was set to 1/3 since for this simulation the BT of the filter was 1 thus

$$\begin{aligned} BT &= B * (\text{Symbol Period}) = B * (1 / \text{Symbol Rate}) = B / R_s \\ &= B / (R_B / \lambda) = B * \lambda / R_B \end{aligned}$$

where R_s = Symbol Rate (symbols/sec);

R_B = Bit Rate = 1 bit/sec (set by default for these simulations);

$\lambda = \log_2 8 = 3$; and

B = Passband Edge Frequency or Single-Sided 3dB Bandwidth .

Thus $BT = B * (3/1) = 3B = 1$ which implies that the Passband Edge Frequency = $B = 1/3$ as shown in Figure A.2 and explained above. If the simulation had to be performed for $BT=2$, then the Passband Edge Frequency, B, would be equal to $2/3$ and for $BT=3$, $B=1$. The output of this filter is also saved in a file for later use. The next block of Figure A.1 is the SSPA which is explained in detail in Appendix B. It is to be noted that the output of the SSPA is also saved in a file. Finally in the study of the PSD of 8 PSK, a 2nd Harmonic Filter (4th Order Butterworth Filter) follows the power amplifier. This type of filter is frequently used after the power amplifier to protect users of other bands. The parameters of this filter can be set in the same manner as explained above for the 5th Order Butterworth. Also for this filter, the output is sent into a file.

In the case where non-ideal data had to be simulated in the system the parameter “zeta” or data asymmetry in the top left corner box in Figure A.1 had to be set in following manner. First the parameter “Symbol Rate (Hz) or R_{sym} ” was set to $1/3 (R_B / \lambda)$ as explained above. Using this result, the parameter “N (#samples/symbol = f_s/R_{sym})“ is equal to

$$\frac{f_s}{R_{sym}} = \frac{250 \text{ samples / sec}}{(1/3) \text{ symbol / sec}} = 750 \text{ samples / symbol}$$

and the parameter “zeta” is defined as $N \times 0.02$ since, as explained in this report, CCSDS limits data asymmetry (or zeta in our case) to $\pm 2\%$ (ratio of time duration of a 1 to time duration of a 0). Thus using the formula and result for N shown above:

$$N \times 0.02 = 750 \times 0.02 = 15 \text{ samples/symbol of data asymmetry.}$$

This number would then be entered next to the zeta parameter. Also another parameter that has to be changed when simulating with non-ideal data are the “Probability of Zero” or data imbalance which was defined in this report as the probability of a bit 1 versus the probability of a bit 0. CCSDS limits data imbalance to 0.45. Thus this value of 0.45 would then be entered for the “Probability of Zero”.

The “Carrier Frequency W_c (Hz)” parameter was set to 0 for all the simulations since these were performed at baseband. Also the “SSPA Backoff (dB)” parameter was set to 0 since the simulations were performed at saturation level (except when the 10 dB Backoff simulations were performed; then the value of SSPA Backoff was set to 10 dB).

When these parameters are set, the simulation is started by using the “run” function in SPW. For the PSD simulations, 300 000 samples were used. After the simulation is terminated, the FFT function in SPW is used (FFT Points was set to 524288 for better accuracy as discussed in section 3.2 of this report) to plot the PSD diagrams. The final diagrams of the PSD are shown in this report, section 3.2.

A.2 SER Detailed Diagram

The detailed diagram from SPW that was used to measure the SER and produce the corresponding SER Curves is shown in Figure A.3. Basically this circuit takes the output signal of the matched filter (since NRZ-L is the data format, a sliding integrator was used as the matched filter. For more information about the matched filter refer to section 2.7 in this report) which is the signal that was distorted through the channel and compares it with the input signal. This comparison is performed by a delay & phase meter which tries to correlate the non-distorted signal with the distorted one. When the best correlation is found, the distorted and non-distorted PSK signals are converted to their corresponding symbol numbers. Afterwards these symbol numbers are compared in a “Simple Error Rate Estimator” to find the Symbol Error Rate (SER).

All this is performed in real time and is shown on the screen of the Sparc-10 Sun Station as it can be seen in the two boxes “ Display and Control” and “Error Rate Display” in Figure A.3. Finally Figure A.4 shows a detailed block diagram for the AWGN that was used in the SPW simulations.

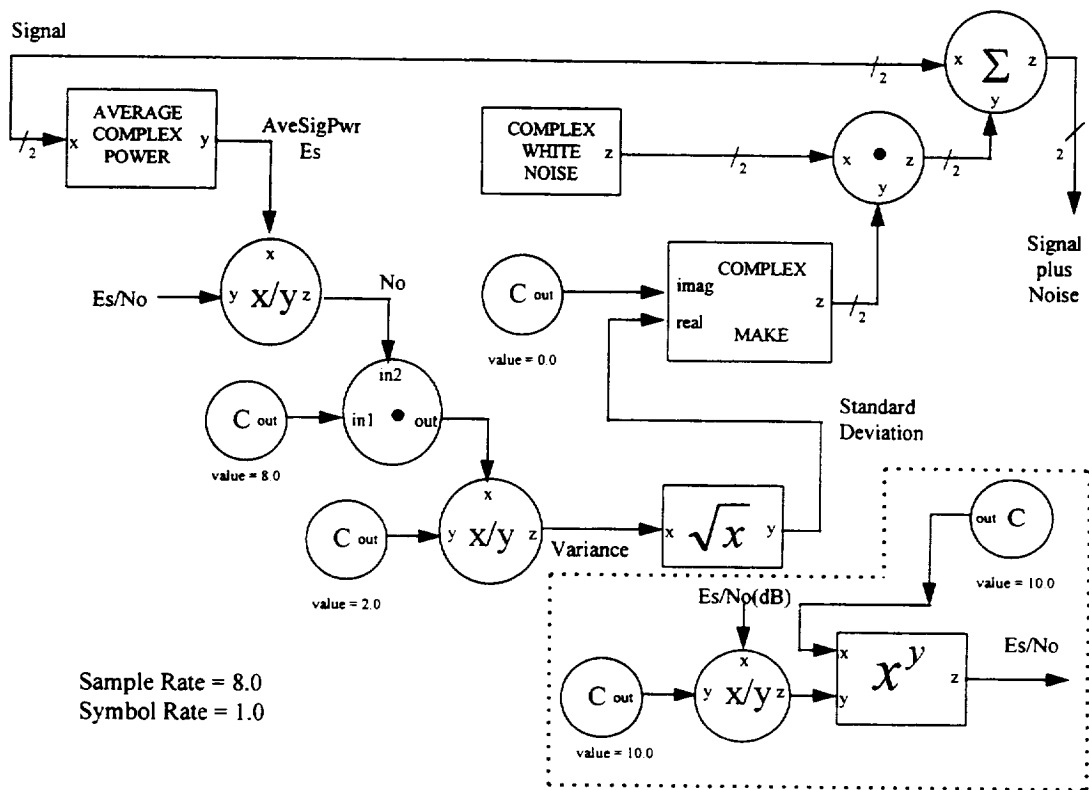


Figure A.4 - Detailed Block Diagram for the AWGN

APPENDIX B

SSPA, ESA 10 Watts

This appendix shows the SSPA model used in SPW. The magnitude and phase plots of the SSPA used in the simulations performed with 8PSK modulation with different spectrum shaping filters are shown in Figure B.1.

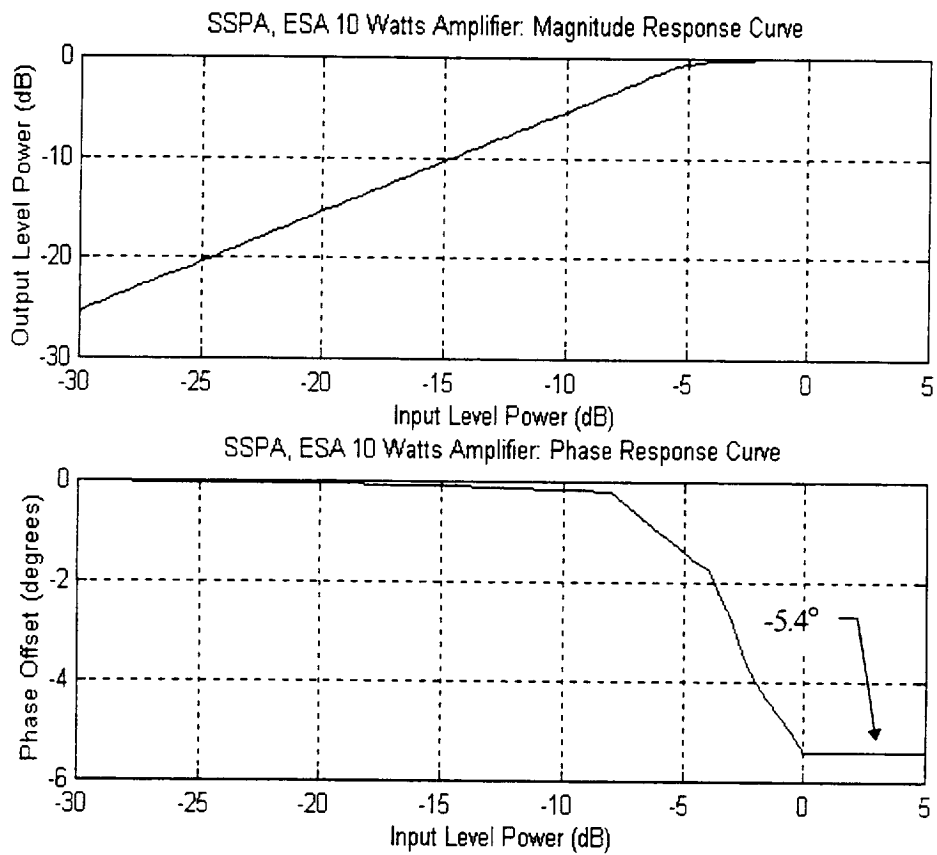


Figure B.1 - Magnitude and Phase of SSPA, ESA 10 Watts

The data used to produce these plots is listed in page 114 and was obtained from JPL (the same amplifier was used by JPL for their simulations at saturation level). The data file consists of three columns: the first column is the input power in dB, the second column is the output power in dB, and the third column is the output phase in degrees ($^{\circ}$). Therefore, the data are formatted in such a way that SPW can have access to the different numbers in the file. The block "TWT" in the "Communication Library" in SPW was utilized. Figure B.2, shows the aspect of this block.

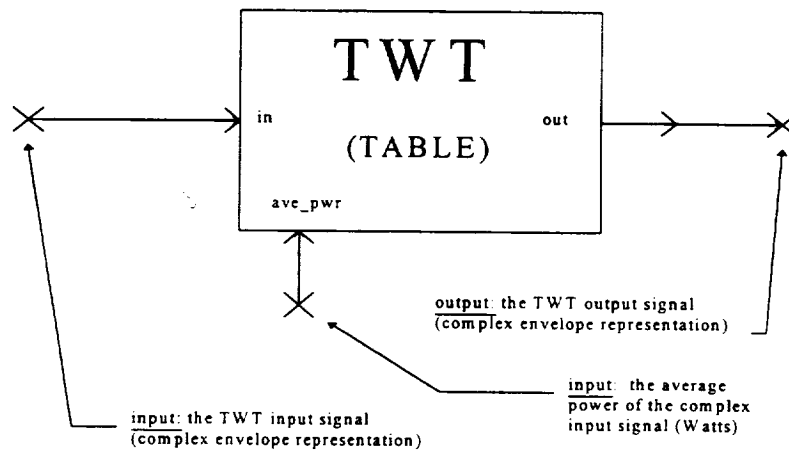


Figure B.2 - SPW Amplifier Model: Block Diagram

This block implements the AM-to-AM and AM-to-PM characteristics for a typical TWT or in this case a SSPA. Parameters to this block include the operating point in dB (0 dB for saturation level), the name of the TWT or SSPA file, and the number of interpolated points (for the simulation performed, 240 interpolated points were used). Figure B.3 - Detailed SPW TWT Model, shows a detailed version of Figure B.2. SSPAs or TWTs are generally modeled using AM/AM and AM/PM conversion characteristics. The characteristics give output power versus input power (AM/AM conversion) and output phase shift versus input power (AM/PM conversion). In this block, these characteristics are specified by a file of measured input/output data as mentioned earlier. This data file represents, for these simulations, the specifications of the SSPA, 10 Watt, S-band power amplifier

IHI_TABLE BLOCK PARAMETERS	
MAIN PARAMETERS:	
Operating point(id)	0.0
File path	'com_deno/hi_table'
Number of interpolated points	248
MISCELLANEOUS PARAMETERS:	
Initial value	0.0
Overflow value	0.0
Error count before action	1
Action taken (stop or continue)	'stop'

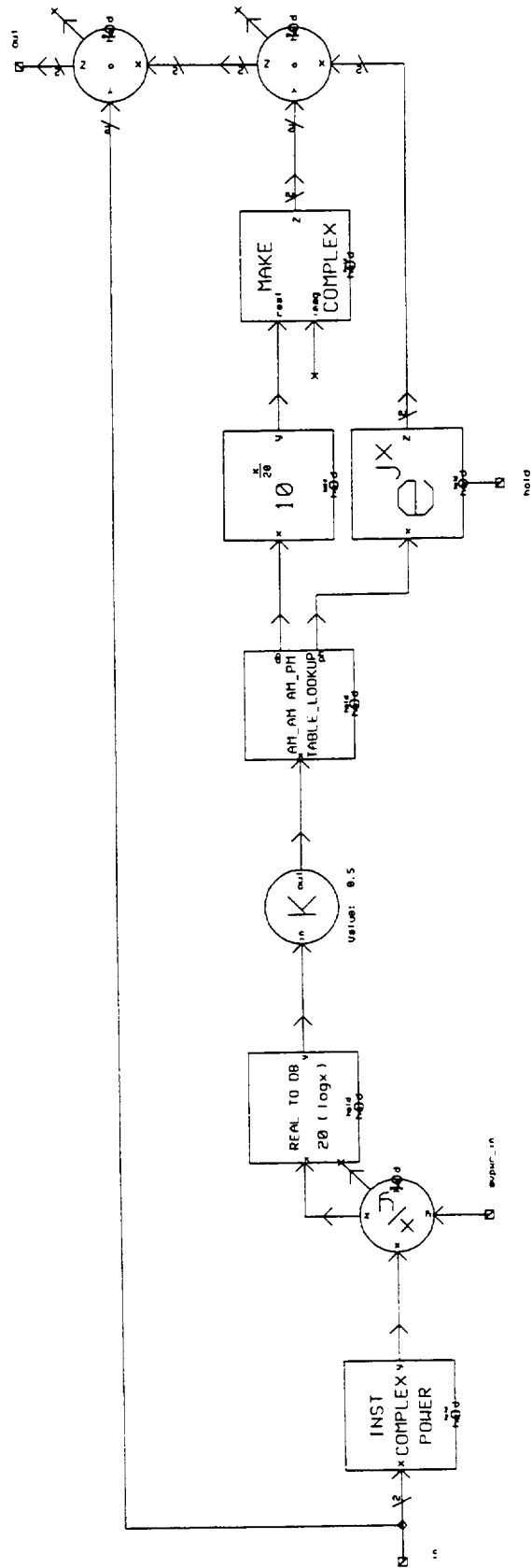


Figure B.3 - Detailed SPW TWT Model

used by the European Space Agency (ESA). As stipulated in [14], “ the measured data in the data file, consists of relative power levels, referenced to saturation point. That is, the input power data are the input power relative to that which causes saturation at the output, and the output power data are the output power relative to the power at saturation. This allows the characteristics to be modeled around the point where an input envelope value of unity gives an output envelope value of unity. Thus, in the measured data , 0 dB input power corresponds to 0 dB output power.”

SSPA3 TABLE

\$

SIGNAL TYPE = double

VECTOR TYPE = interlaced

VECTOR LENGTH = 210

NUMBER OF VECTORS = 3

NUMBER OF SIGNAL POINTS = 210

SAMPLING FREQUENCY = 1

STARTING TIME = 0

\$

-3.000000e+01	-2.534000e+01	-1.588660e-02
-2.950000e+01	-2.484000e+01	-1.682790e-02
-2.900000e+01	-2.434000e+01	-1.782500e-02
-2.850000e+01	-2.384000e+01	-1.888120e-02
-2.800000e+01	-2.334000e+01	-2.000000e-02
-2.750000e+01	-2.284000e+01	-2.118510e-02
-2.700000e+01	-2.234000e+01	-2.244040e-02
-2.650000e+01	-2.184000e+01	-2.377000e-02
-2.600000e+01	-2.134000e+01	-2.517850e-02
-2.550000e+01	-2.084000e+01	-2.667040e-02
-2.500000e+01	-2.034000e+01	-2.825070e-02
-2.450000e+01	-1.984000e+01	-2.992470e-02
-2.400000e+01	-1.934000e+01	-3.169790e-02
-2.350000e+01	-1.884000e+01	-3.357610e-02
-2.300000e+01	-1.834000e+01	-3.556500e-02
-2.250000e+01	-1.784000e+01	-3.767300e-02
-2.200000e+01	-1.734000e+01	-3.990520e-02
-2.150000e+01	-1.684000e+01	-4.226980e-02
-2.100000e+01	-1.634000e+01	-4.477440e-02
-2.050000e+01	-1.584000e+01	-4.742750e-02
-2.000000e+01	-1.534000e+01	-5.023770e-02
-1.950000e+01	-1.484000e+01	-5.321450e-02
-1.900000e+01	-1.434000e+01	-5.636770e-02

-1.8500000e+01	-1.3840000e+01	-5.9707600e-02
-1.8000000e+01	-1.3340000e+01	-6.3245600e-02
-1.7500000e+01	-1.2840000e+01	-6.6993100e-02
-1.7000000e+01	-1.2340000e+01	-7.0962700e-02
-1.6500000e+01	-1.1840000e+01	-7.5167500e-02
-1.6000000e+01	-1.1340000e+01	-7.9621400e-02
-1.5500000e+01	-1.0840000e+01	-8.4339300e-02
-1.5000000e+01	-1.0340000e+01	-8.9336700e-02
-1.4500000e+01	-9.8400000e+00	-9.4630200e-02
-1.4000000e+01	-9.3400000e+00	-1.0023700e-01
-1.3500000e+01	-8.8400000e+00	-1.0617700e-01
-1.3000000e+01	-8.3400000e+00	-1.1246800e-01
-1.2500000e+01	-7.8400000e+00	-1.1913200e-01
-1.2000000e+01	-7.3400000e+00	-1.2619100e-01
-1.1500000e+01	-6.8400000e+00	-1.3366900e-01
-1.1000000e+01	-6.3400000e+00	-1.4158900e-01
-1.0500000e+01	-5.8400000e+00	-1.4997900e-01
-1.0000000e+01	-5.3400000e+00	-1.5886600e-01
-9.5000000e+00	-4.8400000e+00	-1.6827900e-01
-9.0000000e+00	-4.3400000e+00	-1.7825000e-01
-8.5000000e+00	-3.8400000e+00	-1.8812000e-01
-8.0000000e+00	-3.3400000e+00	-2.0000000e-01
-7.5000000e+00	-2.8400000e+00	-4.0000000e-01
-7.0000000e+00	-2.3400000e+00	-6.0000000e-01
-6.5000000e+00	-1.8400000e+00	-8.0000000e-01
-6.0000000e+00	-1.3400000e+00	-1.0000000e+00
-5.5000000e+00	-8.4000000e-01	-1.2000000e+00
-5.0000000e+00	-5.9000000e-01	-1.4000000e+00
-4.5000000e+00	-3.7999900e-01	-1.6000000e+00
-4.0000000e+00	-2.6000000e-01	-1.7500000e+00
-3.5000000e+00	-2.0000100e-01	-2.2500000e+00
-3.0000000e+00	-1.6000000e-01	-2.7500000e+00
-2.5000000e+00	-1.2000200e-01	-3.5000000e+00
-2.0000000e+00	-7.9999800e-02	-4.0000000e+00

-1.5000000e+00	-4.0001400e-02	-4.3500000e+00
-5.0000000e-01	0.0000000e+00	-5.0000000e+00
0.0000000e+00	-5.1771900e-07	-5.4000000e+00
5.0000000e-01	-5.1771900e-07	-5.4000000e+00
1.0000000e+00	-5.1771900e-07	-5.4000000e+00
1.5000000e+00	-5.1771900e-07	-5.4000000e+00
2.0000000e+00	-5.1771900e-07	-5.4000000e+00
2.5000000e+00	-5.1771900e-07	-5.4000000e+00
3.0000000e+00	-5.1771900e-07	-5.4000000e+00
3.5000000e+00	-5.1771900e-07	-5.4000000e+00
4.0000000e+00	-5.1771900e-07	-5.4000000e+00
4.5000000e+00	-5.1771900e-07	-5.4000000e+00
5.0000000e+00	-5.1771900e-07	-5.4000000e+00

APPENDIX C
NON-CONSTANT ENVELOPE
SIMULATION
BLOCK DIAGRAM

This appendix contains a detailed diagram of the non-constant envelope simulation circuit used on SPW to be able to measure the effect of the non-constant envelope through the SSPA. A brief explanation of this circuit will be given.

Figure C.1 shows the detailed SPW diagram of the Non-Constant Envelope Simulations also described in Figure 3.34 of section 3.4 in this report. Note the similarity of Figure C.1 with the Figures in Appendix A. One of the only differences is the model of the SSPA which has been slightly modified. In fact, Figure C.2 shows a detailed diagram of this new model of SSPA. This new model was created to get a better rotation accuracy due to the AM/PM conversion in the SSPA. In this new SSPA model, the SSPA table shown in Appendix B has been modified in the sense that two new tables were created ,i.e., one table which was named “outdb.ascsig” contained the input dB column (first column of the table in Appendix B) and the output dB (second column of table in Appendix B). Therefore this first file was the AM/AM conversion created by the SSPA. The second file that was created was called “outphase.ascsig” and contains the columns from the table in Appendix B that produced the AM/PM conversion ,i.e., column 1 and 3.

Therefore the two TABULAR NON LINEAR blocks in Figure C.2 refer to these files to output the corresponding amplitude or phase conversion. The highest TABULAR NON LINEAR block in the figure refers to the “outdb.ascsig” table and the second block refers to the “outphase.ascsig” table. The rest of the block diagram is self explanatory.

PARAMETERS

sampling rate (Hz) or fs: 16.0
 symbol rate (Hz) or Rsym: (...)
 N (" samples/symbol = fs/Rsym) : (...)
 zeta (data asymmetry: N*0.02) : 0.0
 Carrier Frequency fc (Hz) : 0.0
 Probability of zero: 0.5
 SSPA Backoff (dB): 0.0

MPSK MODULATOR PARAMETERS

MPSK (BPSK = 2, QPSK = 4, 8PSK=8) = 8.0
 C1 (BPSK = 0.0, QPSK = 2.0, 8PSK=2.0) = 2.0
 C2 (BPSK = 0.0, QPSK = 0.0, 8PSK=4.0) = 4.0
 C3 (BPSK = 0.0, QPSK = 0.5, 8PSK=0.5) = 0.5

BANK OF FILTERS

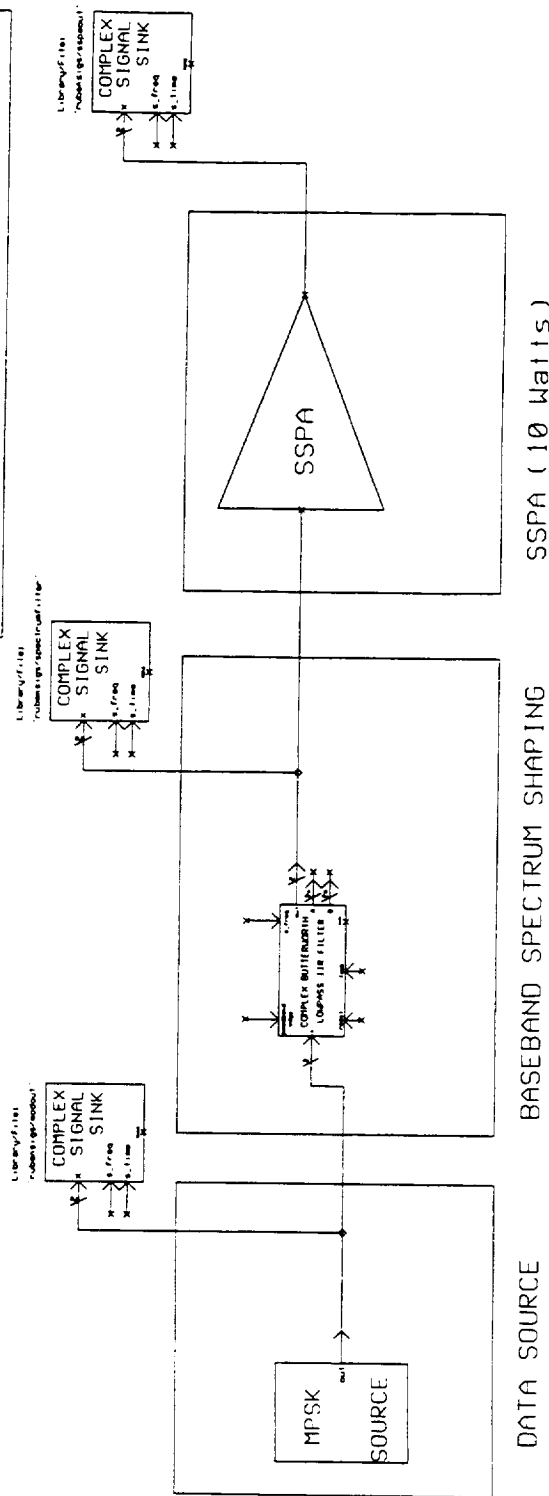
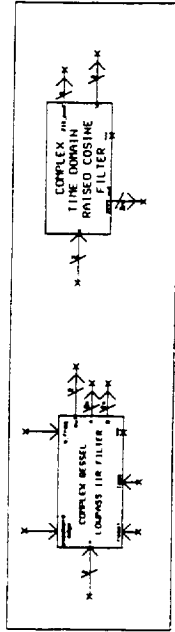
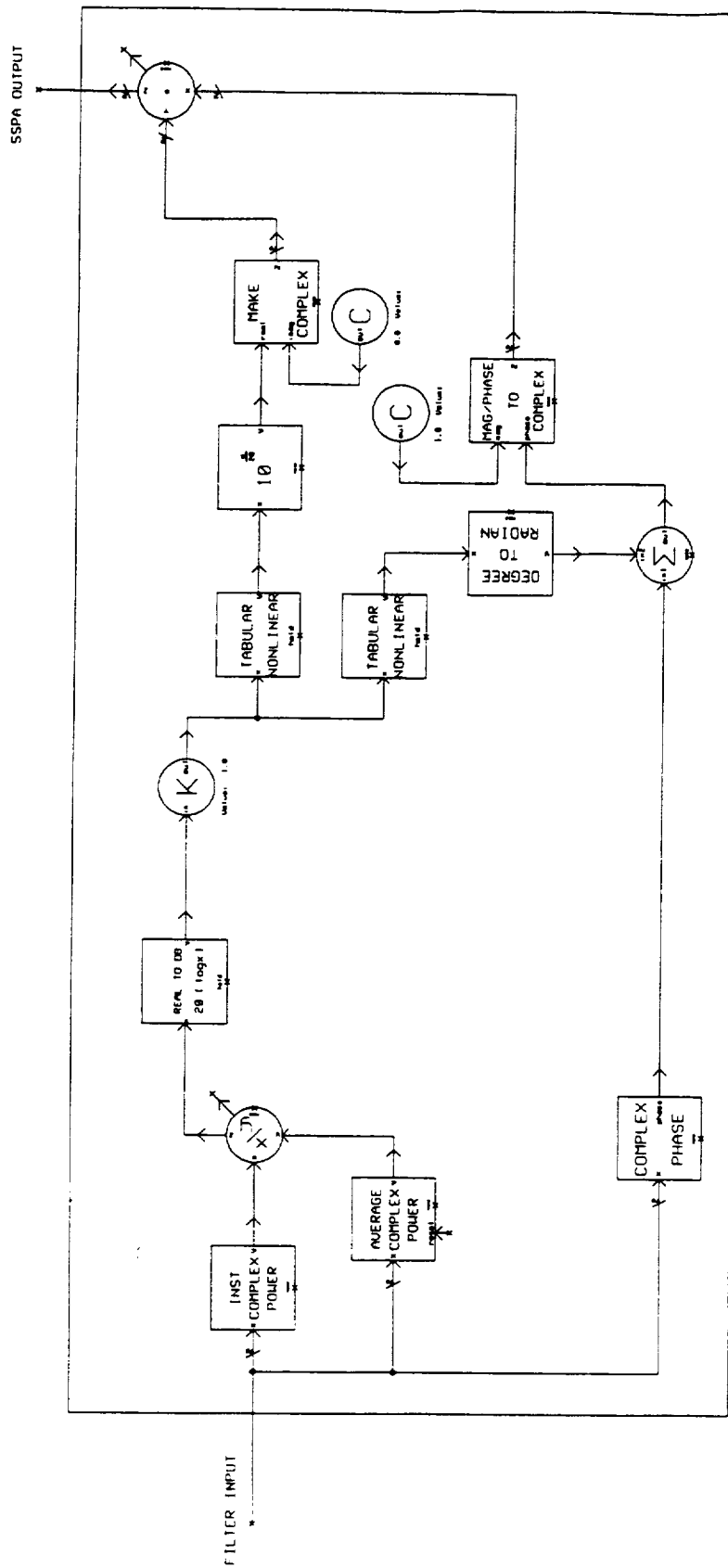


Figure C.1 - Detailed SPW Diagram of Non-Constant Envelope Simulations



SSPA (10 Watts)

Figure C.2 - Detailed SPW Diagram Of New SSPA

The most important point that was considered during these non-constant envelope simulations using the diagram shown in Figure C.1 was the selection of the sampling frequency parameter, f_s , first parameter in the top left corner of Figure C.1). As mentioned in [15], “ Watch out for frequency warping if the filter bandwidth is larger than about 20% of the simulation bandwidth (1/sampling period);; the passband frequencies will be correct, but out-of-band characteristics may be warped.” Thus, to avoid frequency warping, the following condition has to be met:

$$BT < (0.2) \cdot f_s$$

where BT = Bandwidth-Time product (defined in Appendix A); and

f_s = sampling frequency.

For simulations involving BT=1, $f_s=16$ was used and for BT=2,3 values of $f_s=32, 48$ were used to avoid frequency warping. But what causes frequency warping? As described in [10], frequency warping is caused by the nonlinear relationship between corresponding digital and analog frequencies. Therefore if the sampling frequency is not high enough the high frequencies for the digital filter will be warped compared to its corresponding analog filter.

APPENDIX D

PROGRAM LISTING:

“SPWSOBRE.M”

This appendix contains the listing of the program SPWSOBRE.M written in Matlab that was used to produce the scatter plots output from the Non-Constant Envelope simulations. It calculates the Average Symbol Variance of each of the 8 decision regions for different values of BT.

Program Listing: SPWSOBRE.M

```
% Program : SPWSOBRE.M
% Written by : Rubén Caballero
% Developed using MATLAB V4.2B and Signal Processing Toolbox V3.0b
% Copyright 1996 - Rubén Caballero
% New Mexico State University
%
% This function loads the file from the non-constant envelope simulations performed
% in SPW, and locates the decision region where each symbol belongs. Afterwards,
% the function will calculate the mean and variance of each decision region using
% the symbols. For each simulation, 625 symbols were used to produce the output
% scatter plots and calculate the average symbol variance.

%*****
%*****
%*****INPUTS: CHANGE THESE VARIABLES*****
%*****
%*****
clear;
tic;
load sambut17.asc;          % file containing the symbols

jj=1;
for ii=38:length(sambut17); % 38 specifies the filter delay: change this value depending ...
    for jjj=1:2             % ... on the simulation and filter
        A(jj,jjj)=sambut17(ii,jjj); % Change also the name of the ASCII file
    end;
    jj=jj+1;
end;

nsymbol=48;                % sampling frequency to be changed depending on the ...
                           % the simulation
```

```

%*****
%*****
%*****PROGRAM STARTS*****
%*****
%*****

[nr nc]=size(A);

for q=1:nr
    x(q)=A(q,1)*(cos(A(q,2))+sin(A(q,2))*i);
end;

[nr nc]=size(x);
Ksymbols=floor(nc/nsymbol);
x=x(1:Ksymbols*nsymbol);

z=[-1:0.01:1];                % Create the axis for the Scatter Plot
[rz nz]=size(z);
y=sqrt(ones(1,nz)-z.*z);
plot(z,y,'b-',z,-y,'b-');
grid
axis('square');
hold on;

avg=sum(abs(x));
avg=avg/nc;

for i=1:Ksymbols
    m=(nsymbol)*i;
    symbols(i)=x(m)/avg;
end

% Determine the location of the symbols.

RxSig=angle(symbols);

dec0=1;
dec1=1;
dec2=1;
dec3=1;
dec4=1;
dec5=1;
dec6=1;
dec7=1;

for i=1:length(RxSig)                % Decision Region 0
    if ((RxSig(i)>=0) & (RxSig(i) <=pi/4))
        decision0(dec0)=symbols(i);
        dec0=dec0+1;
    end;
end;

```

```

if ((RxSig(i)>=pi/4) & (RxSig(i) <=pi/2))           % Decision Region 1
    decision1(dec1)=symbols(i);
    dec1=dec1+1;
end;

if ((RxSig(i)>pi/2) & (RxSig(i) <=6*pi/8))         % Decision Region 2
    decision2(dec2)=symbols(i);
    dec2=dec2+1;
end;

if ((RxSig(i)>=6*pi/8) & (RxSig(i) <=pi))         % Decision Region 3
    decision3(dec3)=symbols(i);
    dec3=dec3+1;
end;

if ((RxSig(i)>-pi) & (RxSig(i) <= -6*pi/8))       % Decision Region 4
    decision4(dec4)=symbols(i);
    dec4=dec4+1;
end;

if ((RxSig(i)>-6*pi/8) & (RxSig(i) <=-pi/2))     % Decision Region 5
    decision5(dec5)=symbols(i);
    dec5=dec5+1;
end;

if ((RxSig(i)> -pi/2) & (RxSig(i) <=-pi/4))      % Decision Region 6
    decision6(dec6)=symbols(i);
    dec6=dec6+1;
end;

if ((RxSig(i)>-pi/4) & (RxSig(i) <0))            % Decision Region 7
    decision7(dec7)=symbols(i);
    dec7=dec7+1;
end;

end; % end FOR

plot(symbols,'go');

axis([-1.25 +1.25 -1.25 +1.25]);
title('Output of SSPA (saturation level), 5th Order Butterworth Filter (BT=3.8)');
xlabel('real');
ylabel('imag');
% Calculation of the Mean of the Symbols in the Decision Regions

meanrad(1)=(mean(angle(decision0)));           % mean in rads
meandeg(1)=(meanrad(1)*180/pi);              % mean in degrees

meanrad(2)=(mean(angle(decision1)));           % mean in rads
meandeg(2)=(meanrad(2)*180/pi);              % mean in degrees

```

```

meanrad(3)=(mean(angle(decision2))); % mean in rads
meandeg(3)=(meanrad(3)*180/pi); % mean in degrees

meanrad(4)=(mean(angle(decision3))); % mean in rads
meandeg(4)=(meanrad(4)*180/pi); % mean in degrees

meanrad(5)=(mean(angle(decision4))); % mean in rads
meandeg(5)=(meanrad(5)*180/pi); % mean in degrees

meanrad(6)=(mean(angle(decision5))); % mean in rads
meandeg(6)=(meanrad(6)*180/pi); % mean in degrees

meanrad(7)=(mean(angle(decision6))); % mean in rads
meandeg(7)=(meanrad(7)*180/pi); % mean in degrees

meanrad(8)=(mean(angle(decision7))); % mean in rads
meandeg(8)=(meanrad(8)*180/pi); % mean in degrees

% Calculation of the Variance of the Symbols in the Decision Regions

varrad(1)=(std(angle(decision0))).^2; % variance in rads
vardeg(1)=(varrad(1)*180/pi); % variance in degrees

varrad(2)=(std(angle(decision1))).^2; % variance in rads
vardeg(2)=(varrad(2)*180/pi); % variance in degrees

varrad(3)=(std(angle(decision2))).^2; % variance in rads
vardeg(3)=(varrad(3)*180/pi); % variance in degrees

varrad(4)=(std(angle(decision3))).^2; % variance in rads
vardeg(4)=(varrad(4)*180/pi); % variance in degrees

varrad(5)=(std(angle(decision4))).^2; % variance in rads
vardeg(5)=(varrad(5)*180/pi); % variance in degrees

varrad(6)=(std(angle(decision5))).^2; % variance in rads
vardeg(6)=(varrad(6)*180/pi); % variance in degrees

varrad(7)=(std(angle(decision6))).^2; % variance in rads
vardeg(7)=(varrad(7)*180/pi); % variance in degrees

varrad(8)=(std(angle(decision7))).^2; % variance in rads
vardeg(8)=(varrad(8)*180/pi); % variance in degrees

save meandeg; save vardeg;
time=(toc/60); % in minutes

```

APPENDIX E

SCATTER PLOTS:

5TH Order BUTTERWORTH FILTER

This appendix contains the Scatter Plots of the output of the SSPA when a 5th Order Butterworth Spectrum Filter is used after the 8PSK Modulator. The Scatter Plots were produced for BT=1 to 4 using the SPWSOBRE.M function. Also, the listing of the program BUTTPLOT.M written in Matlab which was used to produce the Average Symbol Variance plots (see Figure 3.43 and 3.44 in this report) is included. All the values of mean and variance in this program were calculated in the program SPWSOBRE.M.

E.1 Scatter Plots

Output of SSPA (saturation level), 5th Order Butterworth Filter (BT=1)

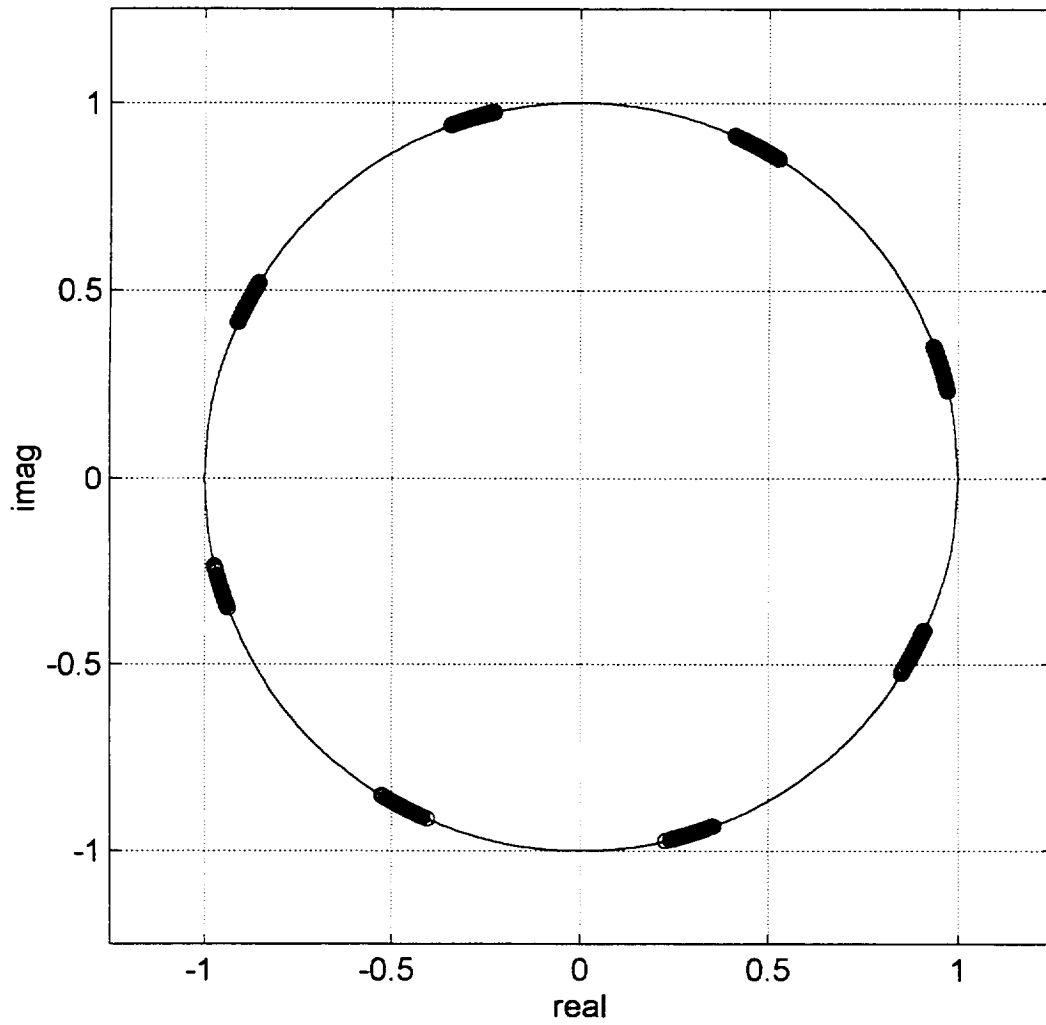


Figure E.1 - Output of SSPA (Saturation Level)
Spectrum Shaping Filter: 5th Order Butterworth BT=1

Output of SSPA (saturation level), 5th Order Butterworth Filter (BT=1.05)

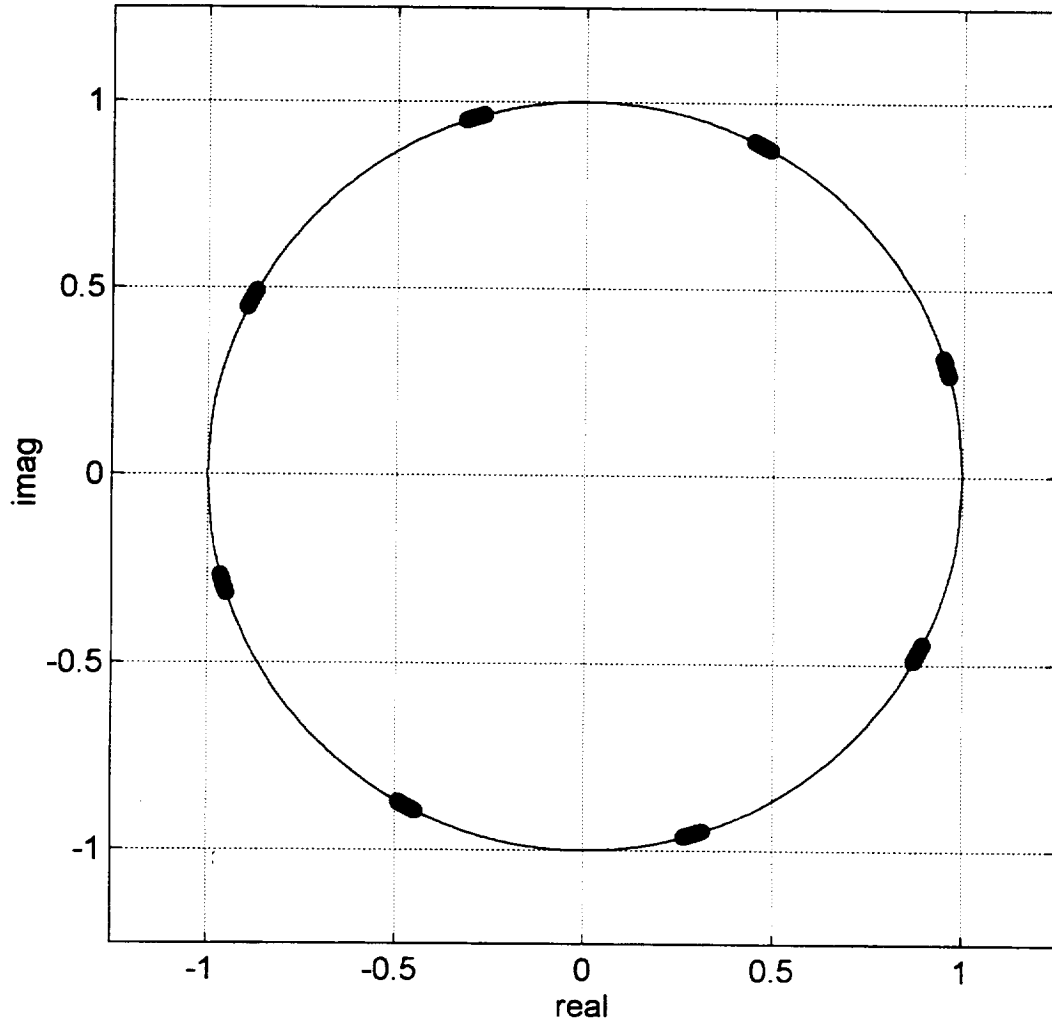


Figure E.2 - Output of SSPA (Saturation Level)
Spectrum Shaping Filter: 5th Order Butterworth BT=1.05

Output of SSPA (saturation level), 5th Order Butterworth Filter (BT=1.1)

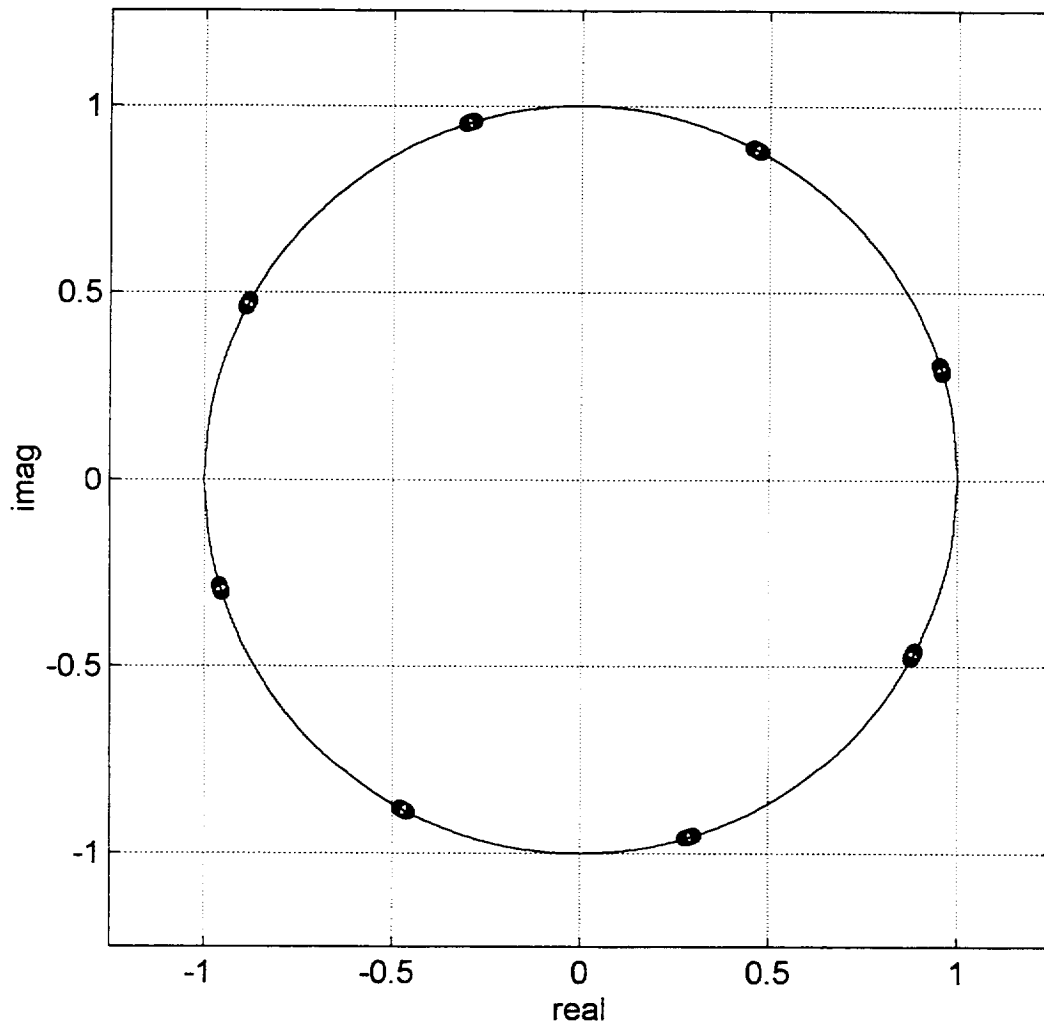


Figure E.3 - Output of SSPA (Saturation Level)
Spectrum Shaping Filter: 5th Order Butterworth BT=1.1

Output of SSPA (saturation level), 5th Order Butterworth Filter (BT=1.2)

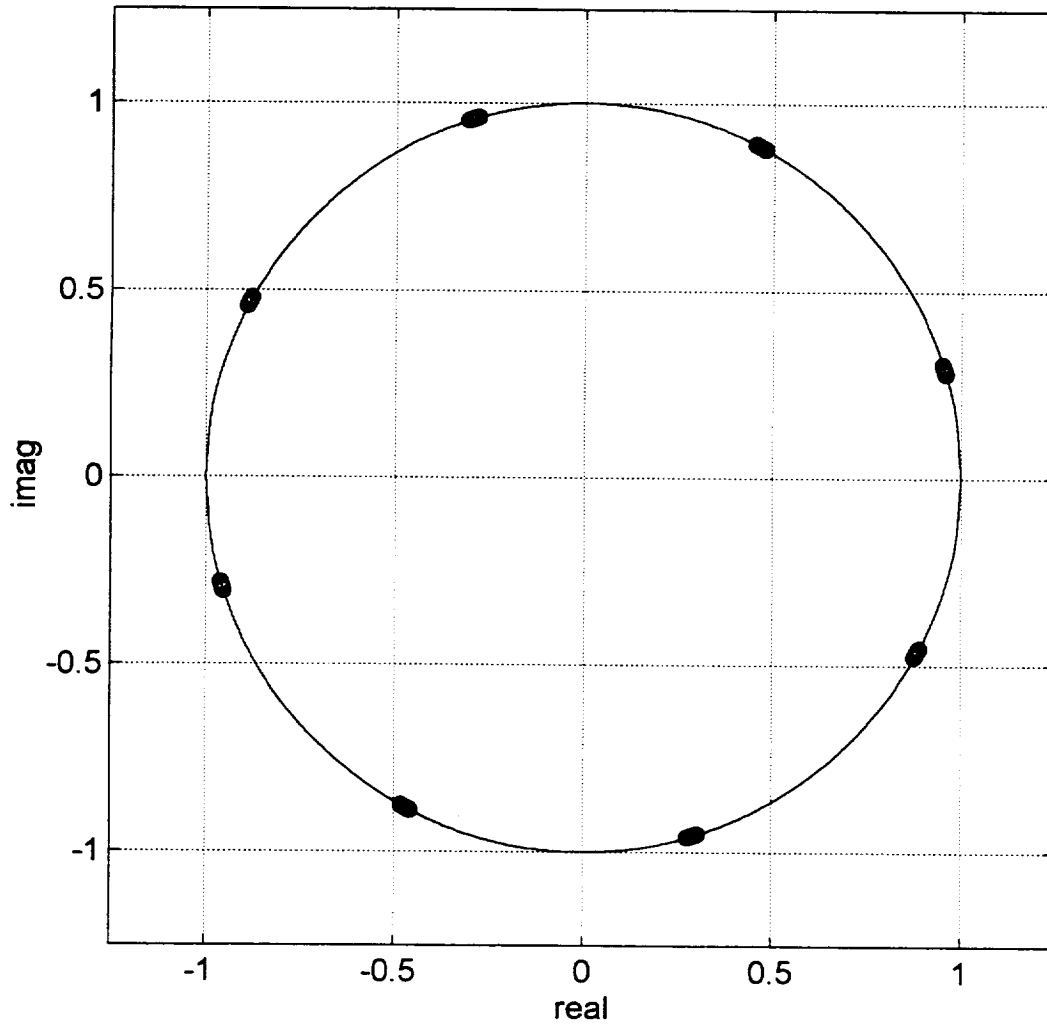


Figure E.4 - Output of SSPA (Saturation Level)
Spectrum Shaping Filter: 5th Order Butterworth BT=1.2

Output of SSPA (saturation level), 5th Order Butterworth Filter (BT=1.4)

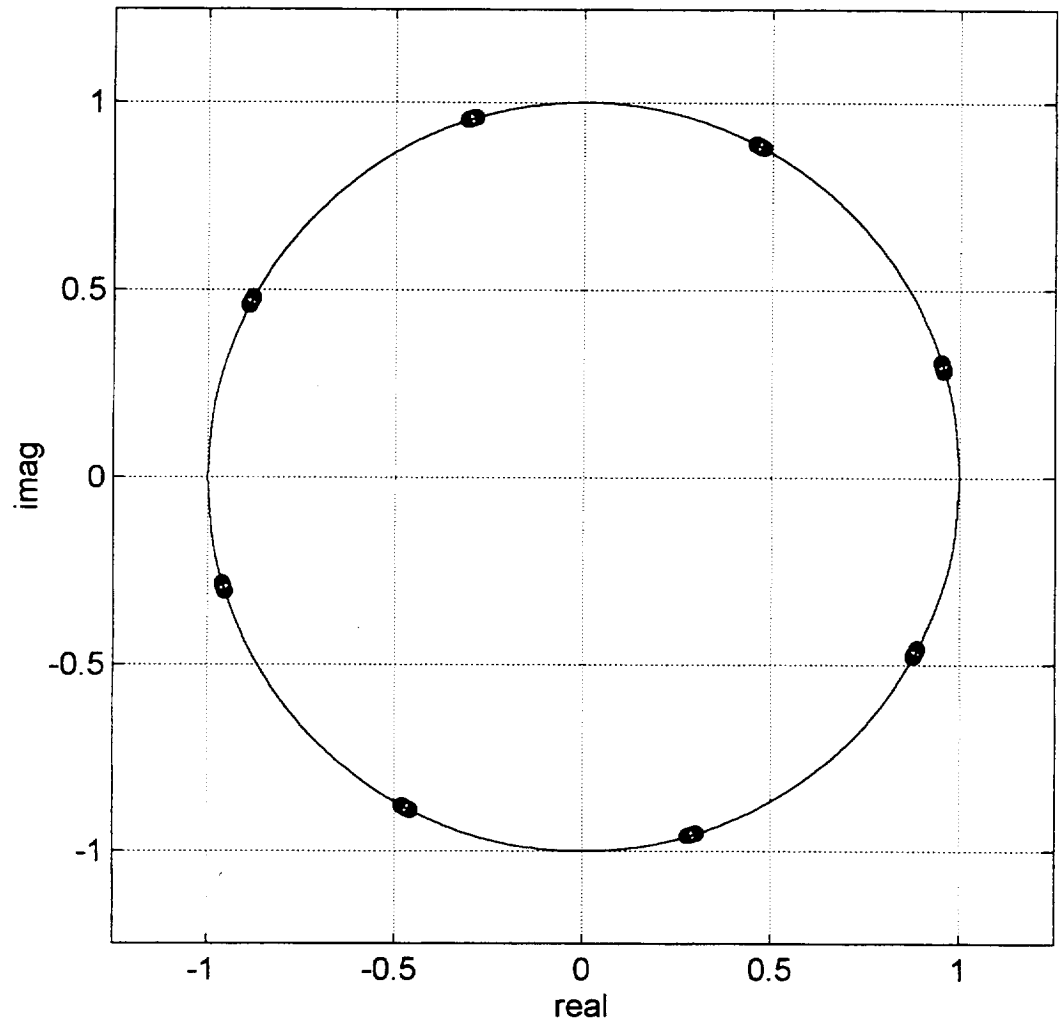


Figure E.5 - Output of SSPA (Saturation Level)
Spectrum Shaping Filter: 5th Order Butterworth BT=1.4

Output of SSPA (saturation level), 5th Order Butterworth Filter (BT=1.6)

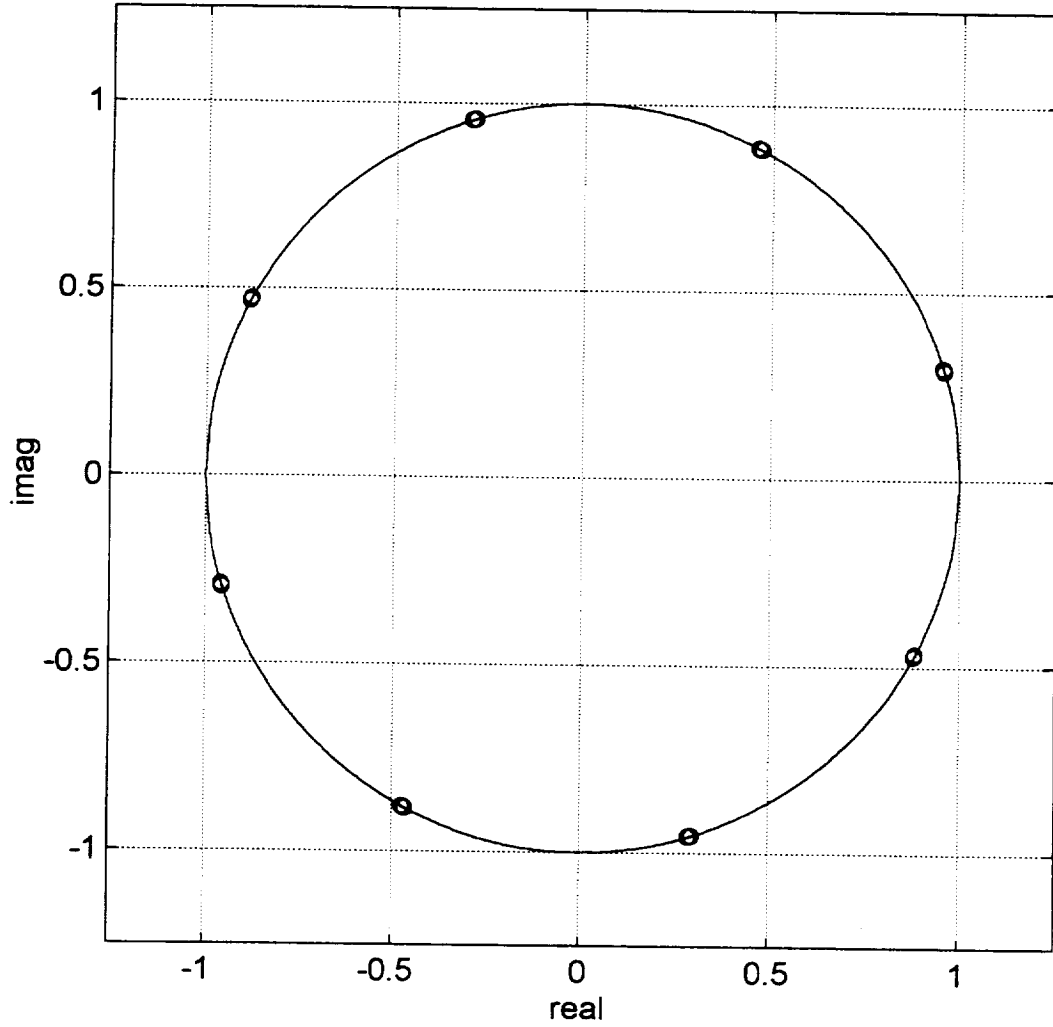


Figure E.6 - Output of SSPA (Saturation Level)
Spectrum Shaping Filter: 5th Order Butterworth BT=1.6

Output of SSPA (saturation level), 5th Order Butterworth Filter (BT=1.8)

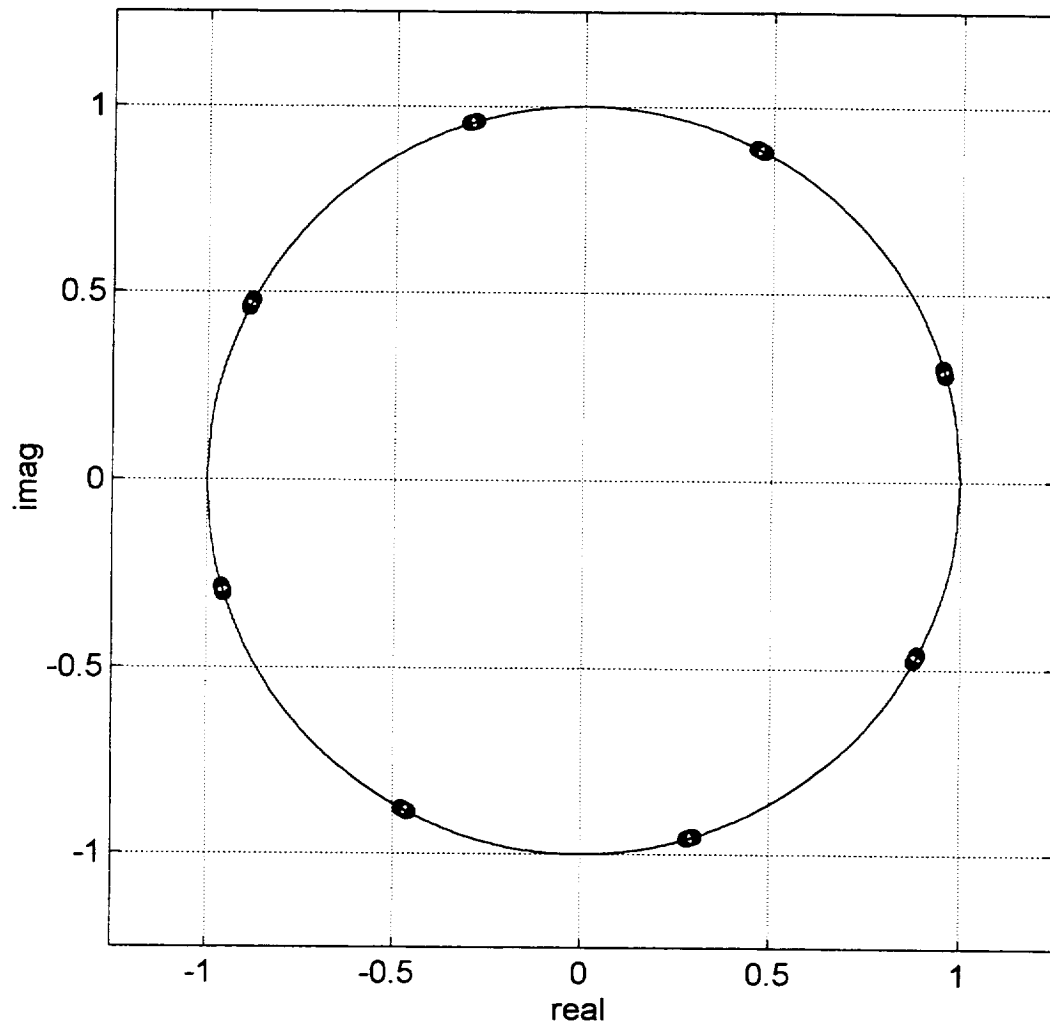


Figure E.7 - Output of SSPA (Saturation Level)
Spectrum Shaping Filter: 5th Order Butterworth BT=1.8

Output of SSPA (saturation level), 5th Order Butterworth Filter (BT=2)

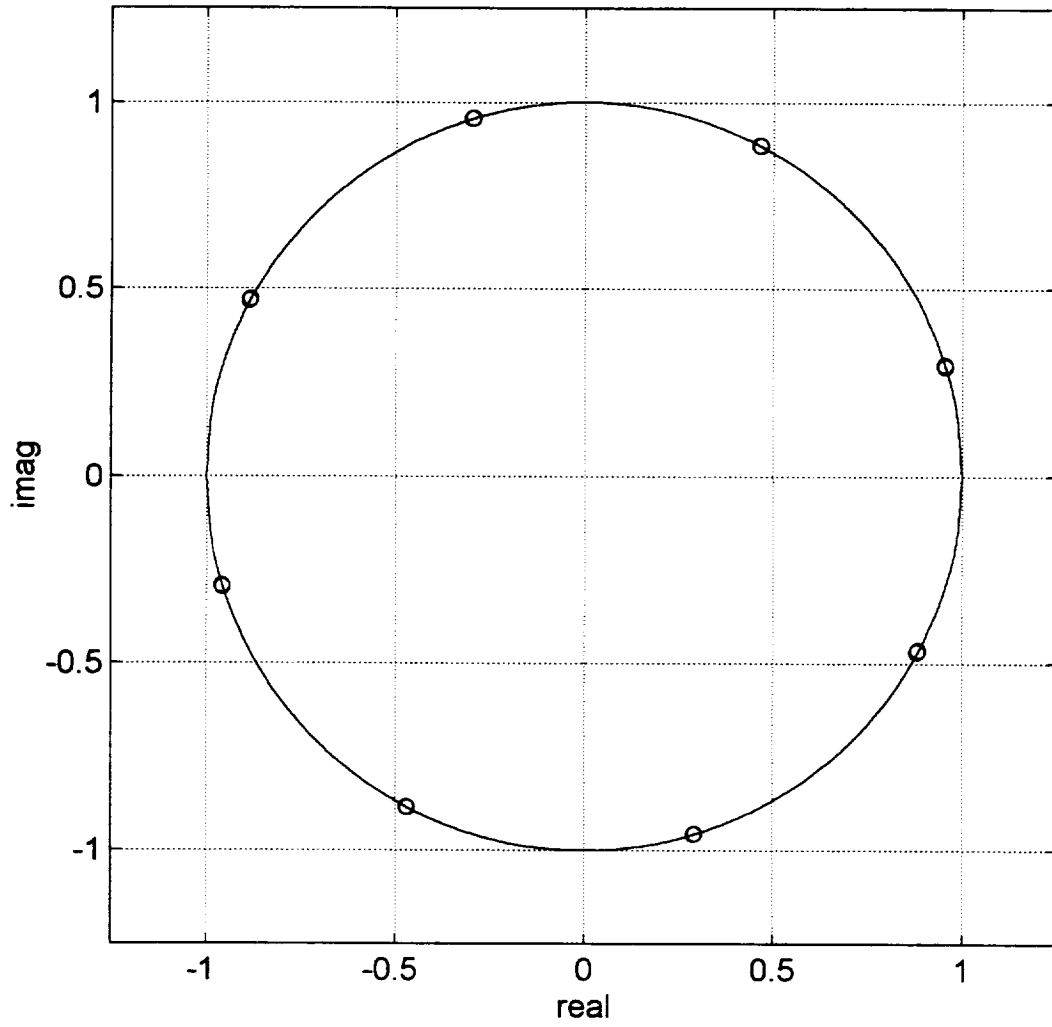


Figure E.8 - Output of SSPA (Saturation Level)
Spectrum Shaping Filter: 5th Order Butterworth BT=2

Output of SSPA (saturation level), 5th Order Butterworth Filter (BT=2.2)

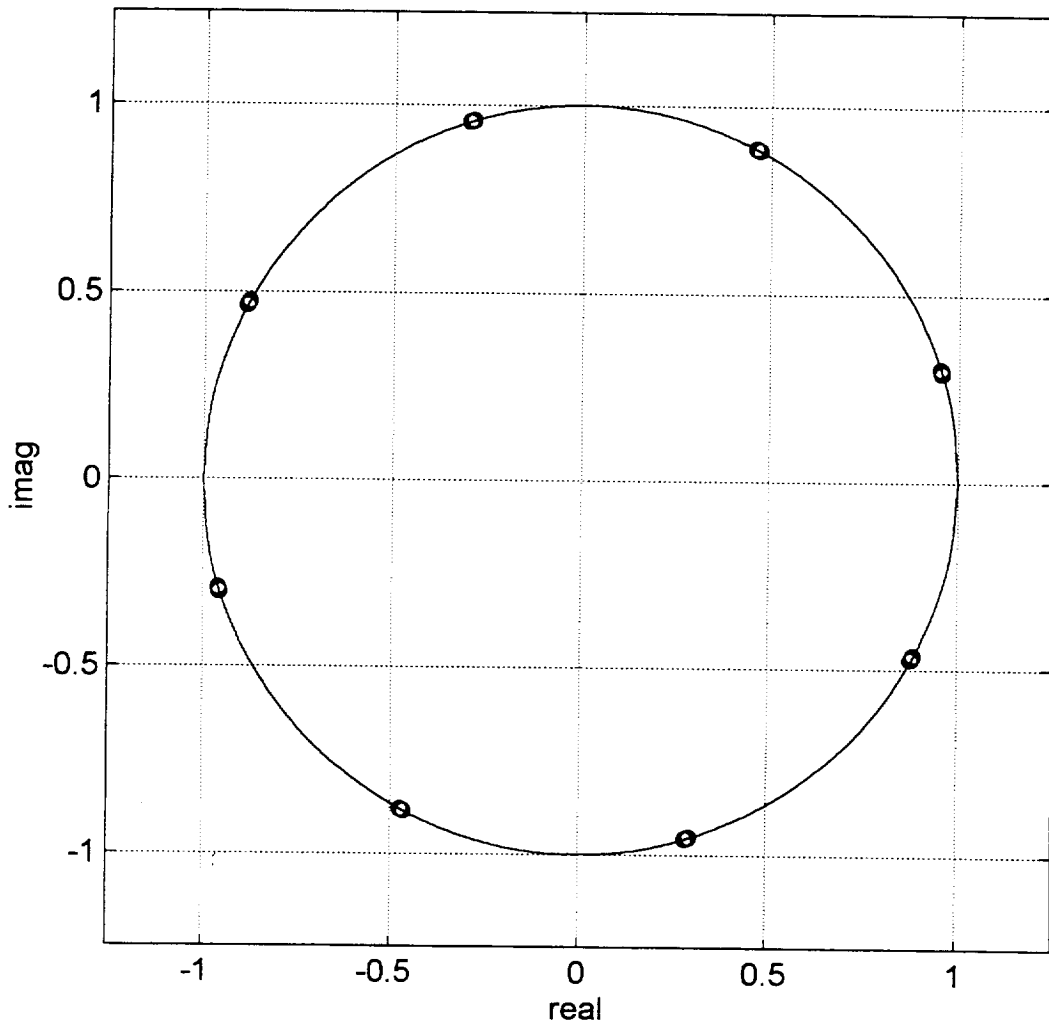


Figure E.9 - Output of SSPA (Saturation Level)
Spectrum Shaping Filter: 5th Order Butterworth BT=2.2

Output of SSPA (saturation level), 5th Order Butterworth Filter (BT=2.4)

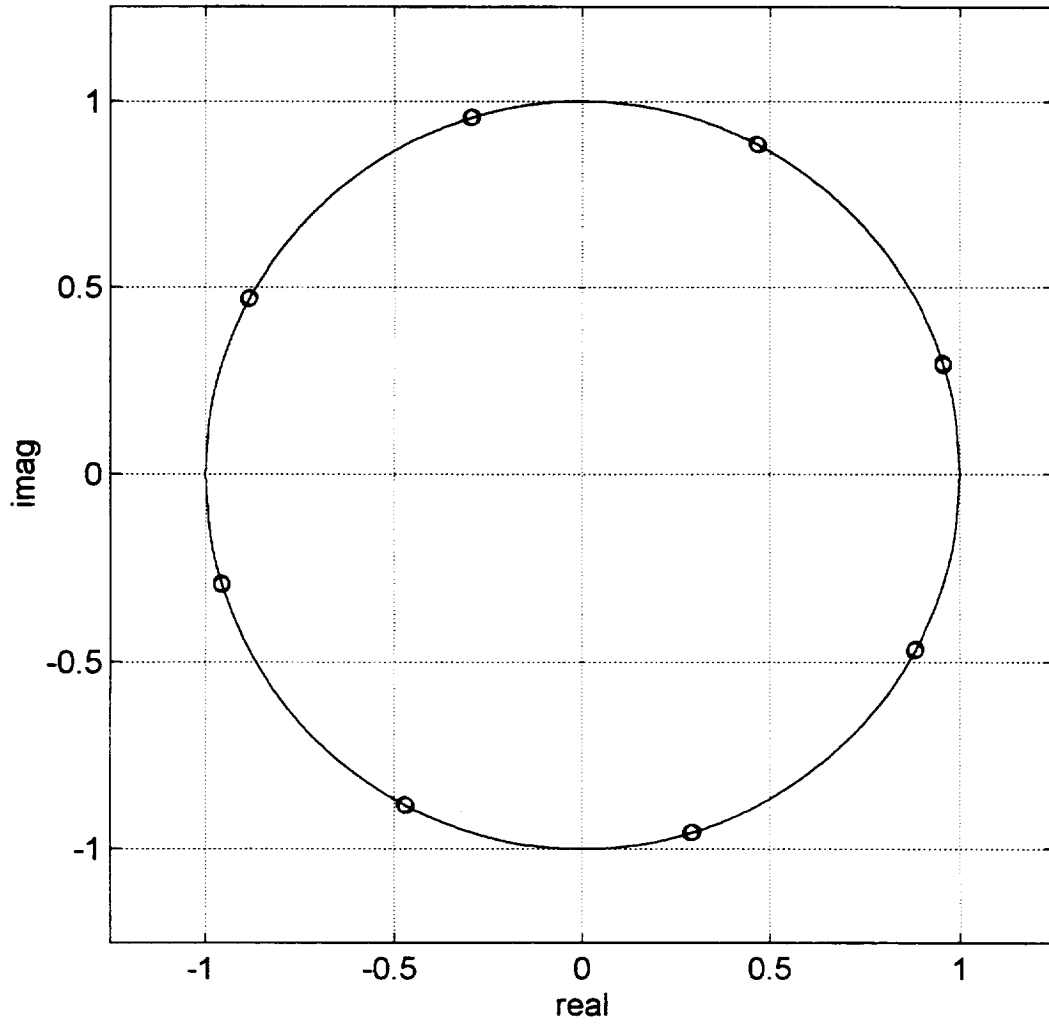


Figure E.10 - Output of SSPA (Saturation Level)
Spectrum Shaping Filter: 5th Order Butterworth BT=2.4

Output of SSPA (saturation level), 5th Order Butterworth Filter (BT=2.6)

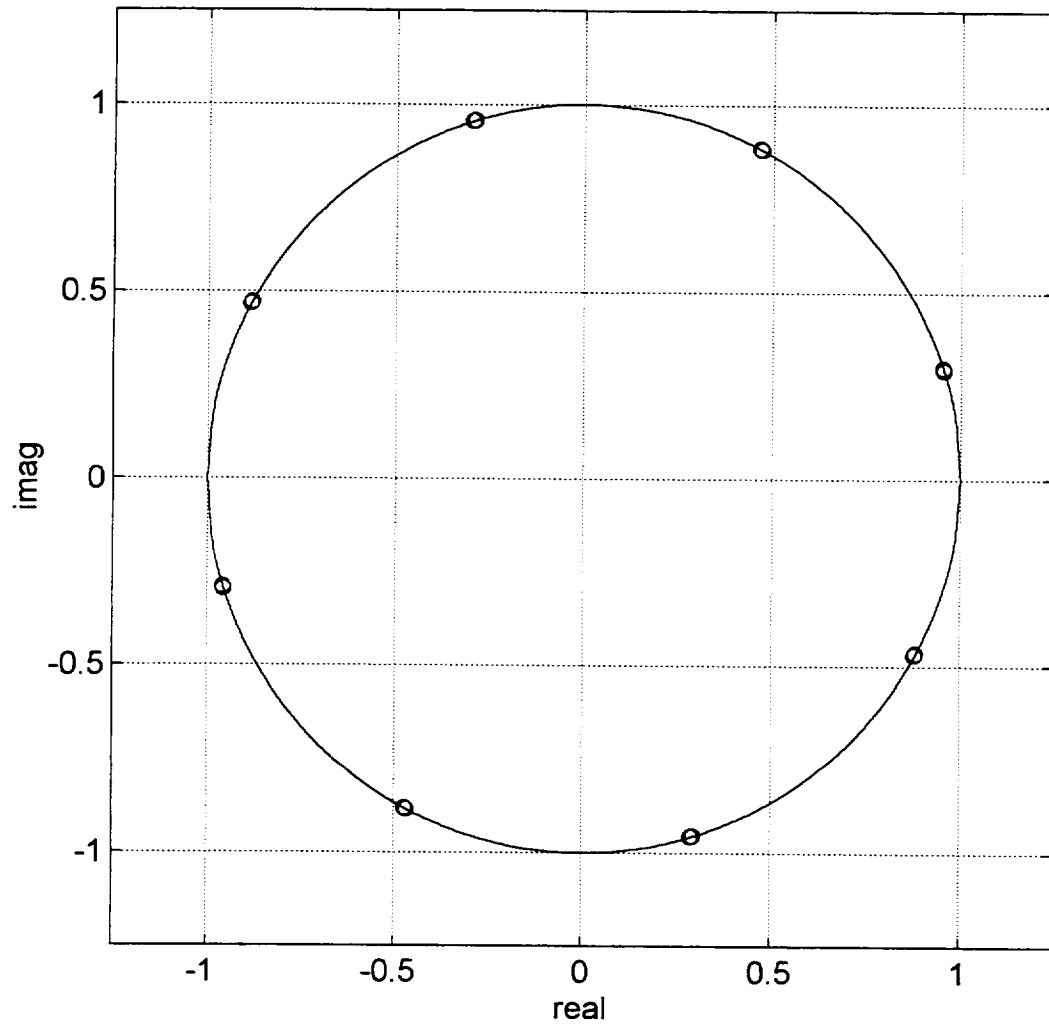


Figure E.11 - Output of SSPA (Saturation Level)
Spectrum Shaping Filter: 5th Order Butterworth BT=2.6

Output of SSPA (saturation level), 5th Order Butterworth Filter (BT=2.8)

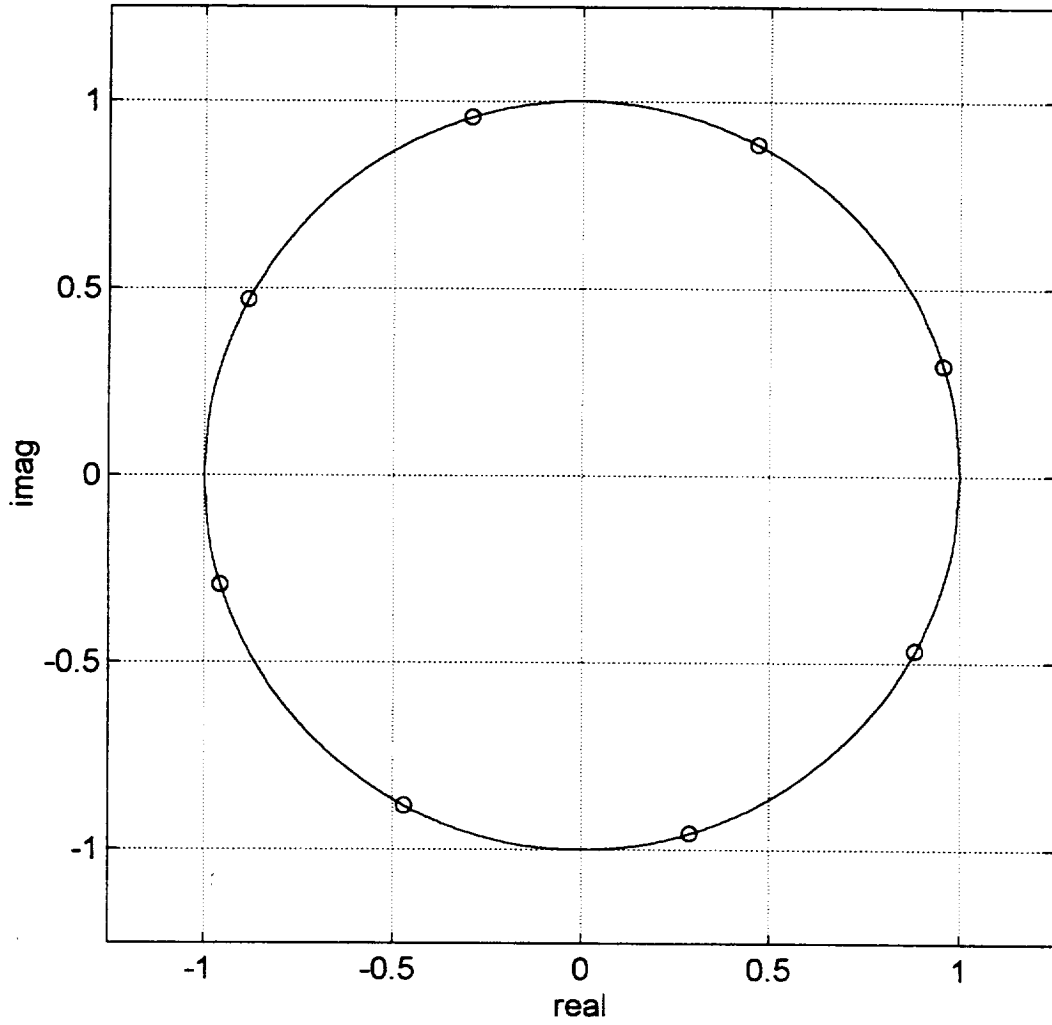


Figure E.12 - Output of SSPA (Saturation Level)
Spectrum Shaping Filter: 5th Order Butterworth BT=2.8

Output of SSPA (saturation level), 5th Order Butterworth Filter (BT=3)

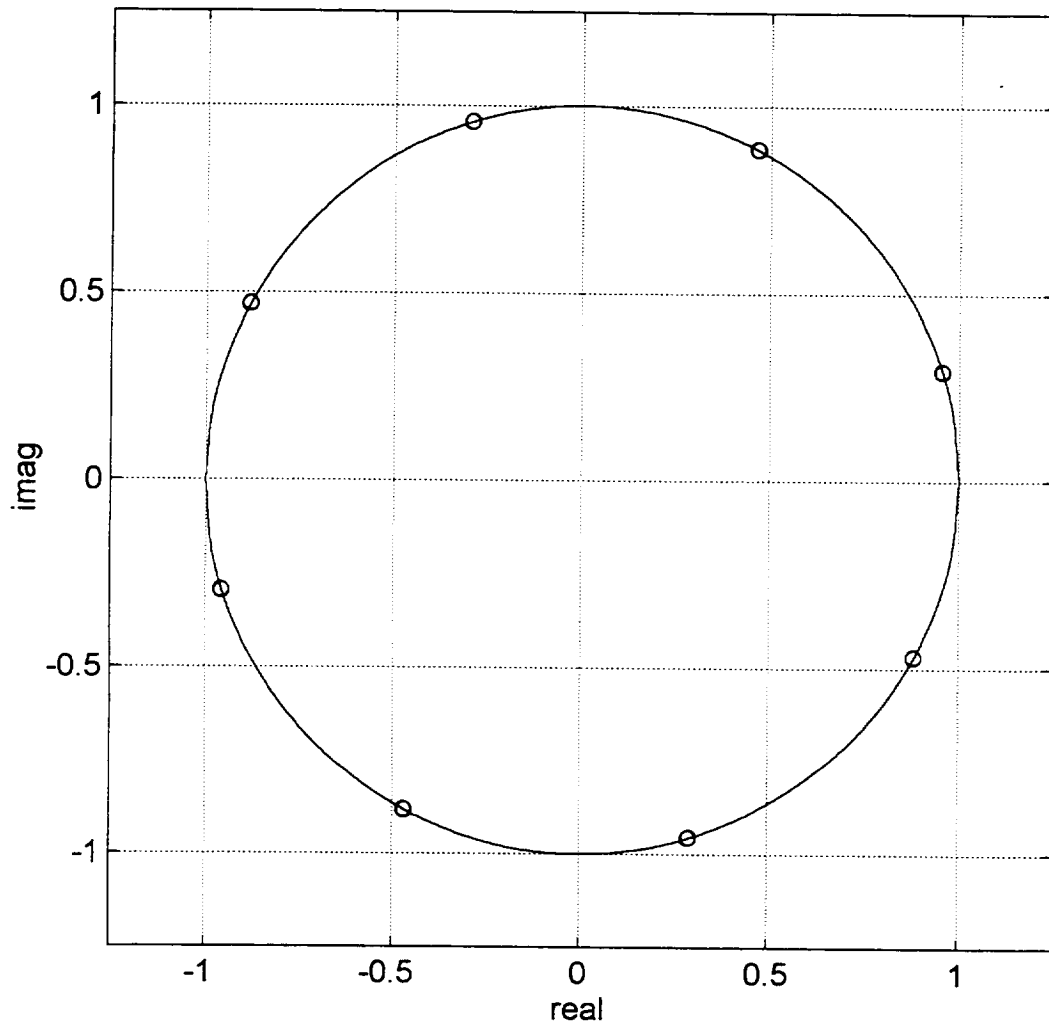


Figure E.13- Output of SSPA (Saturation Level)
Spectrum Shaping Filter: 5th Order Butterworth BT=3

Output of SSPA (saturation level), 5th Order Butterworth Filter (BT=3.2)

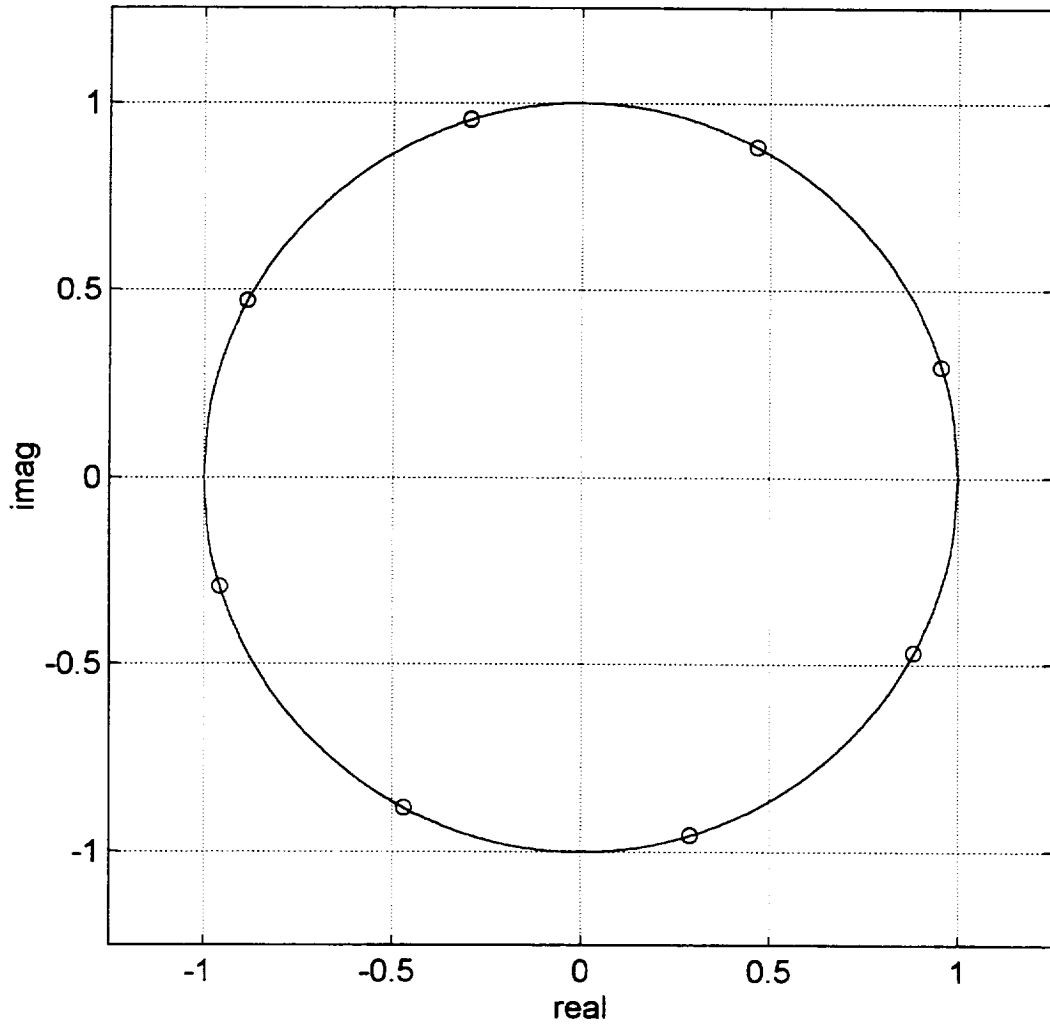


Figure E.14- Output of SSPA (Saturation Level)
Spectrum Shaping Filter: 5th Order Butterworth BT=3.2

Output of SSPA (saturation level), 5th Order Butterworth Filter (BT=3.4)

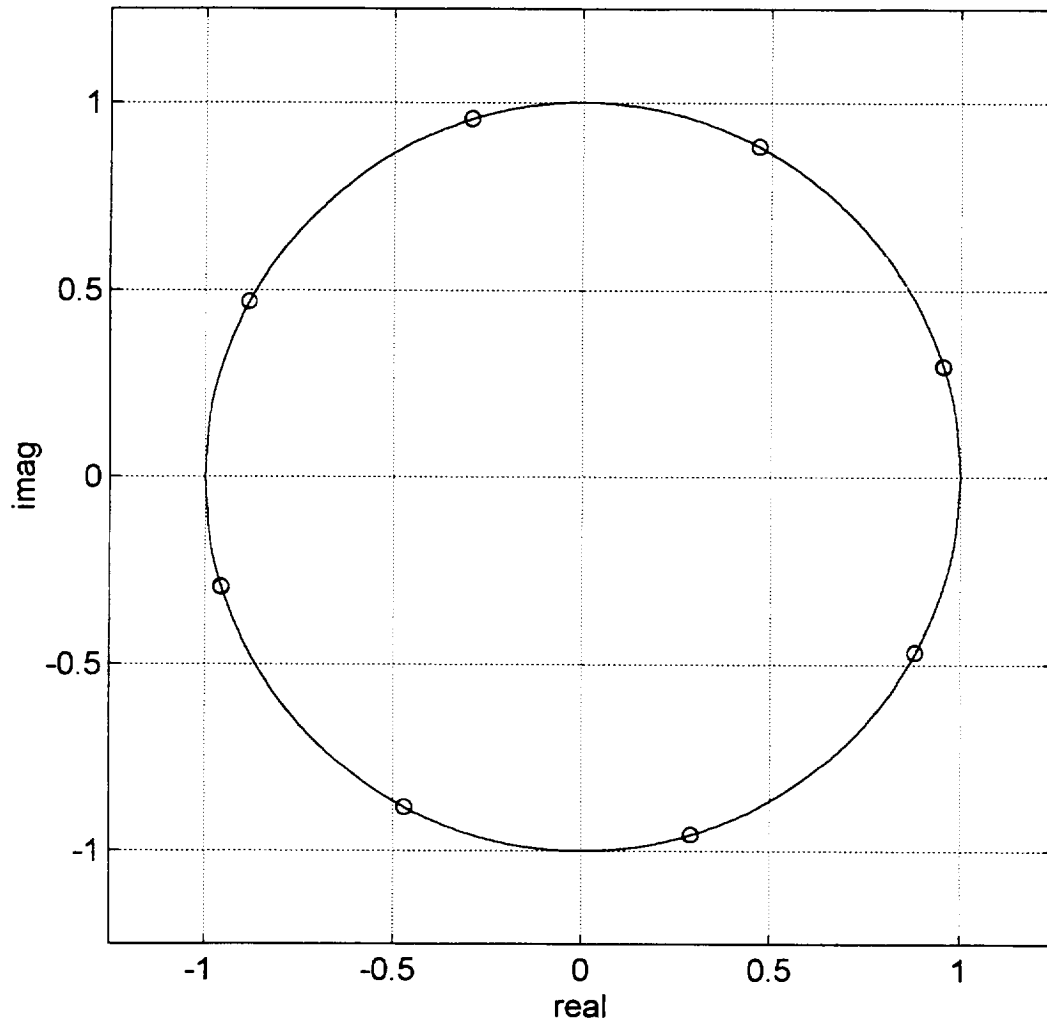


Figure E.15 - Output of SSPA (Saturation Level)
Spectrum Shaping Filter: 5th Order Butterworth BT=3.4

Output of SSPA (saturation level), 5th Order Butterworth Filter (BT=3.6)

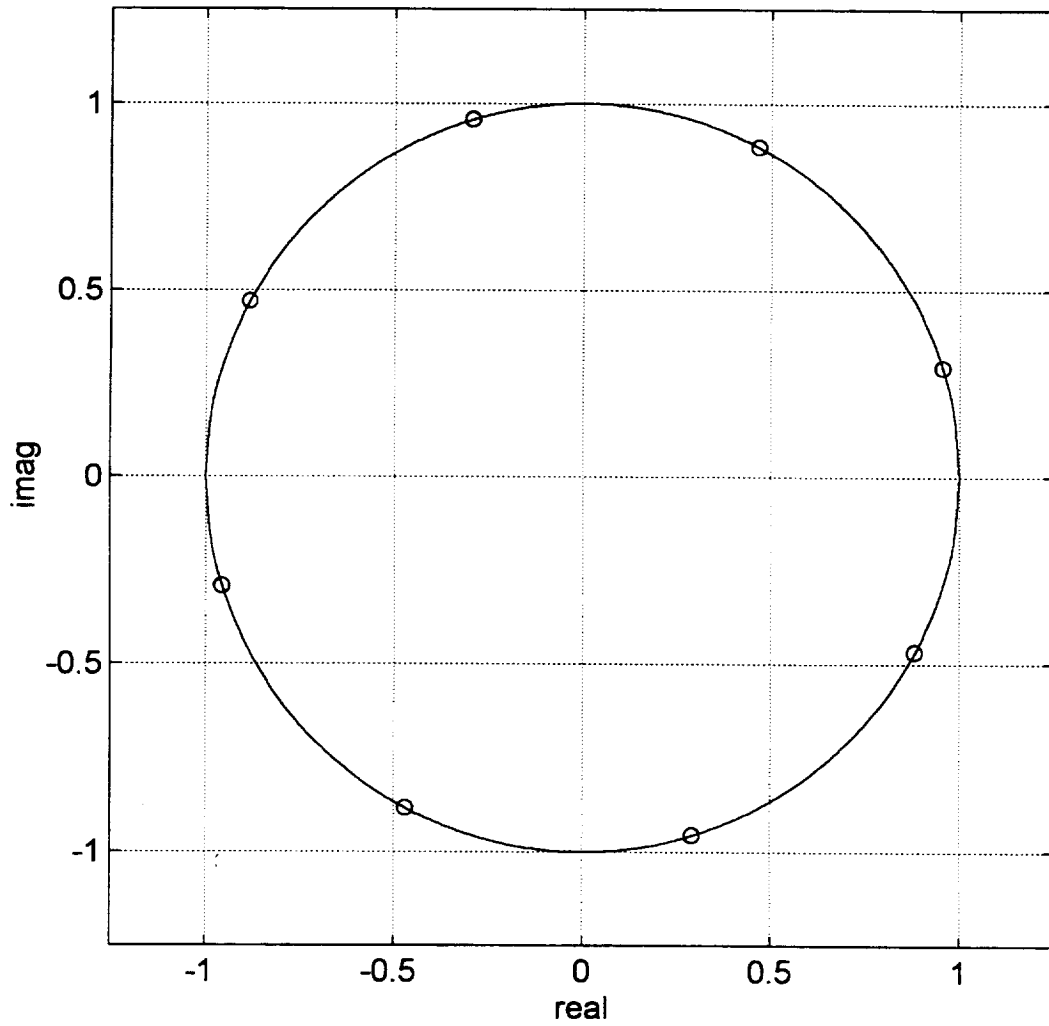


Figure E.16 - Output of SSPA (Saturation Level)
Spectrum Shaping Filter: 5th Order Butterworth BT=3.6

Output of SSPA (saturation level), 5th Order Butterworth Filter (BT=3.8)

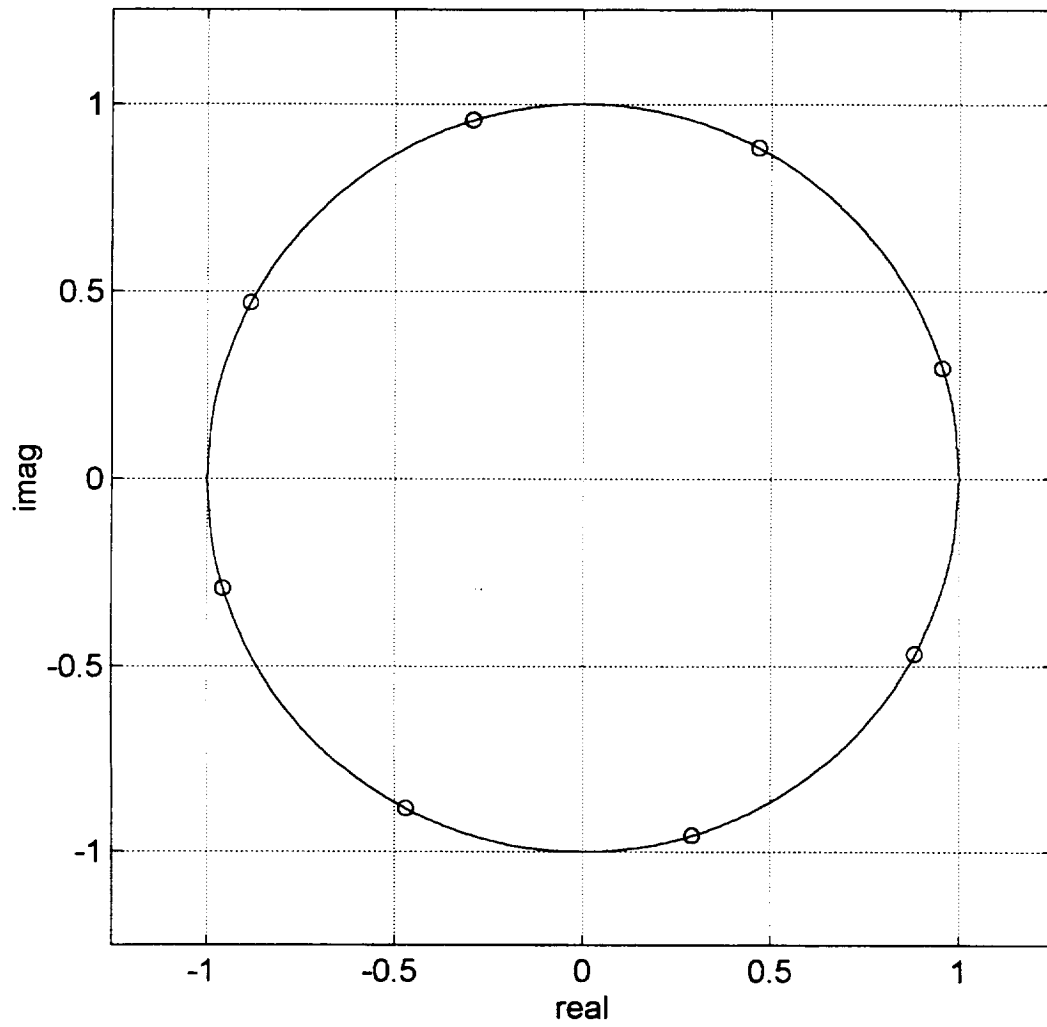


Figure E.17 - Output of SSPA (Saturation Level)
Spectrum Shaping Filter: 5th Order Butterworth BT=3.8

Output of SSPA (saturation level), 5th Order Butterworth Filter (BT=4)

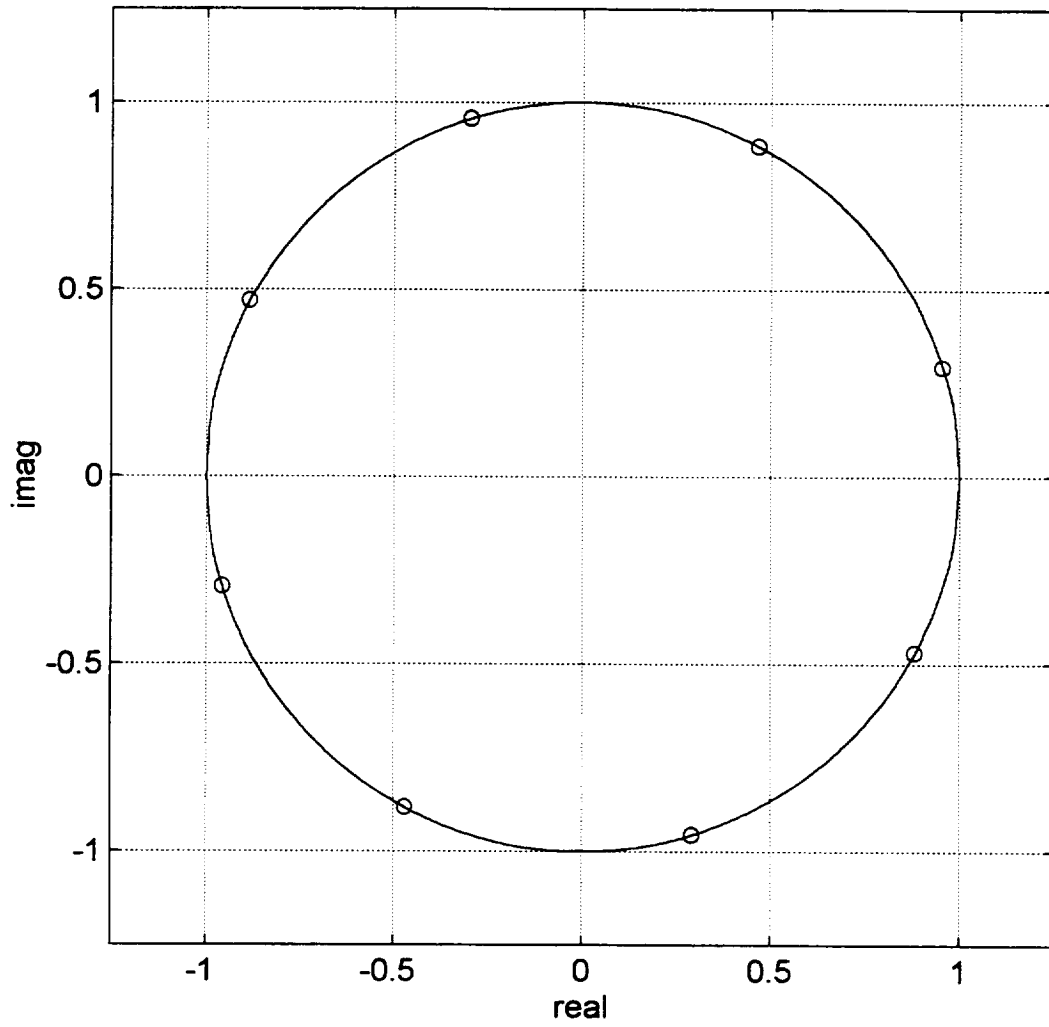


Figure E.18 - Output of SSPA (Saturation Level)
Spectrum Shaping Filter: 5th Order Butterworth BT=4

E.2 Program Listing: BUTTPLOT.M

```
% Program : BUTTPLOT.M
% Written by : Rubén Caballero
% Developed using MATLAB V4.2B and Signal Processing Toolbox V3.0b
% Copyright 1996 - Rubén Caballero
% New Mexico State University
%
% This function uses the mean and variance calculated by the function SPWSOBRE.M to
% calculate the Average Symbol Variance. The result is a plot of the Average Symbol Variance
% versus BT for the 5th Order Butterworth filter as the spectrum shaping filter.

clear;

%*****
%***** Butterworth Filters *****
%*****

BT=[1 1.05 1.1 1.2 1.4 1.6 1.8 2 2.2 2.4 2.6 2.8 3 3.2 3.4 3.6 3.8 4.0]; % set BT values

%*****
%***** BT=1 fs =16 *****
%*****

% BUTTERWORTH: BT=1 (using delay =20, ascii file: sampbut1.asc)

meandeg(1,:) = [1.7020e+001 6.2250e+001 1.0680e+002 1.5258e+002 -1.6298e+002
               -1.1786e+002 -7.2650e+001 -2.7753e+001];
vardeg(1,:) = [7.1477e-002 6.3547e-002 5.2001e-002 6.6354e-002 5.4146e-002 5.4370e-002
               6.6427e-002 7.4719e-002];
avgvardeg1 = sum(vardeg(1,:))/8;

%*****
%***** BT=1.05 fs =16 *****
%*****

% BUTTERWORTH: BT=1.05 (using delay =13, ascii file: sampbut13.asc)

meandeg(13,:) = [1.7092e+001 6.2220e+001 1.0703e+002 1.5225e+002 -1.6294e+002
                -1.1794e+002 -7.2843e+001 -2.7899e+001];
vardeg(13,:) = [1.6673e-002 1.3528e-002 1.2779e-002 1.4959e-002 1.2526e-002 1.2054e-002
                1.3539e-002 1.5471e-002];
avgvardeg13 = sum(vardeg(13,:))/8;
```

```

%*****
%***** BT=1.1 fs =32 *****
%*****

```

```

% BUTTERWORTH: BT=1.1 (using delay =24, ascii file: sampbut8.asc)

```

```

meandeg(8,:) = [1.7103e+001 6.2082e+001 1.0716e+002 1.5204e+002 -1.6296e+002
               -1.1789e+002 -7.2971e+001 -2.7915e+001];
vardeg(8,:) = [1.8056e-003 1.8445e-003 1.9903e-003 2.0978e-003 2.0085e-003 2.1336e-003
               1.7640e-003 1.8487e-003];
avgvardeg8 = sum(vardeg(8,:))/8;

```

```

%*****
%***** BT=1.2 fs =16 *****
%*****

```

```

% BUTTERWORTH: BT=1.2 (using delay =18, ascii file: sampbut4.asc)

```

```

meandeg(4,:) = [1.7096e+001 6.2134e+001 1.0702e+002 1.5222e+002 -1.6285e+002
               -1.1789e+002 -7.2802e+001 -2.7860e+001];
vardeg(4,:) = [2.7145e-003 2.6749e-003 2.5493e-003 2.6131e-003 2.0687e-003 2.9801e-003
               2.5173e-003 2.3366e-003];
avgvardeg4 = sum(vardeg(4,:))/8;

```

```

%*****
%***** BT=1.4 fs =32 *****
%*****

```

```

% BUTTERWORTH: BT=1.4 (using delay =19, ascii file: sampbut5.asc)

```

```

meandeg(5,:) = [1.7092e+001 6.2088e+001 1.0717e+002 1.5205e+002 -1.6299e+002
               -1.1789e+002 -7.2985e+001 -2.7915e+001];
vardeg(5,:) = [3.6223e-003 3.0185e-003 3.5466e-003 3.6122e-003 3.3108e-003 3.5702e-003
               3.4100e-003 2.9896e-003];
avgvardeg5 = sum(vardeg(5,:))/8;

```

```

%*****
%***** BT=1.6 fs =32 *****
%*****

```

```

% BUTTERWORTH: BT=1.6 (delay =27, ascii file: sampbut6.asc)

```

```

meandeg(6,:) = [1.7105e+001 6.2079e+001 1.0712e+002 1.5207e+002 -1.6290e+002
               -1.1789e+002 -7.2922e+001 -2.7901e+001];
vardeg(6,:) = [5.7935e-004 4.9844e-004 4.7372e-004 5.3648e-004 4.6827e-004 5.2152e-004
               4.4754e-004 4.9717e-004];
avgvardeg6 = sum(vardeg(6,:))/8;

```

```

%*****
%***** BT=1.8 fs=48 *****
%*****

% BUTTERWORTH: BT=1.8 (delay =35, ascii file: sampbut7.asc)

meandeg(7,:) = [1.7103e+001 6.2156e+001 1.0708e+002 1.5217e+002 -1.6291e+002
               -1.1791e+002 -7.2871e+001 -2.7893e+001];
vardeg(7,:) = [3.0054e-003 2.4409e-003 2.3048e-003 2.7448e-003 2.2233e-003 2.1648e-003
               2.4702e-003 2.8097e-003];
avgvardeg7 = sum(vardeg(7,:))/8;

%*****
%***** BT=2 fs=48 *****
%*****

% BUTTERWORTH: BT=2 (using delay = 32, ascii file: sampbut2.asc)

meandeg(2,:) = [1.7100e+001 6.2111e+001 1.0710e+002 1.5211e+002 -1.6290e+002 -
               1.1790e+002 -7.2897e+001 -2.7899e+001];
vardeg(2,:) = [1.2757e-004 1.0112e-004 9.9469e-005 1.1625e-004 9.3600e-005 8.5729e-005
               1.0797e-004 1.2218e-004];
avgvardeg2 = sum(vardeg(2,:))/8;

%*****
%***** BT=2.2 fs=48 *****
%*****

% BUTTERWORTH: BT=2.2 (using delay = 29, ascii file: sampbut9.asc)

meandeg(9,:) = [1.7098e+001 6.2134e+001 1.0707e+002 1.5215e+002 -1.6289e+002
               -1.1791e+002 -7.2870e+001 -2.7895e+001];
vardeg(9,:) = [1.1019e-003 9.3545e-004 8.7686e-004 1.0168e-003 8.5896e-004 9.3158e-004
               8.5970e-004 9.7456e-004];
avgvardeg9 = sum(vardeg(9,:))/8;

%*****
%***** BT=2.4 fs=48 *****
%*****

% BUTTERWORTH: BT=2.4 (using delay = 27, ascii file: sambut10.asc)

meandeg(10,:) = [1.7080e+001 6.2064e+001 1.0709e+002 1.5206e+002 -1.6292e+002
                -1.1792e+002 -7.2927e+001 -2.7922e+001];
vardeg(10,:) = [2.5908e-004 2.1067e-004 2.0091e-004 2.3544e-004 1.9016e-004 1.8373e-004
                2.0921e-004 2.4034e-004];
avgvardeg10 = sum(vardeg(10,:))/8;

```

```

%*****
%***** BT=2.6 fs=48 *****
%*****

%*****
%***** BT=2.8 fs=48 *****
%*****

%*****
%***** BT=3 fs=48 *****
%*****

%*****
%***** BT=3.2 fs=48 *****
%*****

%*****
%***** BT=3.2 fs=48 *****
%*****

```

%BUTTERWORTH: BT=2.6 (using delay =34, ascii file: sambut11.asc)

```

meandeg(11,:) = [1.7076e+001 6.2055e+001 1.0709e+002 1.5205e+002 -1.6293e+002
                -1.1792e+002 -7.2940e+001 -2.7928e+001];
vardeg(11,:) = [3.9346e-004 3.3146e-004 3.0956e-004 3.6135e-004 3.0312e-004 3.1763e-004
                3.0654e-004 3.5248e-004];
avgvardeg11 = sum(vardeg(11,:))/8;

```

%BUTTERWORTH: BT=2.8 (using delay =32, ascii file: sambut12.asc)

```

meandeg(12,:) = [1.7078e+001 6.2083e+001 1.0708e+002 1.5209e+002 -1.6292e+002
                -1.1792e+002 -7.2917e+001 -2.7921e+001];
vardeg(12,:) = [1.4141e-005 1.2143e-005 1.2144e-005 1.3224e-005 1.1092e-005 1.2642e-005
                1.1685e-005 1.2637e-005];
avgvardeg12 = sum(vardeg(12,:))/8;

```

%BUTTERWORTH: BT=3 (using delay =30, ascii file: sampbut3.asc)

```

meandeg(3,:) = [1.7077e+001 6.2088e+001 1.0707e+002 1.5209e+002 -1.6292e+002
                -1.1792e+002 -7.2913e+001 -2.7921e+001];
vardeg(3,:) = [9.9154e-005 8.3102e-005 7.9266e-005 9.1259e-005 7.4914e-005 8.1407e-005
                7.9067e-005 8.9380e-005];
avgvardeg3 = sum(vardeg(3,:))/8;

```

%BUTTERWORTH: BT=3.2 (using delay = 28, ascii file: sambut14.asc)

```

meandeg(14,:) = [1.7072e+001 6.2073e+001 1.0707e+002 1.5207e+002 -1.6293e+002
                -1.1793e+002 -7.2927e+001 -2.7928e+001];
vardeg(14,:) = [5.8964e-007 5.0913e-007 9.2412e-007 6.3686e-007 6.4852e-007 4.5768e-007
                1.0022e-006 5.8489e-007];
avgvardeg14 = sum(vardeg(14,:))/8;

```

```
%*****  
%***** BT=3.4 fs=48 *****  
%*****
```

```
%BUTTERWORTH: BT=3.4 (using delay = 34, ascii file: sambut15.asc)
```

```
meandeg(15,:) = [1.7069e+001 6.2062e+001 1.0707e+002 1.5206e+002 -1.6293e+002  
-1.1793e+002 -7.2936e+001 -2.7932e+001];  
vardeg(15,:) = [4.8152e-005 4.0562e-005 3.7986e-005 4.4103e-005 3.8410e-005 3.8316e-005  
3.7664e-005 4.3210e-005];  
avgvardeg15 = sum(vardeg(15,:))/8;
```

```
%*****  
%***** BT=3.6 fs=48 *****  
%*****
```

```
%BUTTERWORTH: BT=3.6 (using delay = 32, ascii file: sambut16.asc)
```

```
meandeg(16,:) = [1.7068e+001 6.2064e+001 1.0707e+002 1.5206e+002 -1.6293e+002  
-1.1793e+002 -7.2934e+001 -2.7933e+001];  
vardeg(16,:) = [1.6145e-005 1.3681e-005 1.2928e-005 1.4785e-005 1.3520e-005 1.2891e-005  
1.2778e-005 1.4431e-005];  
avgvardeg16 = sum(vardeg(16,:))/8;
```

```
%*****  
%***** BT=3.8 fs=48 *****  
%*****
```

```
% BUTTERWORTH: BT=3.8 (using delay =37, ascii file: sambut17.asc)
```

```
meandeg(17,:) = [1.7068e+001 6.2071e+001 1.0707e+002 1.5207e+002 -1.6293e+002  
-1.1793e+002 -7.2929e+001 -2.7932e+001];  
vardeg(17,:) = [6.0818e-006 5.0583e-006 5.1543e-006 5.6452e-006 4.5621e-006 4.9250e-006  
5.5862e-006 5.5223e-006];  
avgvardeg17 = sum(vardeg(17,:))/8;
```

```
%*****  
%***** BT=4.0 fs=48 *****  
%*****
```

```
% BUTTERWORTH: BT=4.0 (using delay =35, ascii file: sambut18.asc)
```

```
meandeg(18,:) = [1.7067e+001 6.2068e+001 1.0707e+002 1.5207e+002 -1.6293e+002  
-1.1793e+002 -7.2932e+001 -2.7933e+001];  
vardeg(18,:) = [6.3159e-007 5.2962e-007 7.6612e-007 6.0844e-007 7.0038e-007 5.1824e-007  
1.1054e-006 5.8058e-007];  
avgvardeg18 = sum(vardeg(18,:))/8;
```

```

%*****
%***** PLOTS*****
%*****

% Average Variance for the Symbols Plot

figure(1);
whitebg;

AMPMavgvar = [avgvardeg1 avgvardeg13 avgvardeg8 avgvardeg4 avgvardeg5 avgvardeg6
              avgvardeg7 avgvardeg2 avgvardeg9 avgvardeg10 avgvardeg11 avgvardeg12
              avgvardeg3 avgvardeg14 avgvardeg15 avgvardeg16 avgvardeg17 avgvardeg18];

% interpolation using spline fit

interBT=1:0.01:4.0;
interpol=spline(BT,AMPMavgvar,interBT);

plot(BT,AMPMavgvar,'ok',interBT,interpol,'k');
title('5th Order Butterworth Filter Symbol Average Variance vs BT');
xlabel('Bandwidth-Time Product (BT)');
ylabel('Variance in Degrees');

```

APPENDIX F

SCATTER PLOTS:

3RD Order BESSEL FILTER

This appendix contains the Scatter Plots of the output of the SSPA when a 3rd Order Bessel Spectrum Filter is used after the 8PSK Modulator. The Scatter Plots were produced for BT=1 to 4 using the SPWSOBRE.M function. Also, the listing of the program BESSPLOT.M written in Matlab which was used to produce the Average Symbol Variance plots (see Figure 3.45 and 3.46 in this report) is included. All the values of mean and variance in this program were calculated in the program SPWSOBRE.M.

F.1 Scatter Plots

Output of SSPA (saturation level), 3rd Order Bessel Filter (BT=1)

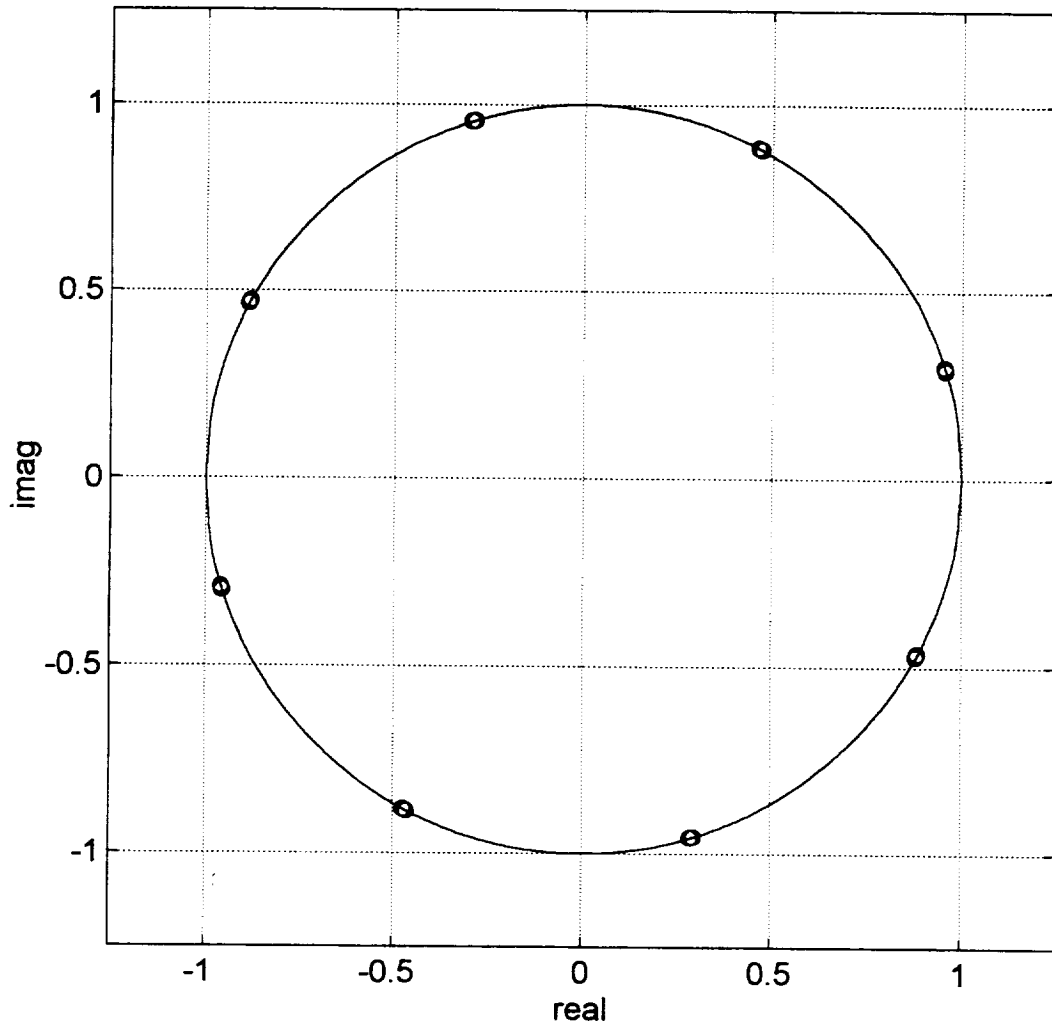


Figure F.1 - Output of SSPA (Saturation Level)
Spectrum Shaping Filter: 3rd Order Bessel BT=1

Output of SSPA (saturation level), 3rd Order Bessel Filter (BT=1.05)

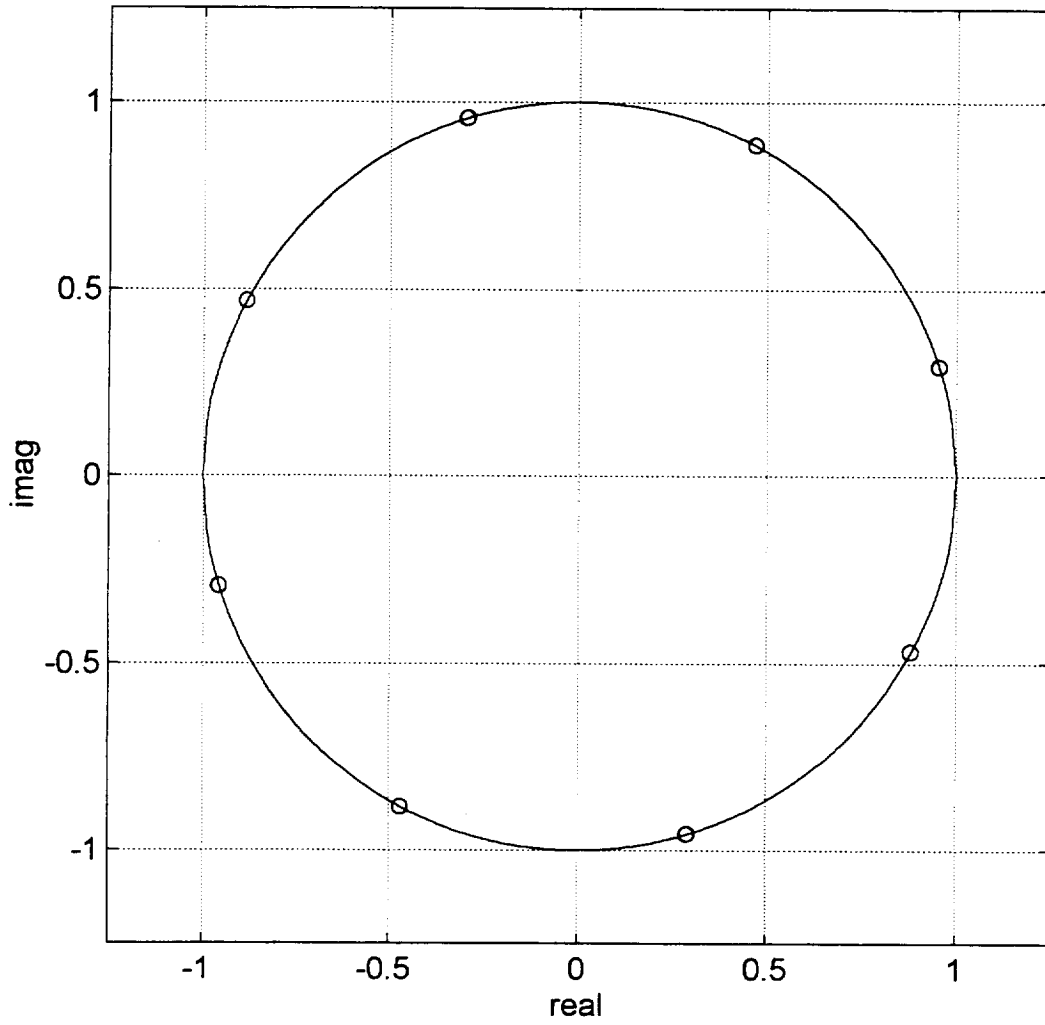


Figure F.2 - Output of SSPA (Saturation Level)
Spectrum Shaping Filter: 3rd Order Bessel BT=1.05

Output of SSPA (saturation level), 3rd Order Bessel Filter (BT=1.1)

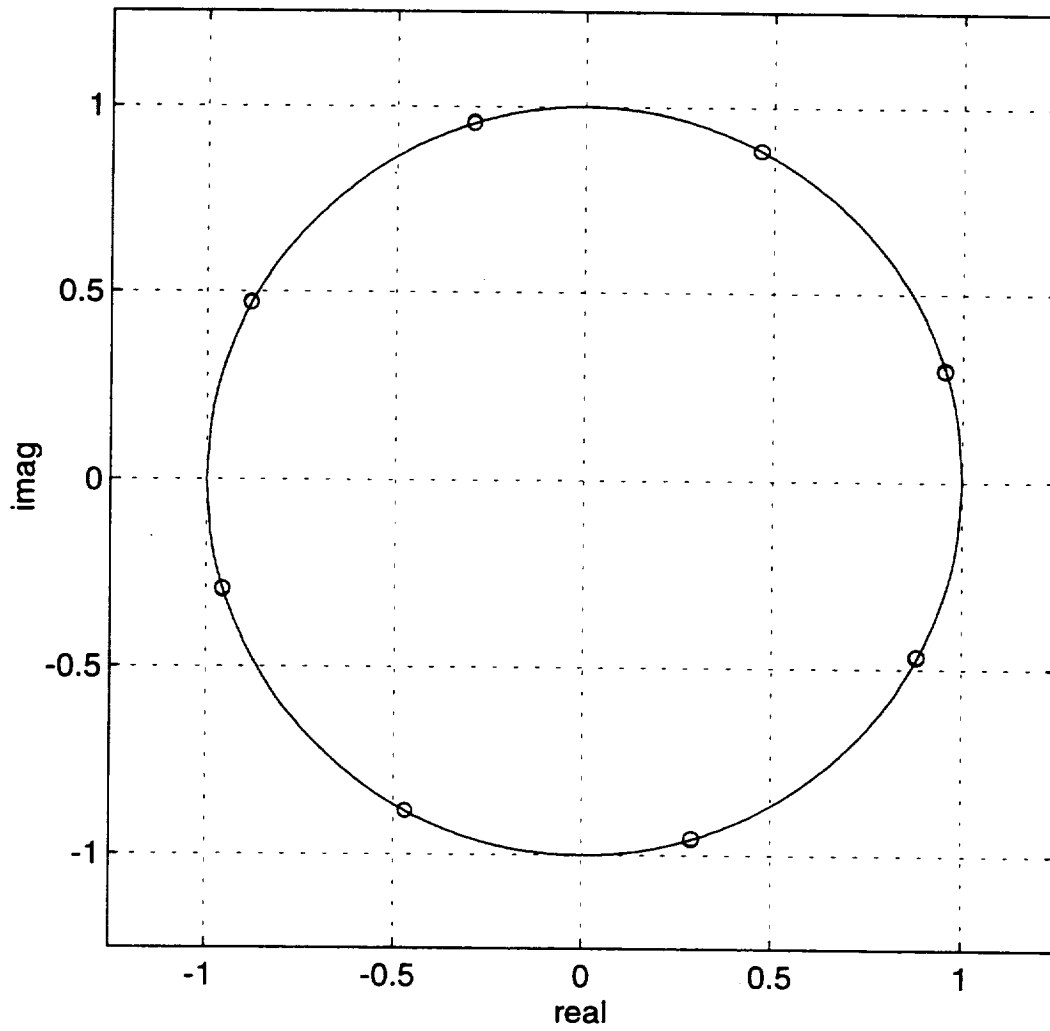


Figure F.3 - Output of SSPA (Saturation Level)
Spectrum Shaping Filter: 3rd Order Bessel BT=1.1

Output of SSPA (saturation level), 3rd Order Bessel Filter (BT=1.2)

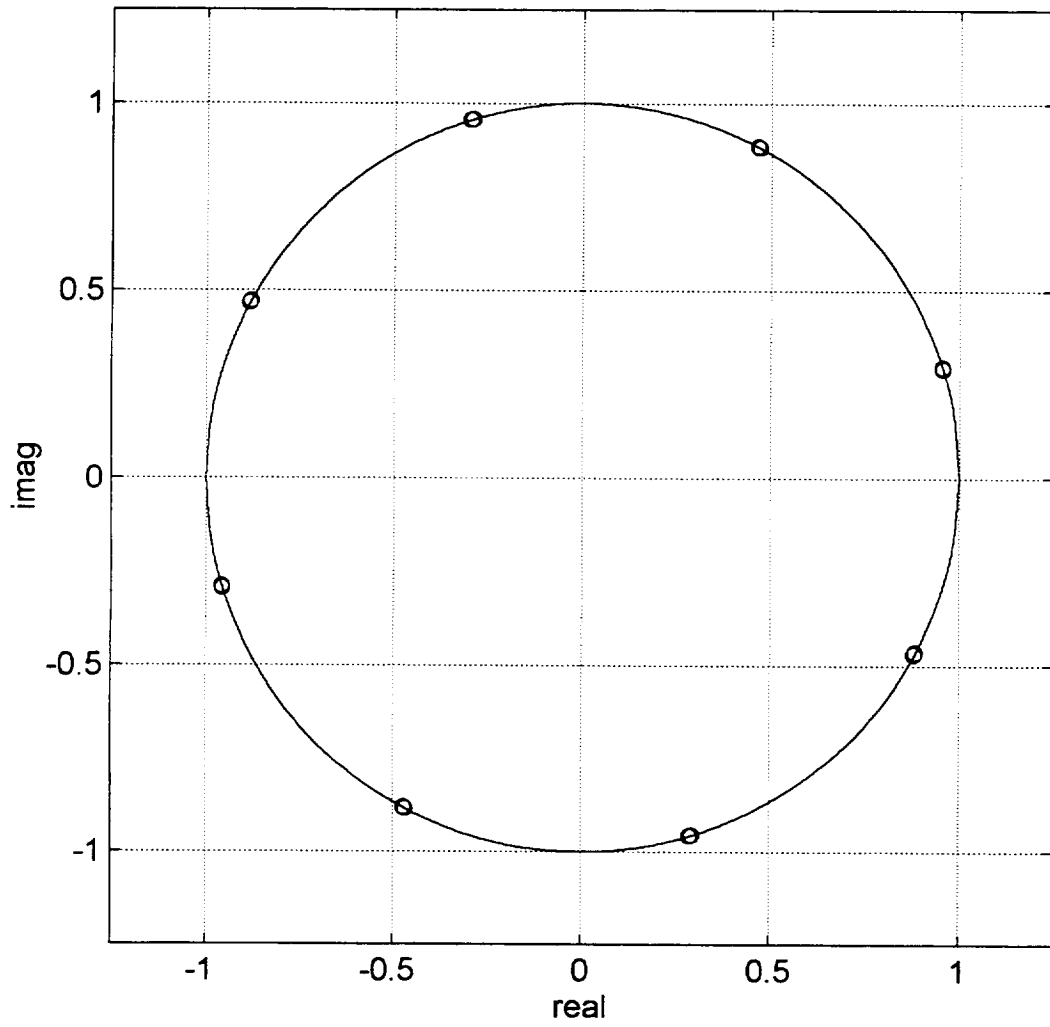


Figure F.4 - Output of SSPA (Saturation Level)
Spectrum Shaping Filter: 3rd Order Bessel BT=1.2

Output of SSPA (saturation level), 3rd Order Bessel Filter (BT=1.4)

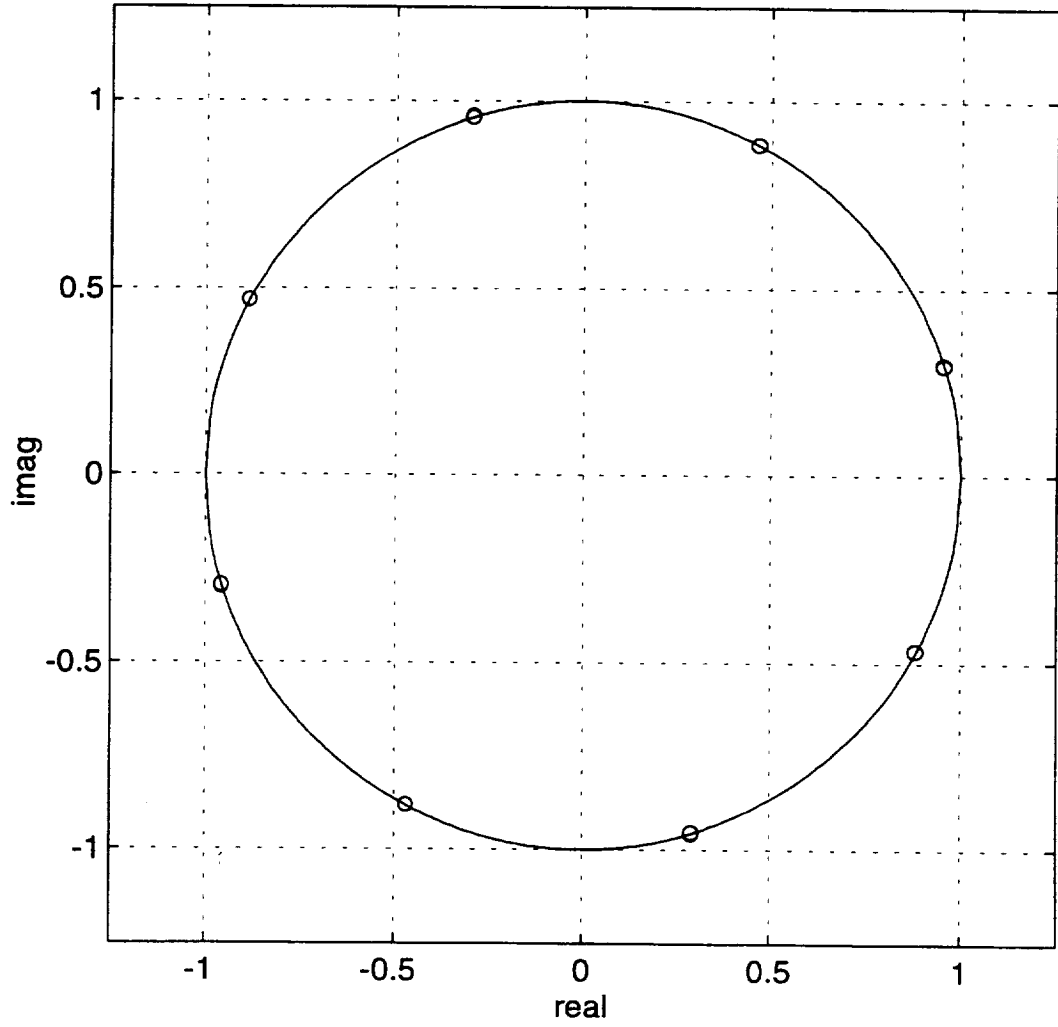


Figure F.5 - Output of SSPA (Saturation Level)
Spectrum Shaping Filter: 3rd Order Bessel BT=1.4

Output of SSPA (saturation level), 3rd Order Bessel Filter (BT=1.6)

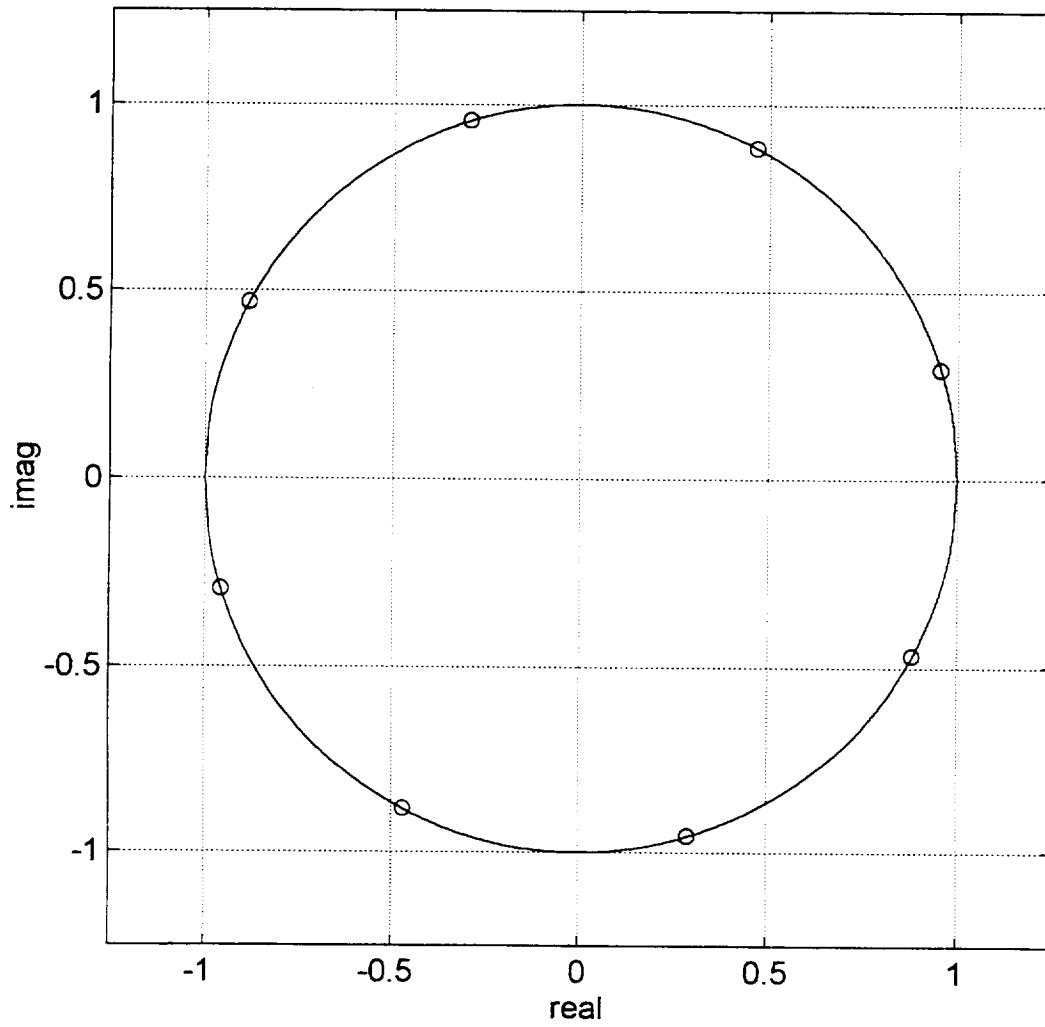


Figure F.6 - Output of SSPA (Saturation Level)
Spectrum Shaping Filter: 3rd Order Bessel BT=1.6

Output of SSPA (saturation level), 3rd Order Bessel Filter (BT=1.8)

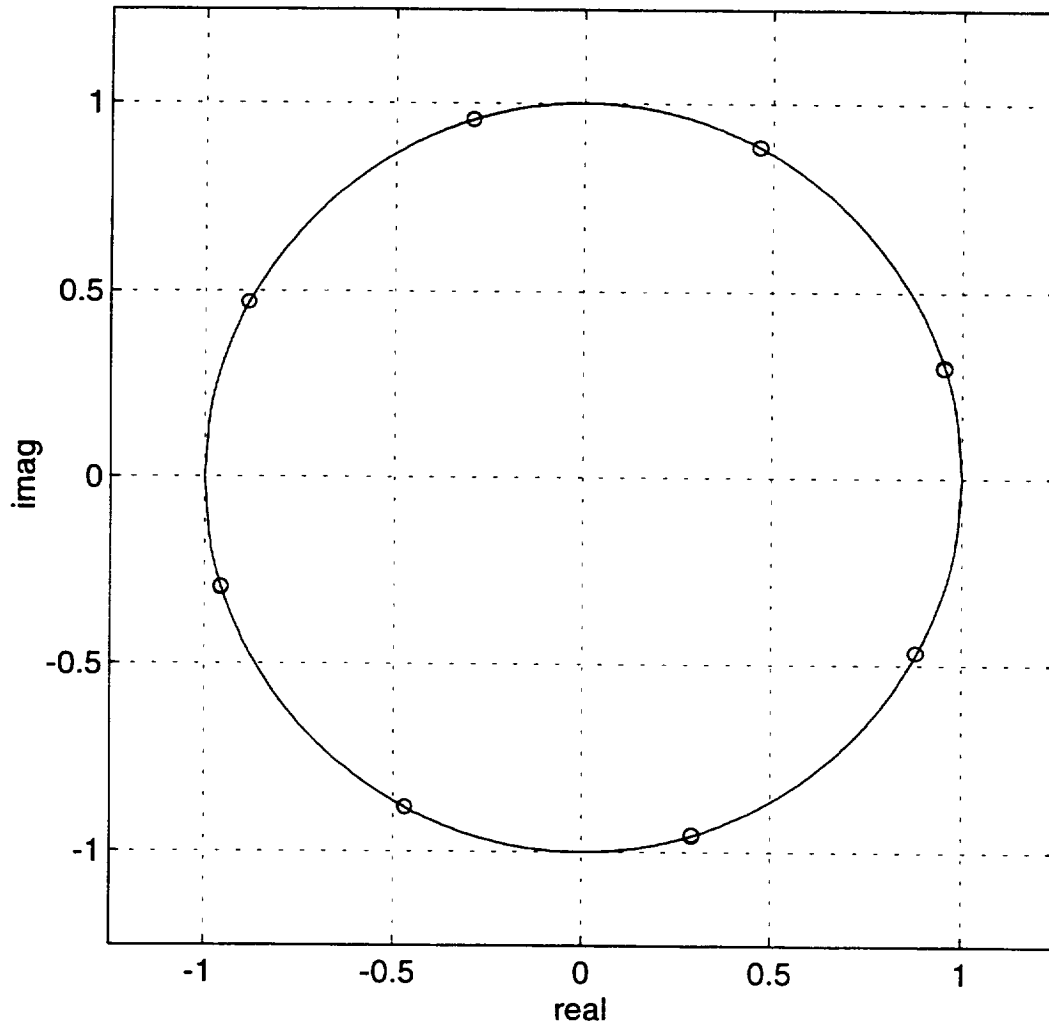


Figure F.7 - Output of SSPA (Saturation Level)
Spectrum Shaping Filter: 3rd Order Bessel BT=1.8

Output of SSPA (saturation level), 3rd Order Bessel Filter (BT=2)

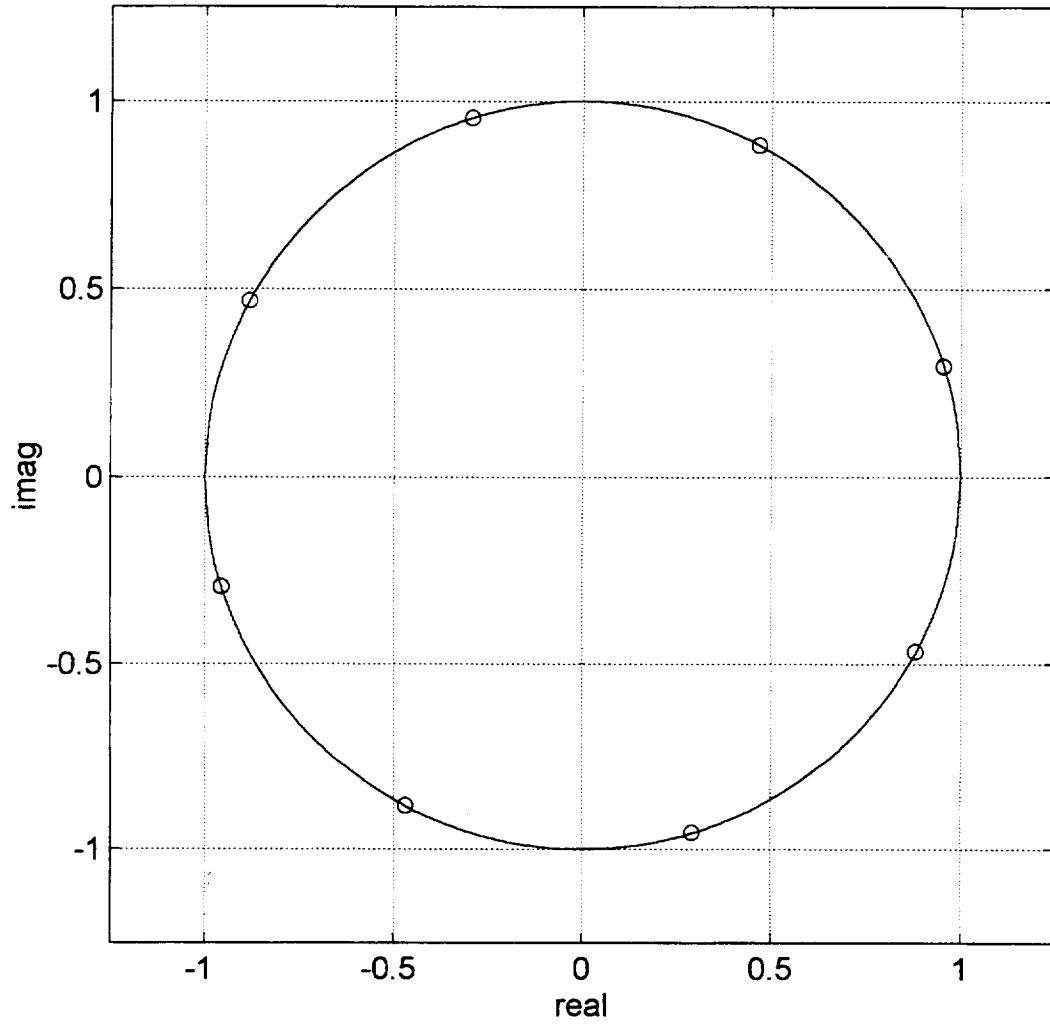


Figure F.8 - Output of SSPA (Saturation Level)
Spectrum Shaping Filter: 3rd Order Bessel BT=2

Output of SSPA (saturation level), 3rd Order Bessel Filter (BT=2.2)

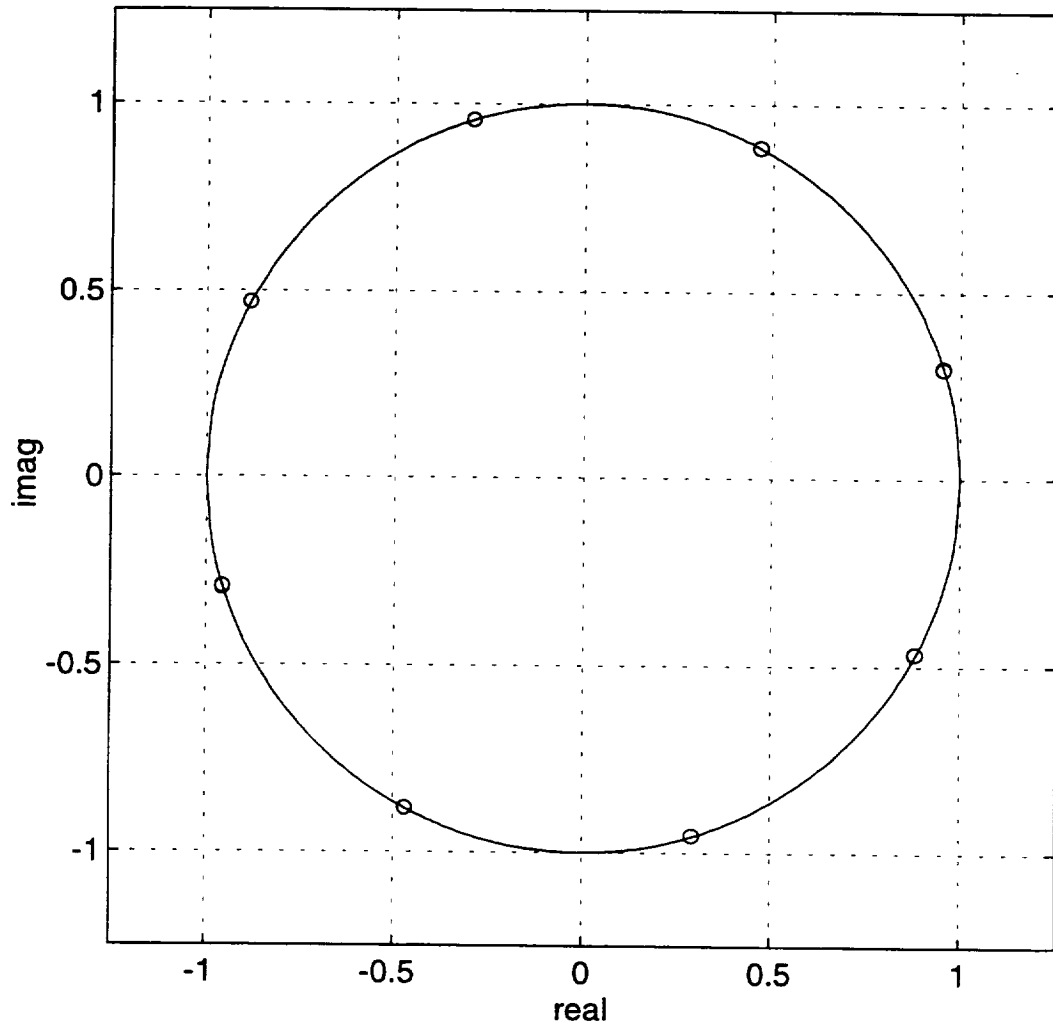


Figure F.9 - Output of SSPA (Saturation Level)
Spectrum Shaping Filter: 3rd Order Bessel BT=2.2

Output of SSPA (saturation level), 3rd Order Bessel Filter (BT=2.4)

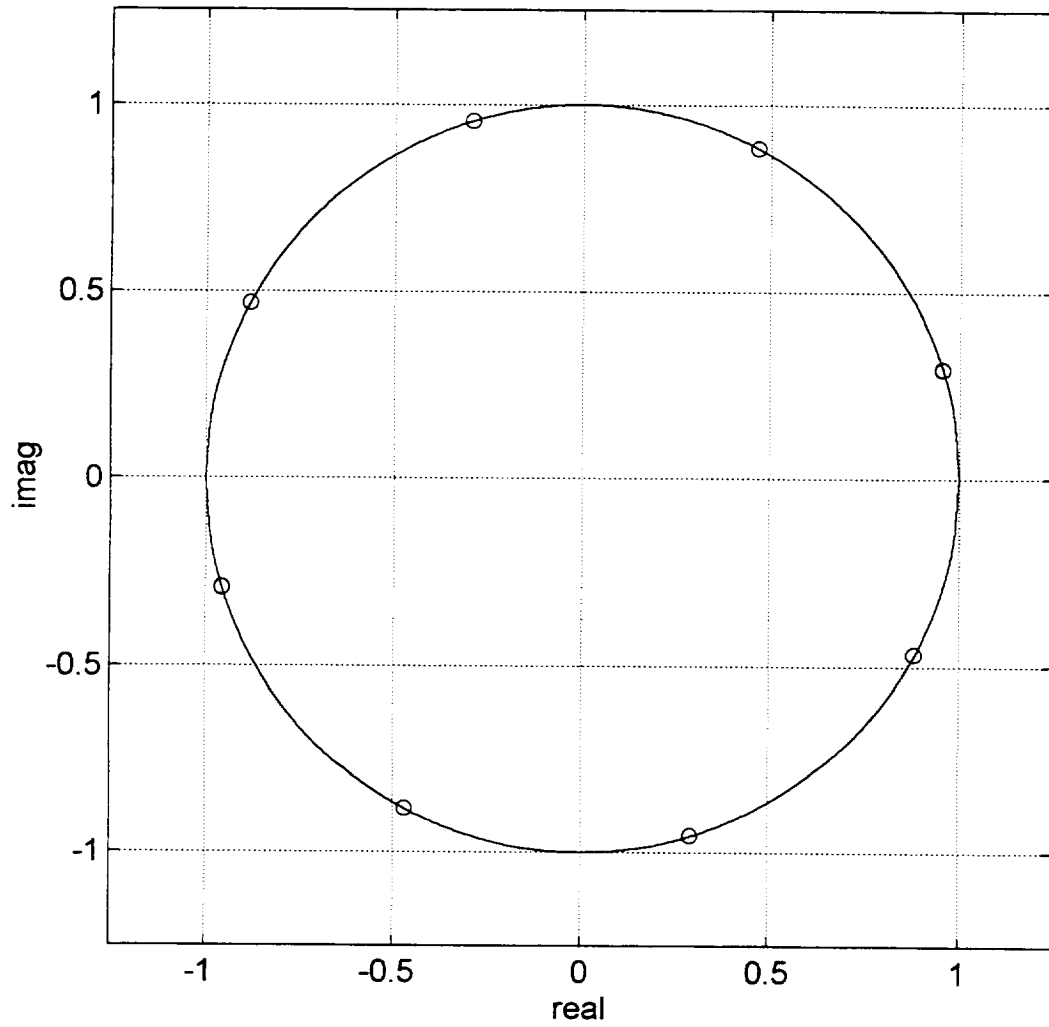


Figure F.10 - Output of SSPA (Saturation Level)
Spectrum Shaping Filter: 3rd Order Bessel BT=2.4

Output of SSPA (saturation level), 3rd Order Bessel Filter (BT=2.6)

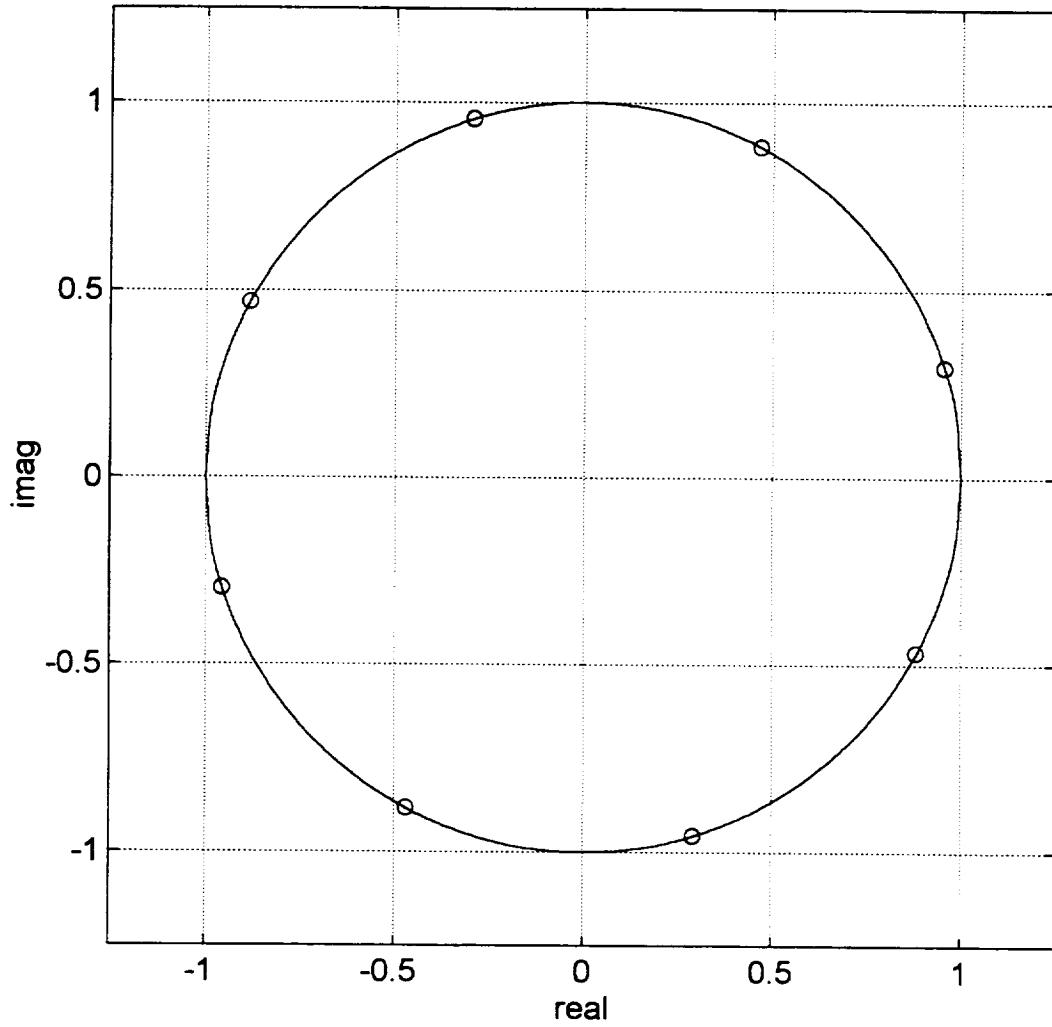


Figure F.11 - Output of SSPA (Saturation Level)
Spectrum Shaping Filter: 3rd Order Bessel BT=2.6

Output of SSPA (saturation level), 3rd Order Bessel Filter (BT=2.8)

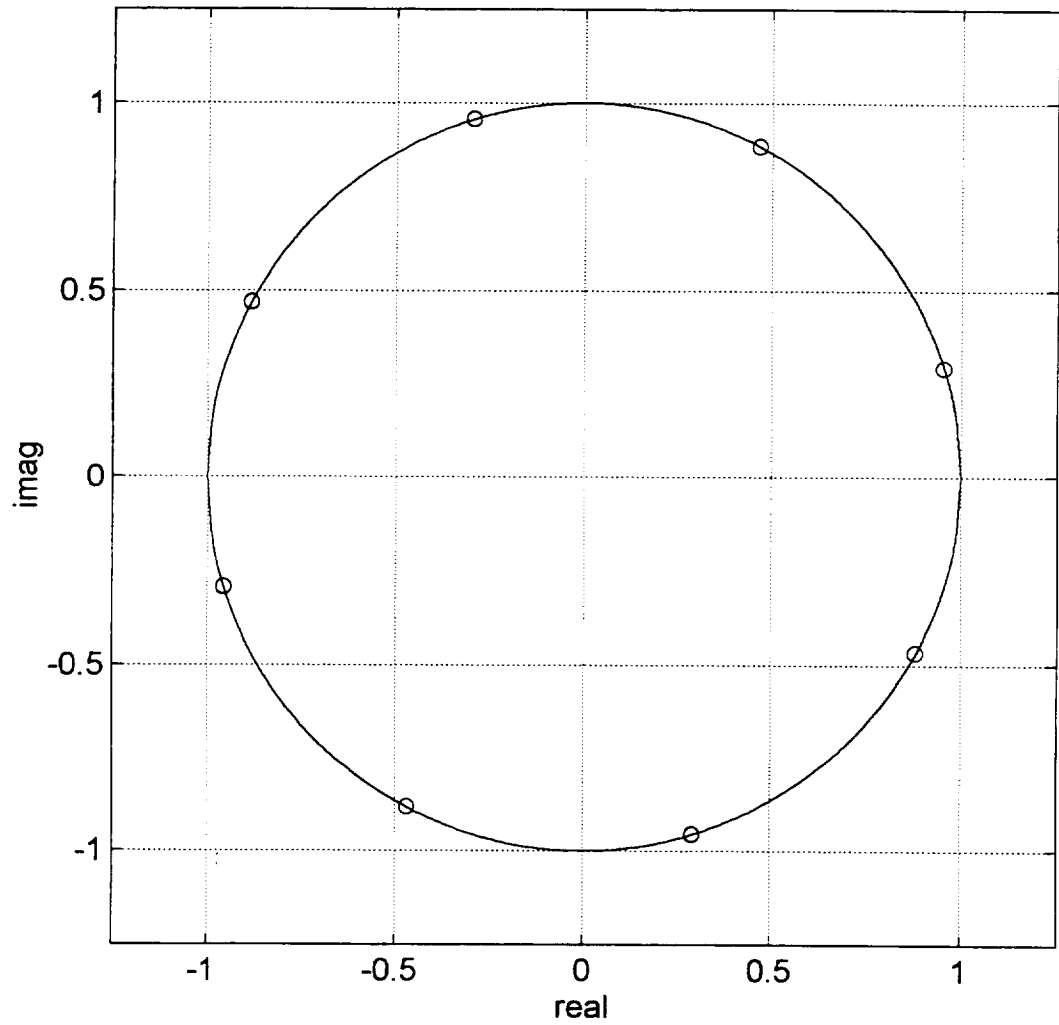


Figure F.12 - Output of SSPA (Saturation Level)
Spectrum Shaping Filter: 3rd Order Bessel BT=2.8

Output of SSPA (saturation level), 3rd Order Bessel Filter (BT=3)

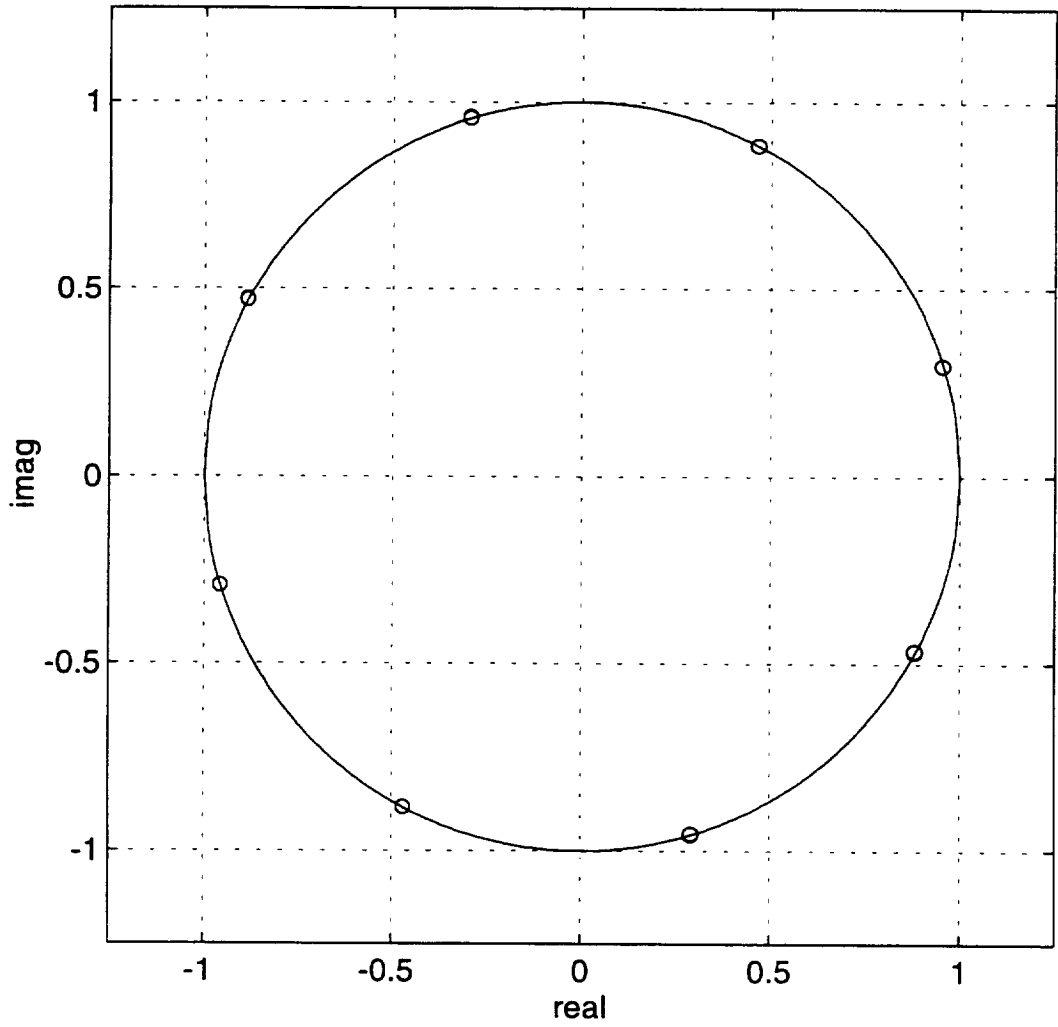


Figure F.13- Output of SSPA (Saturation Level)
Spectrum Shaping Filter: 3rd Order Bessel BT=3

Output of SSPA (saturation level), 3rd Order Bessel Filter (BT=3.2)

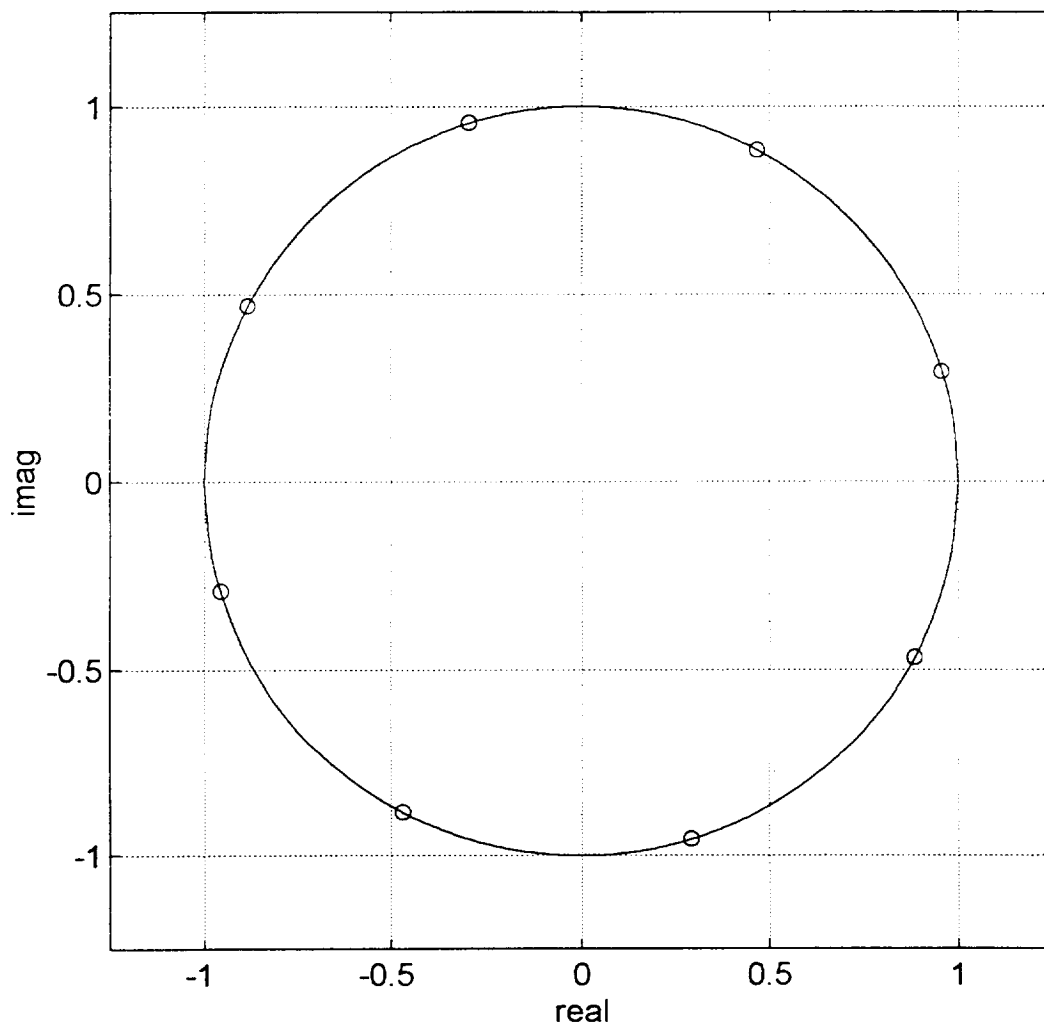


Figure F.14- Output of SSPA (Saturation Level)
Spectrum Shaping Filter: 3rd Order Bessel BT=3.2

Output of SSPA (saturation level), 3rd Order Bessel Filter (BT=3.4)

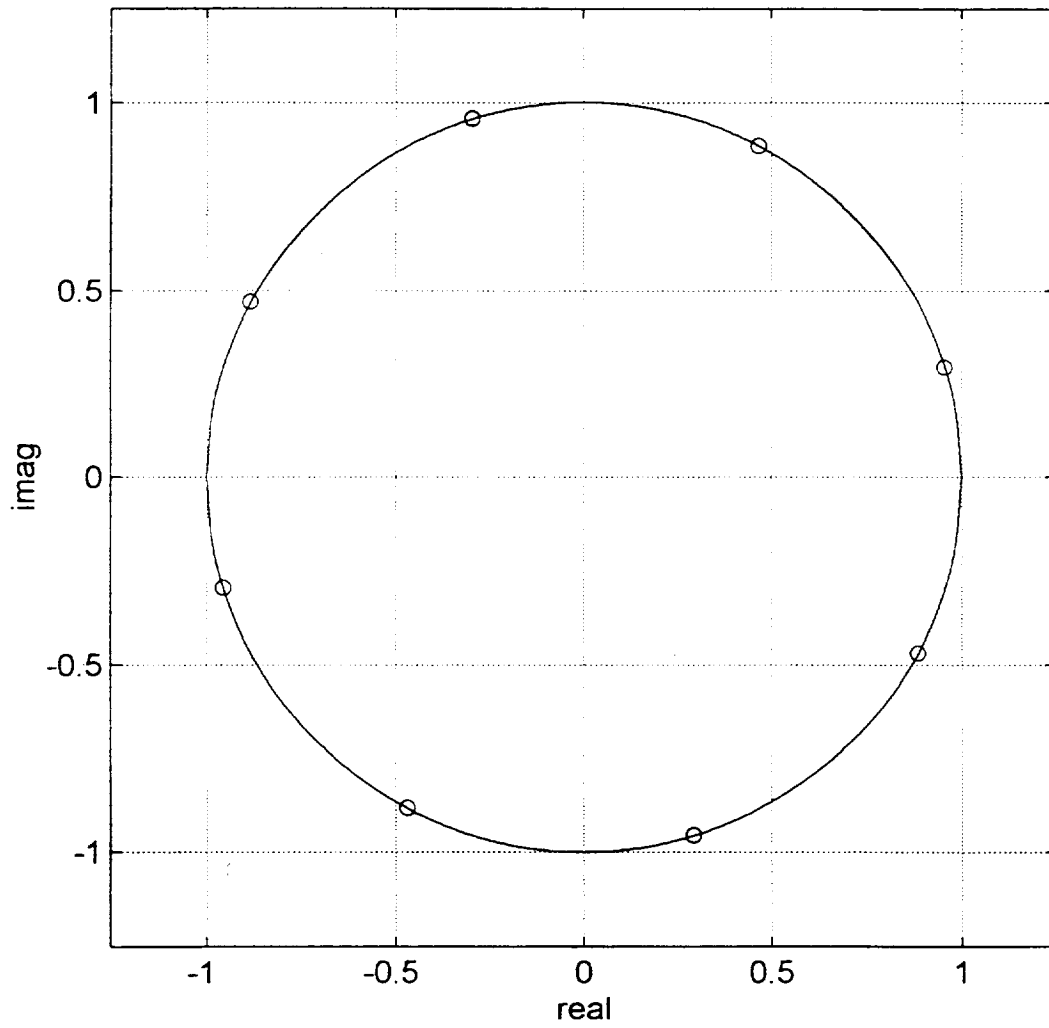


Figure F.15 - Output of SSPA (Saturation Level)
Spectrum Shaping Filter: 3rd Order Bessel BT=3.4

Output of SSPA (saturation level), 3rd Order Bessel Filter (BT=3.6)

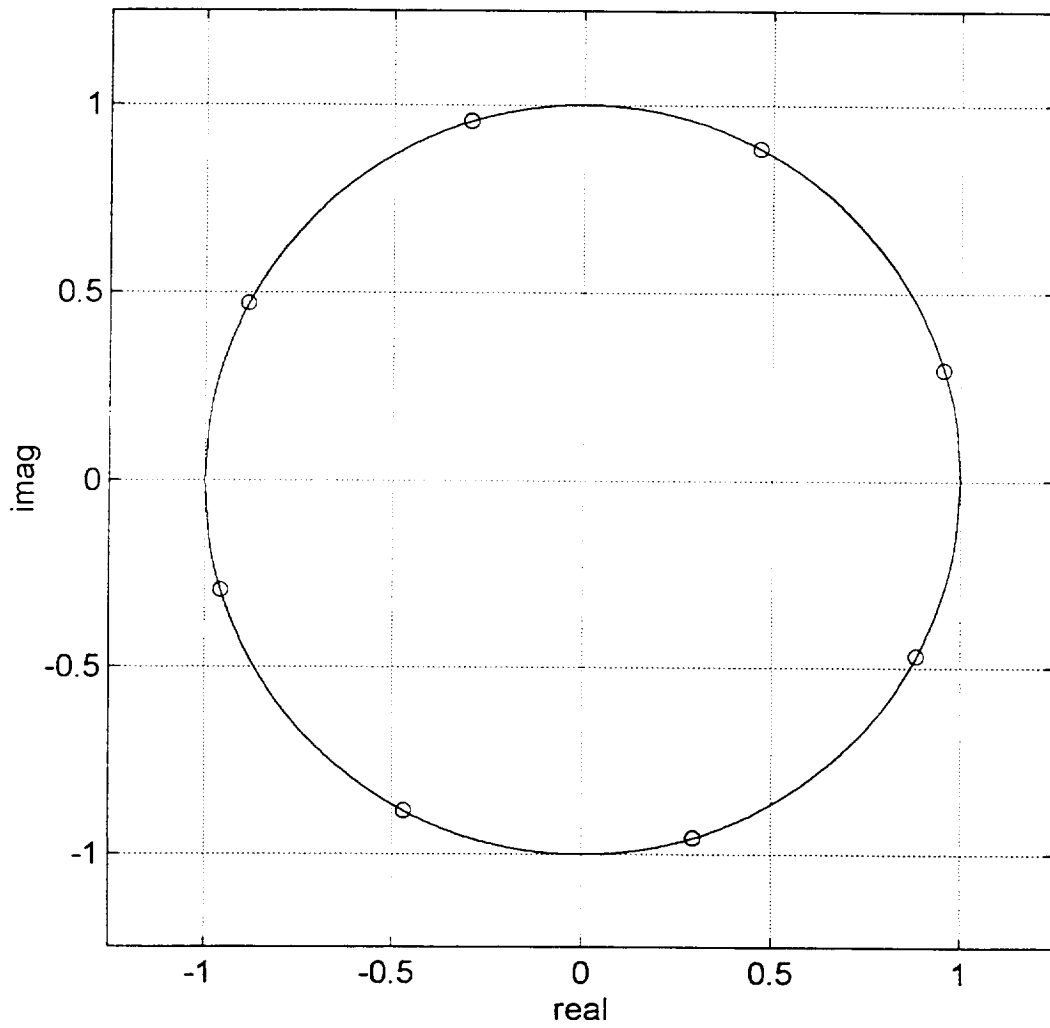


Figure F.16 - Output of SSPA (Saturation Level)
Spectrum Shaping Filter: 3rd Order Bessel BT=3.6

Output of SSPA (saturation level), 3rd Order Bessel Filter (BT=3.8)

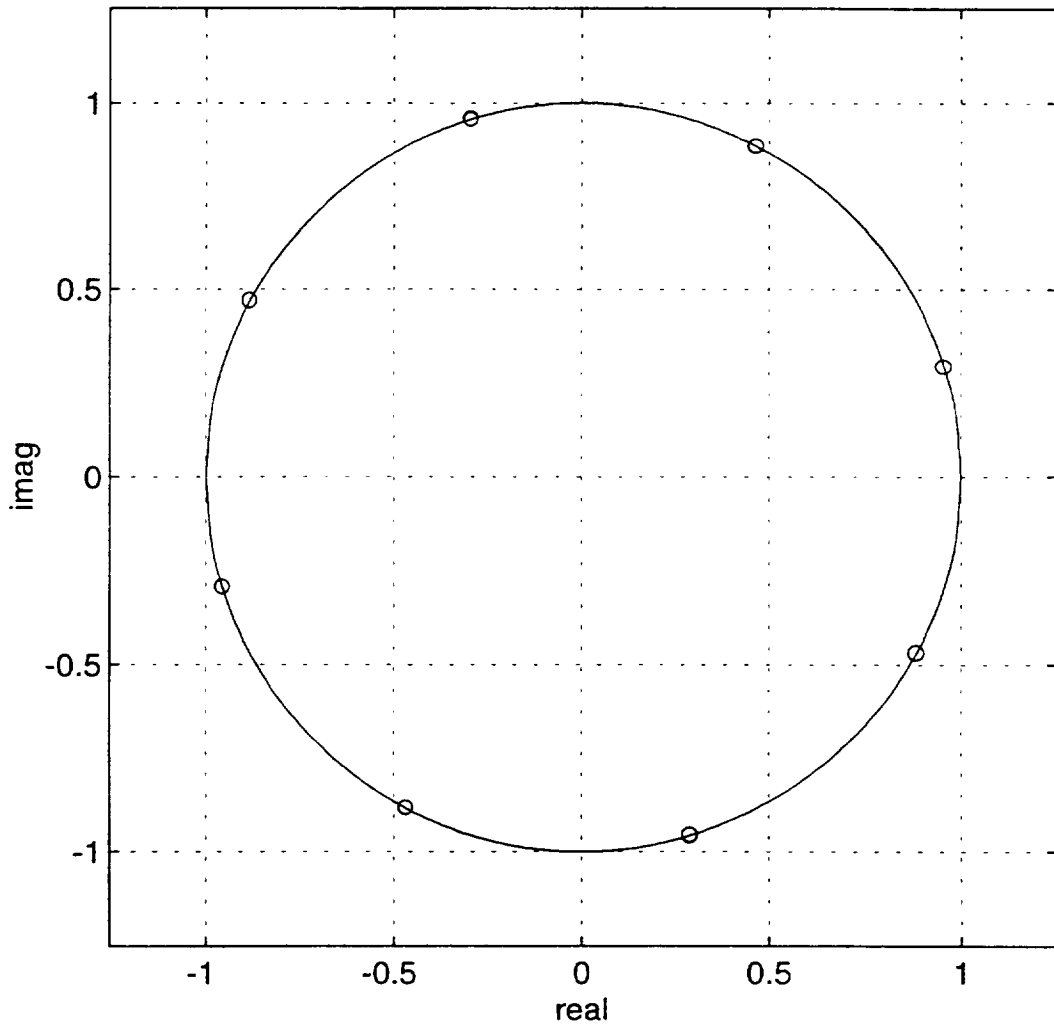


Figure F.17 - Output of SSPA (Saturation Level)
Spectrum Shaping Filter: 3rd Order Bessel BT=3.8

Output of SSPA (saturation level), 3rd Order Bessel Filter (BT=4)

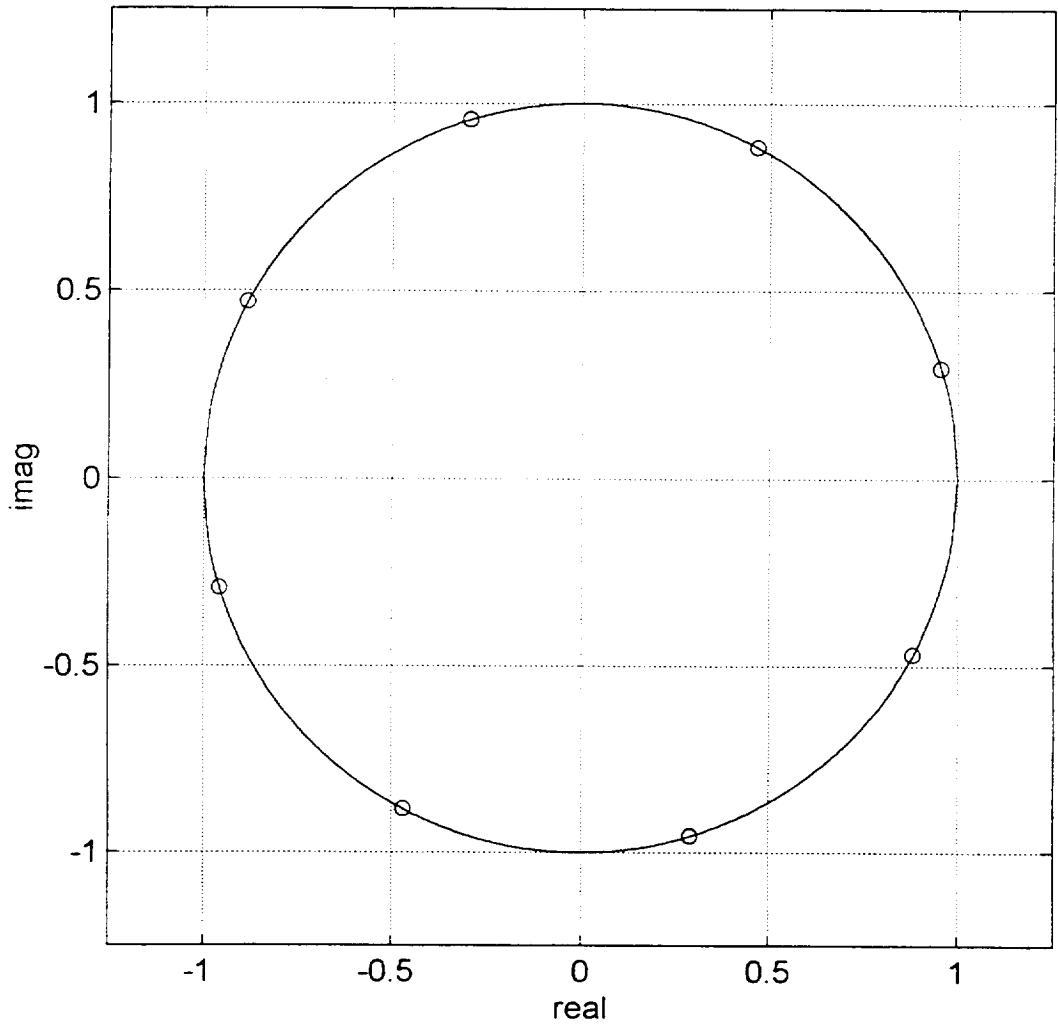


Figure F.18 - Output of SSPA (Saturation Level)
Spectrum Shaping Filter: 3rd Order Bessel BT=4

F.2 Program Listing: BESSPLOT.M

```
% Program : BESSPLOT.M
% Written by : Rubén Caballero
% Developed using MATLAB V4.2B and Signal Processing Toolbox V3.0b
% Copyright 1996 - Rubén Caballero
% New Mexico State University
%
% This function uses the mean and variance calculated by the function SPWSOBRE.M to
% calculate the Average Symbol Variance. The result is a plot of the Average Symbol Variance
% versus BT for the 3rd Order Bessel filter as the spectrum shaping filter.

clear;

%*****
%***** Bessel Filters *****
%*****

BT=[1 1.05 1.1 1.2 1.4 1.6 1.8 2 2.2 2.4 2.6 2.8 3 3.2 3.4 3.6 3.8 4.0];

%*****
%***** BT=1 fs=16 *****
%*****

% BESSEL : BT=1 (using delay=10, ascii file: sampbes1.asc)

meandeg(1,:) = [1.7100e+001 6.2067e+001 1.0712e+002 1.5205e+002 -1.6290e+002
               -1.1789e+002 -7.2926e+001 -2.7905e+001];
vardeg(1,:) = [1.0221e-003 8.5808e-004 8.0633e-004 9.4189e-004 7.8621e-004 8.2393e-004
               8.1116e-004 9.1752e-004];
avgvardeg1 = sum(vardeg(1,:))/8;

%*****
%***** BT=1.05 fs=32 *****
%*****

% BESSEL : BT=1.05 (using delay =20, ascii file: sampbes13.asc)

meandeg(13,:) = [1.7098e+001 6.2105e+001 1.0709e+002 1.5211e+002 -1.6290e+002
                -1.1790e+002 -7.2897e+001 -2.7901e+001];
vardeg(13,:) = [4.0437e-005 3.3809e-005 3.1692e-005 3.7052e-005 3.0734e-005 3.2129e-005
                 3.2110e-005 3.6434e-005];
avgvardeg13 = sum(vardeg(13,:))/8;
```

```

%*****
%***** BT=1.1 fs=32 *****
%*****

% BESSEL : BT=1.1 (using delay =19, ascii file: sampbes8.asc)

meandeg(8,:) = [1.7098e+001 6.2101e+001 1.0710e+002 1.5210e+002 -1.6290e+002
               -1.1790e+002 -7.2900e+001 -2.7902e+001];
vardeg(8,:) = [9.9913e-006 8.3489e-006 7.8251e-006 9.1203e-006 7.5720e-006 7.9193e-006
               7.9803e-006 9.0411e-006];
avgvardeg8 = sum(vardeg(8,:))/8;

%*****
%***** BT=1.2 fs=32 *****
%*****

% BESSEL : BT=1.2 (using delay =17, ascii file: sampbes4.asc)

meandeg(4,:) = [1.7099e+001 6.2083e+001 1.0711e+002 1.5208e+002 -1.6290e+002
               -1.1790e+002 -7.2914e+001 -2.7903e+001];
vardeg(4,:) = [2.4972e-004 2.0951e-004 1.9659e-004 2.3032e-004 1.9168e-004 2.0041e-004
               1.9809e-004 2.2399e-004];
avgvardeg4 = sum(vardeg(4,:))/8;

%*****
%***** BT=1.4 fs=32 *****
%*****

% BESSEL : BT=1.4 (using delay = 24, ascii file: sampbes5.asc)

meandeg(5,:) = [1.7101e+001 6.2102e+001 1.0710e+002 1.5210e+002 -1.6290e+002
               -1.1790e+002 -7.2899e+001 -2.7899e+001];
vardeg(5,:) = [1.3749e-006 1.1572e-006 1.1217e-006 1.2701e-006 1.1957e-006 1.2262e-006
               1.1256e-006 1.2264e-006];
avgvardeg5 = sum(vardeg(5,:))/8;

%*****
%***** BT=1.6 fs=32 *****
%*****

% BESSEL : BT=1.6 (using delay = 22, ascii file: sampbes6.asc)

meandeg(6,:) = [1.7106e+001 6.2104e+001 1.0711e+002 1.5210e+002 -1.6289e+002
               -1.1789e+002 -7.2896e+001 -2.7894e+001];
vardeg(6,:) = [4.5746e-006 3.8329e-006 3.5877e-006 4.2036e-006 3.3338e-006 3.5724e-006
               3.6400e-006 4.1172e-006];
avgvardeg6 = sum(vardeg(6,:))/8;

```

```

%*****
%***** BT=1.8 fs=48 *****
%*****

% BESSEL : BT=1.8 (using delay = 29, ascii file: sampbes7.asc)

meandeg(7,:) = [1.7109e+001 6.2107e+001 1.0711e+002 1.5211e+002 -1.6289e+002
               -1.1789e+002 -7.2892e+001 -2.7891e+001];
vardeg(7,:) = [1.6004e-006 1.3463e-006 1.2807e-006 1.4545e-006 1.1838e-006 1.2862e-006
               1.3147e-006 1.4452e-006];
avgvardeg7 = sum(vardeg(7,:))/8;

%*****
%***** BT=2 fs=32 *****
%*****

% BESSEL : BT=2 (using delay = 17, ascii file: sampbes2.asc)

meandeg(2,:) = [1.7109e+001 6.2109e+001 1.0711e+002 1.5211e+002 -1.6289e+002
               -1.1789e+002 -7.2891e+001 -2.7891e+001];
vardeg(2,:) = [4.4990e-008 3.8308e-008 5.1507e-008 5.3124e-008 5.0042e-008 5.9081e-008
               6.3786e-008 4.0034e-008];
avgvardeg2 = sum(vardeg(2,:))/8;

%*****
%***** BT=2.2 fs=48 *****
%*****

% BESSEL : BT=2.2 (using delay = 31, ascii file: sampbes9.asc)

meandeg(9,:) = [1.7108e+001 6.2106e+001 1.0711e+002 1.5211e+002 -1.6289e+002 -1.1789e+002
               -7.2893e+001 -2.7893e+001];
vardeg(9,:) = [1.0595e-006 8.9530e-007 8.6564e-007 9.7955e-007 9.1845e-007 9.8303e-007
               8.6531e-007 9.4939e-007];
avgvardeg9 = sum(vardeg(9,:))/8;

%*****
%***** BT=2.4 fs=48 *****
%*****

% BESSEL : BT=2.4 (using delay = 29, ascii file: sambes10.asc)

meandeg(10,:) = [1.7105e+001 6.2104e+001 1.0711e+002 1.5210e+002 -1.6290e+002
                -1.1790e+002 -7.2896e+001 -2.7895e+001];
vardeg(10,:) = [5.5214e-007 4.6563e-007 4.7792e-007 5.3915e-007 5.5696e-007 5.8688e-007
                4.5275e-007 4.8757e-007];
avgvardeg10 = sum(vardeg(10,:))/8;

```

```
%*****
%***** BT=2.6 fs=48 *****
%*****
```

```
% BESSEL : BT=2.6 (using delay = 27, ascii file: sambes11.asc)
```

```
meandeg(11,:) = [1.7101e+001 6.2100e+001 1.0710e+002 1.5210e+002 -1.6290e+002
                -1.1790e+002 -7.2899e+001 -2.7899e+001];
vardeg(11,:) = [4.0654e-007 3.4041e-007 3.8516e-007 4.1756e-007 4.7282e-007 4.7462e-007
                3.4439e-007 3.5223e-007];
avgvardeg11 = sum(vardeg(11,:))/8;
```

```
%*****
%***** BT=2.8 fs=48 *****
%*****
```

```
% BESSEL : BT=2.8 (using delay = 25, ascii file: sambes12.asc)
```

```
meandeg(12,:) = [1.7096e+001 6.2095e+001 1.0710e+002 1.5209e+002 -1.6290e+002
                -1.1790e+002 -7.2904e+001 -2.7904e+001];
vardeg(12,:) = [4.5417e-007 3.8038e-007 4.5201e-007 4.5872e-007 5.5238e-007 5.1875e-007
                4.0865e-007 3.9254e-007];
avgvardeg12 = sum(vardeg(12,:))/8;
```

```
%*****
%***** BT=3 fs=48 *****
%*****
```

```
% BESSEL : BT=3 (using delay = 40, ascii file: sampbes3.asc)
```

```
meandeg(3,:) = [1.7092e+001 6.2092e+001 1.0709e+002 1.5209e+002 -1.6291e+002
                -1.1791e+002 -7.2908e+001 -2.7908e+001];
vardeg(3,:) = [5.8291e-008 3.9094e-008 1.2009e-007 1.2832e-007 1.0620e-007 1.1197e-007
                7.1450e-008 3.9674e-008];
avgvardeg3 = sum(vardeg(3,:))/8;
```

```
%*****
%***** BT=3.2 fs=48 *****
%*****
```

```
% BESSEL : BT=3.2 (using delay = 28, ascii file: sambes14.asc)
```

```
meandeg(14,:) = [1.7088e+001 6.2088e+001 1.0709e+002 1.5209e+002 -1.6291e+002
                -1.1791e+002 -7.2911e+001 -2.7912e+001];
vardeg(14,:) = [5.4259e-008 3.5312e-008 1.4483e-007 1.0340e-007 1.1655e-007 8.1064e-008
                1.3418e-007 4.1300e-008];
avgvardeg14 = sum(vardeg(14,:))/8;
```

```

%*****
%***** BT=3.4 fs=48 *****
%*****

% BESSEL : BT=3.4 (using delay = 28, ascii file: sambes15.asc)

meandeg(15,:) = [1.7084e+001 6.2084e+001 1.0708e+002 1.5208e+002 -1.6292e+002
                -1.1792e+002 -7.2915e+001 -2.7916e+001];
vardeg(15,:) = [4.0005e-008 2.5838e-008 1.4176e-007 7.8527e-008 1.1756e-007 6.8254e-008
                1.4721e-007 2.9590e-008];
avgvardeg15 = sum(vardeg(15,:))/8;

%*****
%***** BT=3.6 fs=48 *****
%*****

% BESSEL : BT=3.6 (using delay = 28, ascii file: sambes16.asc)

meandeg(16,:) = [1.7081e+001 6.2081e+001 1.0708e+002 1.5208e+002 -1.6292e+002
                -1.1792e+002 -7.2919e+001 -2.7919e+001];
vardeg(16,:) = [3.1934e-008 2.0872e-008 1.3377e-007 6.1400e-008 1.0893e-007 5.5746e-008
                1.5336e-007 2.3636e-008];
avgvardeg16 = sum(vardeg(16,:))/8;

%*****
%***** BT=3.8 fs=48 *****
%*****

% BESSEL : BT=3.8 (using delay = 28, sambes17.asc)

meandeg(17,:) = [1.7078e+001 6.2078e+001 1.0708e+002 1.5208e+002 -1.6292e+002
                -1.1792e+002 -7.2921e+001 -2.7922e+001];
vardeg(17,:) = [2.5426e-008 1.6786e-008 1.2010e-007 4.7555e-008 9.4054e-008 4.3259e-008
                1.5054e-007 1.9058e-008];
avgvardeg17 = sum(vardeg(17,:))/8;

%*****
%***** BT=4 fs=48 *****
%*****

% BESSEL : BT=4 (using delay = 28, sambes18.asc)

meandeg(18,:) = [1.7076e+001 6.2075e+001 1.0708e+002 1.5208e+002 -1.6292e+002
                -1.1792e+002 -7.2924e+001 -2.7924e+001];
vardeg(18,:) = [1.9867e-008 1.3236e-008 1.0380e-007 3.6088e-008 7.8051e-008 3.2460e-008
                1.4042e-007 1.5133e-008];
avgvardeg18 = sum(vardeg(18,:))/8;

```

```

%*****
%***** PLOTS*****
%*****

% Average Variance for the Symbols

figure(1);
whitebg;

AMPMAvgvar = [avgvardeg1 avgvardeg13 avgvardeg8 avgvardeg4 avgvardeg5 avgvardeg6
              avgvardeg7 avgvardeg2 avgvardeg9 avgvardeg10 avgvardeg11 avgvardeg12
              avgvardeg3 avgvardeg14 avgvardeg15 avgvardeg16 avgvardeg17 avgvardeg18];

% interpolation using spline fit

interBT1=1:0.1:4.0;
interpol1=interp1(BT,AMPMAvgvar,interBT1,'spline');
plot(BT,AMPMAvgvar,'ok',interBT1,(interpol1),'k');

plot(BT,AMPMAvgvar,'ok');

title('3rd Order Bessel Filter Symbol Average Variance vs BT');
xlabel('Bandwidth-Time Product (BT)');
ylabel(' Variance in Degrees');
grid;

```

APPENDIX G
SCATTER PLOTS:
SRRC FILTER

This appendix contains the Scatter Plots of the output of the SSPA when a Square Root Raised Cosine (SRRC) Filter is used after the 8PSK Modulator. The Scatter Plots were produced for $\alpha=0.1$ to 1 using the SPWSOBRE.M function. Also, the listing of the program SRRCPLOT.M written in Matlab which was used to produce the Average Symbol Variance plot (see Figure 3.47 in this report) is included. All the values of mean and variance in this program were calculated in the program SPWSOBRE.M.

G.1 Scatter Plots

Output of SSPA (saturation level), SRRC Filter (alpha=0.1)

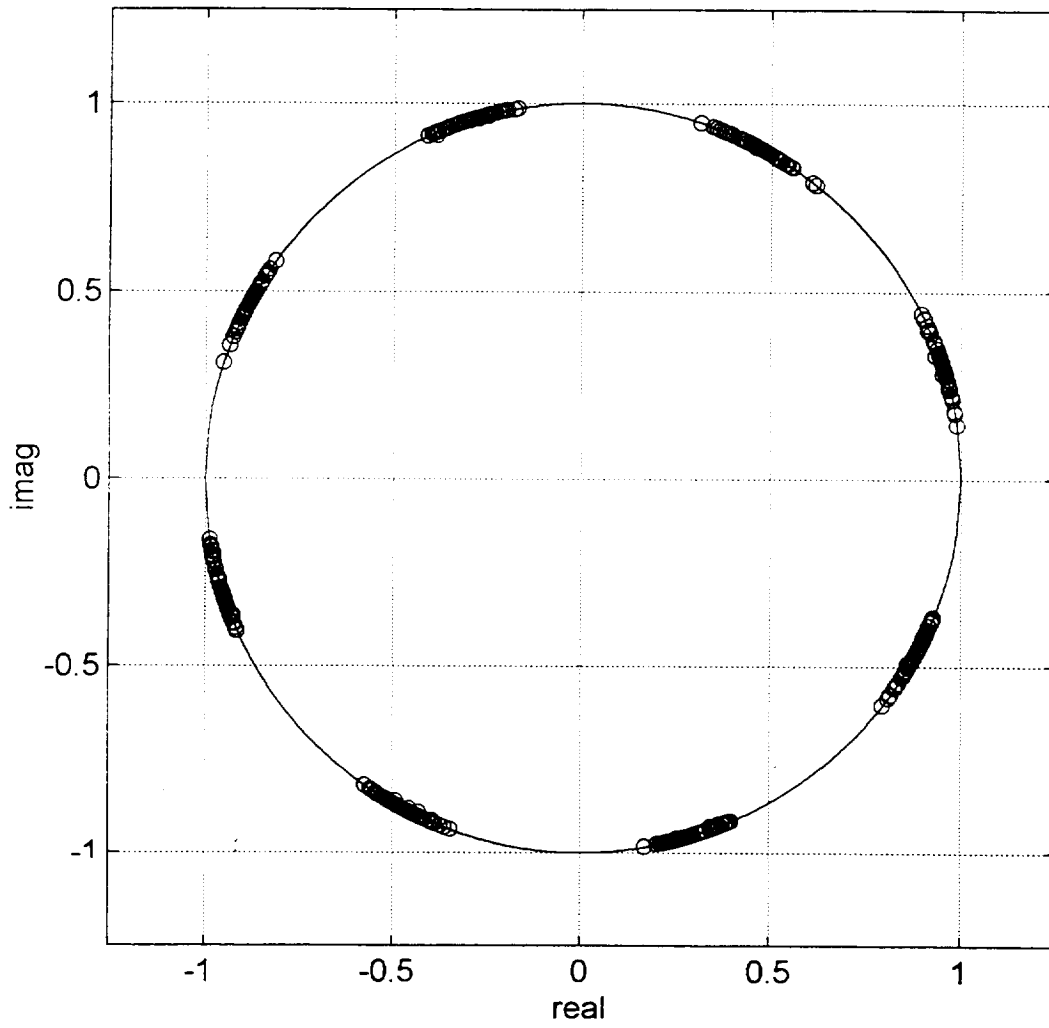


Figure G.1 - Output of SSPA (Saturation Level)
Spectrum Shaping Filter: SRRC $\alpha = 0.1$

Output of SSPA (saturation level), SRRRC Filter (alpha=0.15)

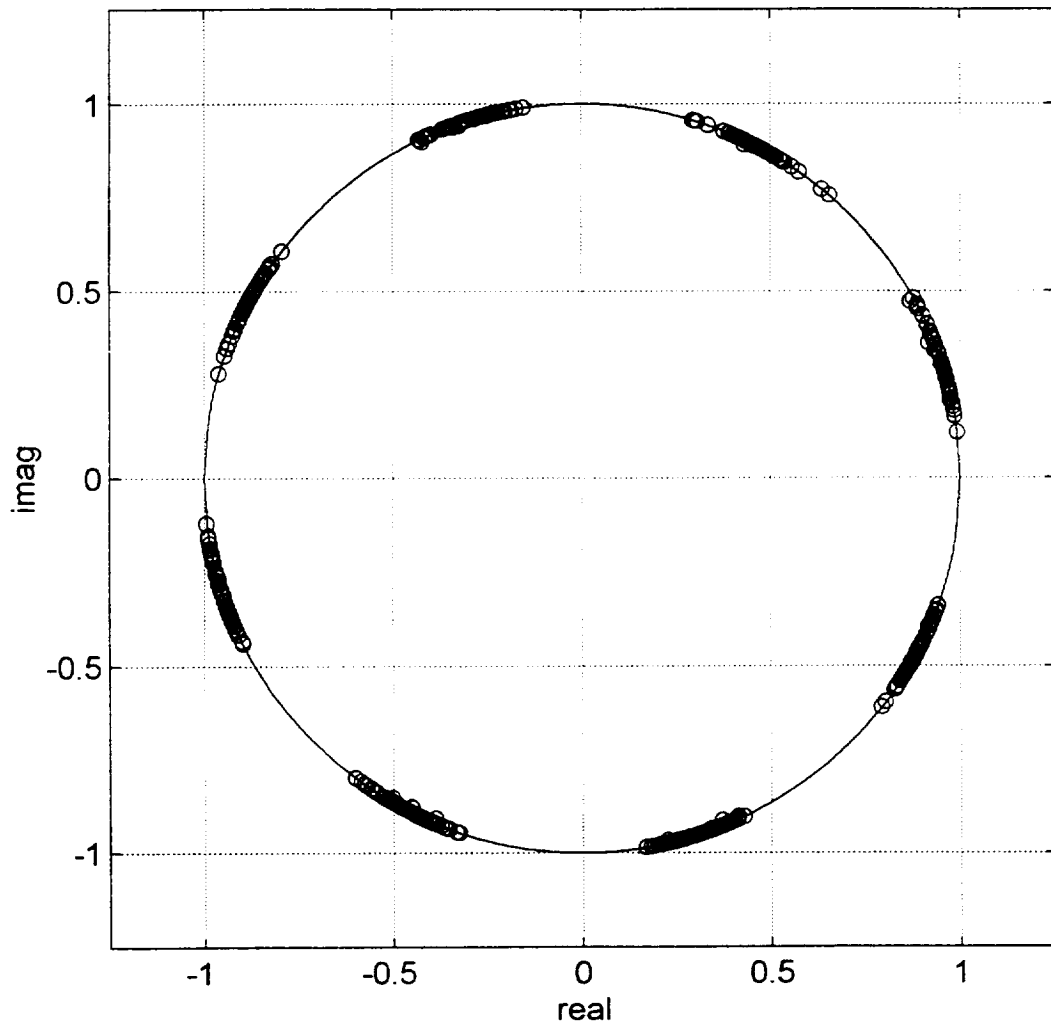


Figure G.2 - Output of SSPA (Saturation Level)
Spectrum Shaping Filter: SRRRC $\alpha=0.15$

Output of SSPA (saturation level), SRRC Filter ($\alpha=0.2$)

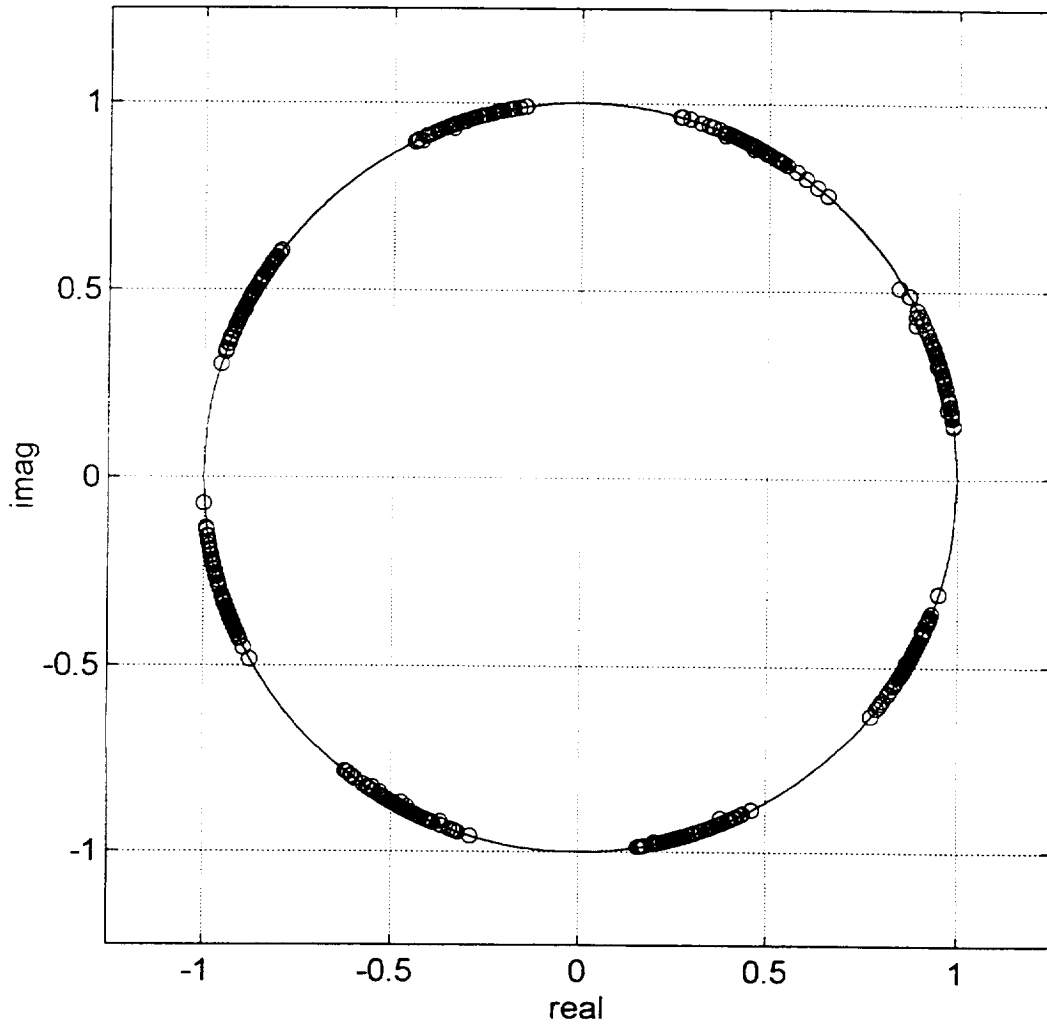


Figure G.3 - Output of SSPA (Saturation Level)
Spectrum Shaping Filter: SRRC $\alpha=0.2$

Output of SSPA (saturation level), SRRC Filter (alpha=0.25)

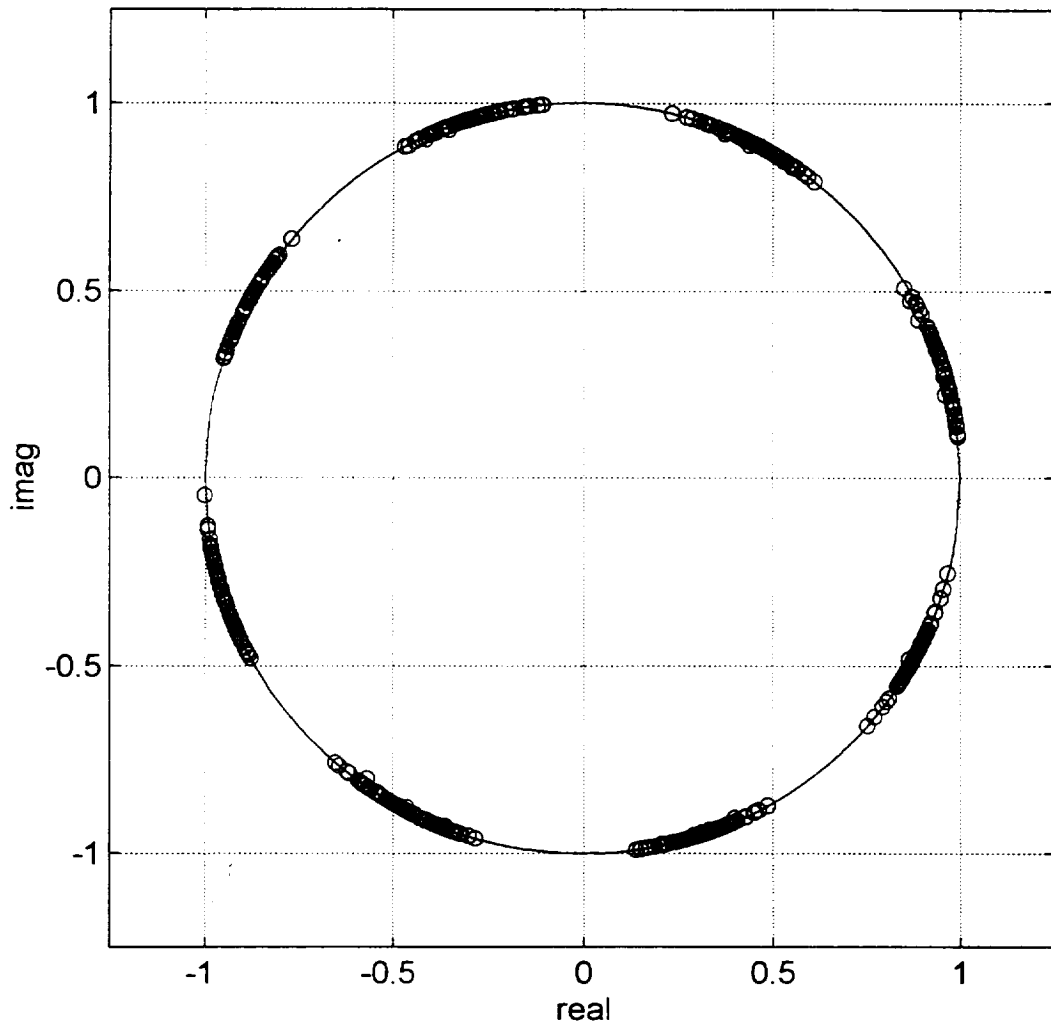


Figure G.4 - Output of SSPA (Saturation Level)
Spectrum Shaping Filter: SRRC $\alpha=0.25$

Output of SSPA (saturation level), SRRC Filter (alpha=0.3)

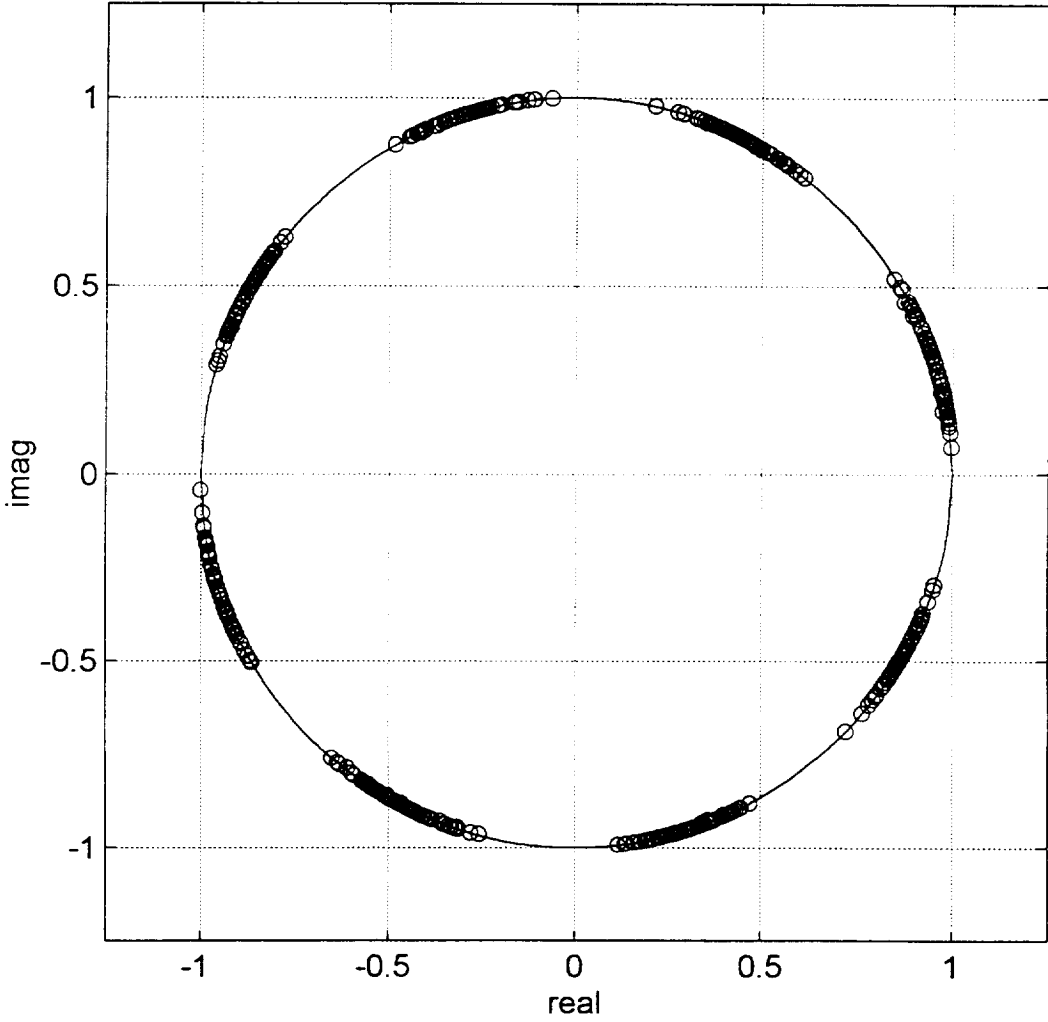


Figure G.5 - Output of SSPA (Saturation Level)
Spectrum Shaping Filter: SRRC $\alpha=0.3$

Output of SSPA (saturation level), SRRC Filter (alpha=0.35)

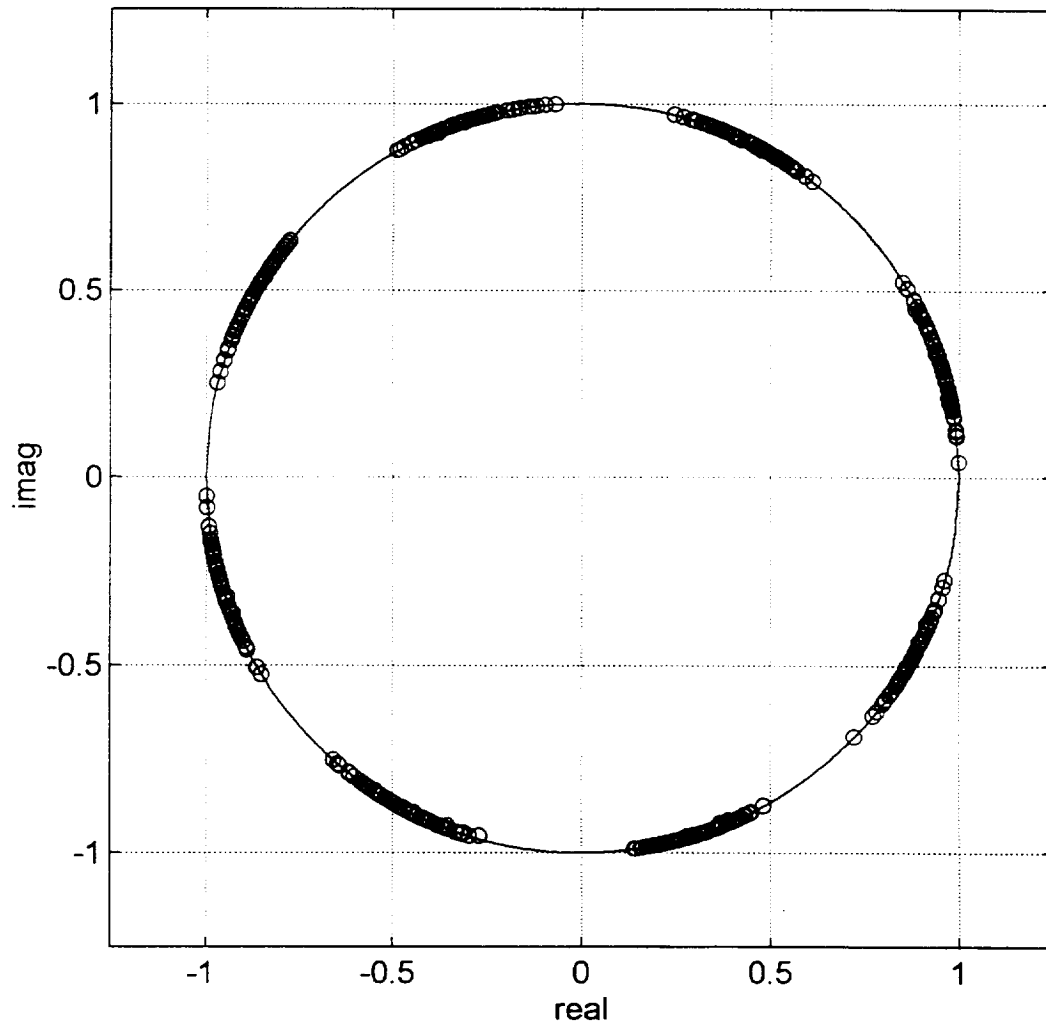


Figure G.6 - Output of SSPA (Saturation Level)
Spectrum Shaping Filter: SRRC $\alpha=0.35$

Output of SSPA (saturation level), SRRC Filter (alpha=0.4)

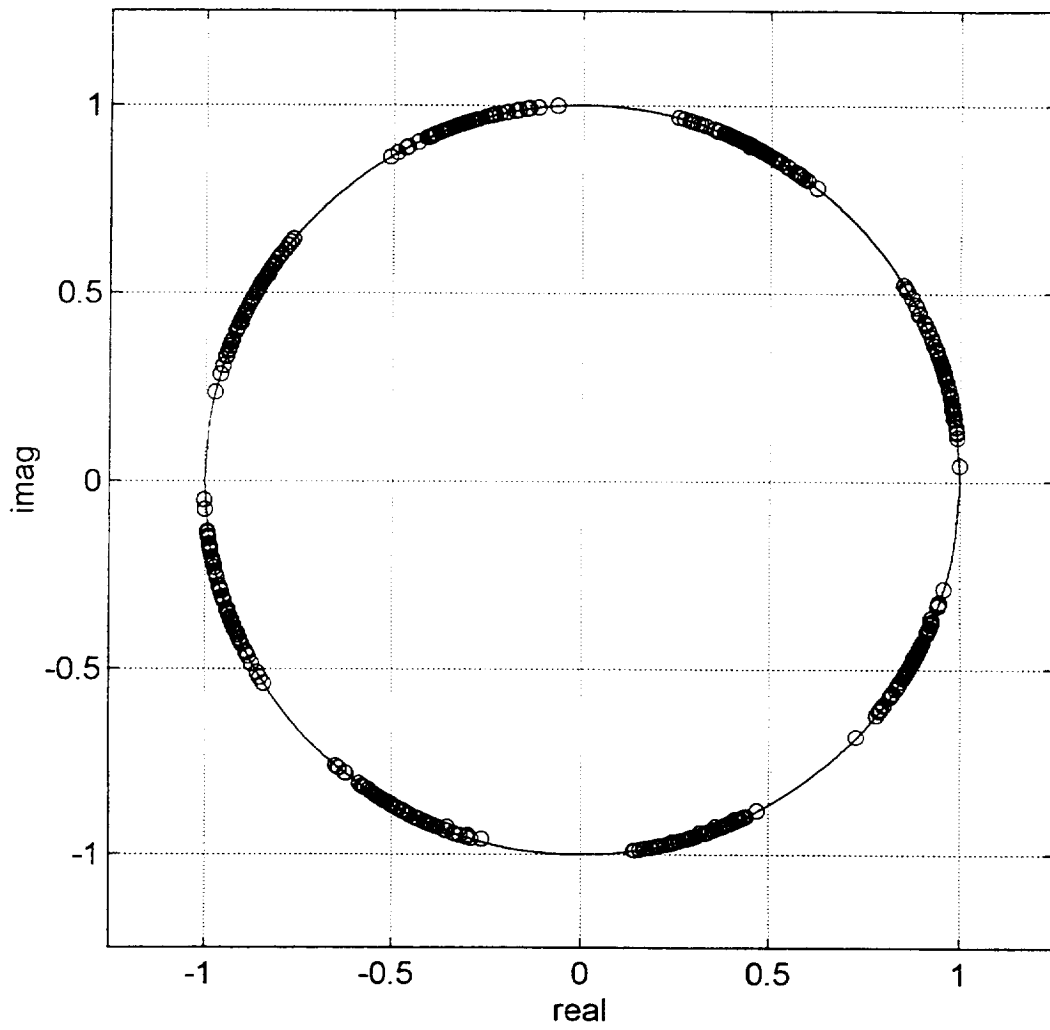


Figure G.7 - Output of SSPA (Saturation Level)
Spectrum Shaping Filter: SRRC $\alpha=0.4$

Output of SSPA (saturation level), SRRC Filter (alpha=0.45)

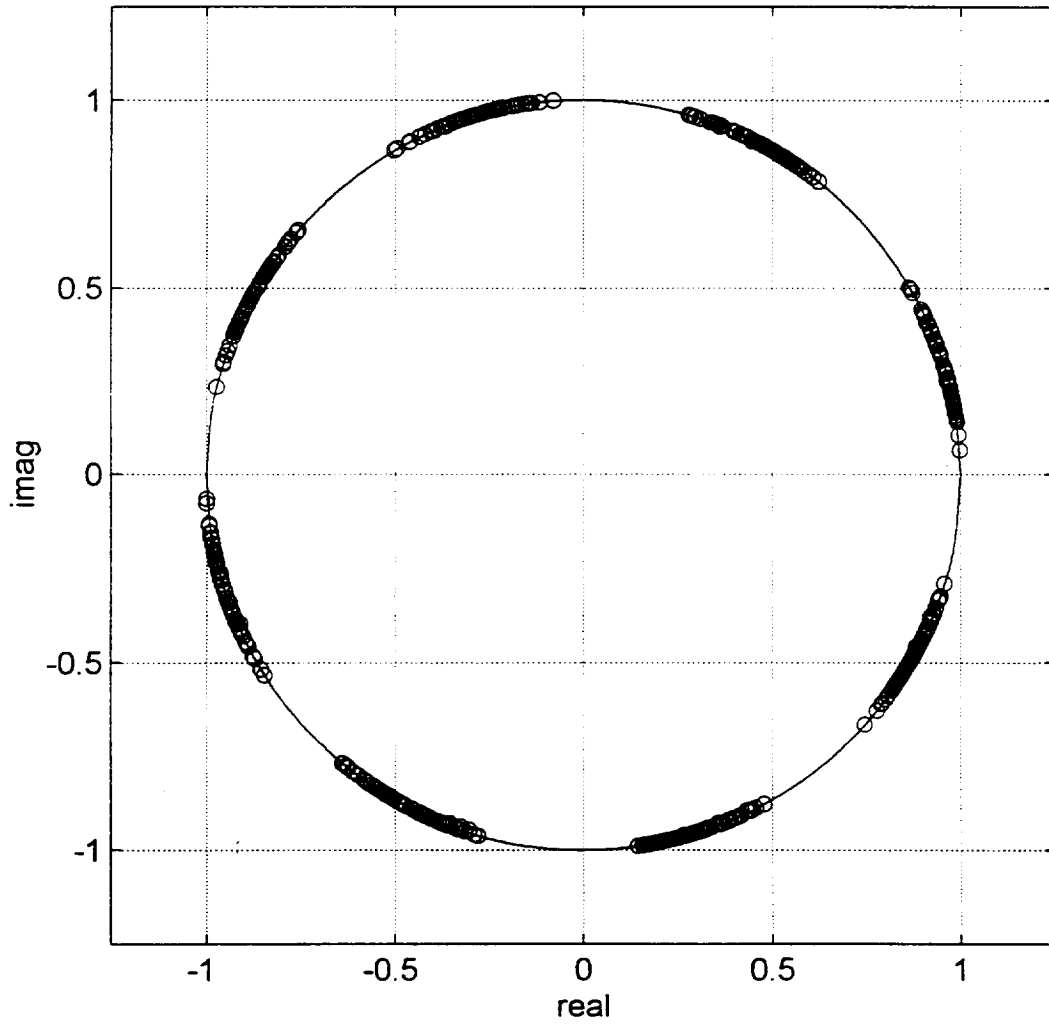


Figure G.8 - Output of SSPA (Saturation Level)
Spectrum Shaping Filter: SRRC $\alpha=0.45$

Output of SSPA (saturation level), SRRRC Filter ($\alpha=0.5$)

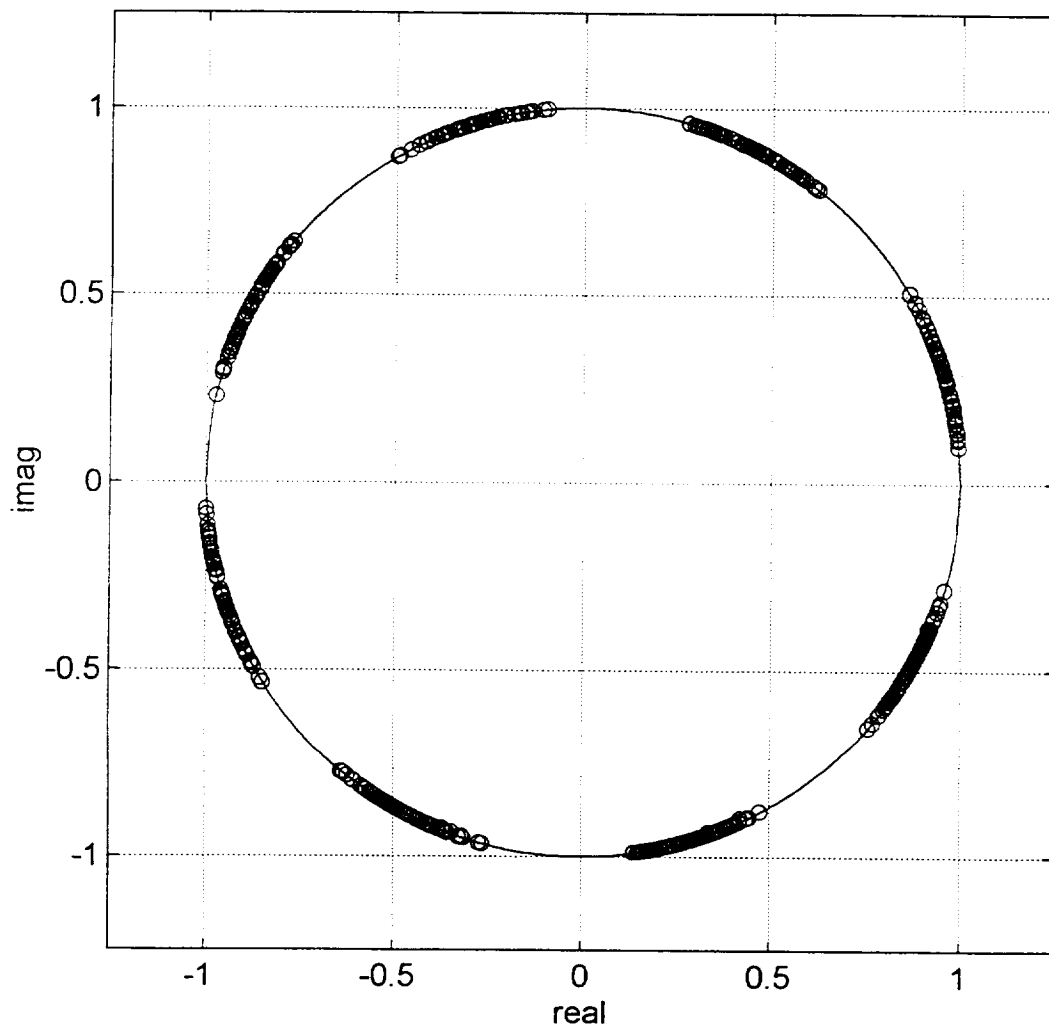


Figure G.9 - Output of SSPA (Saturation Level)
Spectrum Shaping Filter: SRRRC $\alpha=0.5$

Output of SSPA (saturation level), SRRC Filter (alpha=0.55)

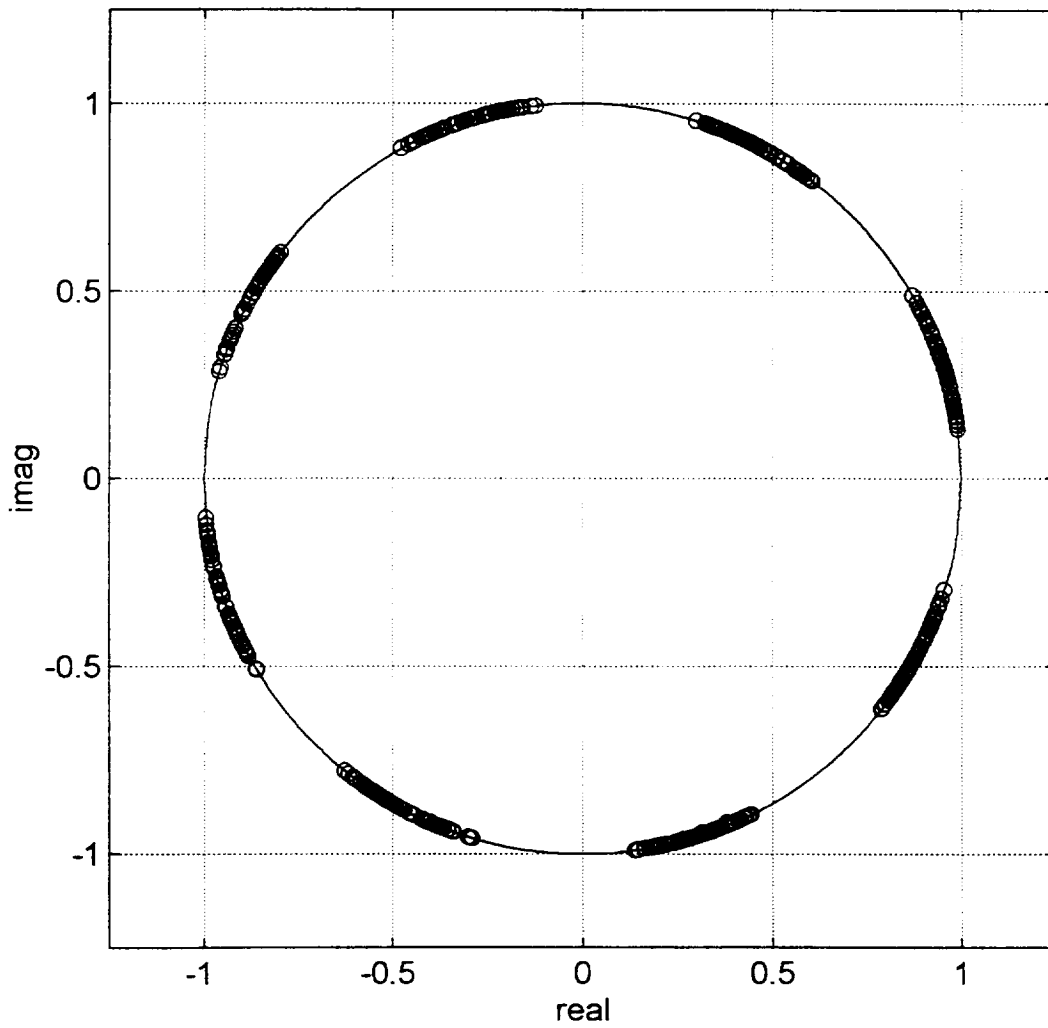


Figure G.10 - Output of SSPA (Saturation Level)
Spectrum Shaping Filter: SRRC $\alpha=0.55$

Output of SSPA (saturation level), SRRC Filter (alpha=0.6)

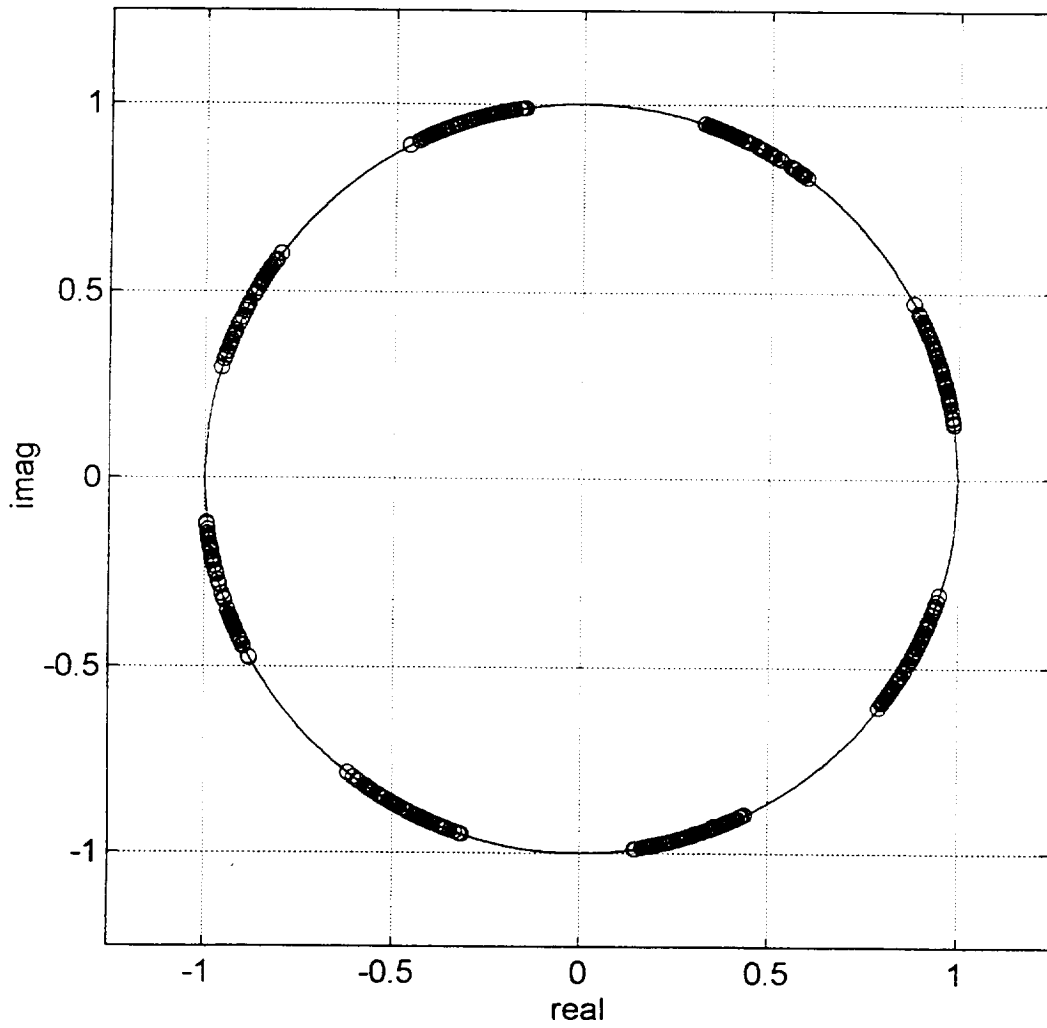


Figure G.11 - Output of SSPA (Saturation Level)
Spectrum Shaping Filter: SRRC $\alpha=0.6$

Output of SSPA (saturation level), SRRRC Filter (alpha=0.65)

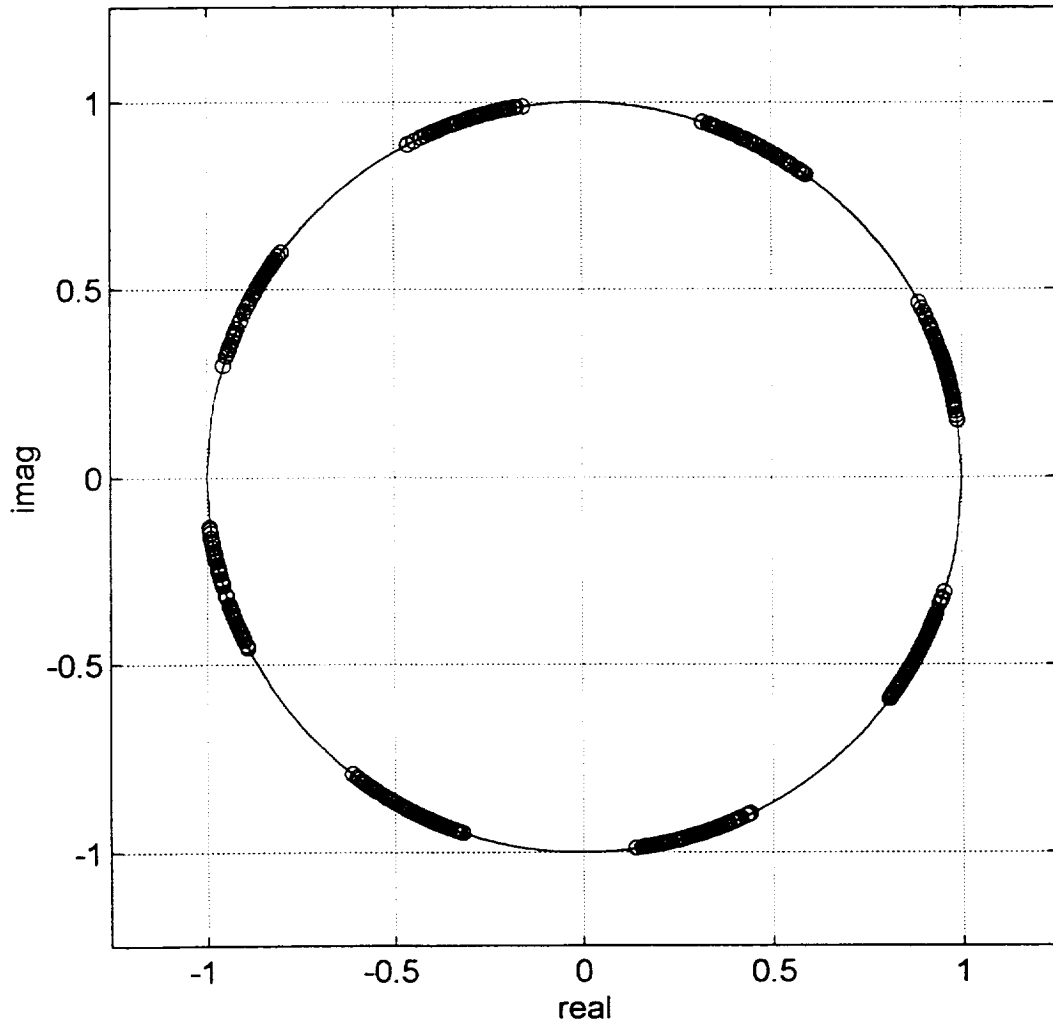


Figure G.12 - Output of SSPA (Saturation Level)
Spectrum Shaping Filter: SRRRC $\alpha=0.65$

Output of SSPA (saturation level), SRRC Filter (alpha=0.7)

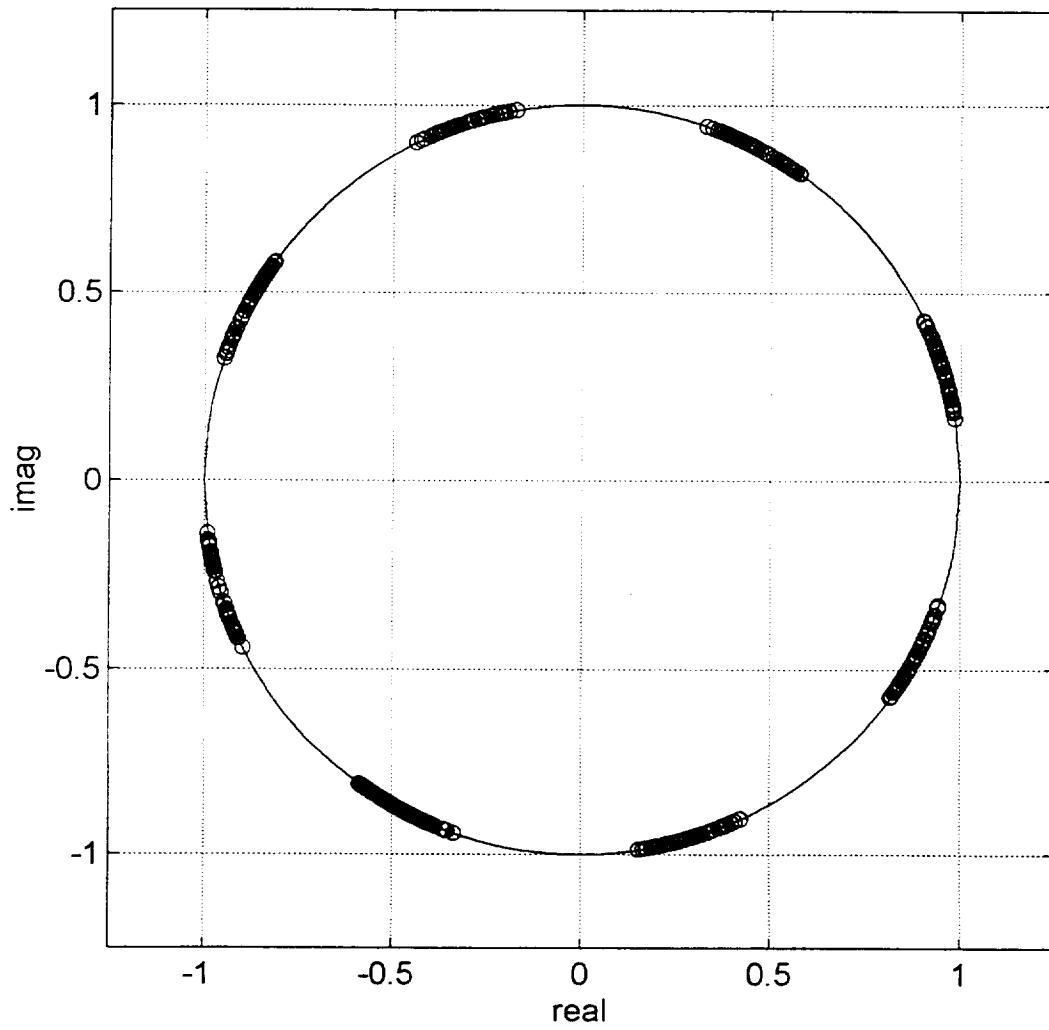


Figure G.13- Output of SSPA (Saturation Level)
Spectrum Shaping Filter: SRRC $\alpha=0.7$

Output of SSPA (saturation level), SRRC Filter (alpha=0.75)

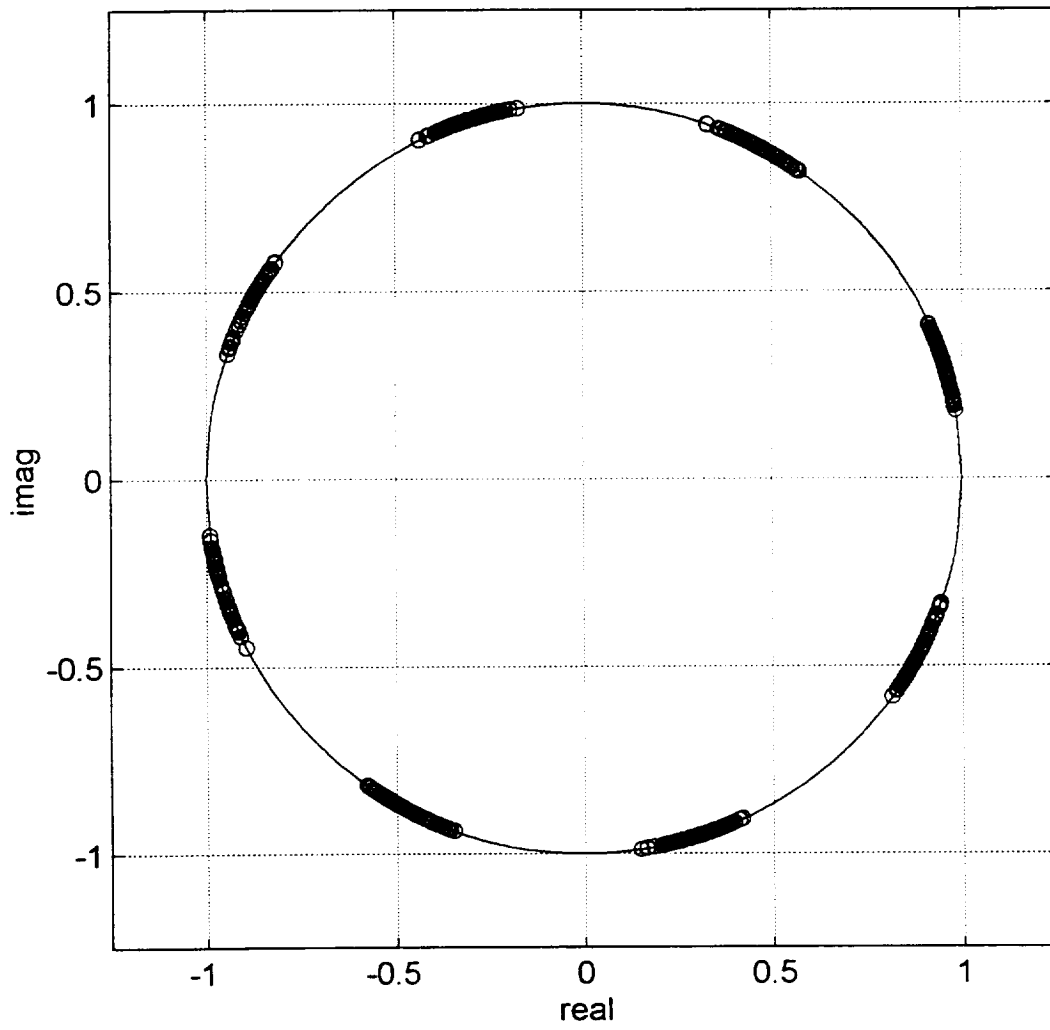


Figure G.14- Output of SSPA (Saturation Level)
Spectrum Shaping Filter: SRRC $\alpha=0.75$

Output of SSPA (saturation level), SRRC Filter (alpha=0.80)

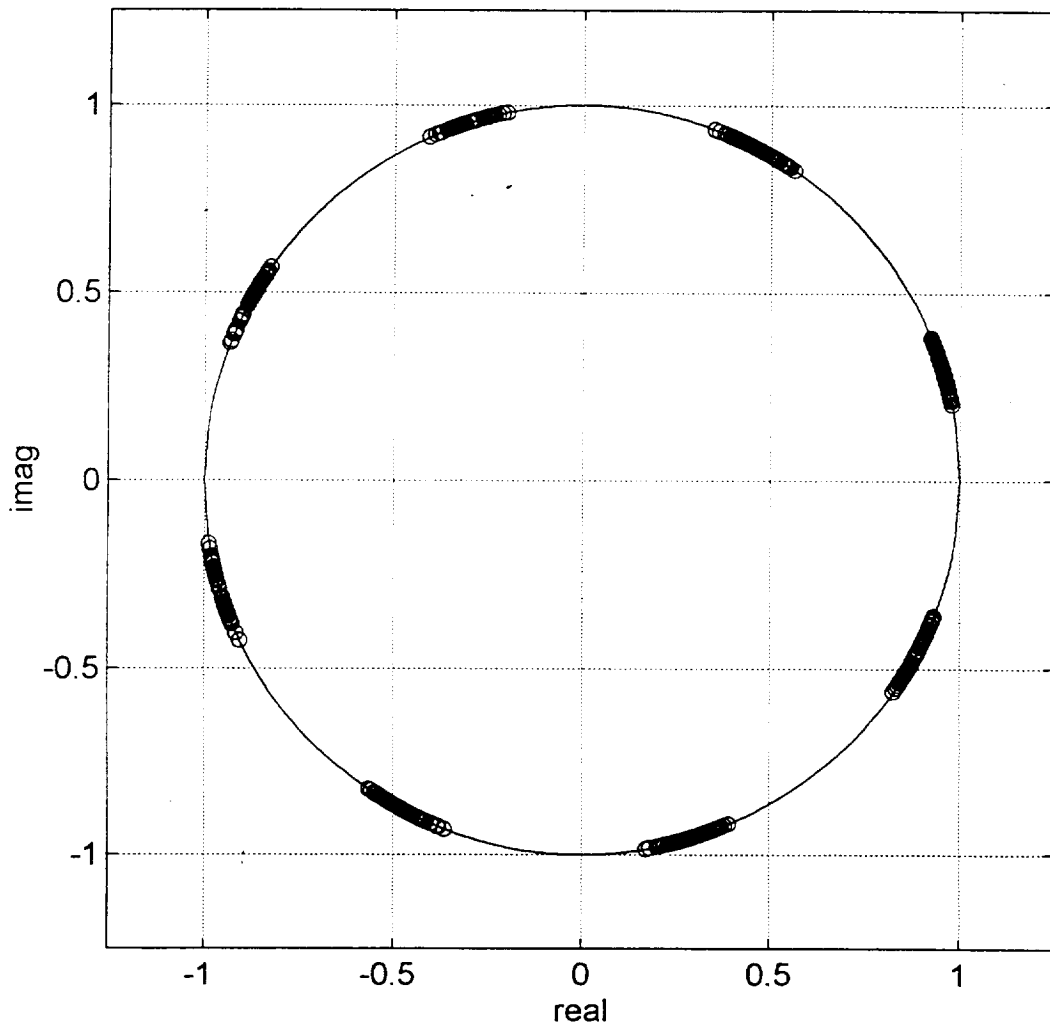


Figure G.15 - Output of SSPA (Saturation Level)
Spectrum Shaping Filter: SRRC $\alpha=0.8$

Output of SSPA (saturation level), SRRC Filter (alpha=0.85)

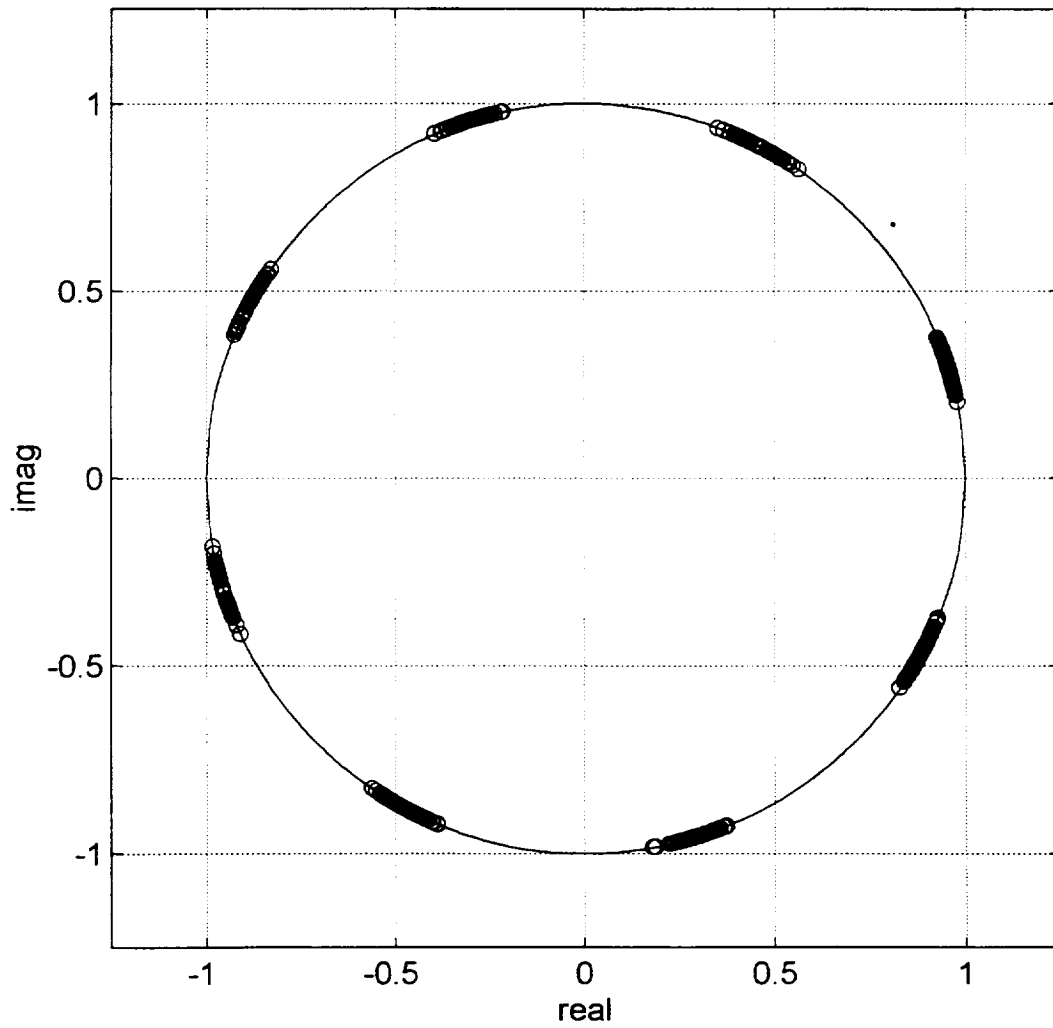


Figure G.16 - Output of SSPA (Saturation Level)
Spectrum Shaping Filter: SRRC $\alpha=0.85$

Output of SSPA (saturation level), SRRC Filter (alpha=0.9)

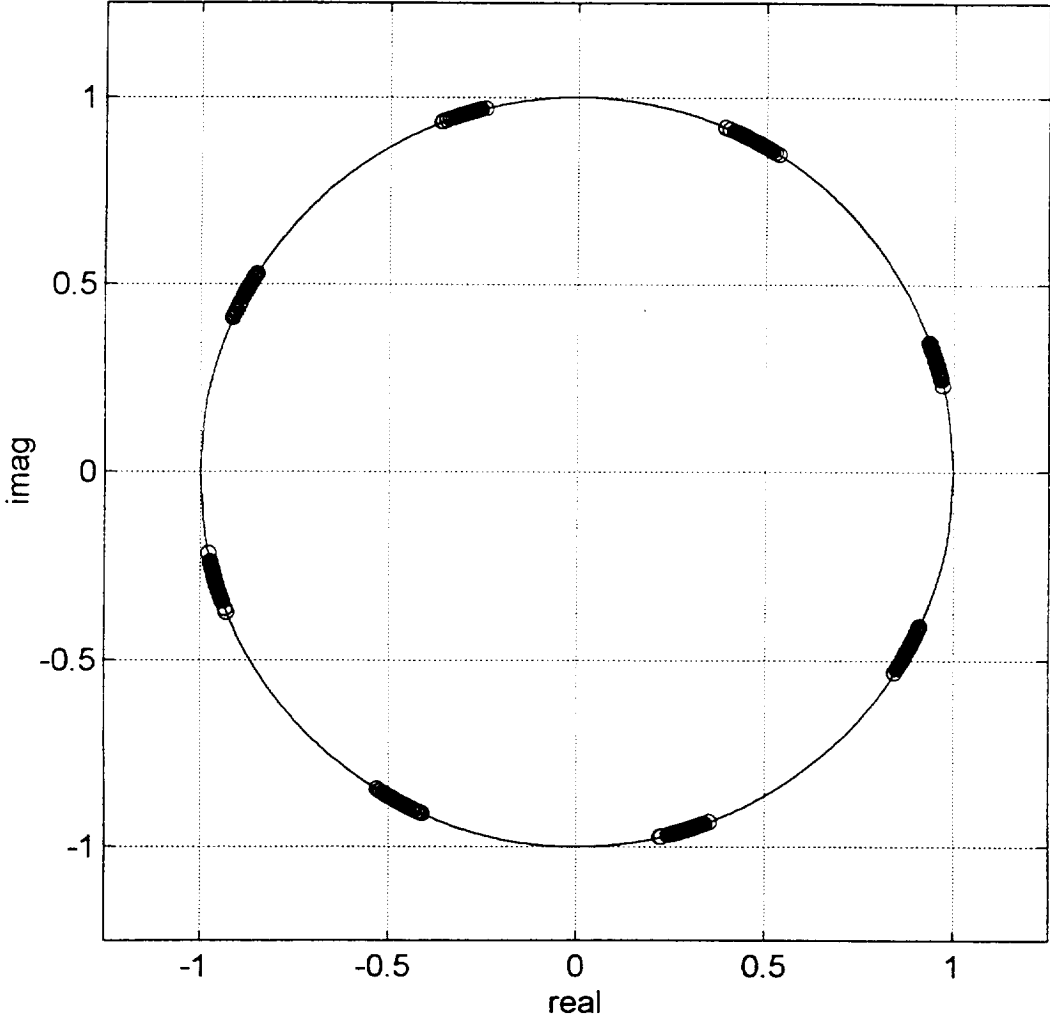


Figure G.17 - Output of SSPA (Saturation Level)
Spectrum Shaping Filter: SRRC $\alpha=0.9$

Output of SSPA (saturation level), SRRC Filter (alpha=0.95)

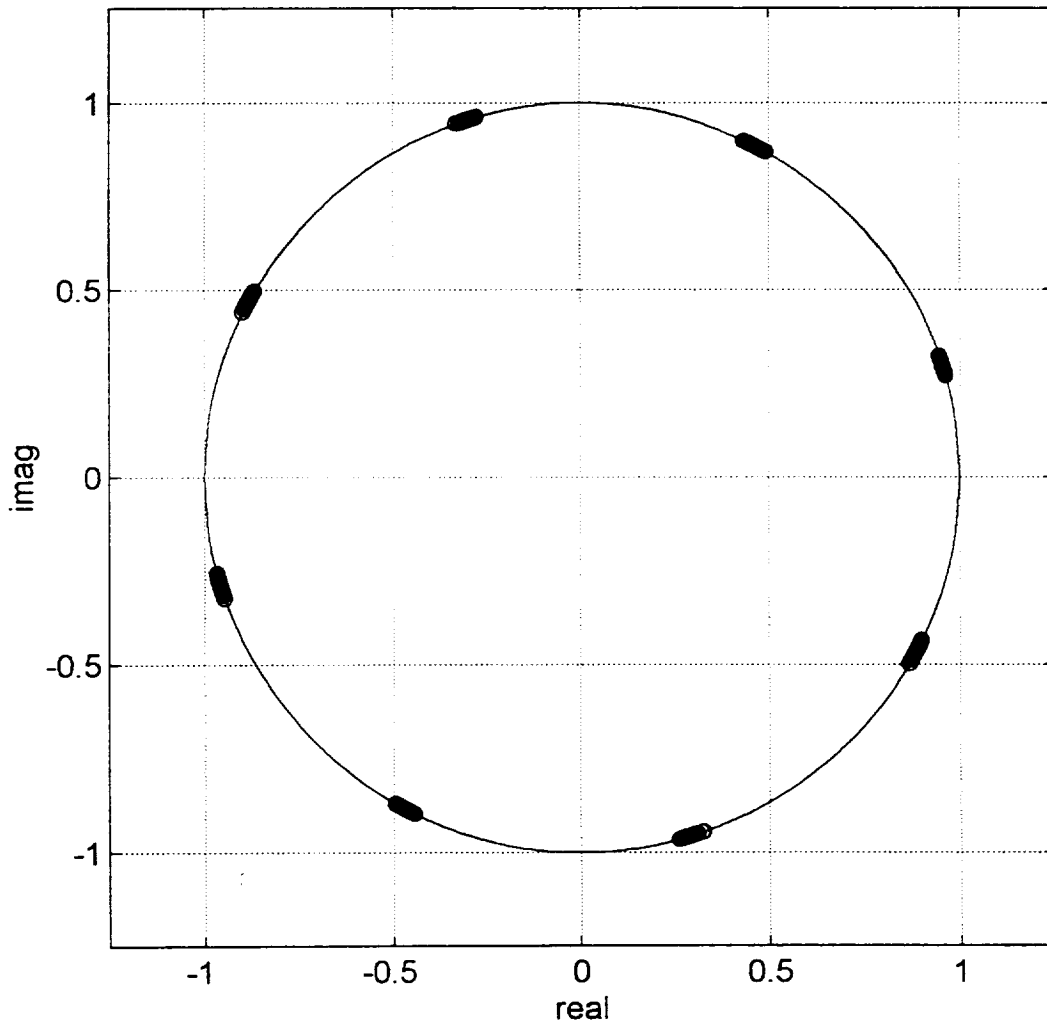


Figure G.18 - Output of SSPA (Saturation Level)
Spectrum Shaping Filter: SRRC $\alpha=0.95$

Output of SSPA (saturation level), SRRC Filter (alpha=1)

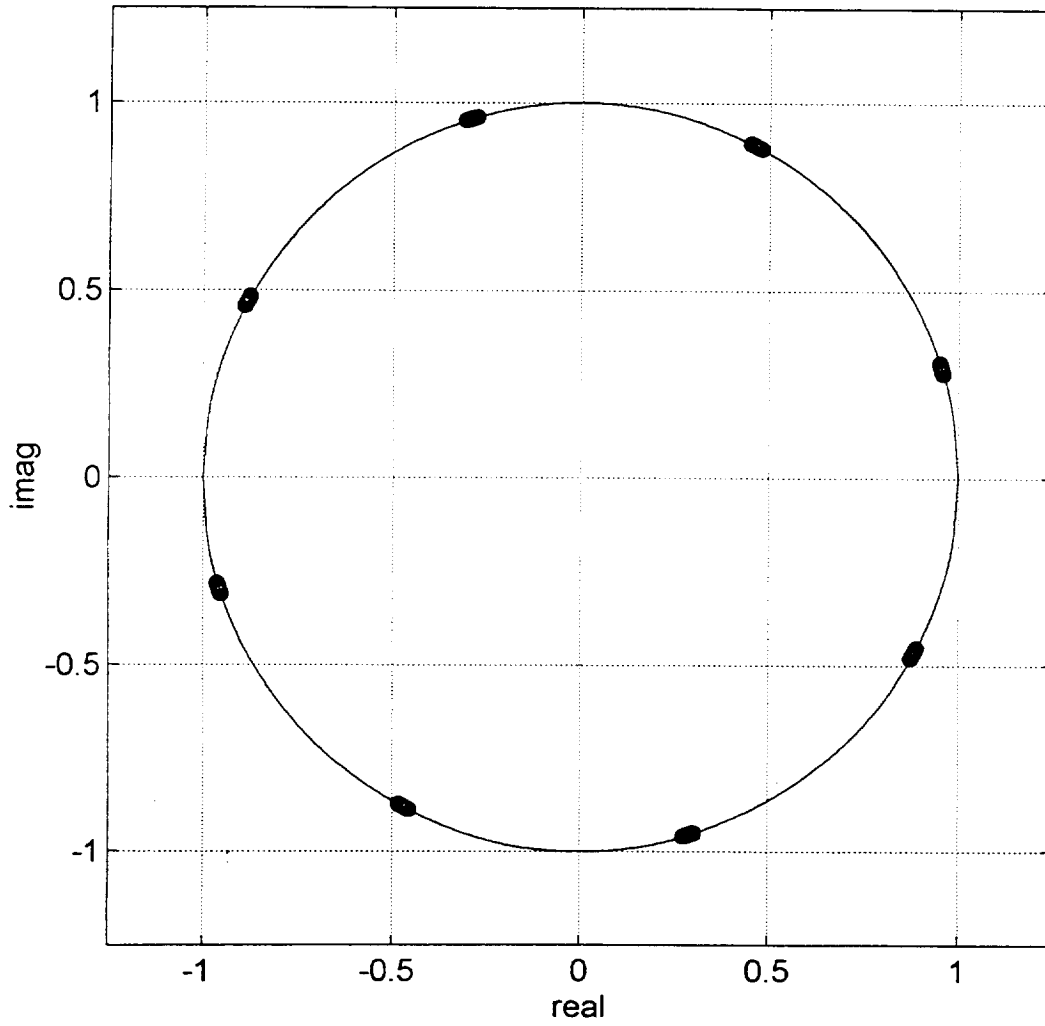


Figure G.19 - Output of SSPA (Saturation Level)
Spectrum Shaping Filter: SRRC $\alpha=1$

G.2 Program Listing: SRRCPLOT.M

```
% Program : SRRCPLOT.M
% Written by : Rubén Caballero
% Developed using MATLAB V4.2B and Signal Processing Toolbox V3.0b
% Copyright 1996 - Rubén Caballero
% New Mexico State University
%
% This function uses the mean and variance calculated by the function SPWSOBRE.M to
% calculate the Average Symbol Variance. The result is a plot of the Average Symbol Variance
% versus  $\alpha$  for the SRRC filter as the spectrum shaping filter.

clear;

%*****
%***** SRRC Filters *****
%*****

alpha=[0.1 0.15 0.2 0.25 0.3 0.35 0.4 0.45 0.5 0.55 0.6 0.65 0.7 0.75 0.8 0.85 0.9 0.95 1.0];

%*****
%***** alpha=1 fs= 33 *****
%*****

%SRRC = 1 (using delay=521, ascii file: samprc1.asc)

meandeg(1,:) = [1.7111e+001 6.2204e+001 1.0710e+002 1.5211e+002 -1.6292e+002
               -1.1793e+002 -7.2849e+001 -2.7908e+001];
vardeg(1,:) = [3.2534e-003 3.0962e-003 3.7946e-003 3.8191e-003 3.0762e-003 3.4823e-003
               2.8293e-003 3.7601e-003];
avgvardeg1 = sum(vardeg(1:))/8;

%*****
%***** alpha=0.95 fs= 33 *****
%*****

%SRRC = 0.95 (using delay=521, ascii file: samprc6.asc)

meandeg(9,:) = [1.7127e+001 6.2099e+001 1.0722e+002 1.5195e+002 -1.6292e+002
               -1.1800e+002 -7.2911e+001 -2.7973e+001];
vardeg(9,:) = [9.2975e-003 1.2104e-002 8.6912e-003 1.2401e-002 1.5264e-002 1.0330e-002
               1.0367e-002 1.4794e-002];
avgvardeg9 = sum(vardeg(9:))/8;
```

```
%*****:*****  
%***** alpha=0.90 fs= 33 *****  
%*****
```

%SRRC = 0.90 (using delay=522, ascii file: samprc19.asc)

```
meandeg(19,:) = [1.7205e+001 6.2291e+001 1.0734e+002 1.5186e+002 -1.6286e+002  
                -1.1816e+002 -7.2892e+001 -2.8051e+001];  
vardeg(19,:) = [4.5507e-002 6.7076e-002 4.2139e-002 6.1049e-002 8.0428e-002 6.1238e-002  
                4.5872e-002 6.4998e-002];  
avgvardeg19 = sum(vardeg(19,:))/8;
```

```
%*****:*****  
%***** alpha=0.85 fs= 33 *****  
%*****
```

%SRRC = 0.85 (using delay=523, ascii file: samprc5.asc)

```
meandeg(8,:) = [1.7292e+001 6.2435e+001 1.0743e+002 1.5174e+002 -1.6279e+002  
                -1.1834e+002 -7.2930e+001 -2.8151e+001];  
vardeg(8,:) = [1.1523e-001 1.5848e-001 1.0640e-001 1.4940e-001 1.9194e-001 1.4397e-001  
                1.1206e-001 1.4847e-001];  
avgvardeg8 = sum(vardeg(8,:))/8;
```

```
%*****:*****  
%***** alpha=0.8 fs= 33 *****  
%*****
```

%SRRC = 0.8 (using delay=523, ascii file: samprc18.asc)

```
meandeg(18,:) = [1.7320e+001 6.2427e+001 1.0752e+002 1.5156e+002 -1.6276e+002  
                -1.1840e+002 -7.2974e+001 -2.8241e+001];  
vardeg(18,:) = [1.5747e-001 1.9982e-001 1.4313e-001 1.9965e-001 2.6472e-001 1.8456e-001  
                1.5906e-001 2.0486e-001];  
avgvardeg18 = sum(vardeg(18,:))/8;
```

```
%*****:*****  
%***** alpha=0.75 fs= 33 *****  
%*****
```

%SRRC = 0.75 (using delay=524, ascii file: samprc4.asc)

```
meandeg(7,:) = [1.7400e+001 6.2585e+001 1.0763e+002 1.5153e+002 -1.6272e+002  
                -1.1851e+002 -7.2991e+001 -2.8415e+001];  
vardeg(7,:) = [2.5221e-001 3.0434e-001 2.4381e-001 2.9943e-001 4.1604e-001 2.9389e-001  
                2.4814e-001 3.0076e-001];  
avgvardeg7 = sum(vardeg(7,:))/8;
```

```

%*****
%***** alpha=0.70 fs= 33 *****
%*****

%SRRC=0.7 (using delay= 524, ascii file: samprc17.asc)

meandeg(17,:) = [1.7472e+001 6.2628e+001 1.0776e+002 1.5139e+002 -1.6270e+002
                -1.1846e+002 -7.3051e+001 -2.8555e+001];
vardeg(17,:) = [3.0576e-001 3.5998e-001 3.0909e-001 3.5684e-001 5.0074e-001 3.5077e-001
                3.1454e-001 3.6826e-001];
avgvardeg17 = sum(vardeg(17,:))/8;

%*****
%***** alpha=0.65 fs= 33 *****
%*****

%SRRC = 0.65 (using delay=525, ascii file: samprc7.asc)

meandeg(6,:) = [1.7547e+001 6.2769e+001 1.0778e+002 1.5138e+002 -1.6262e+002
                -1.1851e+002 -7.3048e+001 -2.8670e+001];
vardeg(6,:) = [4.0793e-001 4.6687e-001 4.1356e-001 4.4883e-001 6.4636e-001 4.5084e-001
                3.9264e-001 4.4991e-001];
avgvardeg6 = sum(vardeg(6,:))/8;

%*****
%***** alpha=0.60 fs= 33 *****
%*****

%SRRC=0.6 (using delay= 525, ascii file: samprc16.asc)

meandeg(16,:) = [1.7568e+001 6.2800e+001 1.0775e+002 1.5123e+002 -1.6252e+002
                -1.1847e+002 -7.3137e+001 -2.8757e+001];
vardeg(16,:) = [4.8162e-001 5.3695e-001 4.7133e-001 5.0882e-001 7.2892e-001 4.9668e-001
                4.4502e-001 5.1539e-001];
avgvardeg16 = sum(vardeg(16,:))/8;

%*****
%***** alpha=0.55 fs= 33 *****
%*****

%SRRC = 0.55 (using delay=526, ascii file: samprc8.asc)

meandeg(5,:) = [1.7492e+001 6.2998e+001 1.0763e+002 1.5124e+002 -1.6239e+002
                -1.1850e+002 -7.3114e+001 -2.8836e+001];
vardeg(5,:) = [5.6558e-001 6.0821e-001 5.2558e-001 5.8436e-001 8.3203e-001 5.5564e-001
                4.7571e-001 5.4309e-001];
avgvardeg5 = sum(vardeg(5,:))/8;

```

```

%*****
%***** alpha=0.50 fs= 33 *****
%*****

%SRRC = 0.5 (using delay = 529, ascii file: samprc2.asc)

meandeg(4,:) = [1.7304e+001 6.3239e+001 1.0737e+002 1.5178e+002 -1.6229e+002
               -1.1858e+002 -7.2771e+001 -2.8588e+001];
vardeg(4,:) = [6.5188e-001 6.0204e-001 5.4793e-001 6.7353e-001 8.6404e-001 6.0872e-001
               4.6567e-001 4.8212e-001];
avgvardeg4 = sum(vardeg(4,:))/8;

%*****
%***** alpha=0.45 fs= 33 *****
%*****

%SRRC = 0.45 (using delay = 530, ascii file: samprc9.asc)

meandeg(3,:) = [1.7206e+001 6.3302e+001 1.0730e+002 1.5201e+002 -1.6223e+002
               -1.1857e+002 -7.2514e+001 -2.8389e+001];
vardeg(3,:) = [7.2511e-001 5.9837e-001 5.5998e-001 6.7928e-001 8.3062e-001 6.4724e-001
               4.8553e-001 4.6707e-001];
avgvardeg3 = sum(vardeg(3,:))/8;

%*****
%***** alpha=0.40 fs= 33 *****
%*****

%SRRC=0.4 (using delay= 529, ascii file: samprc14.asc)

meandeg(14,:) = [1.7222e+001 6.3314e+001 1.0752e+002 1.5155e+002 -1.6219e+002
                 -1.1854e+002 -7.2540e+001 -2.8581e+001];
vardeg(14,:) = [7.4356e-001 6.0301e-001 5.5130e-001 6.2800e-001 8.3997e-001 6.3238e-001
                 4.7616e-001 4.6947e-001];
avgvardeg14 = sum(vardeg(14,:))/8;

%*****
%***** alpha=0.35 fs= 33 *****
%*****

%SRRC=0.35 (using delay= 530, ascii file: samprc10.asc)

meandeg(2,:) = [1.7173e+001 6.3371e+001 1.0727e+002 1.5196e+002 -1.6212e+002
                -1.1848e+002 -7.2149e+001 -2.8407e+001];
vardeg(2,:) = [8.1269e-001 5.5102e-001 5.7030e-001 5.9333e-001 7.6520e-001 6.3595e-001
                4.7928e-001 4.5532e-001];
avgvardeg2 = sum(vardeg(2,:))/8;

```

```

%*****
%***** alpha=0.3 fs= 33 *****
%*****

%SRRC=0.30 (using delay= 529, ascii file: samprc12.asc)

meandeg(12,:) = [1.7161e+001 6.3261e+001 1.0737e+002 1.5159e+002 -1.6217e+002
                -1.1837e+002 -7.2458e+001 -2.8654e+001];
vardeg(12,:) = [7.2397e-001 5.3567e-001 5.4030e-001 5.1729e-001 7.4123e-001 5.5889e-001
                4.3710e-001 4.4035e-001];
avgvardeg12 = sum(vardeg(12,:))/8;

%*****
%***** alpha=0.25 fs= 33 *****
%*****

%SRRC =0.25 (using delay = 530, ascii file: samprc10.asc)

meandeg(10,:) = [1.7306e+001 6.3191e+001 1.0709e+002 1.5227e+002 -1.6221e+002
                -1.1813e+002 -7.2247e+001 -2.8346e+001];
vardeg(10,:) = [7.0668e-001 4.8405e-001 5.1696e-001 4.7003e-001 6.3451e-001 5.6028e-001
                4.2029e-001 3.7706e-001];
avgvardeg10 = sum(vardeg(10,:))/8;

%*****
%***** alpha=0.2 fs= 33 *****
%*****

%SRRC=0.2 (using delay= 529, ascii file: samprc11.asc)

meandeg(11,:) = [1.7496e+001 6.2861e+001 1.0736e+002 1.5191e+002 -1.6257e+002
                -1.1796e+002 -7.2788e+001 -2.8484e+001];
vardeg(11,:) = [5.4128e-001 3.9687e-001 4.2458e-001 3.7001e-001 5.6274e-001 4.0052e-001
                3.6781e-001 3.4022e-001];
avgvardeg11 = sum(vardeg(11,:))/8;

%*****
%***** alpha=0.15 fs= 33 *****
%*****

%SRRC=0.15 (using delay= 529, ascii file: samprc15.asc)

meandeg(15,:) = [1.7699e+001 6.2560e+001 1.0740e+002 1.5213e+002 -1.6284e+002
                -1.1792e+002 -7.2878e+001 -2.8250e+001];
vardeg(15,:) = [4.0597e-001 3.2023e-001 3.5618e-001 2.8089e-001 4.1931e-001 2.9815e-001
                3.1036e-001 2.9837e-001];
avgvardeg15 = sum(vardeg(15,:))/8;

```

```

%*****
%***** alpha=0.1 fs=33 *****
%*****

%SRRC=0.1 (using delay= 529, ascii file: samprc13.asc)

meandeg(13,:) = [1.7752e+001 6.2291e+001 1.0743e+002 1.5202e+002 -1.6291e+002
                -1.1790e+002 -7.2870e+001 -2.8113e+001];
vardeg(13,:) = [2.5572e-001 2.4821e-001 2.4306e-001 1.8168e-001 2.5692e-001 2.0489e-001
                1.9270e-001 2.1830e-001];
avgvardeg13 = sum(vardeg(13,:))/8;

%*****
%***** PLOTS *****
%*****

% Average Variance for the Symbols

figure(1);
whitebg;

AMPMAvgvar = [avgvardeg13 avgvardeg15 avgvardeg11 avgvardeg10 avgvardeg12 avgvardeg2
              avgvardeg14 avgvardeg3  avgvardeg4 avgvardeg5 avgvardeg16 avgvardeg6
              avgvardeg17 avgvardeg7 avgvardeg18 avgvardeg8 avgvardeg19 avgvardeg9
              avgvardeg1];

% interpolation using spline fit

interalpha=0.1:0.0001:1;
interpol=spline(alpha,AMPMAvgvar,interalpha);

plot(alpha,AMPMAvgvar,'ok',interalpha,interpol,'k');

title('SRRC Filter Average Symbol Variance vs Roll-of Factor (alpha)');
xlabel('SRRC Rolloff factor (alpha)');
ylabel(' Average Variance (degrees)');
grid;

```

